Karlsruhe Institute of Technology

Processes Influencing Radionuclide Transport and Retention - Investigations Across Scales

TransRet 2020

(October 12-13, 2021, Karlsruhe, Germany)

Workshop Summary - Book of Abstracts

F. Heberling, J. Lützenkirchen (eds.)

INE SCIENTIFIC WORKING DOCUMENTS 05

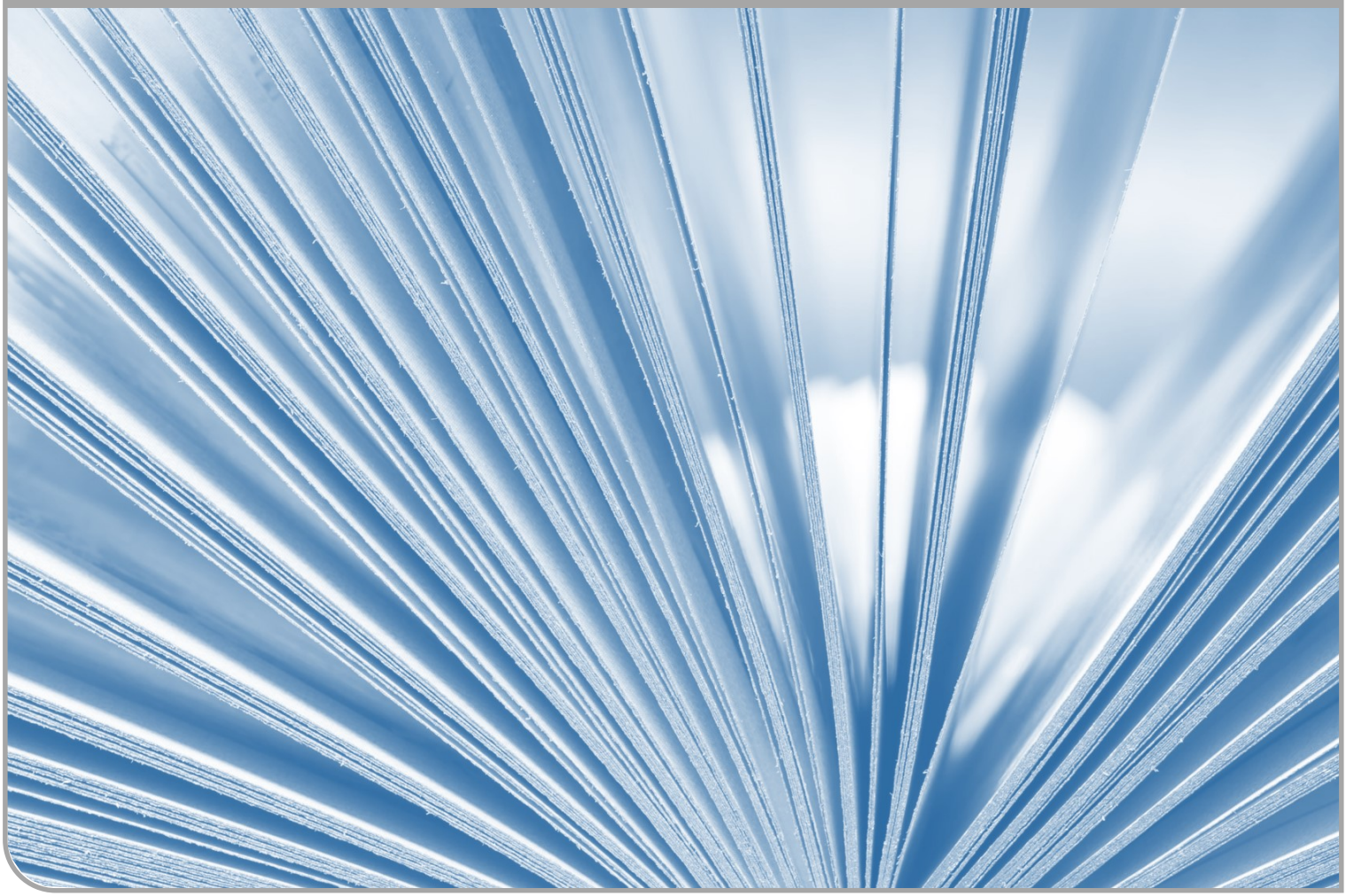

Institut für Nukleare Entsorgung (INE)

Hermann-von-Helmholtz-Platz 1
76344 Eggenstein-Leopoldshafen
www.ine.kit.edu

Impressum

Karlsruher Institut für Technologie (KIT)
www.kit.edu

2022

URL: http://www.ine.kit.edu/53.php
ISSN: 2701-262X
DOI: 10.5445/IR/1000142975

Preface

TransRet2020 (October 12-13, 2021) was the seventh meeting in the series of the Karlsruhe Geochemical Workshops. It had originally been planned to take place in summer 2020 on the occasion of the 40th anniversary of the foundation of the Institute for Nuclear Waste Disposal (INE) at the Karlsruhe Institute of Technology (KIT) in association with a symposium celebrating the anniversary. Due to the COVID pandemic it was decided to postpone the workshop to spring 2021. Due to persisting restrictions it had to be again rescheduled and was finally organized as a hybrid onsite/online meeting starting one day after the postponed symposium held on October 11, 2021.

The first workshop in the series was held in 1997 at Forschungszentrum Karlsruhe, the KIT predecessor. Its main topic was “Geochemical modelling – radiotoxic and chemical toxic substances in natural aquatic systems”.

The second meeting took place in 1999 in nearby town of Speyer, focusing on “Mineral/water interactions close to equilibrium”.

TRePro 2002 held in 2002 in Karlsruhe dealt with “Modelling of coupled **T**ransport **Re**action **Pro**cesses”.

SoPro 2005, again in Karlsruhe, treated **So**rption **Pro**cesses on oxide and carbonate minerals.

TRePro II 2009 was more focusing on the transport aspects.

TRePro III 2014 took up the ideas of TRePro 2002 and TRePro II 2009.

The intention of the workshops has always been to enhance the discussion between experimentalists and modelers from different domains.

Concerning **TransRet2020**, the organizers gratefully acknowledge the willingness of all contributors to attend the meeting onsite and/or online. The hybrid form was new to most of us. In particular, the poster session in the proposed format - involving flash presentations and virtual poster-rooms - cannot be as interesting and productive as a real poster event.

Overall, we were very happy with the course of the workshop at the given boundary conditions!

Without the help of many colleagues at INE, the organization of the workshop would not have been possible. In particular, Susanne Fanghänel and Dominik Mayer managed to surmount all the difficulties imposed by the virus.

The team of our IT service provider Tooltec arranged a very smooth and stable hybrid conference format.

The helpful input from various departments at KIT who were involved in the organization is gratefully acknowledged.

Finally, we thank all participants and in particular the contributors to this book of abstracts.

Eggenstein-Leopoldshafen, December 2020

Program

Processes Influencing Radionuclide Transport and Retention

-

Investigations Across Scales

TransRet2020

Karlsruhe, Germany

12th & 13th October, 2021

KIT 1980 - 2020
INE - 40
Institute for Nuclear Waste Disposal

Karlsruhe Institute of Technology

TransRet2020, Agenda

Tuesday, 12th October:

8:00 *Registration opens*

8:30 – 8:40 *Announcements (Frank Heberling)*

8:40 – 8:45 *Welcome (Horst Geckeis)*

Session 1: Kinetics and dynamics of alteration, mobilization, and retention processes (Chair: Marcus Altmaier)

Keynote:

8:45 – 9:15 **Gilles Montavon (Subatech)**: Assessment of contaminant lability in the environment: a key issue for understanding their mobility/(bio)availability (online/onsite to be confirmed)

Orals, session 1:

9:15 – 9:35 **Jenna Poonoosamy (FZJ)**: A lab-on-a-chip approach for resolving controversies on crystallization processes in porous media (online)

9:35 – 9:55 **Lionel Mercury (Uni Orléans)**: Supersolubility and cold boiling in nano/milli-metric dual porous media subject to capillarity (online)

9:55 – 10:25 *Coffee break*

10:25 – 11:00 *Poster Flash-talks, session 1:*

Cynthia Rieckhof (CIEMAT): Kinetic study of ^{233}U(VI) and ^{99}Tc(VII) retention in nontronite: role of accessory Fe (online)

Maximilian Demnitz (HZDR): Influence of surface roughness on the sorption of Cm(III) (online)

Jonas Schabernack (HZDR): Surface reactivity parameterization for the simulation of mineral dissolution in pore-scale reactive transport models (onsite)

Tiziana Missana (CIEMAT): Radiobarite stability under cementitious condition (online)

Kaifeng Wang (Uni Grenoble): Corrosion of borosilicate glass under hydraulically saturated conditions (onsite)

Agost Tasi (KIT): Hydrolytic degradation of the polyacrylonitrile-based UP2 ion exchange resin under cementitious conditions (onsite)

Vladyslav Sushko (HZDR): Microcosm study of indigenous microorganisms in bentonite and its effect on corrosion of cast iron (online)

Stephan Hilpmann (HZDR): Microscopic and spectroscopic study of the Uranium(VI) reduction by a sulfate-reducing microorganism (online)

Orals, session 1 continued:

11:00 – 11:20 Natalia Mayordomo-Herranz (HZDR): Technetium immobilization by chloride green rust (online)

11:20 – 11:40 Kaifeng Wang (Uni Grenoble): Selenite interaction with mackinawite in cement pore water (onsite)

11:40 – 12:00 Anna Dabizha (Uni Mainz): Effect of temperature on molybdate adsorption by goethite (online)

12:00 – 13:30 Lunch break

Session 2: Thermodynamics of aqueous speciation, solubility, and sorption (Chair: Lara Duro)

Keynote:

13:30 – 14:00 Lara Duro (AMPHOS): Solubility of lanthanides for environmental and performance assessments (onsite)

Orals, session 2:

14:00 – 14:20 Xavier Gaona (KIT): Radionuclide retention in cementitious systems: research activities at KIT-INE (onsite)

14:20 – 14:40 Pierre Hencoq (ANDRA): Towards a global model of radionuclide sorption in cement-based materials. Focus on cesium uptake (online)

14:40 – 15:00 David Garcia (AMPHOS): Radionuclide sorption onto calcareous gravels. Experimental results for K_d determination and first insights on adsorption mechanisms (onsite)

15:00 – 15:20 Michal Arbel-Haddad (NRCN): NMR and XRD provide evidence for preferential binding of cesium to crystalline zeolite phases in geopolymers (online)

15:20 – 15:40 Julia Neumann (HZDR): Structural investigation of the adsorption of Y(III) on orthoclase (001) single crystals using resonant surface X-ray diffraction (onsite)

15:40 – 16:10 Coffee break

16:10 – 17:10 Poster Flash-talks, session 2:

Xavier Gaona (KIT): THEREDA thermodynamic database (onsite)

Oscar Almendros (CIEMAT): Sorption of ^{233}U on ettringite and effects of the presence of isosaccharinic acid, citrate and phthalate (online)

Yongheum Jo (KIT): Solubility of Niobium(V) in cementitious systems: identification of the solubility-controlling solid phases in hyperalkaline systems containing Ca (onsite)

Janina Stietz (Uni Mainz): Influence of EDTA on the sorption of Am(III), Th(IV) and Pu(IV) on hardened cement paste (onsite)

Andrey Kalinichev (Subatech): Atomistic computer simulation of the structure and properties of iodide-containing hydrocalumite (AFm phase) (online)

Marcus Altmaier (KIT): R&D performed in the EURAD-CORI project (onsite)

Volodymyr Svitlyk (HZDR): Towards nuclear waste confinement: solid solutions and phase stability in (Th/Ce)-Y-zirconia systems (online)

Nicole DiBlasi (KIT): Investigation of the solubility, redox behavior, and aqueous speciation of the ternary Plutonium-EDTA-calcium system (onsite)

Sarah Duckworth (KIT): Impact of inorganic and organic ligands on the solubility and redox chemistry of Tc under reducing saline conditions (onsite)

Christian Kiefer (KIT): Solubility and structural characterization of M(IV) hydrous oxides: the case of Zr(IV) and Th(IV) (onsite)

Torben Weyand (BASE): Converting thermodynamic data using the Pitzer approach for the geochemical code TOUGHREACT (online)

Andrej Skerencak-Frech (KIT): The complexation and thermodynamics of Cm(III) with F^- at T = 25 to 200 °C studied by time resolved laser fluorescence spectroscopy (onsite)

Jessica Lessing (HZDR): Structural and modeling study of the retention of trivalent f-elements (Am, Cm, Eu) by natural and synthetic Ca-feldspars (onsite)

Frank Heberling (KIT): Surface complexation models for rough and heterogeneous surfaces - the charge regulation concept applied to simple 2D geometries (onsite)

Orals, session 2 continued:

17:10 – 17:30 Brian Powell (Uni Clemson): Understanding tetravalent actinide oxide formation, stability, and dissolution under far field environmental conditions (online)

17:30 – 17:50 Jordi Bruno (AMPHOS): The contribution of natural analogue studies to the safety assessment of nuclear waste repositories (onsite)

19:00 – 21:00 Workshop dinner, KIT Cafeteria

Wednesday, 13th October

8:00 Venue opens

Session 3: Radionuclide transport phenomena (Chair: Volker Metz)

Keynote:

8:30 – 9:00 Sergey Churakov (PSI): Reactive transport and retention of solutes in porous media: Current state of the art and the challenges (online)

Orals, session 3:

9:00 – 9:20 Raphael Wüst (NAGRA): Coupled radionuclide transport reactions in shale rocks interpreted based on laboratory diffusive tests and data modelling – a novel approach (online)

9:20 – 9:40 Yuankai Yang (FZJ): A hybrid pore-scale and continuum-scale model for solute transport and local precipitation in porous media (online)

9:40 – 10:00 Tao Yuan (HZDR): Numerical modeling and simulation of diffusive transport of radionuclides in the sandy facies of Opalinus Clay using multi-scale digital rock physics (onsite)

10:00 – 10:30 Coffee break

10:30 – 11:05 Poster Flash-talks, session 3:

Claudia Joseph (KIT): Autoradiography and SEM–EDX analysis of diffusion samples of sandy facies of Opalinus Clay (onsite)

Naila Ait-Mouheb (FZJ): Migration behaviour of Ra-226 in the sandy facies of Opalinus Clay (online)

Yasmine Kouhail (KIT): Long term bentonite erosion experiments in an artificial fracture: Radionuclide diffusion in FEBEX bentonite (onsite)

Madlen Stockmann (HZDR): Radionuclide transport modelling: The Smart Kd-Concept in reactive transport codes (online)

Teba Gil-Diaz (Uni Jena): Anion transport mechanisms: applications to radionuclide migration and cementitious systems (onsite)

Mara Lönartz (FZJ): Deciphering mineral precipitation induced porosity clogging in diffusion-controlled porous media (online)

Bruce Yardley (Uni Leeds): Processes contributing to rock matrix diffusion in fractured crystalline rock (online)

Orals, session 3 continued:

11:05 – 11:25 Daniel Glückman (KIT): Diffusion of U(VI) and Am(III) through Opalinus Clay studied down to ultra-trace levels (onsite)

11:25 – 11:45 Cornelius Fischer (HZDR): Pore network and flow field analysis toward improved predictability of diffusive transport in argillaceous host rocks (online)

11:45 – 12:05 Claudia Joseph (KIT): Diffusion of HTO, $^{36}Cl^-$, and $^{85}Sr^{2+}$ in compacted natural and reduced-charge dioctahedral smectites (onsite)

12:05 – 13:30 Lunch break

Session 3: Radionuclide transport phenomena, continued (Chair: Olaf Kolditz)

Keynote:

13:30 – 14:00 Olaf Kolditz (UFZ): Workflow development for Thermo-Hydro-Mechanical (THM) and Reactive Transport Processes (RTP) and software integration for deep geological repository simulation (onsite)

Orals, session 3 continued:

14:00 – 14:20 Jörg Buchwald (UFZ): A framework for risk analysis of clayrock fracturing due to high gas pressures in repository systems (online)

14:20 – 14:40 Jaime Garibay-Rodriguez (UFZ): Reactive transport model of a low and intermediate-level waste disposal cell evolution in clay rock (online)

14:40 – 15:00 Theresa Hennig (GFZ): Geochemical gradients within the Opalinus Clay system at Mont Terri (Switzerland) enhance uranium migration (online)

15:00 – 15:30 Coffee break

15:30 – 15:50 Francesca Quinto (KIT): Breakthrough of ^{99}Tc and actinide tracers from the Long-term-In-situ-Test (LIT) (onsite)

15:50 – 16:10 Richard Metcalfe (Quintessa): Evolution of radionuclide transport and retardation processes in uplifting crystalline rock (online)

16:10 – 16:30 Renchao Lu (UFZ): A new operator-splitting finite element scheme for reactive transport modelling in saturated porous media (online)

16:30 – 17:00 Workshop closes (Johannes Lützenkirchen)

Abstracts

Assessment of contaminant lability in the environment: a key issue for understanding their mobility/(bio)availability.

G. Montavon

SUBATECH, IMTA/CNRS-IN2P3/Université de Nantes, 4, rue Alfred Kastler, F- 44304-Nantes
e-mail: montavon@subatech.in2p3.fr

INTRODUCTION

In the context of the management of contaminated sites or waste disposal sites, it is essential to assess the reactivity/mobility/ (bio)availability of the elements of interest in the environment and their potential effects. A significant number of work has shown that the reactivity / mobility / (bio)availability of retained elements in soil/sediment is directly related to the labile fraction (e.g. [1]).

As this term is not clearly defined by IUPAC, we specify its meaning in the context we are interested in (which is generally found in the literature), namely that it is the reactive fraction retained by the soil/sediment in rapid equilibrium with the dissolved fraction (and more generally the free fraction). From a more mechanistic point of view, it depends on retention mechanism leading to the interaction between the element and the soil/sediment, which is directly related to the chemical form (or speciation) of the element.

Given the heterogeneity of natural systems, the difficulty of reproducing natural conditions in the laboratory, the presence of metals at the trace level which generally does not allow the use of spectroscopic tools to directly characterize the species, and the existence of several mechanisms that can lead to retention, the characterization of this labile fraction, and the link with speciation, is a real challenge and remains a growing field of research.

DESCRIPTION OF THE WORK

The issue of lability has been widely addressed at Subatech since 2000, with a particular interest in colloidal Organic Matter (OM), free or adsorbed on mineral surfaces, and clay materials.

This work is carried out in connection with the management of radioactive waste, the problem of NOR (Naturally-Occuring Radionuclides) and the question of the impact of anthropogenic radionuclides release into the environment. In this presentation, the main results obtained will be presented.

RESULTS AND DISCUSSION

THE CASE OF ORGANICALLY BOUND TRITRIUM (OBT). An important action focuses on the issue of OBT and the labile nature of the interactions (Exchangeable/Non-Exchangeable, E/NE). A novel isotope exchange method is proposed to quantify OBT-E/NE in solid matrices of interest; the exchange is carried out in a solid-gas system under well-controlled conditions (tritium content, temperature, humidity...) [2,3]. It has been shown that the exchangeability/lability is not only related to the nature of the bond, i.e. covalent and iono-covalent bonds are related to inert and labile fraction, respectively. In fact, there is a "non-labile" fraction that does not depend on the type of bonding, but is associated with the complex three-dimensional arrangement of certain components (case of proteins, cellulose) [4], i.e. the so-called buried fraction. This result was validated using model systems based on cellulose: the greater the degree of crystallinity, the more effective the arrangement of molecules in three dimensions, and the greater the quantity of buried tritrium. In particular, a linear relationship is proposed between the degree of crystallinity and the proportion of non-exchangeable tritium [5]. To our knowledge, this is the first correlation that would allow to trace back to quantitative values for the buried fraction, at least for matrices rich in cellulose.

METALS AND COLLOIDAL ORGANIC MATTER. The formation of inert complexes between metals and natural colloidal organic matter is also a subject of interest. This aspect was evaluated by studying simplified model systems (γ-alumina (in colloidal form), synthetic PolyCarboxylic Acids (PCAs) and trivalent M(III) elements (M=Eu, Cm, Gd)). PCAs are not strictly speaking models of OM and more specifically of humic substances. On the other hand, the study of simplified model systems can lead to a better understanding of ternary systems; the main result is that the behaviour of PAC towards M(III) is not the same depending on whether the polyelectrolye is free in solution or adsorbed [6-9]. While the M(III)-PCA interaction leads to labile complexes, inert complexes are formed over time when M(III) reacts with the adsorbed PCA. The difference in behaviour is not related to a difference in local environment (i.e. the first coordination sphere), but is

related to the difference in "structure" of PCA. At the surface of the solid, the polyelectrolytes are no longer isolated and aggregate to form an organic layer in which the metal is less "available" (slow equilibration kinetics). This brings us back to a question of accessibility, as in the case of buried tritium. Note that the method used to characterise the OBT-NE fraction has also been used to characterise a reserve of 'exchangeable' protons in humic substances that cannot be identified by the usual titration methods [10]; this result opens up new research perspectives.

The question of the lability of metals with natural organic matter is currently being studied within the framework of the ZATU ("zone Atelier Territoires Uranifères") in a wetland contaminated with U as a result of mining activities [11]. First profiles carried out in the soil by coupling DGT (Diffusive Gradients in Thin films) and DET (Diffusive equilibrium in Thin films) sensors have been obtained and indicate a difference in lability of U depending on the depth and the type of environment; the labile nature of the interaction is particularly limited in the area rich in organic matter [12].

CHARACTERIZATION OF THE LABILE FRACTION OF METALS IN INTERACTION WITH CLAY MATERIALS. If we come back to the labile fraction in soil/sediment, beyond the species identification, it is crucial to have operational methods to characterize it, i.e. to evaluate the coefficient that characterizes the distribution of the element between the two compartments (the Kd value), the content of the labile part in relation to the total quantity of the element present or even the kinetic parameters that characterize the re-supply of the element from the soil/sediment to the pore water.

In a recent work, a new and simple approach has been proposed; it is based on the desorption of the elements of interest as a function of the solid-liquid ratio under conditions representative of the *in-situ* conditions. As for the isotope exchange method, (i) time is the key parameter to discriminate between labile and non-labile fractions and (ii) modelling of the data allows to obtain two key parameters, the amount of labile species and the Kd value. The method was successfully tested for Ni naturally present in samples of Callovo-Oxfordian (COx) clay, the formation envisaged in France for deep radioactive waste disposal [13]. The results appeared to be consistent with those deduced from isotope exchange experiments. After comparing the results with sorption models developed in this context, this labile fraction, which represents only a small part of the total quantity of naturally-occurring Ni, could be associated with the proportion of Ni adsorbed on the surface of the COx clay fraction. The method is currently being extended to other naturally occurring trace elements in COx (I, Cs, Rb, Co, Fe, Sr, Cu, Mn, Ba, Zn, Sr, Eu and Th) to assess the relevance of such a method in a more general way.

REFERENCES

1. A.L. Nolan et al., "Metal Bioacculation and Toxicity in Soils-Why Bother with Speciation?" *Aust. J. Chem.,* **56**, 77-91 (2003).
2. O. Péron et al. "Towards speciation of organically bound tritium and deuterium: quantification of non-exchangeable form in carbohydrate molecules" *Chemosphere* **196**, 120-128 (2018)
3. A-L. Nivesse et al. "Non-intrusive and reliable speciation of organically bound tritium in environmental matrice" *Talanta*, **224**, 121803 (2021).
4. A-L. Nivesse et al "Cellulose, proteins, starch and simple carbohydrates molecules control the hydrogen exchange capacity of bio-indicators and foodstuffs" *Chemosphere*, **269** 128676 (2021)
5. A-L. Nivesse, N. Baglan, G. Montavon, O. Peron. "New insights into the accessibility of native cellulose to environmental contaminants toward tritium behavior prediction" *Journal of Hazardous Materials* **420**, 126619 (2021).
6. G. Montavon &B. Grambow "Study of the reversibility of the interaction between Eu and polyacrylic acids" *New J. Ch*em., **27**, 1344 (2003)
7. G. Montavon et al. "Interaction of Eu(III)/Cm(III) with alumina-bound poly(acrylic acid): sorption, desorption and spectroscopic studies" *Environ. Sci. Technol.* **38**, 4312 (2004).
8. G. Montavon et al. "Modeling the complexation properties of mineral-bound organic polyelectrolyte; An attempt of comprehension using the model system Alumina/Polyacrylic Acid/M (M=Eu, Cm,Gd)" *J. Coll. Inter. Sci.*, **305,** 32 (2007)
9. G. Montavon et al "Comparison of complexed species of Eu in Alumina-bound and free Polyacrylic Acid. A spectroscopic study" *J. Coll. Inter. Sci.*, **300,** 482 (2006)
10. A.-L. Nivresse et al. "An overlooked pool of hydrogen stored in humic matter revealed by isotopic exchange: implication for radioactive 3H contamination" *Environ. Chem. Lett*., **18**, 475-481 (2020)
11. A. Martin et al. "An integrated approach combining soil profile, records and tree ring analysis to identify the origin of environmental contamination in a former uranium mine (Rophin, France)" *Sci. Total Environ*., **747**, 141295 (2020)
12. A. Martin "A combined DGT - DET approach for an *in situ* investigation of uranium resupply from large soil profiles in a wetland impacted by former mining activities" *Chemosphere*, **279**, 130526 (2021)
13. G. Montavon et al. "Ni sorption on Callovo-Oxfordian clay rock (France) ; transferability from model system to *in-situ* conditions" *Environ. Sci. Technol.*, **54**, 12226–12234 (2020)

A lab-on-a-chip approach for resolving controversies on crystallization processes in porous media

Jenna Poonoosamy[1], Nikolaos Prasianakis[2], Enzo Curti [2], Mohamed Mahrous[2], Guido Deissmann[1], Sergey Churakov[2], Dirk Bosbach[1]

[1]*Institute of Energy and Climate Research (IEK-6): Nuclear Waste Management and Reactor Safety, Forschungszentrum Jülich GmbH, 52425 Jülich, Germany*
[2]*Laboratory for Waste Management, Paul Scherrer Institut, CH-5232 Villigen PSI, Switzerland*
email: j.poonoosamy@fz-juelich.de

INTRODUCTION

The precipitation of minerals in porous media is an important process governing the evolution of many subsurface systems, leading to an alteration of permeability and other physical characteristics of the rock matrix that can have significant effects on subsurface solute and gas transport [1, 2]. Crystallization processes in porous media can lead to phenomena that are rarely observed in batch experiments like (i) oscillatory zoning, or (ii) pore-size dependency on nucleation. Here, we developed a "lab-on-a-chip" approach [3-5] (i.e., micronized experiments combined with *in-situ* Raman spectroscopy and imaging) complemented by reactive transport modelling to unravel and resolve current controversies on these processes. Specifically, we addressed the following questions:

(i) Is oscillatory zoning controlled by the limited diffusion of solutes or by crystallization kinetics?
(ii) Is nucleation pore-size dependent?

DESCRIPTION OF THE WORK

The micromodel to address the formation of oscillatory zoned crystals of (Ba,Sr)SO_4 consisted of two parallel supply channels interconnected by microfluidic reaction chambers. A Na_2SO_4 solution and a mixed solution of $BaCl_2$ and $SrCl_2$ were injected into the supply channels and the co-precipitation of (Ba,Sr)SO_4 was fostered by the counter-diffusion of solutes in the microfluidic reaction chamber. The compositions of the solid solutions were determined by *in situ* Raman spectroscopy. We used reactive transport modelling with newly implemented theoretical approaches such as the supersaturation function and classical nucleation theory (CNT) extended to solid solutions to (i) predict the composition of the nucleating phases, and (ii) determine the driving forces for the oscillatory zoning.

To unravel the pore size-dependency on nucleation, we designed a micromodel consisting of a pore network with circular pores of various diameters and heights interlinked by capillaries with a cross-sectional area of 1 μm^2. The nucleation of $BaSO_4$ was triggered and monitored.

RESULTS AND DISCUSSION

OSCILLATORY ZONED CRYSTALS OF (Ba,Sr)SO_4: Our investigations showed that the composition of the nucleating phases (Fig. 1) can be approximated by using CNT, and that the oscillatory zoning results from a combination of limited diffusional transport of solutes and kinetically controlled precipitation reactions.

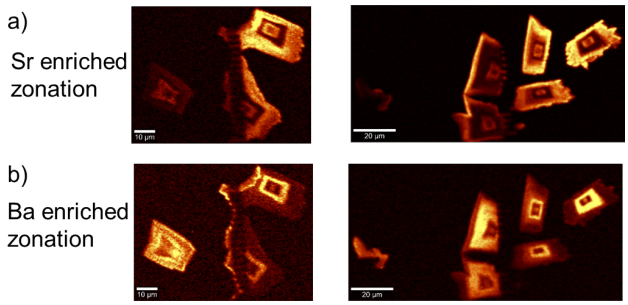

Fig. 1: Raman images of zoned crystal of a) Sr enriched and b) Ba enriched (Ba,Sr)SO_4 solid solutions.

PORE SIZE-DEPENDENCY ON NUCLEATION:
A preferential localization of $BaSO_4$ precipitates and a shorter induction time were observed in the larger pores (Fig. 2). However, the dynamics of nucleation were comparatively accelerated in the 1 μm^2 capillaries. Currently we (i) investigate the nature (amorphous versus crystalline) of the precipitates in the pore network and (ii) explore the theoretical approaches that can explain these phenomena.

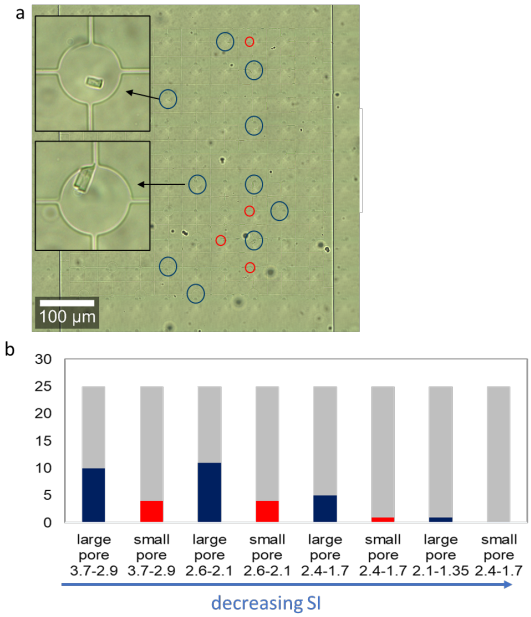

Fig. 2: a) Optical microscopy image of the pore network after barite precipitation, and b) histograms indicating preferential barite precipitation in larger pores than in smaller pores.

ACKNOWLEDGEMENTS

The research leading to these results has received funding from the German Federal Ministry of Education and Research (BMBF, grant agreement 02NUK053A) and from the Initiative and Networking Fund of the Helmholtz Association (HGF grant SO-093) within the iCross project.

REFERENCES

1. XIE et al., "Implementation and evaluation of permeability-porosity and tortuosity-porosity relationships linked to mineral dissolution-precipitation" *Computational Geosciences*, **19**, 655-671 (2015).
2. POONOOSAMY et al., "Benchmarking of reactive transport codes for 2D simulations with mineral dissolution/precipitation reactions and feedback on transport parameters" *Computational Geosciences*, **25**, 1337-1358 (2021).
3. POONOOSAMY et al., "A microfluidic experiment and pore scale modelling diagnostics for assessing mineral precipitation and dissolution in confined spaces", *Chemical Geology*, **528**, 119264 (2019)
4. POONOOSAMY et al., "Microfluidic flow-through reactor and 3D Raman imaging for in situ assessment of mineral reactivity in porous and fractured porous media", *Lab on a chip*, **20**, 2562-2571 (2020).
5. PRASIANAKIS et al., "Neural network based process coupling and parameter upscaling in reactive transport simulations", *Geochimica et Cosmochimica Acta*, **291**, Page 126-143 (2020).

Supersolubility and cold boiling in nano-/millimetric dual porous media subject to capillarity

Lionel Mercury

Institut des Sciences de la Terre d'Orléans - UMR 7327 Université d'Orléans, CNRS, BRGM - Orléans (France).
email: lionel.mercury@univ-orleans.fr

INTRODUCTION

The clay formations targeted for nuclear wastes repositories (Belgium, France, Switzerland) hold a mineralogical variability, described as a composite of clay matrix and detritic grain inclusions (e.g., [1]). This assemblage generates a microstructural heterogeneity yielding to a microscale variability of the geomechanical rock properties (e.g., [2]). Additionally, in the area around the drifts, excavation induces the formation of fractures, thus adding to the complexity of the pore network structure. Clay matrix, matrix-inclusions assemblages, fractures apertures, exhibit pore size from 2 nm up to hundreds of µm [3]. As a rough approximation, argillaceous formations can thus be viewed as strongly contrasted dual (nm-mm)-porosity media.

The porosity of the clay formations is initially water-saturated and at geo/hydro-mechanical equilibrium. During excavation and operating period, air ventilation is responsible for pore water evaporation that propagates radially from the tunnel, and that promotes chemical reactions because of the contrasted conditions in the atmosphere and in the clay formation. Fields studies of gas penetration (e.g., [2,4,5-6]) gave an estimate of the distance attainable by these gases. It was shown (1) that excavation-induced fracture walls were systematically related to geochemical reactions such as pyrite oxidation and calcite dissolution (e.g., [5]), and (2) that gases propagated preferentially along fractures, involving a limited volume of water and reacting materials along these main flow paths.

Long-term ventilation experiments were carried out at different sites (e.g., [7-8]) to estimate the water loss and how it affects the geochemical processes and the fluid transfer. It was demonstrated that the evaporation affected only the first 0.5 meters of the formation around the tunnels and results in a limited water loss (e.g., [4,9]). The geochemical impact on porosity, appeared surprisingly negligible at the scale of the studies (e.g., [6-7]). The propagation of the drying front was over-estimated by numerical modelling [8] despite account of the fracture network and of the permeability evolution and inhomogeneity, leading to the hypothesis of a strong influence of fracture closure mechanisms through self-sealing/healing processes [8].

The present work argues that a full account of the influence of capillary processes is missing in this conceptual scheme. We will show in the following how capillary processes may act to couple geochemical, hydrological and poromechanical processes, which can modify reactivity and transport properties.

At equilibrium, the Young-Laplace law rules the size of the liquid-vapor meniscus (pore size control), and the Kelvin law drives the liquid-vapor equilibrium (air RH control). Internal pressure of the capillary liquid modifies the chemical potential of water and of aqueous components, and so changes gas and solid solubilities [10-11], and exerts an additional stress to the matrix because of the formation of negative pore pressure (pore tension) [12]. Additionally, the aqueous solution becomes metastable when confined in a pore space larger than the capillary bridges, which is typically the case in fractures. Spontaneous boiling (or cavitation process) may occur in such macro-volumes after a certain lifetime (e.g., [13-14], making a dramatic change for hydraulic connectivity and gas pathways.

In the following, I present a simple experimental setup that made it possible to evidence these complex coupled behaviors. Then, I discuss the possible application of these results in the framework of geological repository settings in clay formations.

RESULTS AND DISCUSSION

We developed an experimental procedure to fabricate synthetic dual-media that are analogous to fissures-matrix assemblage while allowing direct observation of phase transitions. Cylindrical microtubes were filled with a saline solution that evaporates in drying conditions. The solution became supersaturated and formed small crystal plugs almost clogging the tube at its two extremities, trapping a large volume of water behind (Fig. 1). Around these plugs, annular nanometric openings remain wherein capillary bridges take place. In the large volume behind, capillary water is metastable.

First, during its lifetime, capillarity can modify significantly the Gibbs free energy of the capillary-bearing phase, and so modify the reactive properties and chemical driving forces in the whole tube (e.g., [10-16]). Using sodium sulphate and sodium chloride salts, we observed a *circa* 30% decrease of the solid volume over 3 months, due to supersolubility ranging from 110% to 130%, related to 30-93 MPa capillary pressure range.

Second, a capillary liquid exerts a direct geomechanical tension on the pore walls through its

negative pore pressure (e.g., [12-14]). Therefore, the poromechanical stress field changes simultaneously along with the capillary bridging. Subsequently, the micro-cracks network is re-organized and the flowlines are re-distributed which impacts the advection/diffusion flow regimes. With the same setup, we observed that the salt plugs were able to slide along the tube with a max displacement reaching 3.5 mm (7-8 times the plug size) over 7 days. Cracks were also observed in the plugs during the experiment.

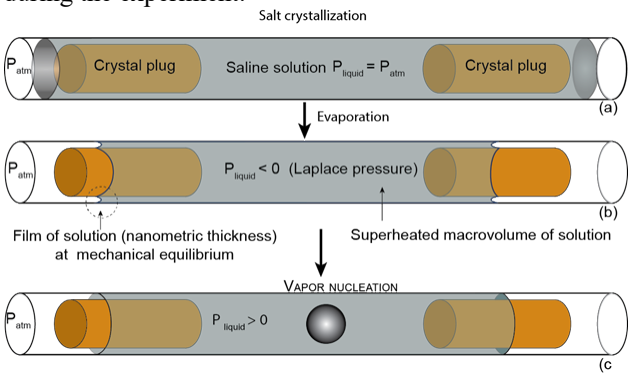

Fig. 1: a. Evaporation-driven salt growth keeping open a thin nanometric film between the crystal and the glass wall. b. RH-controlled capillarity preventing evaporation and generating negative pressure in the entire trapped solution including the macrovolume. c. Relaxation of the tensile state after an induction time inside the trapped macrovolume. From [13].

Third, the lifetime of our experiments (more than 50) varied from 2 days to 24 months, systematically coming to an end by generating bubbles in the large pore bodies. Due to that boiling, we expect that all these processes should be limited to the first weeks after excavation. However, we observed that the capillary state was regenerated by external RH variations [14], most probably by osmotic flow [17]. It means that capillarity is potentially a long-term player.

CONCLUSION AND PERSPECTIVE

During ventilation, a tunnel is at constant RH. Therefore, it exists in the contacting aquifer a pore size threshold fixed by capillarity laws that prevents water from evaporating, keeping the porous network saturated. A negative pore pressure, i.e. a tension or a tensile strength, occurs whenever aqueous solution is trapped in pores smaller than 1.5 µm contacting air at relative humidity (RH) lower than 99.93% RH. Capillary bridges hosted by 2 nm clay (slit-like) pores can reach -113 MPa (at equilibrium with 42 % RH air), while 90 nm pores can host -15 MPa capillary bridges (stable for 98.8% RH contacting air).

The liquid-air interfacial capillary front in the argillite will propagate around a ventilated tunnel until stopped by the not-evaporating capillary frontier. The 3D shape of the front across the aquifer is therefore controlled by the connectivity of water-bearing bridges percolating between adequately-sized pore spaces. Ventilation experiments showed that unsaturated conditions propagate to a 0.5 m distance to the tunnel walls. Behind this capillary front, the whole formation remained saturated irrespective of the pore size variation throughout the formation. In this situation, the capillary pressure was equal to that of the capillary bridges corrected from gravity and osmotic contributions.

Eventually, the practical aspect of our findings is that tiny capillary bridges localized close to a tunnel subject to ventilation, determines the capillary tension in the whole formation behind. The tensile wave propagates freely in the hydraulically connected formation, giving birth to new properties everywhere. These observations constitute a proof-of-concept that capillarity-driven mechanisms do play a role in clay formations in terms of pressure gradient, assessment of the liquid-vapor distribution, water-rock-gas interactions, gas migration/generation, and poromechanical behaviors. The intricacy between the driving forces and the induction time of the different processes remain a challenge to overcome for modelling these complex phenomena on the long term.

REFERENCES

[1] ARMAND G. et al. *Computers & Geotechnics* **85**, 277–286 (2017).
[2] MARSCHALL P. et al. *Oil & Gas Sci. Technol.* **60**(1), 121-139 (2005).
[3] SONG Y. et al. *Marine Petrol. Geol.* **65**, 63-82 (2015).
[4] VINSOT A. et al. *Procedia Earth Planet. Sci.* **7**, 871-874 (2013).
[5] VINSOT A. et al. Geological Society of London, Special Publications **400,** 207-220 (2014).
[6] VINSOT A. et al. *Procedia Earth Planet. Sci.* **17**, 562-565 (2017).
[7] ZHENG L. et al. *Phys. Chem. Earth* **33**, S186-S195 (2008).
[8] PARDOEN B. et al. *Int. J. Rock Mech. Mining Sci.* **85**, 192–208 (2016).
[9] ZHANG et al. *Phys. Chem. Earth* **65**, 79–89 (2013).
[10] MERCURY L., TARDY Y. *Geochim. Cosmochim. Acta* **65**, 3391-3408 (2001).
[11] MERCURY L. et al. *Geochim. Cosmochim. Acta* **67**, 1769-1785 (2003).
[12] MERCURY L. et al. *ACS Earth Space Chem* **5**, 170-185 (2021).
[13] HULIN C., MERCURY L. *Geochim. Cosmochim. Acta* **252**, 144-158 (2019a).
[14] HULIN C., MERCURY L. *Geochim. Cosmochim. Acta* **265**, 279-291 (2019b).
[15] LASSIN A. et al. *Geochim. Cosmochim. Acta* **186**, 91-104 (2016).
[16] LIDON P. et al. *Langmuir* **34**, 12017-12024 (2018).
[17] VINCENT O. et al. *Langmuir* **35**, 2934−2947 (2019).

Kinetic study of ^{233}U(VI) and ^{99}Tc(VII) retention in nontronite: role of accessory Fe

Ursula Alonso, Miguel García-Gutiérrez, Cynthia Rieckhof, Tiziana Missana

[1]*CIEMAT, Physical Chemistry of Actinides and Fission Products Unit*
Avenida Complutense 40, 28040 Madrid (Spain)
email: ursula.alonso@ciemat.es

INTRODUCTION

Smectite-rich clays are widely used to prevent contaminant transport because different mechanisms favour their retention. Amongst other retention processes, it is considered that the natural presence of specific elements, such as Fe, can affect the retention of redox sensitive contaminants as uranium or technetium [1].

This study analysed the sorption of ^{233}U(VI) and ^{99}Tc(VII) on a Fe-rich smectite (nontronite), under anoxic conditions, considering the presence of different Fe sources: (1) Structural Fe naturally present in the clay; (2) Fe(0) and Fe(II/III)-oxides as accessory minerals; (3) Dissolved Fe^{2+} /Fe^{3+}.

DESCRIPTION OF THE WORK

Nontronite NAu-1, an Fe-rich bentonite from Uley Mine (Australia) was purchased in the Clay Minerals Society (www.clays.org). The clay was characterised in detail by different techniques (XRD, FT-IR, potentiometric titration, CEC,…) to characterise the clay surface and to quantify the structural and accessory Fe, present in the system. The accessory Fe was less than 2%, the BET-N_2 was 57.8 m^2/g and the CEC 90 meq/100 g.

Batch sorption experiments were carried out in NAu-1 suspensions in $NaClO_4$ (10 g/L) with ^{233}U or ^{99}Tc, as a function of time, pH, ionic strength and varying tracer concentration.

To elucidate the role of accessory Fe and to evaluate possible kinetic effects on U(VI) or Tc(VII) retention, complementary sorption tests were performed in NAu-1 suspended in $NaClO_4$ 0.1 M at pH 8, including the presence of 5% in weight of different Fe sources: commercial metallic Fe(0) (MERCK), commercial hematite (Fe_2O_3) form Sigma Aldrich and laboratory synthetized magnetite (Fe_3O_4). All Fe-phases were characterised. For sorption experiments, contact times varied from 7 up to 200 days. The pH and Eh of samples was periodically measured.

Non-electrostatic models (NEM) were proposed to describe sorption in the systems.

RESULTS AND DISCUSSION

The sorption of U(VI) and Tc(VII) in raw NAu-1was analysed at short equilibrium times (1 week). Sorption of U(VI) was pH dependent, revealing cation exchange and surface complexation as the main U retention mechanism. The maximum sorption is reached at pH 7, with a maximum distribution coefficient of logKd (mL/g) = 4.2 ± 0.2. The retention of U(VI) by cation exchange mechanisms was limited and the competition of dissolved Fe^{2+} and Fe^{3+} was found to be minimal. ^{99}Tc sorption in NAu-1 was negligible under studied conditions.

The role of accessory Fe on ^{233}U and ^{99}Tc retention was analysed in different NAu-1/Fe mixtures. Fig. 1 shows the time evolution of ^{233}U distribution coefficients in the different NAu-1/Fe mixtures and Fig. 2 shows ^{99}Tc distribution coefficients measured in NAu-1 with Fe(0).

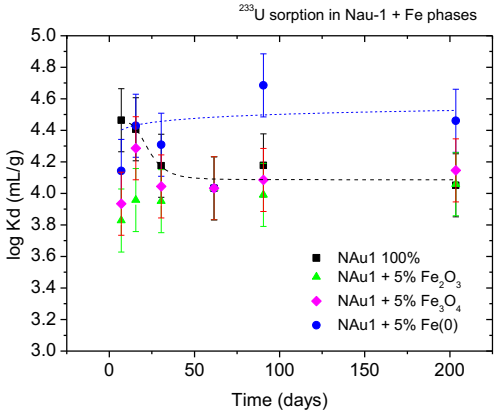

Fig. 1: U(VI) sorption on NAu-1 in presence of different Fe phases, measured under anoxic conditions as a function of time.

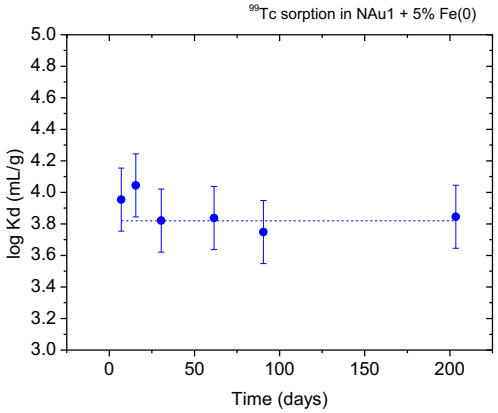

Fig. 2: Tc(VII) sorption on NAu-1 in presence of metallic Fe(0), measured under anoxic conditions as a function of time.

The sorption of U in raw NAu-1 slightly decreased with time, attributed to some kinetic effect of the structural Fe of the clay itself. In the presence of hematite an Fe(III) oxide, no redox change effect expected and U sorption slightly decreased with respect to that of raw bentonite. Both in the presence of magnetite (Fe^{2+}- oxide) and metallic Fe, the Eh of the system was appreciably reduced, but only in presence of Fe(0) the sorption of U was improved with time (Fig. 1).

Tc sorption was negligible in raw NAu-1, and in the mixtures with hematite. With magnetite, only after 200 days a logKd mL/g of 0.8 was measured. In the mixture with metallic Fe(0) Tc sorption was significantly improved **(**Fig. 2) and average sorption values of logKd mL/g = 3.8 ± 0.2 were measured.

The results contribute to weigh the different role played by Fe, as a structural cation or as an accessory oxide, in the immobilization of U(VI) and Tc(VII) in clays.

ACKNOWLEDGMENT

This study has received funding from the European Union`s Horizon 2020 research and innovation programme under grant agreement 847593 (FUTURE-EURAD) and by the Spanish Ministry of Innovation and Science (PID2019-106398GB-I00, ARNO Project).

REFERENCES

1. MA et al., “A review of the retention mechanisms of redox-sensitive radionuclides in multi-barrier systems”. *Applied Geochemistry* **100**, 414-431 (2019).

Influence of surface roughness on the sorption of Cm(III)

M. Demnitz[1], S. Schymura[2], J. Neumann[1], K. Müller[1], M. Schmidt[1]

[1]*Helmholtz-Zentrum Dresden-Rossendorf e.V., Institute of Resource Ecology, Bautzner Landstraße 400, 01328 Dresden, Germany*
[2]*Helmholtz-Zentrum Dresden-Rossendorf e.V., Institute of Resource Ecology, Research Site Leipzig, Permoser Str. 15, 04318 Leipzig, Germany*
email: m.demnitz@hzdr.de

INTRODUCTION

Many countries will use deep geological repositories to dispose of their highly radioactive nuclear waste. With an international perspective, crystalline rock is a potential host rock because of its strong geotechnical stability, low permeability and low solubility. However, its inherent mineralogy is heterogeneous, consisting of a wide set of minerals in varying amounts. Therefore, there is a need for using sophisticated techniques that allow to characterize the nanostructure of such crystalline rock surfaces with spatial resolution and the molecular speciation of the actinides thereon. As a representative for trivalent actinides, such as Am(III), Np(III), and Pu(III), which are expected to be present due to the reducing conditions encountered in a deep geological repository, we have chosen the actinide Cm(III). It possesses excellent luminescence properties, allowing us to determine sorption uptake and molecular speciation of Cm(III) on the surface.

DESCRIPTION OF THE WORK

Investigations focused on cleaved orthoclase (K-feldspar) single crystals as well as different crystalline rocks stemming from various regions in Europe. Cleaved pieces of orthoclase or thin sections of the crystalline rocks were immersed in a sorption solution containing $[Cm(III)] = 5 \cdot 10^{-7} - 10^{-5}$ M. The experiments were undertaken at selected pH values (5.0 and 6.9) and different inherent mineralogical complexity of the systems. Subsequently, we applied correlated spectroscopy to analyze the samples. We combined vertical scanning interferometry, calibrated autoradiography, and Raman microscopy coupled to µTRLFS. Thus, we were able to correlate mineralogy, topography, and grain boundary effects with radionuclide speciation, allowing us to identify important radionuclide retention processes and parameters. For experimental details, see [1].

RESULTS AND DISCUSSION

We observed that Cm(III) sorption uptake and speciation depends not only on the mineral phase, but also the surface roughness. Already on single crystal orthoclase an increasing surface roughness leads to higher sorption uptake (see Fig. 1) and to a stronger coordination of the sorbed Cm(III).

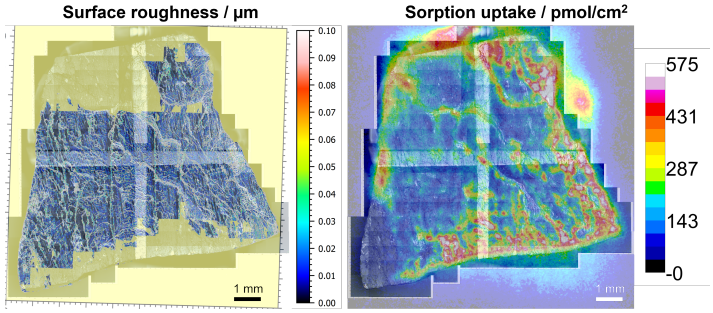

Fig. 1: Cm(III) sorption on an orthoclase single crystal at pH 6.9 comparing (left) surface roughness as determined by interferometry with (right) Cm(III) sorption uptake as determined by calibrated autoradiography.

Increasing the mineral complexity of the system further, we used thin sections of various crystalline rocks, consisting mainly of feldspar, quartz, and mica. We observed significant differences in sorption uptake on individual mineral phases as well as the resulting speciation. In case that one mineral phase dominates the sorption process, e.g. amphibole, sorption of Cm(III) on other mineral phases will only occur at strong binding sites, typically where surface roughness is high. Areas of feldspar and quartz with high surface roughness additionally showed the formation of sorption species with particularly high sorption strength that could either be interpreted as Cm(III) incorporation species or adsorbed ternary complexes on the mineral surface.[2]

At pH values of around 6.8 Cm(III) generally sorbs more weakly to the surface, while preferentially targeting mineral phases such as mica instead of feldspar or quartz. At a higher pH of 8.0 the sorption uptake on other mineral

phases increases, with a general trend towards more strongly bound Cm(III) surface species.

We conclude that in addition to mineral composition, surface roughness needs to be considered adequately by reactive transport models to describe interfacial speciation of contaminants and respective retention patterns for the safety assessments of nuclear waste repositories.

ACKNOWLEDGEMENTS

This work has been developed in the frame of the iCross project. We gratefully acknowledge funding provided by the German Federal Ministry of Education and Research (BMBF, Grant 02NUK053) and the Helmholtz Association (Grant SO-093).

REFERENCES

1. MOLODTSOV et al., "Sorption of Eu(III) on Eibenstock granite studied by µTRLFS: A novel spatially-resolved luminescence-spectroscopic technique" *Scientific Reports,* **9**, 6287 (2019).
2. DEMNITZ et al., "Effects of surface roughness and mineralogy on the sorption of Cm(III) on crystalline rock" *Journal of Hazardous Materials*, **423**, Part A, 127006 (2022).

Surface reactivity parameterization for the simulation of mineral dissolution in pore-scale reactive transport models

Jonas Schabernack, Cornelius Fischer

Department of Reactive Transport, Institute of Resource Ecology, Helmholtz-Zentrum Dresden-Rossendorf, Germany
email: j.schabernack@hzdr.de

INTRODUCTION

The dissolution of crystalline material and the kinetics involved play an important role in many environmental and technical processes, e.g., corrosion, weathering, or host rock characterization for nuclear waste repositories. Mineral dissolution in geological systems is governed by two key parameters: transport and surface reactivity.

Transport of dissolved species in the fluid controls the concentration gradient in the solution and thus the equilibrium conditions at the mineral-fluid interface. High flow velocities and undersaturated fluids lead to far from equilibrium conditions resulting in dissolution rates predominantly controlled by crystal surface reactivity.

Crystal surface reactivity is a material intrinsic property and is heterogeneously distributed over crystal surfaces (1). The distribution of surface reactivity is determined by the distribution of highly reactive atomic surface sites (kink sites) that are highly concentrated at nanotopographical surface structures (etch pits, steps).

In pore-scale reactive transport modeling, mineral dissolution is typically described via rate equations that are based on data from bulk or powder dissolution experiments (2). These rate equations solely include species concentrations in the fluid as variables to compute the local dissolution rates at the interface. Thus, a description of surface reactivity and its influence on the calculated dissolution rates is neglected in the current modeling approach. Recently it has been shown that this exclusion of surface reactivity in reactive transport models can lead to results strongly differing from experimental dissolution rates (2).

DESCRIPTION OF THE WORK

In this work we apply the current reactive transport modeling approach with different transport conditions on an experimentally measured calcite single crystal surface (1). The simulated dissolution rates from 2D and 3D models are then compared to experimentally derived rates and their consistency is tested.

To parameterize surface reactivity in the reactive transport model we follow a recent approach using the surface slope distribution as a proxy parameter (3). The surface slope identifies surface portions showing specific height changes. Contrasting concentrations of surface steps showing specific densities of highly reactive surface sites can be identified using the surface slope data (Fig. 1). We improve the current proxy calculation towards parameterization of 3D rock datasets, e.g., derived from high resolution computer tomography. Additionally, we discuss the normalization of the slope parameter depending on the experimental rate spectra of the specific mineral.

RESULTS AND DISCUSSION

Our results show that the current reactive transport model is not able reproduce the experimental dissolution rate maps over a wide range of transport conditions, which is similar to the results by (2). The surface topography of the single crystal calcite surface has negligible influence on the hydrodynamics and consequently the transport conditions in the system.

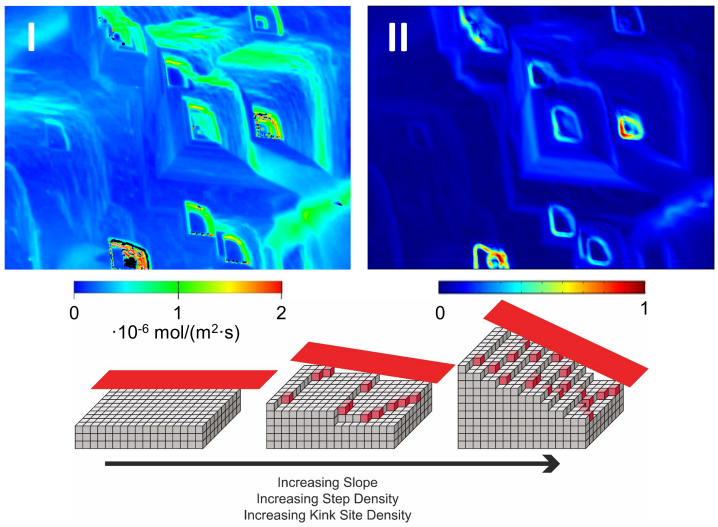

Fig. 1: Comparison of the experimental dissolution rate distribution (I) and the calculated surface slope distribution (II) on a reacting calcite single crystal surface. The field of view in both images is 414 x 313 µm^2. The comparison shows a good fit between dissolution rate and slope. Lower part: Sheme of the distribution of highly reactive surface sites (red cubes) as a function of surface slope (red planes).

As a result, we conclude that it is critical to include surface reactivity in the calculation of dissolution rates in

reactive transport models. The surface slope as a proxy parameter shows a good fit with the experimental dissolution rate maps indicating the reactivity distribution. This new parameterization results in improved predictive capabilities of the model and can be applied to a wide range of systems.

REFERENCES

1. BIBI I et al., "Temporal Evolution of Calcite Surface Dissolution Kinetics" *Minerals*, **8**, 256 (2018)
2. AGRAWAL P et al., "The contribution of hydrodynamic processes to calcite dissolution rates and rate spectra" *Geochimica et Cosmochimica Acta*, **307**, Page 338-350 (2021)
3. KARIMZADEH L et al., "Implementing Heterogeneous Crystal Surface Reactivity in Reactive Transport Simulations: The Example of Calcite Dissolution" *ACS Earth and Space Chemistry*, **5**, 2408-2418 (2021).

Radiobarite stability under cementitious condition

Tiziana Missana, Miguel García-Gutiérrez, Ursula Alonso

CIEMAT, Physical Chemistry of Actinides and Fission Products Unit – Department of Environment
Avenida Complutense 40, 28040 Madrid (Spain)
email: tiziana.missana@ciemat.es

INTRODUCTION

The coprecipitation of radium in barite ($BaSO_4$) can be an effective method to reduce the aqueous radium concentrations in low level long lived (LLLL) radioactive waste disposals. The objective of the present study is to synthetize and characterize a synthetic radiobarite (Ra, Ba)SO_4 and analyze its stability under the chemical conditions generated by cementitious materials.

DESCRIPTION OF THE WORK

Barite and radiobarite were prepared using high purity $BaCl_2$ and Na_2SO_4 salts. For the preparation of radiobarite, a ^{226}Ra-traced $BaCl_2$ was used, of known initial activity. A Ra/Ba relation of $2.9 \cdot 10^{-8}$ gr(Ra)/gr($BaSO_4$) was obtained, in agreement with the target ratio. The activity of ^{226}Ra was measured by liquid scintillation counting, after reaching the equilibrium with ^{222}Rn.

$BaCl_2$ solution was added dropwise to the $NaSO_4$ and, immediately, the solid precipitated. The suspension was stirred for one hour and then decanted overnight. The solid was filtered out (0.1 µm) and the supernatant analyzed (Na, Cl, Ba/Ra and SO_4^{2-}). Then the solid was washed in deionized water to eliminate salt residues. Six cycles of washing/ centrifuging (10 min 9000 rpm) were needed to obtain electrical conductivity lower than 10 $\mu S \cdot cm^{-1}$.

To perform stability tests, the solid (0.1-0.3 g) was suspended in different aqueous solutions (60 mL), which were periodically analyzed to check their chemical evolution. The effects of pH, ionic strength, calcium content (as possible competing ion) sulfate content (common ion effect) on Ra/Ba release from the solid were examined.

Additionally, synthetic waters respectively representative of fresh cement and cement degraded at the Stage II, were used to perform leaching experiments.
For each experimental condition, various samplings were carried out, at variable time from 30 days to 200 days.

RESULTS AND DISCUSSION

Fig. 1 shows a scanning electron microscopy (SEM) image of the solid synthetized for this study. The N_2-BET of this material was 5 m^2/g. In comparison to a commercial barite (Aldrich), with a BET of 2 m^2/g, the grain size was 10 times smaller, also indicating a lower crystallinity.

First, experiments were carried out with the barite (without Ra), which led to determine a mean solubility product (K_{sp}) of $7 \cdot 10^{-10}$ within a range of pH from 7 to 11.

Fig. 2 shows an example of the results obtained for the radiobarite in 0.1 M NaCl + NaOH, as a function of pH.

Measurements shows that Ra release from the solid is always lower than 1%. The minimum solubility is observed in the range of pH between 11 and 12.7, but a sharp increase just above pH 13 is observed.

Experiments as a function of the Ca concentration (from 0 to 0.01 M), indicated a small effect of the content of this cation on Ra release (which remained within a 0.6% maximum of the initial activity), whereas an increase of sulfates (from 0 to 0.01 M) inhibited the release of Ra.

The maximum release of Ra (approximately 1.4 %) was in fact observed for the Ra-barite suspended in the fresh CEM synthetic water.

In general, the combined increase of pH and ionic strength favored Ra release, minimizing Ra retention.

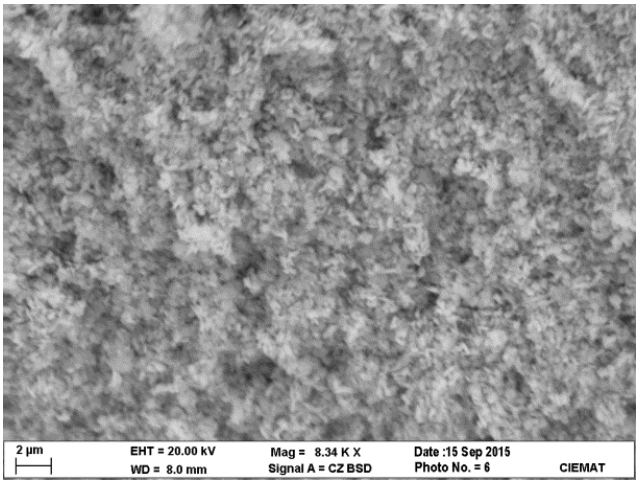

Fig. 1: SEM image of the barite synthetized for this study.

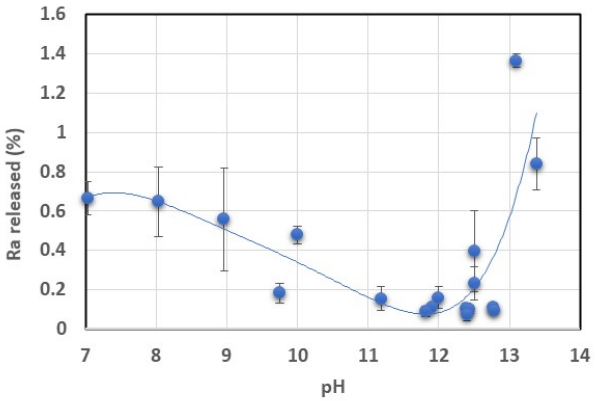

Fig. 2: Mean Ra released) as a function of pH in NaCl (0.1 M) +NaOH solutions. (% calculated from three different samplings upon 108, 147 and 170 days).

ACKNOWLEDMENTS

This study has received funding from the Europeans Union`s Horizon 2020 research and innovation programme under grant agreement 847593 (EURAD) and by the Spanish Ministry of Innovation and Science (PID2019-106398GB-I00, ARNO Project).

Corrosion of borosilicate glass under hydraulically saturated conditions

Kaifeng Wang[1,2], Zhentao Zhang[1]

[1]*Engineering Technology Center of Decommissioning and Remediation, China Institute of Atomic Energy, 102413 Beijing, China*
[2]*University of Grenoble Alpes and CNRS, ISTerre, BP 53, 38041 Grenoble Cedex 9, France*
e-mail: kaifeng.wang@univ-grenoble-alpes.fr

INTRODUCTION

High level nuclear waste to be deposited in deep geological setting will be previously vitrified. The chemical durability of such glasses is important for predicting the long-term radionuclide retention potential in geologic repositories [1]. Studies showed that glass corrosion undergoes a series of processes [2]. At first, a hydrated and cation-depleted altered surface forms on the surface of glass due to the diffusion and the selective cation exchange between H_3O^+ and alkali, alkaline metals and B. Then the hydrated silicic acid is released into solution and the relict silica begins to form a separate porous gel layer by hydrolysis and condensation reactions. As aqueous silica becomes saturated in solution, secondary phases such as phyllosilicates and zeolites may precipitate. In this study, we focuses on evaluating the corrosion kinetics of borosilicate glass and identifying the secondary crystalline phases during corrosion. Our finding will be provide fundamental data to assess the potential uncertainty for long-term glass dissolution, especially in the framework of the high level nuclear waste glasses.

DESCRIPTION OF THE WORK

The size of glass powder was 75-149 µm and the specific surface area was 0.07 m^2/g. The corrosion experiment was performed Milli-Q water (18.2 MΩ·cm) at 90 °C under hydraulically saturated conditions. After reaction for 3, 7, 20, 90, 180, 380, 540 and 760 days, 3.11 mL deionized water was added into the sample and let equilibrate for 2 hours at room temperature. The suspension was filtered by 0.22 µm nitrocellulose membrane. Total aqueous B, Si, Fe, Al, Mg, Na and Ca concentrations of filtrate were analyzed by ICP-OES. The solid was dried at 90 °C for 12 hours and then used for SEM and XRD analysis.

RESULTS AND DISCUSSION

CORROSION KINETICS. The concentrations of Si and B are shown in Figure 1. As we can see that the concentration significantly increased in the first 90 days and then slightly increased from 90 to 540 days. However, a decrease after 760 days reaction occurred, which may be caused by the formation of secondary phases. B was globally released at a rate of 3.4×10^{-6} g m^{-2} d^{-1} at the end of the experiment.

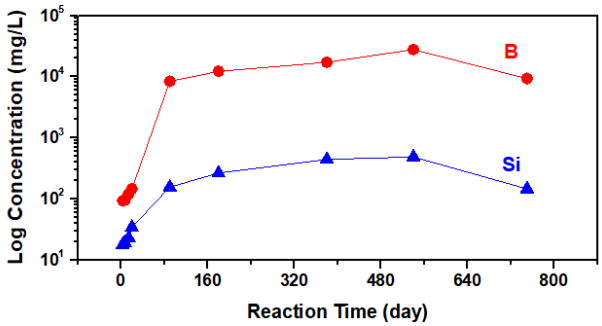

Fig. 1: Concentration of B and Si with reaction time.

SECONDARY PHASES IDENTIFICATION. Figure 2 shows the XRD result of glass samples after reaction for 540 and 760 days. The main secondary crystalline phases of the two samples were analcime and smectite, small amount of zeolite was also checked. The relative SEM images are shown in Figure 3. Smectite and analcime were observed for the two samples, which is in agreement with the XRD result. However, a nano-needle mineral precipitated after reaction for 540 days, which may be calcite. Furthermore, some nano- to micrometer sized crack morphology structure present on the glass surface was also observed by SEM (Figure 3).

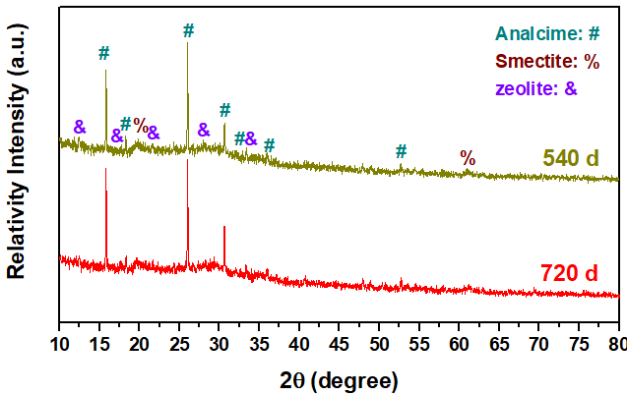

Fig. 2: Secondary phases identification by XRD

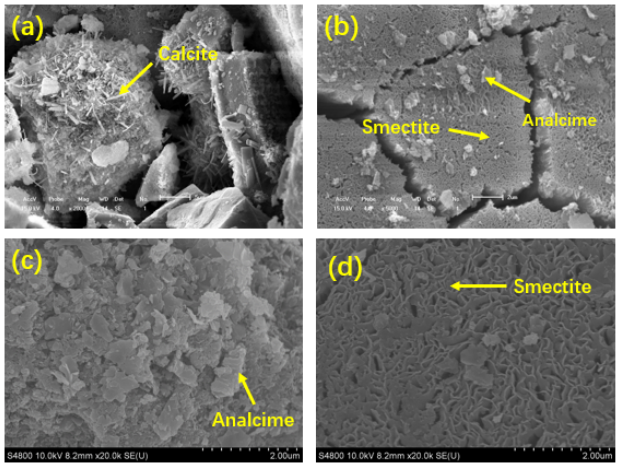

Fig. 3: SEM images of glass samples reaction for 540 days (a, b) and 760 days (c, d).

In conclusion, the corrosion rate of borosilicate glass was 3.4×10^{-6} g m^{-2} d^{-1} conformed by B concentration. Analcime and smectite were the main secondary crystalline phases formed after 760 days corrosion.

REFERENCES

1. GUITTONNEAU C. et al., "A 25-year laboratory experiment on French SON68 nuclear glass leached in a granitic environment – First investigations" *Journal of Nuclear Materials*. **408**, 73-89 (2011).
2. ROLAND H. et al., "Mechanisms of glass corrosion by aqueous solutions" *Encyclopedia of Glass Science, Technology, History, and Culture*, **I**, 647-662 (2021).

Hydrolytic degradation of the polyacrylonitrile-based UP2 ion exchange resin under cementitious conditions

Agost Tasi, Peter Szabo, Xavier Gaona, Marcus Altmaier, Horst Geckeis

Karlsruhe Institute of Technology, Institute for Nuclear Waste Disposal, Karlsruhe, Germany
email: agost.tasi@kit.edu

INTRODUCTION

The UP2 filter aid, mainly composed of polyacrylonitrile (PAN), is disposed of in high quantities along with low- and intermediate-level ion-exchange resins in underground repositories for radioactive waste, such as SFR1 in Sweden [1]. In the post-closure period, the developing reducing, alkaline conditions of the intruding ground water may lead to the generation of dissolved organic compounds due to the hydrolytic degradation of PAN. These ligands can have an impact on the mobility of radionuclides in the near field of a waste disposal facility, posing a potential risk in the aspects of long-term safety. Experimental observations on the degradation mechanism of PAN [2,3] indicate a significant uncertainty in the predictive calculations for radionuclide retention under relevant conditions. This work aims at resolving the existing controversy and setting the basis for investigations on the impact of the degradation products of UP2 on the solubility and sorption of selected radionuclides in cementitious systems under the conditions of interest.

DESCRIPTION OF THE WORK

All experiments were performed under Ar atmosphere. Long term degradations studies (up to 3 a) involving the original UP2 material with solid to liquid ratios (S:L) of ~50 g·dm^{-3} were conducted in various NaOH media (pH = constant = 12.5, where the pH was re-adjusted and with c(NaOH) = 0.10, 1.00 M) as well as in $Ca(OH)_2$-buffered solutions (pH = 12.5) at T = 25 and 80 °C in the absence and presence of Fe(0), respectively. All solutions were stored in polytetrafluoroethylene (PTFE) vials and continuous stirring was maintained throughout the study. Supernatant solutions were systematically monitored for pH, E_h and Ca total concentrations (via inductively coupled plasma – optical emission spectroscopy: ICP-OES). Leachates were further characterized by means of non-purgeable organic carbon content (NPOC) measurements and various spectroscopic (nuclear magnetic resonance: ^1H / ^{13}C NMR, Fourier-transform infrared: FT-IR, UV-visible light absorption spectroscopic techniques), as well as chromatographic analyses (size-exclusion - liquid chromatography - organic carbon/nitrogen detection technique: SEC-LC-OCD-OND, ion chromatography: IC). Degraded UP2 solid phases retrieved from the experiments were characterized by X-ray photoelectron spectroscopy (XPS), solid-state infrared spectroscopy (IR) and thermogravimetry - differential scanning calorimetry (TG-DSC).

RESULTS AND DISCUSSION

Degradation kinetics related to chain scission and the consequent release of dissolved organics at T = 80 °C and in $Ca(OH)_2$-buffered media were observed to be substantially slower than in Ca-free, NaOH systems. Figure 1 displays the evolution of NPOC values at the same pH of 12.5 for the two media at room temperature. Monitored E_h and $[Ca]_{tot}$ concentrations were constant till the equilibration time of ~1000 days. As for the pH condition, NaOH-degraded systems indicated a significant consumption of OH^- ions resulting in lowered pH values necessitating a rigorous re-adjustment of the pH for the sample at pH = constant = 12.5. The SEC-LC-OCD-OND characterization results of filtered degradation leachates at t = 1 a revealed average molecular weight distribution-ranges of ~1 – 3 kDa and ~10 – 40 kDa for the polymeric fragments leached in $Ca(OH)_2$-buffered and NaOH media, respectively.

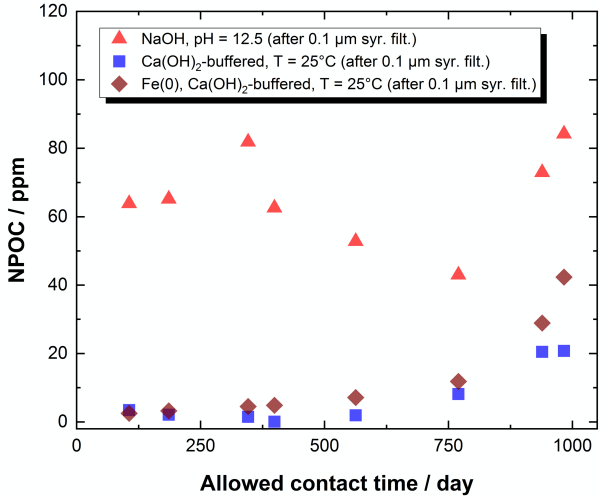

Fig. 1: NPOC values as a function of time determined in UP2 degradation experiments at pH = 12.5 and room temperature in NaOH media or in $Ca(OH)_2$-buffered solutions (with or without Fe(0)) as quantified after centrifugation and syringe filtration through 0.1 µm PTFE disk filters.

The 1D ^{1}H and ^{13}C NMR spectra of the degradation leachate in the 1.0 M NaOH experiment displayed signals in the chemical shift range corresponding to aliphatic and carboxylic acid functional groups. The heteronuclear ^{1}H – ^{13}C multiple-bond correlation NMR spectra of the 1.0 M NaOH leachate (Fig 2) revealed a single long-range coupling between one of the aliphatic proton signals with a carboxylic carbon NMR peak. This indicates that the generated fragments do carry identical structural traits to the original PAN polymer and the overall hydrolytic process in NaOH media can be understood as the nucleophilic attack of OH^- ions on the nitrile-groups coupled to the release of NH_3(g). An exemplary dissolved polymer fragment generated in NaOH media from PAN can be seen in Figure 2.

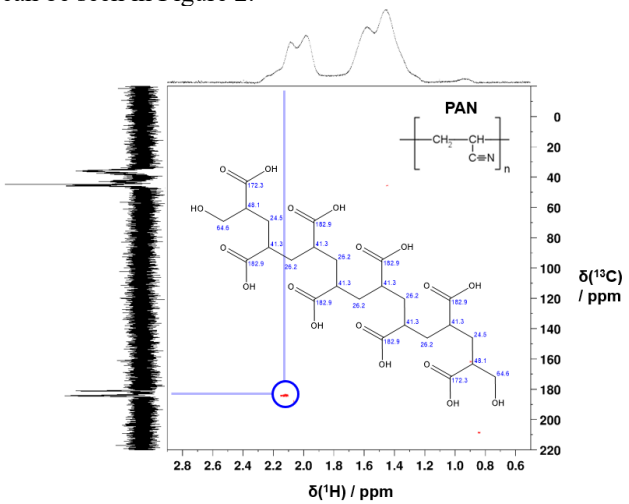

Fig. 2: Heteronuclear multiple-bond correlation 2D: ^{1}H - ^{13}C NMR spectrum of the degraded leachate after filtration (through 0.45 µm Teflon syringe filter) taken from the UP2 degradation experiment in 1.0 M NaOH (with 20% D_2O) after an allowed contact time of 2.5 a.

Solid state FT-IR and XPS spectra of the retrieved UP2 solid material collectively hint towards relevant differences in the hydrolytic degradation process for PAN in NaOH vs. $Ca(OH)_2$-buffered media. In contrast to the rather high dissolution rate owing to the sequential chain scission of the polymer in NaOH media, the $Ca(OH)_2$-buffered case indicated the full conversion of nitrile groups to carboxamide and/or carboxylate groups at an earlier stage. The latter process was driven presumably by the preferential complexation with the readily available Ca^{2+} ions from the solution, which, in turn, stabilized the intermediate resulting in a slower dissolution rate of the fiber mass.

In accordance with all experimental observations, 3 initial proxy ligands were assigned to simulate the chemical characteristics of the degradation products in both media.

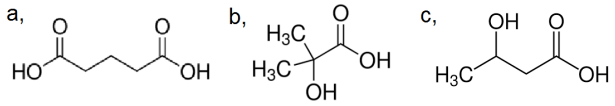

Fig. 3: Proxy ligands: (a) glutaric acid, (b) α-hydroxy-isobutyric acid, (c) 3-hydroxy-butyric acid.

Glutaric acid was chosen to represent the complexing capability of the bulk chain of the generated polymer fragments, whilst α-hydroxy-isobutyric acid and 3-hydroxy-isobutyric acids were selected with the aim to re-create the overall effect of the end groups.

Further characterization results gained within this study and comparison of the obtained findings with published data will be detailed in this contribution.

ACKNOWLEDGEMENTS.

This work was partially funded by SKB. The EURAD project leading to this application has received funding from the European Union's Horizon 2020 research and innovation programme under grant agreement No 847593. Annika Maier and Svante Hedström at SKB are thanked for discussions and feedback. The support of Dieter Schild, Muriel Bouby, Stephanie Kraft and Thomas Sittel is gratefully acknowledged for the XPS, TG-DSC, SEC-LC-OCD-OND and NMR measurements, respectively.

REFERENCES

1. KEITH-ROACH M. et al. "Assessment of complexing agent concentrations in SFR", *Swedish Nuclear Fuel and Waste Management Co, SKB Technical Report,* R-14-03, (2014).
2. LITMANOVICH A. D. et al. "Alkaline hydrolysis of polyacrylonitrile. On the reaction mechanism" *Macromolecular Chemistry and Physics* **201**, 2176–2180 (2000).
3. DURO L. et al. "Study of the effect of the fibre mass UP2 degradation products on radionuclide mobilization" *Swedish Nuclear Fuel and Waste Management Co, SKB Technical Report,* R-12-15, (2012).

Microcosm study of indigenous microorganisms in bentonite and its effect on corrosion of cast iron

V. Sushko, S. Kluge, N. Matschiavelli, A. Schierz, T. Stumpf, A. Cherkouk

Helmholtz-Zentrum Dresden-Rossendorf, Bautzner Landstraße 400, 01328 Dresden - Germany
email:v.sushko@hzdr.de

INTRODUCTION

Bentonite is a potential barrier material in deep geological repositories (DGR) for nuclear waste and spent fuel [1] and it is critical to maintain its functionality for long periods of time. Bacteria, that can originate from the bentonite itself, can affect important properties of the engineered barrier system, including bentonite's swelling capability and integrity of the container material [2]. Cast iron is often considered as a suitable material for constructing the containers for the radioactive waste storage [3]. But the container material could be unstable and can corrode to insoluble corrosion products, which react with the bentonite barrier. In a DGR, anaerobic corrosion and microbially influenced corrosion are dominant forms of corrosion and the interactions at the metal/bentonite interface determine the long-term performance of bentonite-based radioactive waste barriers [4].

DESCRIPTION OF THE WORK

The microcosm-type setup described in [5] was used for the current study. Three types of bentonite with different indigenous microorganisms were chosen for the setup: B25, Calcigel, MX-80. Incubation of the microcosms, containing GGG40 cast iron coupons, synthetic Opalinus Clay porewater (OPA) and bentonite, was performed in N_2/CO_2 atmosphere at 30 °C. Some of the microcosms were supplemented with 5 mM sodium lactate or 0.5 bar of hydrogen to stimulate microbial activity. After a 271-day incubation period, the microcosms were investigated by various geochemical analyses (as e.g. ICP-MS, ion and high-performance liquid chromatography), DNA isolation and amplification of the ribosomal RNA (rRNA) intergenic spacer (RISA) for microbial community analysis, SEM-EDX and RAMAN spectroscopy to characterize the surface structure of the cast iron coupons. In addition, a similar 3-component experiment was set up with Calcigel including 4 time points to study in more detail the microbial-induced process of cast iron corrosion in Calcigel-microcosms.

RESULTS AND DISCUSSION

After 271 days of incubation under anaerobic conditions at 30 °C, the presence of black precipitants in microcosms containing Calcigel and sodium lactate, and all substrate-containing MX-80 samples became apparent. Geochemical investigation of the respective samples showed a decrease in sulphate concentration which was dominant in microcosms containing MX-80.

Surface analysis with SEM-EDX showed severe damage for all the samples, except B25 without substrates. Two types of crystalline structures were found: iron and/or calcium carbonates and iron sulphide. The presence of the latter could be an indication of the activity of sulphate-reducing bacteria.

Different microbial community structures were observed by RISA analysis depending on the used bentonite and the applied conditions.

Overall, the results show that the reactivity at the bentonite/metal interface and the microbial activity are bentonite-type dependent and the selection of the bentonite for the DGR is highly important for preventing possible microbial implications that could lead to a faster deterioration of the metal container.

ACKNOWLEDGEMENT

Funding was provided by the German Federal Ministry of Education and Research (BMBF, Grant 02NUK053) and the Helmholtz Association (Grant SO-093).

REFERENCES

1. P. SELLIN et al., "The Use of Clay as an Engineered Barrier in Radioactive-Waste Management – A Review" Clays and Clay Minerals, **61**, 477-498 (2014).
2. F. KING, "Container Materials for the Storage and Disposal of Nuclear Waste" Corrosion, **69**, 986-1011 (2013).
3. F. KING et al., "Nature of the near-field environment in a deep geological repository and the implications for the corrosion behaviour of the container" Corrosion Engineering, Science and Technology, **52**, 25-30 (2017).
4. S. KAUFHOLD et al., "About the Corrosion Mechanism of Metal Iron in Contact with Bentonite" ACS Earth Space Chem., **4**, 711–721 (2020).
5. N. MATSCHIAVELLI et al., "The Year-Long Development of Microorganisms in Uncompacted Bavarian Bentonite Slurries at 30 and 60 °C" Environ. Sci. Technol., **53**, 10514–10524 (2019)

Microscopic and spectroscopic study of the uranium(VI) reduction by a sulfate-reducing microorganism

Stephan Hilpmann[1], Robin Steudtner[1], René Hübner[2], André Rossberg[1,3], Damien Prieur[1,3], Stephen Bauters[1,3], Kristina Kvashnina[1,3], Thorsten Stumpf[1], Andrea Cherkouk[1]

[1]Helmholtz-Zentrum Dresden-Rossendorf, Institute of Resource Ecology, Dresden, Germany
Email: s.hilpmann@hzdr.de
[2]Helmholtz-Zentrum Dresden-Rossendorf, Institute of Ion Beam Physics and Materials Research, Dresden, Germany
[3]The Rossendorf Beamline (BM20-ROBL), European Synchrotron Radiation Facility, Grenoble, France

INTRODUCTION

Clay rock is a possible host rock for the long-term storage of high-level radioactive waste, and bentonites are a suitable backfill material for a final repository in clay rock and crystalline rock. For a comprehensive safety assessment of such a repository over a long period, different aspects must be taken into account. Besides intensive research regarding geological, geochemical, and geophysical properties, these surroundings represent a habitat for naturally occurring microorganisms. In the event of a worst-case scenario, water can enter the repository. It is possible that microorganisms can interact with the radionuclides and thereby change the chemical speciation or the oxidation state by various processes.

Desulfosporosinus spp. play an important role as a representative of anaerobic, sulphate-reducing, and spore-forming microorganisms. These bacteria occur in different clay formations as well as in bentonites.[1,2] A very closely related bacterium to an isolated species from bentonite is *Desulfosporosinus hippei* DSM 8344, which was originally found in permafrost soils.[3] Therefore, this strain was selected to get a more profound insight into the uranium(VI) interactions with naturally occurring microorganisms from deep geological layers by different microscopic and spectroscopic techniques.

DESCRIPTION OF THE WORK

For the time-dependent experiments in artificial Opalinus Clay pore water[4] (100/500 µM uranium(VI), pH 5.5), the cells were cultivated in specific media and harvested in the late exponential growing phase. After washing, suspensions containing cells, uranium(VI), and lactate were incubated at room temperature and samples were taken between zero hours and one week.

RESULTS AND DISCUSSION

The experiments showed the removal of about 80% of the initial uranium(VI) from the supernatants within 48 h at a concentration of 100 µM. Corresponding UV/Vis measurements of the dissolved cell pellets revealed an increasing proportion of uranium(IV) in the samples with time. After one week, round about 40% of the uranium in the cell pellets was reduced from VI to IV. Therefore, the interaction mechanisms can be assigned to a combined sorption-reduction process.

TEM images of the uranium-incubated cells reveal the formation of uranium aggregates on the cell surface. Uranium can be found not only outside the cell in vesicles, but also inside the cell.

HERFD-XANES measurements at the U M4 edge show the presence of three oxidation states in the cell pellets. Besides uranium(VI) and uranium(IV), also uranium(V) plays a major role in the cellular reduction process. With the help of EXAFS measurements, three cell-related uranium species were detected.

This study helps to close existing gaps in a comprehensive safeguard concept for a final repository for high-level radioactive waste in clay rock. Moreover, new insights into the interaction mechanisms of sulfate-reducing microorganisms with uranium are presented.

ACKNOWLEDGEMENT

Funding provided by the German Federal Ministry of Education and Research (BMBF, Grant 02NUK053) and the Helmholtz Association (Grant SO-093) is acknowledged.

REFERENCES

1. A. BAGNOUD et al., “Reconstructing a hydrogen-driven microbial metabolic network in Opalinus Clay rock” *Nat. Commun*., **7**, 1-10 (2016).
2. N. MATSCHIVELLI et al., “The year-long development of microorganisms in uncompacted Bavarian bentonite slurries at 30 °C and 60 °C” *Environ. Sci. Technol*., **53**, 10514-10524 (2019).
3. A. VATSURINA et al., “Desulfosporosinus hippei sp. nov., a mesophilic sulfate-reducing bacterium isolated from permafrost” *Int. J. Syst. Evol. Microbiol*., **58**, 1228-1232 (2008).
4. P. WERSIN et al., “Biogeochemical processes in a clay formation in situ experiment: Part A - Overview, experimental design and water data of an experiment in the Opalinus Clay at the Mont Terri Underground Research Laboratory, Switzerland” *Appl. Geochemistry*, **26**, 931-953 (2011).

Technetium immobilization by chloride green rust

Natalia Mayordomo,[1] Diana M. Rodríguez,[1] Dieter Schild,[2] André Rossberg,[1,3] Andreas C. Scheinost,[1,3] Vinzenz Brendler,[1] Katharina Müller[1]

[1]*Institute of Resource Ecology, Helmholtz-Zentrum Dresden – Rossendorf (HZDR), 01328 Dresden (Germany)*
[2]*Institute for Nuclear Waste Disposal, Karlsruhe Institute of Technology (KIT), 76344, Eggenstein-Leopoldshafen (Germany)*
[3]*The Rossendorf Beamline at ESRF (ROBL), 38043, Grenoble (France)*
e-mail: n.mayordomo-herranz@hzdr.de

INTRODUCTION

Technium-99 (^{99}Tc) is one of the most concerning fission products due to its long half-life ($2.14 \cdot 10^5$ years) and the high mobility of the anion pertechnetate (TcO_4^-). [1]

Tc migration decreases when Tc(VII) is reduced to Tc(IV). This scavenging step is carried out by Fe(II) minerals, which have been widely studied due to their versatility, low cost and ubiquity. [2] Green rust is a Fe(II)-Fe(III) hydroxide that possesses adsorption, anion exchange and reduction capabilities. Its presence is expected in the near- and far-field of a nuclear waste repository because it is an iron corrosion product, and it is also formed in the environment when Fe^{2+} interacts with Fe(III) minerals. [3] Thus, further studies are needed to both identify the optimal Tc scavenging conditions by green rust and the mechanism responsible of Tc retention.

DESCRIPTION OF THE WORK

Batch contact studies have been performed under a wide range of conditions, i.e. pH (3-11), Tc concentration (nM-mM), and ionic strength (0-0.1 M). X-ray powder diffraction, Raman microscopy, X-ray photoelectron spectroscopy (XPS), and X-ray absorption spectroscopy (XAS) provided information on Tc oxidation state and speciation as well as on secondary redox products related to the Tc interaction with chloride green rust (GR(Cl)). In addition, re-oxidation experiments have been performed for one year to analyze the Tc retention reversibility.

RESULTS AND DISCUSSION

The results show that GR(Cl) removes Tc from solution with efficiencies between 80% ($Kd = 8.0 \cdot 10^3$ mL/g) and ≈100% ($Kd = 9.9 \cdot 10^5$ mL/g) for pH > 6.0.

In contrast, Tc removal for pH < 6.0 drops with decreasing pH, and ranges from 80% to 50% ($Kd = 2.0 \cdot 10^3$ mL/g), reaching a minimum at pH 3.5. XPS analysis reveals the predominance of Tc(IV) at all evaluated pH values (3.5 to 11.5), supporting that Tc reductive immobilization is the main retention mechanism. Re-oxidation experiments show that Tc is slowly solubilized when time increases.

The analysis of the extended X-ray absorption fine structure (EXAFS) reveals a change on Tc(IV) environment depending on pH and Tc loading. The most probable structural rearrangements are represented by Tc(IV) sorption on Fe(III) minerals formed as secondary phases with Tc polynuclear species contribution.

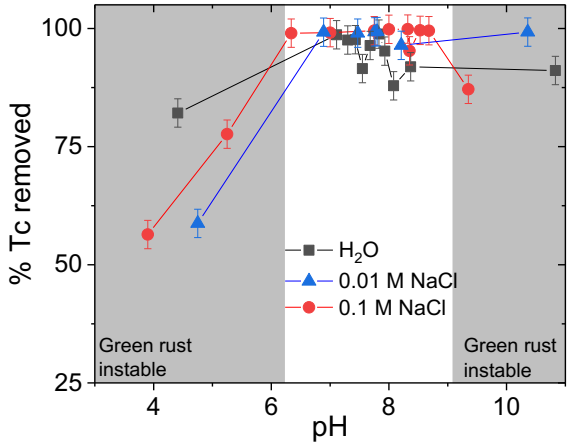

Fig. 1: Tc removal (%) by GR(Cl) as a function of pH for different ionic strengths (square) H_2O, (triangle) 0.01 M NaCl and (circle) 0.1 M NaCl.

ACKNOWLEDGMENT

We thank the German Federal Ministry of Economic Affairs and Energy (BMWi) for funding the VESPA II project (02E11607B).

REFERENCES

1. MEENA, A.H.; ARAI, Y. "Environmental geochemistry of technetium" *Env. Chem Lett*, **15**, 241–263 (2017).
2. PEARCE, C.I. et al., "Technetium immobilization by materials through sorption and redox-driven processes: A literature review" *Sci. Total Environ,.*

716, 132849 (2020).
3. USMAN, M.; et al., "Magnetite and Green Rust: Synthesis, Properties, and Environmental Applications of Mixed-Valent Iron Minerals" *Chem. Rev.* **118**, 3251–3304, (2018).

Chemical interaction between selenite and mackinawite in cement pore water

K. Wang [1,2], A.F. Martinez[1], L. Simonelli[3], B. Madé[4], P. Hénocq[4], B. Ma[1,5], L. Charlet[1]

[1] *University of Grenoble Alpes and CNRS, ISTerre, BP 53, 38041 Grenoble Cedex 9, France*
[2] *Engineering Technology Center of Decommissioning and Remediation, China Institute of Atomic Energy, 102413 Beijing, China*
[3] *BL22 – CLAESS, ALBA Synchrotron Light Source, 08290 Barcelona, Spain*
[4] *ANDRA, 1/7 rue Jean Monnet, Parc de la Croix Blanche, 92298 Chatenay-Malabry Cedex, France*
[5] *Paul Scherrer Institut, Laboratory for Waste Management, 5232 Villigen PSI, Switzerland*
e-mail: kaifeng.wang@univ-grenoble-alpes.fr

INTRODUCTION

^{79}Se is one of radioactive isotope with half-life of 4.8×10^5 years. Usually, under oxidizing conditions, aqueous oxyanions (SeO_3^{2-} and SeO_4^{2-}) are particularly mobile. In contrast, Se(0, -I and -II) present in low solubility under reducing conditions. The CEM-V/A type of cement is being evaluated as engineered barrier for deep underground radioactive waste disposal in France and the cement pore water (CPW) has hyperalkaline (pH ~ 13.5) and high resistance to sulfate corrosion[1]. Mackinawite (FeS), a redox-active nanosized layer ferrous sulfide mineral, a phase that can form at steel surface of reinforced concrete in CPW, makes it have tremendous potential to immobilize radionuclides. The fate of selenite induced by FeS in CPW and reducing conditions remains unclear and requires investigation.

DESCRIPTION OF THE WORK

In this work, we identify the reduced species of selenium, oxidation state mineral composition of Fe and S by a combination of XAS, XPS and TEM. Analytical investigations (ICP and ion chromatography) is used to measure the concentration of selenite (SeO_3^{2-}) and sulfur species (S^{2-}/S_n^{2-}, SO_3^{2-} and SO_4^{2-}). The results shows distinct kinetic steps. After 192 h reaction, ~95 % SeO_3^{2-} is reduced to Se^0-S_n species by oxidation of S^{2-}/S_n^{2-} to SO_4^{2-} and Fe(II) to Fe(III). In 0.22 µm filtered solution, ~99% of reduced selenium is present as nano-Se_4S particles due to the dissolution of Se^0-S_n at high pH. Meanwhile, ~62 % S^{2-}/S_n^{2-} dissolves from solid, and FeS is first totally transformed to nano-magnetite (Fe_3O_4), present in part in the solution after 192 h reaction.

RESULTS AND DISCUSSION

THE FATE OF SELENIUM. Equilibrium kinetics of SeO_3^{2-} by FeS in CPW is conducted and the concentrations of SeO_3^{2-} and the total Se are shown in Fig. 1(a). The total concentration of Se are equal to the SeO_3^{2-} free ion concentration in the first 24 h reaction time, indicating that SeO_3^{2-} is the only species in suspension and that reduction products are absorbed or co-precipitated Se species. After 50 h, the concentration of SeO_3^{2-} continues to decrease while the total concentration of Se is increasing with reaction time. It means the reduction product, such as nano-Se^0, are released to the suspension and are not filtered out by the < 0.22µm membrane. Meanwhile, the color of the filtered supernatant solution turns yellow after 24 h reaction from clear (1 h) to orange (50 h), olive (73 h) and black (138 h and 192 h), as shown in Fig. 1(b). The orange color may indicate that SeO_3^{2-} is reduced to red Se^0 nanoparticles released to the solution, as other studies have observed [2]. Therefore, the total concentration of Se includes SeO_3^{2-} and the dissolved nano-Se^0 species. After 192 h reaction, ~95 % SeO_3^{2-} is reduced and ~99 % of reduced selenium species are present in the solution.

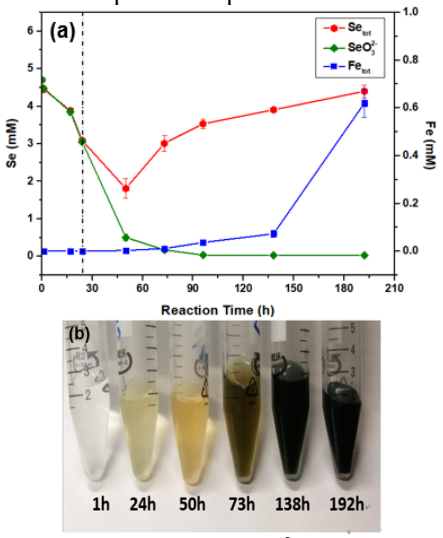

Fig. 1: (a) Concentration of SeO_3^{2-} and the total Se with reaction time, (b) Picture of the supernatant solution.

After reacting for 1 h, SeO_3^{2-} was mainly reduced into 35.8(3.0)% $FeSe_2$, 35.5(9.2) % FeSe and 19.2(1.0) % SeS_2, while only 4.9(2.9)% Se^0 and 4.9(1.2)% SeO_3^{2-} could be identified, indicating that SeO_3^{2-} can be quickly adsorbed on the surface and reduced to Se (0, -I, -II). From 24 h to 196 h, all the spectra showed similar features, with ~63% SeS_2 and 30-32% Se^0 identified to be the primary solid Se species (Fig. 2). After 192 h, the nanoparticles present in supernatant are observed by TEM (Fig. 3). The nanoparticles formed are made of Se, S, Fe and O with a

Se to S of roughly 4:1 according to EDS analysis (Fig 3d). The HRTEM data proves however that reduced Se transforms to Se_4S. The interplanar spacing in Fig. 3(c) is 0.25 nm, corresponds to the (330) lattice plane of magnetite (Fe_3O_4). It means FeS is transformed to nano-magnetite in filtered supernatant during the reaction, resulting in an apparent Fe concentration in Fig. 1(a). We suggest SeO_3^{2-} is reduced to atom/fine phase of Se(0) and then Se^0-S species are formed though the bonding of Se(0) and S(0) immediately. Furthermore, ≡Fe-S/S_n-Se^0 breaks down to its constituent parts in CPW, i.e. into ≡Fe-S/S_n and nano-Se^0 or ≡Fe-OH and nano-Se^0-S/S_n.

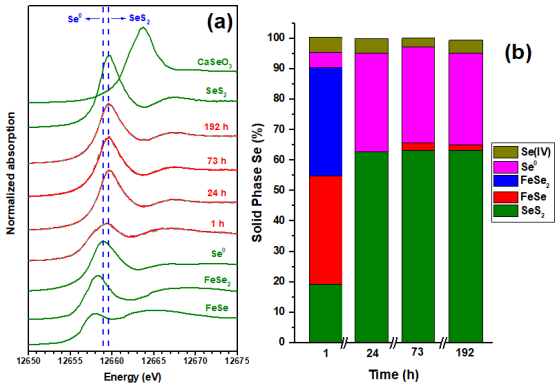

Fig. 2: Se K-edge normalized XANES spectra of solid samples, comparing to Se references.

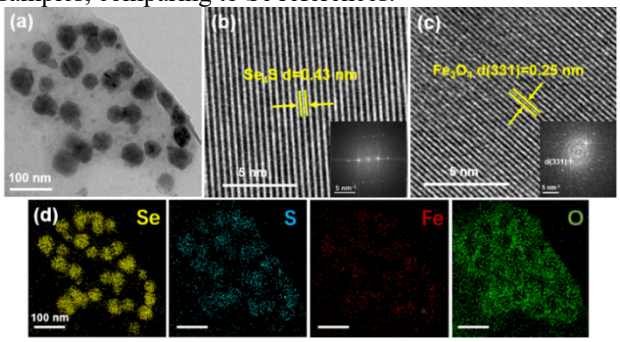

Fig. 3:. TEM of nanoparticle in supernatant at 192 h. (a) TEM image; (b), (c) Fe_3O_4 and SeS_4 HRTEM image with FFT; (d) EDS mapping of Se, S, Fe and O.

DISSOLUTION KINETICS OF FES WITH/WITHOUT SEO_3^{2-}. A plot of S concentration versus reaction time is shown in Fig. 4. From the ionic composition without SeO_3^{2-} (Fig. 4a), The concentration of (poly)sulfide (blank) (S^{2-}/S_n^{2-}) concentration increases very slowly and aqueous SO_4^{2-} (blank) remains at the CPW value, suggesting there is no apparent dissolution of FeS and no significant quantities of aqueous SO_4^{2-} absorbs on FeS. However, in the presence of SeO_3^{2-}, a critical threshold of reaction time (73 h) is observed from (ploy)sulfide (S^{2-}/S_n^{2-}) concentration. The concentration of dissolved S^{2-}/S_n^{2-} originating from solid increases quickly during first 73 h and remains rather constant and equals to 13~14 mM thereafter. After 192h, 14.12 mM S^{2-}/S_n^{2-} dissolves in the suspension and the dissolution efficiency is 62 % (22.8 mM FeS). The sulfate (SO_4^{2-}) concentration remains equal to 1.55 mM during the reaction. Some sulfite (SO_3^{2-}) is observed in the suspension with a concentration following the kinetic trend of sulfide.

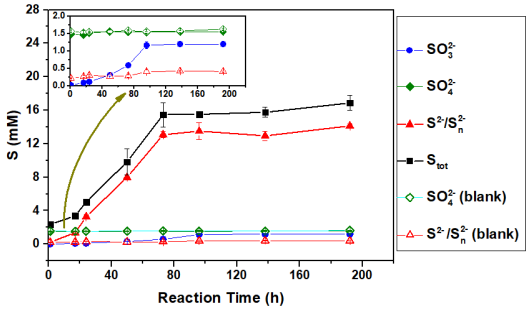

Fig. 4: The concentration profiles of S^{2-}/S_n^{2-}, SO_4^{2-} and SO_3^{2-} with/without SeO_3^{2-} as a function of reaction time.

POSSIBLE REACTION INVOLVING FE, S AND SE. Fig. 5 shows the XPS spectra of S 2p and Fe 2p3/2 for filtered FeS reacted with SeO_3^{2-} for various times. In Fig. 5(a), from 1 h to 192 h, a decrease in S^{2-}/S_n^{2-} with an increase in SO_4^{2-} suggests S^{2-}/S_n^{2-} on the surface of FeS to be oxidized to SO_4^{2-} following SeO_3^{2-} reduction. Compared with pure FeS XPS result, an increase of Fe(II)-O and Fe(III)-O peaks and the absence of Fe(II)-S observe at 73 h. It means SeO_3^{2-} is reduced by oxidation of Fe(II) to Fe(III) and Fe(II)-O forms due to the dissolution of S^{2-}/S_n^{2-} at high pH. At 192 h, the content of Fe(II)-O and Fe(III)-O keep constant. Mixtures of Fe(II)-O and Fe(III)-O observed may represent the formation of magnetite.

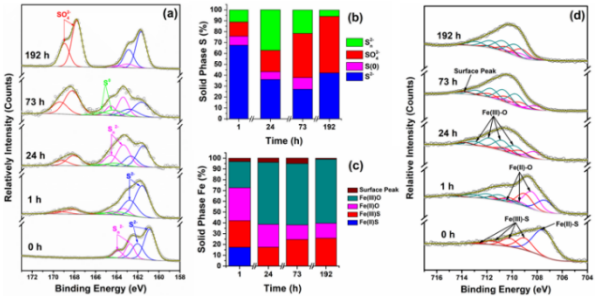

Fig. 5: XPS spectra of S(2p)(a) and Fe($2p_{3/2}$) (d) and the fractions of components of S(b) and Fe(c) species.

In brief, SeO_3^{2-} reacted with FeS in CPW, and produced magnetite, absorbed SO_4^2 and Se^0. Also, Se^0 combined with S_n immediately to form Se-S_n species. The simplified reaction equations should be:

$$6FeS + 7SeO_3^{2-} + 10H^+ \rightarrow 7Se^0 + 4S^0 + 2Fe_3O_4 + 2SO_4^{2-}{}_{(s)} + 5H_2O,\ Se^0 + nS^0 \rightarrow SeS_n$$

REFERENCES

1. BIN M. et al., *Applied Geochemistry*, **100**, 414-431 (2019).
2. HAN, D. S. et al., *Journal of Hazardous Materials*, **186**, 451-457 (2011).

Effect of Temperature on Molybdate Adsorption by Goethite

Anna Dabizha, Michael Kersten

Geosciences Institute, Johannes Gutenberg-University, 55099 Mainz, Germany
e-mail: dabizha@uni-mainz.de

INTRODUCTION

There is increased interest in understanding adsorption behaviour at elevated temperatures typical of the nearfield of nuclear waste repositories. However, this is not only for radionuclides, but also for other toxic elements abundant in such repositories like those included in canister material such as chromium, vanadium, and molybdenum. In a previous publication we already reported the adsorption behaviour of chromate at elevated temperatures [1]. The aim of this study is to implement a surface complexation model for molybdate at elevated temperatures.

DESCRIPTION OF THE WORK

Synthetic goethite was prepared as reported previously [1]. A series of subsamples were prepared with solutions of different ionic strengths ($NaNO_3$) and goethite suspensions of 5 g L^{-1}. The pH values were set to the desired value between 3 and 10 by NaOH or HNO_3 respectively. Adsorption experiments were conducted with different molybdate concentrations of 0.1, 0.2, and 0.3 mM in a thermostat at temperatures between 10 °C and 75 °C. All samples were centrifuged and membrane-filtrated (0.2 µm). The residual dissolved molybdate was measured by ICP-MS.

RESULTS AND DISCUSSION

The adsorption data were plotted against pH for different ionic strengths, Mo concentrations, and temperatures (example for 25°C in Fig. 1). In general, the higher the temperature, the less molybdate was adsorbed by the goethite surfaces at the same total Mo concentration resulting in an exothermic behaviour. A CD-MUSIC surface complexation model was set on basis of previously published spectroscopic results [2]. The resulting entropy of adsorption of 325 J K^{-1} mol^{-1} for the bidentate inner-spheric surface complex $(\equiv FeO)_2MoO_2$ nicely fits to those previously found for other oxyanions, if their entropies are plotted vs. the volume of the molecules as derived from the EXAFS results following an approach published by Housecroft et. al. [3] (Fig. 2):

$$\Delta_r S_{IS,298} = k V_m^{-1/3} + c \quad (1)$$

where V_m is the formula unit volume (nm3), and k and c are the linear correlation constants.

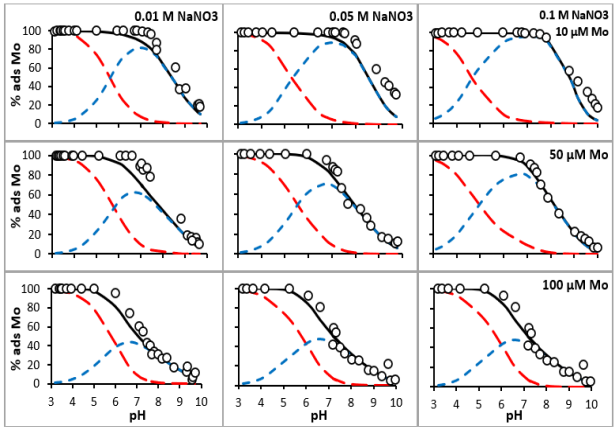

Fig. 1. The red model lines represent the inner-sphere surface complex, the blue lines represent the outer-sphere surface complex, and the black lines total Mo adsorbed.

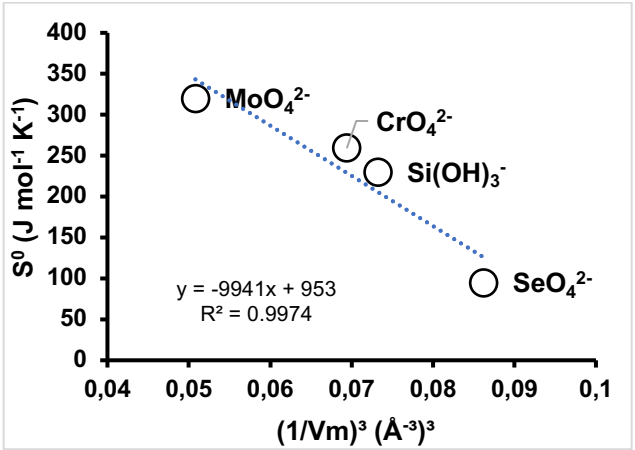

Fig. 2. Plot of the molar entropies of adsorption vs. the cubic of inverse adsorbate molecule volume $(1/Vm)^3$.

REFERENCES

1. DABIZHA et al., "Exothermic adsorption of chromate by goethite" *Applied Geochemistry*, **123**, 104785 (2020).
2. GUSTAFSSON et. al., "Molybdenum binding to soil constituents in acid soils: An XAS and modeling study" *Chemical Geology*, **417**, 279-288 (2015).
3. HOUSECROFT et. al., "Absolute ion hydration enthalpies and the role of volume within hydration thermodynamics" *J. RSC Adv.*, **7**, 27881–27894 (2017).

Solubility of Lanthanides for environmental and performance assessments

Lara Duro

Amphos21, Calle Venezuela 103, 2º 1ª, Barcelona, E-08019 (Spain)
email: lara.duro@amphos21.com

INTRODUCTION

Lanthanides (lanthanoids according to IUPAC), are a group of 15 elements (when including Lanthanum) whose atomic number varies between 57 and 71 and whose 4f orbital is being filled progressively from the electronic configuration of Lanthanum. Given that the internal 4f orbitals do not intervene very importantly to the chemical bonds, and that all of them have the same external electronic configuration, the most important oxidation state is M^{3+} for all lanthanoids, ionizing by losing their external 6s electrons and 1 electron of the 4f orbitals.

The electronic configuration along the lanthanoids series gives them specific properties of interest for technological applications, for example high magnetic moments. The Rare Earth Metals category (REE) includes lanthanoids plus scandium and yttrium. Although Sc and Y have similar chemical properties to lanthanoids, they have different magnetic behaviour.

REE have many different uses, as seen in Figure 1. They have also important nuclear applications for example as neutron poisons, hydrogen-moderators, alloys for modification of the components of the reactors, etc.

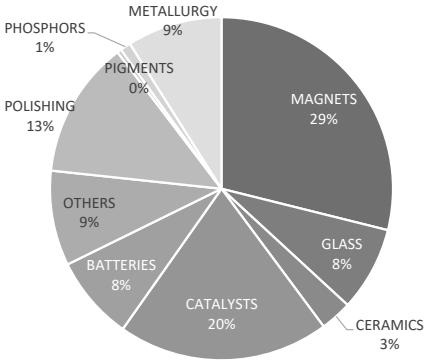

Fig. 1: Use of REE in the US [1].

In the last years, the recovery of REE have received special relevance due, predominantly, to their relative high price (121 USD /kg Nd vs. 109€/kg U as of September 2021 [2]), what has contributed to a rebound of the study of their chemistry. This, together with their evident interest in radioactive waste management, justifies that the development of sound thermodynamic databases to properly account for the chemical behaviour of lanthanides receives more attention.

DESCRIPTION OF THE WORK

A review of the solubility of lanthanoids selected in supporting calculations for radioactive waste management is presented in this work.

Experimental supporting experiments are from results obtained with synthetic carbonates of Nd, Eu and Yb are used to illustrate the case. After synthesis and characterisation of the solid phases, the solubility of solid carbonates was determined in the pH range 5 to 11 and at temperatures 25°C and 40°C [3].

RESULTS AND DISCUSSION

The conclusions of the literature analyses highlighted the relevance of both, hydroxides, carbonates and phosphates as solubility limiting phases, depending on the geochemical conditions of the environment.

Spahiu and Bruno [4] highlight in their database compilation that the solid carbonates of lanthanoids may suffer hydrolysis, being converted into hydroxy-carbonate solids and producing a change in the solubility of the metals. The extent to which this hydrolysis can occur may depend on the Ln in question, being more important for heavier REE.

Different authors have studied the solubility of carbonates and hydroxycarbonates of lanthanoids and trivalent actinides in the literature, and point out the possible influence of the temperature on phase transformation [5,6,7,8]. This work compares the data so far obtained and presents additional data on solubility experiments of synthetic Nd, Eu and Yb solid carbonates.

The results (see Fig. 2) did not show important differences between light and heavy lanthanoids with regards to the solid phase formed and indicated no important temperature effect in the range 25-40°C [3].

These results suggest that a more detailed investigation and assessment of the thermodynamic data and hypothesis on lanthanoids behaviour in support of recovery of these metals and radioactive waste management.

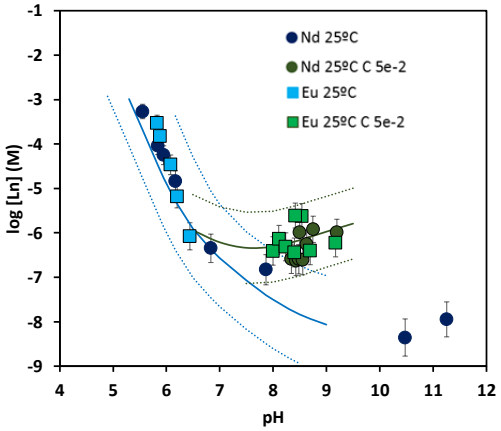

Fig. 2: Experimental results of the solubility of synthetic Ln-CO_3 solid phases [3].

REFERENCES

1. ROSKILL — Rare Earths Market Outlook Report, (2021).
2. Daily Metal Price: Uranium Price (USD / Kilogram) for the Last Month. https://www.dailymetalprice.com/metalprices.php?c=nd&u=oz&d=20
3. LOPEZ, M., in preparation (2021).
4. SPAHIU, K., BRUNO, J., A selected thermodynamic database for REE to be used in HLNW performance assessment exercises, SKB TR 95-35 (1995).
5. RUNDE, W., Meinrath, G., Kim, J.I., A study of solid-liquid phase equilibria of trivalent lanthanide and actinide ions in carbonate systems. *Radiochim Acta* **58/59**, 93–100 (1992).
6. VITORGE, P., $Am(OH)_3(s)$, $AmOHCO_3(s)$, $Am_2(CO_3)_3(s)$ stabilities in environmental conditions. *Radiochim. Acta* **58/59**, 105–107 (1992).
7. FELMY, A.R., et al. The solubility of AmOHCO3(c) and the aqueous thermodynamics of the system Na^+-Am^{3+}-HCO_3^--OH^--H_2O. *Radiochim. Acta* **50**, 193–204 (1990).
8. GIFFAUT, E., Influence des ions chlorure sur la chimie des actinides. Effets de la radiolyse et de la température. Universite de Paris-Sud U.F.R. Scientifique D'Orsay (1994).

Radionuclide retention in cementitious systems: research activities at KIT-INE

Xavier Gaona[1], Marcus Altmaier[1], Iuliia Androniuk[1], Nese Çevirim-Papaioannou[1], Rosa Ester Guidone[1,2], Yongheum Jo[1], Andrej Skerencak-Frech[1], Peter Szabo[1], Agost Tasi[1], Horst Geckeis[1]

[1]*Institute for Nuclear Waste Disposal (INE), Karlsruhe Institute of Technology (KIT), Karlsruhe, 76344, Germany*
[2]*Swiss Federal Laboratories for Materials Science and Technology (Empa), 8600 Dübendorf, Switzerland*

email: xavier.gaona@kit.edu

Safety concepts regarding nuclear waste disposal in underground repositories generally rely on a combination of engineered and geological barriers, which minimize the potential release of radionuclides out of the containment-providing rock zone or even the transport into the biosphere. Cementitious materials are used for the conditioning of certain nuclear waste types, as components of waste containers and overpacks as well as constituents of structural materials at the interface between backfilling and host-rock in some repository concepts.

In the event of formation water interacting with cementitious materials, pore water solutions characterized by (highly) alkaline pH conditions will form. These boundary conditions define the chemical response of the radionuclides, but also influence the behaviour of neighbouring components of the multi-barrier system, *e.g.* bentonitic or argillaceous backfilling and host-rock, respectively. Hardened cement paste or Sorel cement are typically the main sorbing materials present in the near field of repositories for low and intermediate level waste (LILW). Hence, interactions of radionuclides with cementitious materials represent a very important mechanism retarding their mobility and potential migration from the near field (Wieland, 2014; Ochs et al., 2016). While the quantitative description of the sorption processes (usually in terms of sorption coefficients, *i.e.* K_d values) is a key input in the safety analyses of nuclear waste repositories, the detailed mechanistic analysis and understanding of sorption phenomena provide additional scientific arguments and important process understanding and thus enhance both the quality of safety arguments and the overall confidence in the safety assessment.

Research at KIT–INE dedicated to the interaction of cementitious materials with radionuclides is conducted in the context of different repository concepts, including clay (low and high ionic strength conditions), crystalline rock or rock salt. Experimental and theoretical studies are performed in the frame of national (GRAZ, BMWi) and international (CEBAMA and EURAD-CORI, EU Horizon 2020 Programme) projects, extending to third-party projects with several waste management organizations in Europe, *e.g.* SKB (Sweden) or ONDRAF-NIRAS (Belgium). The combination of classical experimental (wet-chemistry) methods, advanced spectroscopic techniques and theoretical calculations provides both an accurate quantitative evaluation and a fundamental understanding of the sorption processes. Examples on recent studies at KIT-INE on the radionuclide behaviour in cementitious systems in the context of LILW will be presented in this contribution to explain methodologies, scientific approaches and results. This includes activities with actinides (Pu), fission and activation products (Ni, Nb, Cl), as well as with chemotoxic elements (Be). The contribution will also elaborate on the role of organic ligands expected in LILW (*e.g.* isosaccharinate, citrate, etc.) in the retention of radionuclides. The present state-of-knowledge as well as main remaining uncertainties affecting the retention processes of radionuclides in cementitious environments under different conditions will be critically discussed, also in the view of current international research activities and repository projects.

ACKNOWLEDGEMENTS

Some of the studies in this contribution were partly funded by SKB (Sweden), ONDRAF-NIRAS (Belgium) and BMWi (Germany). The EURAD project leading to some examples in this application has received funding from the European Union's Horizon 2020 research and innovation programme under grant agreement No 847593. The research leading to some of these results has received funding from the European Union's European Atomic Energy Community's (Euratom) Horizon 2020 Programme (NFRP-2014/2015) under grant agreement, 662147 – Cebama. A. Maier and S. Hedström (SKB), B. de Blochouse (ONDRAF-NIRAS), B. Lothenbach (Empa) and J. Bruno, E. Colàs and L. Duro (Amphos 21) are gratefully acknowledged for their contribution to different studies and fruitful discussions.

REFERENCES

1. OCHS, M. et al., "Radionuclide and metal sorption on cement and concrete", Springer, Switzerland (2016).
2. WIELAND, E., et al. "Sorption database for the cementitious near field of L/ILW and ILW repositories for provisional safety analyses for SGT-E2", Nagra Technical Report 14-08. Paul Scherrer Institut, Villigen, Switzerland (2014).

Towards a global model of radionuclide sorption in cement-based materials. Focus on cesium uptake.

Pierre Henocq[1], Catherine Landesman[2], Nicolas Bessaguet[2], Solange Ribet[2], Karine David[2], and Véronique Baty[2]

[1]*Andra, rue Jean Monnet, 92298 Châtenay-Malabry, France*
[2]*Subatech, UMR 6457 (IMT-Atlantique, Université de Nantes, CNRS-IN2P3), 4 Rue Alfred Kastler, 44307, Nantes, France*
email: pierre.henocq@andra.fr

INTRODUCTION

In the framework of the radioactive waste management, the behaviour of radionuclides is deeply investigated in the different components of the underground and surface repositories. In particular, the behaviour in the cement-based materials is widely studied due to the expected massive amounts of concrete as vault structure or waste packages. The objectives of such studies consist to provide retention parameters, such as the distribution coefficient Kd, and transport parameters, such as the effective diffusion coefficient De. Most of the radionuclides interact with the Calcium Silicates Hydrates (C-S-H), the main component of the hydrated cement paste. Theses interactions can be assumed as a surface adsorption mechanism such as surface complexation. This work presents an approach for building a global retention model integrating a large range of radionuclides and major species associated to cementitious systems. This retention model is based on the surface complexation model CD-MUSIC in Phreeqc software. The development of such a surface complexation model requires to assess the logK values related to each surface reaction. The logK determination is based on experimental sorption data and/or zeta potential measurements. The present work focuses on the behaviour of cesium in cement-based materials in various environments.

DESCRIPTION OF THE WORK

The retention of radionuclides in cement-based materials is mainly controlled by C-S-H due to their surface properties and their high specific surface area. Many works have been made for providing experimental data on the radionuclide sorption in C-S-H, which are mostly cited by Evans (2008). The interpretation of these data by a surface complexation model has been proposed by several authors (Viallis et al., 2001; Kulik, 2002; Pointeau et al., 2006; Missana et al., 2017,2018). Most of these works are dedicated to specific radionuclides or species in solution. The present approach, described in a previous work (Henocq, 2017), aims to develop a global model with a unique logK dataset for all the C-S-H, i.e. for all the calcium-to-silicon (C/S) ratio between 0.7 and 1.6. Here, the case of cesium is presented. Pure C-S-H systems have been used to determine log parameters from experimental data by Missana et al. (2018). Furthermore, the retention and diffusion of cesium in hydrated cement pastes (HCP) were studied; in particular, the effect of high concentrations of Na_2SO_4 has been investigated. The diffusion of Cs is modelled with Phreeqc, using the Transport block for the diffusion part, coupled with the Surface block for the retention.

RESULTS AND DISCUSSION

A unique set of parameters is found to reproduce the experimental data related to C-S-H with the following C/S ratios: 0.8, 1.0, 1.2, and 1.6. In parallel, the parameters for sulfate sorption on C-S-H are determined for a large range of C/S ratios from Barbarulo (2002); Na sorption has been already characterized in Henocq (2017). By this way, the effect of the Na^+ and SO_4^{2-} sorption on Cs uptake is modelled showing that the amount of Cs in C-S-H decreases as Na_2SO_4 increases as experimentally observed. This result is remarkably confirmed by diffusion tests performed in the presence of Na_2SO_4 (Fig.1).

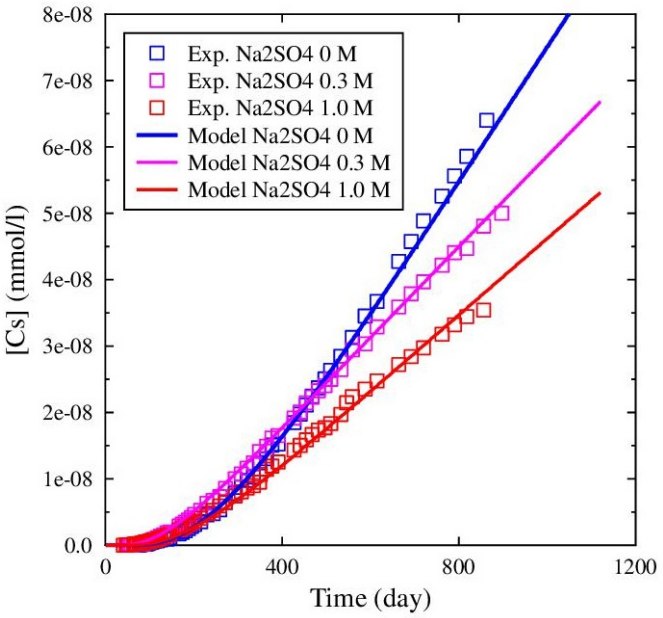

Fig. 1: Modelling of the cumulative amount of Cs in the downstream cell during a diffusion test in the presence of different Na_2SO_4 concentrations.

In the presence of 1M of Na_2SO_4, the modeling of the diffusion data (cumulative amount of Cs in the downstream cell) can reproduce the experimental data by assuming only the absence of Cs retention, while without Na_2SO_4, the modeling clearly shows a Cs retention. This observation illustrates the relationship between sorption tests (batch tests) and the diffusion tests. That shows the capability here to model the diffusion of Cs by considering a coupling *transport/surface complexation*, and consequently, that establishes a relationship between tests on crushed samples (batch tests) and consolidated samples (diffusion tests). Some issues remain such as the accessible C-S-H surface for sorption in the consolidated systems which should not correspond to the total amount of C-S-H. Regardless the remaining uncertainties, these results open the way for a deeper characterization of the diffusion tests for providing accurate sorption properties related to the consolidated cement-based materials.

REFERENCES

1. BARBARULO, R. "Comportement des matériaux cimentaires: actions des sulfates et de la température." LMT-ENS de Cachan, France, Doctorat thesis (2002).
2. EVANS, N. "Binding mechanisms of radionuclides to cement." *Cement and Concrete Research*, **38**, 543-553 (2008).
3. HENOCQ, P. "A sorption model for alkalis in cement-based materials–correlations with solubility and electrokinetic properties." *Physics and Chemistry of the Earth*, *Parts A/B/C,* **99**, 184-193 (2017).
4. KULIK, D.A. "Sorption modelling by Gibbs energy minimisation: Towards a uniform thermodynamic database for surface complexes of radionuclides." *Radiochimica Acta*, **90**, 815-832 (2002).
5. MISSANA, T., et al. "Analysis of barium retention mechanisms on calcium silicate hydrate phases." *Cement and Concrete Research*, **93**, 8-16 (2017).
6. MISSANA, T., et al. "Comparison between cesium and sodium retention on calcium silicate hydrate (CSH) phases." *Applied Geochemistry*, **98**, 36-44 (2018).
7. POINTEAU, I., et al. "Measurement and modeling of the surface potential evolution of hydrated cement pastes as a function of degradation." *Journal of Colloid and Interface Science*, **300**, 33-44 (2006).
8. VIALLIS-TERRISSE, H., et al., "Zeta-potential study of calcium silicate hydrates interacting with alkaline cations." *Journal of Colloid and Interface Science*, **244**, 58-65 (2001).

Radionuclide sorption onto calcareous gravels. Experimental results for Kd determination and first insights on adsorption mechanisms

David García[1], Benoît Madé[2], Marta López-García[1], Alba Valls[1], Jean-Charles Robinet[2], Lara Duro[1]

[1]*Amphos21, Barcelona, Spain*
[2]*Agence Nationale pour la gestion des Déchets Radioactifs (Andra) Châtenay-Malabry Cedex, France*
email: david.garcia@amphos21.com

INTRODUCTION

Sorption is a general term that includes different types of individual interaction processes such as ion exchange, surface complexation, etc. that, combined, lead to distribution factors (K_d) of a chemical element onto a solid material. In the context of radioactive waste management, sorption processes are one of the main processes able to retard the migration of radionuclides. The value of K_d ($L.kg^{-1}$) is very sensitive to the experimental conditions under which it has been determined and thus, it must be evaluated under the specific conditions of interest that are most representative of a repository.

Andra (Agence Nationale pour la gestion des Déchets RAdioactifs, France) is interested in determining experimental distribution coefficients of a range of radionuclides (Sr, U, Ni, Ag, Eu, Th, Pu, Tc and ^{14}C) onto specific gravels, which are used in the CIRES (Centre Industriel de Regroupement, d'Entreposage et de Stockage) facility. At present, there is an evident lack of sufficient experimental data on the adsorption of these elements on the targeted calcareous gravels, making it necessary to develop experimental studies to gain knowledge on the interaction between gravels and the selected radionuclides. In this contribution, we present:

- The set up of sorption experiments of selected chemical elements onto calcareous gravels, and
- the interpretation of the results in terms of K_d values, for their used in safety assessment applications, and also the first steps in developing mechanistic geochemical models.

DESCRIPTION OF THE EXPERIMENTAL WORK

Gravels coming from CIRES were crushed and sieved with a mesh opening below 250 µm to obtain a homogeneous sample. These samples were characterised by XRD to determine the main mineralogical composition (98% calcite) and by BET isotherms to obtain the specific surface area (3.1 ± 0.14 $m^2 \cdot g^{-1}$).

Synthetic water, representative of calcareous gravel pore water, used in sorption experiments was established by dissolving appropriate amounts of the solid reagents NaCl, $CaSO_4$, $MgSO_4$, SiO_2 and $CaCO_3$ in Milli-Q water and equilibrating the mixture for 24 h. Then, the pH was adjusted by adding little volumes of HCl up to pH 7.9, which did not affect the solution composition. After 24 hours of equilibration, the solution was filtered using a nylon filter (mesh size of 0.22 µm). Then, the synthetic porewater was contacted with the grinded gravels for 24 h and the resulting solution was filtered again (nylon filter, mesh opening of 0.22 µm).

Sorption experiments were performed using 0.1 g of grinded and sieved calcareous gravels equilibrated with 10 mL of synthetic water for 24 h (solid:liquid ratio, S:L, 10 $g \cdot L^{-1}$). After this time, the appropriate amount of each tracer (selected radionuclides) was spiked into solution to obtain the desired initial concentration and the experiment was left for the selected time under continuous stirring. The pH was measured at the end of the sorption experiments using a pH sensitive electrode. After completion of the experiments, the aqueous concentration of the target element in solution was determined by: (a) ICP-MS for Ag, C, Eu, Ni, Pu, Sr, Th, Tc and U, and (b) LSC for ^{14}C, ^{99}Tc, ^{238}Pu and ^{228}Th.

Kinetic sorption tests were performed to determine the equilibrium time for each system. Three different times were tested (i.e., 1, 7, 14 days) at one S:L (10 $g \cdot L^{-1}$) for one single tracer concentration. Sorption isotherms are obtained by varying the tracer concentration at equilibrium time of 14 days with S:L 10 $g \cdot L^{-1}$.

RESULTS AND DISCUSSION

The distribution coefficients determined in this work are summarized in Table 1. The results obtained indicate that the calcareous gravels studied have high adsorption capacities for ^{238}Pu and/or ^{152}Eu, but are not effective in retaining ^{99}Tc or Sr. This result can be related both to the chemical characteristics of each individual element (^{238}Pu and ^{152}Eu speciation dominated by cationic species) and to the physicochemical properties of the calcareous gravels themselves (negative zeta potential for calcite [1]). This behaviour highlights the importance of the electrostatic component on the adsorption mechanism.

Comparison of the results obtained in this work for ^{152}Eu, Ni, ^{238}Pu and U with previous literature data [2, 3, 4], under similar experimental conditions, showed good agreement in the case of Ni, U (Fig. 1) or ^{152}Eu. Higher

discrepancies were found in the case of ^{238}Pu with differences of more than one logarithmic unit observed [2]. Differences in solution pH (pH ~ 7.5 in the present work and 8.0-9.8 in [2] may explain the discrepancy observed in the experimental data as changes in pH leads to changes in the ^{238}Pu speciation. In the case of Pu, a pH variation from 9 to 7 increases the amount of the cationic species $Pu(OH)_3^+$ versus $Pu(OH)_4(aq)$, favouring the retention of ^{238}Pu and causing the increase observed in the K_d values determined in this work.

Element	K_d (mL·g^{-1})
Ag	1702 ± 308
^{14}C	49 ± 7
^{152}Eu	9622 ± 1712
Ni	322 ± 75
^{238}Pu	17895 ± 8272
Sr	18.4 ± 0.2
^{228}Th	560 ± 22
^{99}Tc	Not adsorbed
U	38 ± 10

Table 1: Distribution coefficient (Kd) determined in this work for stable and non-natural elements on calcareous gravels.

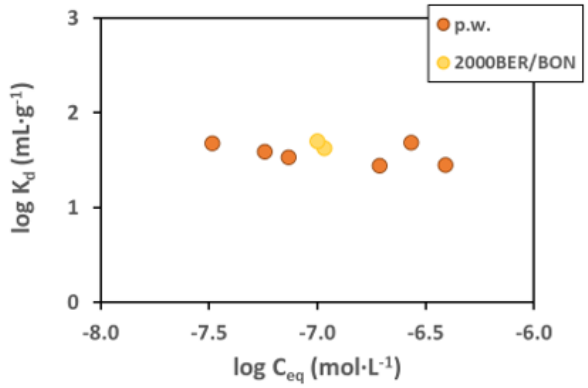

Figure

Fig. 1: Comparison of adsorption data obtained in this work (p.w.) with other data available in literature for U [4].

After analysis of the experimental results, we can conclude that the calcareous gravels are able to effectively retain ^{238}Pu, ^{152}Eu, Ag, ^{228}Th, and Ni. The electrostatic component of the adsorption process was highlighted after analysing both the surface properties of calcite and the chemical speciation of the targeted elements. Finally, the results obtained in this work are in agreement with those obtained in the literature, accounting for the strong dependence of the sorption data on the specific experimental conditions used.

REFERENCES

1. AL MAHROUQI et al. ”Zeta potential of artificial and natural calcite in aqueous solution”, *Advances in Colloid and Interface Science,* **240**, 60–76 (2017).
2. ZAVARIN et al. “Eu (III), Sm (III), Np (V), Pu (V), and Pu (IV) Sorption to Calcite”, *Radiochimica Acta,* **93**, 93–10 (2005).
3. TAHERVAND and JALALI “Sorption and desorption of potentially toxic metals (Cd, Cu, Ni and Zn) by soil amended with bentonite, calcite and zeolite as a function of pH”, *Journal of Geochemical Exploration,* **181**, 148–159 (2017).
4. BERRY et al. “An experimental study of actinide sorption onto calcite, aluminium oxide and hematite” - A report produced for United Kingdom Nirex Limited, AEAT/R/ENV/0205 (2000).

NMR and XRD provide evidence for preferential binding of cesium to crystalline zeolite phases in geopolymers

M. Arbel-Haddad[1], Y. Harnik[2], Y. Schlosser[3], A. Goldbourt[3]

[1]*Nuclear Research Center Negev, PO Box 9001, Beer Sheva 84901, Israel*
[2]*Israel Atomic Energy Commission (IAEC), Israel*
[3]*School of Chemistry, Tel Aviv University, Ramat Aviv 6997801, Tel Aviv, Israel*
e-mail: arbel.haddad@gmail.com

INTRODUCTION

Geopolymers are a class of inorganic cementitious materials obtained by alkali activation of various aluminosilicate raw materials. Whereas the preparation of geopolymers is similar to that of traditional Portland cement, their chemical nature is akin to that of zeolites, having an interconnected network of silicate and aluminate groups. The ion-binding preoperties of geoplymers, much like those of zeolites, are due to the negatively-charged tetrahedral aluminate groups. This property, together with their high chemical resistance, have made the geopolymers attractive candidates for waste immobilization applications, including nuclear waste. Special attention has been given to the immobilization of low-level radioactive wastes containing ^{137}Cs species in geopolymer matrices.

Whereas the formulation of most Cs-bearing geopolymers reported in the litterature had a relatively high SiO_2:Al_2O_3 ratio, thus yielding materials of a non-crystalline amorphous nature[1-4], our studies have focused on low-Si compositions (SiO_2:Al_2O_3 ratio < 2.0) which lead to the formation of a composite structure, with crystalline Cs-bearing zeolite domains embedded within an amorphous geopolymer matrix[5,6]. In the current study we correlated between data obtained from ^{133}Cs solid state NMR measurements and XRD measurements of the same samples. Whereas XRD data yields structural information concerning the ensemble of phases within the matrix, the chemical shift of ^{133}Cs obtained in NMR measurements is known to be sensitive to the chemical environment of the Cs ions, and is influenced by its concentration within the specific phase, by the type of nearest neighbors, and by its hydration state[7,8]. By combining the data from the two measurements we were able to identify the Cs binding sites within the geopolymers studied, and to follow the changes in the distribution of Cs between these sites upon geopolymer leaching

DESCRIPTION OF THE WORK

A series of geopolymer samples was prepared by manually mixing metakaolin (MK, PowerPozzTM) with mixed NaOH+CsOH solutions. The molar fraction of CsOH in the mixed activating solutions, CsOH:MOH (M = Na+Cs), was varied between 2.5% to 100%, while the overall water to alkali molar ratio was kept at a constant value of H_2O:MOH=5.5, (~10 M). The ratios between MK and the activating solutions were adjusted to obtain a M_2O:Al_2O_3 ratio of 1 (M = Na+Cs).

Cast samples were cured at 40ºC±3 for 3 months and consequently kept at room temperature. Cured samples were ground to yield powder samples for XRD and NMR measurements as well as for leaching experiments.

Leaching experiments were conducted by contacting 1 g powder samples with 10 ml of deionized water. The extent of leaching was determined from Cs and Na concentrations in the aqueous phase following 24 and 46 hours of contact; the leached powder samples were characterized once more by both XRD and NMR.

RESULTS AND DISCUSSION

XRD diffraction patterns of geopolymer samples with varying Cs content (Fig. 1) show diffraction peaks due to crystalline phases for all of the compositions studied. These are superimposed on a broad band due to an amorphous geopolymer phase.

The diffraction pattern for the sample with the lowest Cs content (2.5%Cs sample) is essentially the same as that observed previously for similar NaOH-based samples[6], showing distinct diffraction peaks due to zeolite A and zeolite X. As the Cs content increases, additional diffraction peaks which correspond to the Cs-bearing zeolite F were also observed. Zeolite F is the only crystalline phase indicated in the diffraction patterns of the 10%Cs sample and all samples with higher Cs content.

The ^{133}Cs MAS NMR spectra of the Cs-bearing MK-based geopolymers (Fig. 1) report on the existence of several Cs sites within the geopolymer matrices. The distribution of Cs between the different sites varies with Cs content. These changes can be correlated with the structural data obtained from XRD data, hence allowing for assignment of the features in the NMR spectra to the different phases making up the geopolymer matrix. The two ^{133}Cs signals observed in the 2.5%Cs sample spectrum correspond to zeolites A (-3.5 ppm) and X (28.0 ppm). These are also observed, albeit at slightly lower values, in the 5%Cs sample. The signal at 51.6 ppm, which is first observed in the 5%Cs sample, corresponds to the zeolite F phase, in agreement with XRD data for

this sample. It is interesting to note that the area of the peak assigned to zeolite F in the NMR spectrum of the 5%Cs sample is of the same order of magnitude as that of the remaining two peaks, although its contribution to the diffraction pattern is rather small. This result indicates preferential binding of Cs to zeolite F.

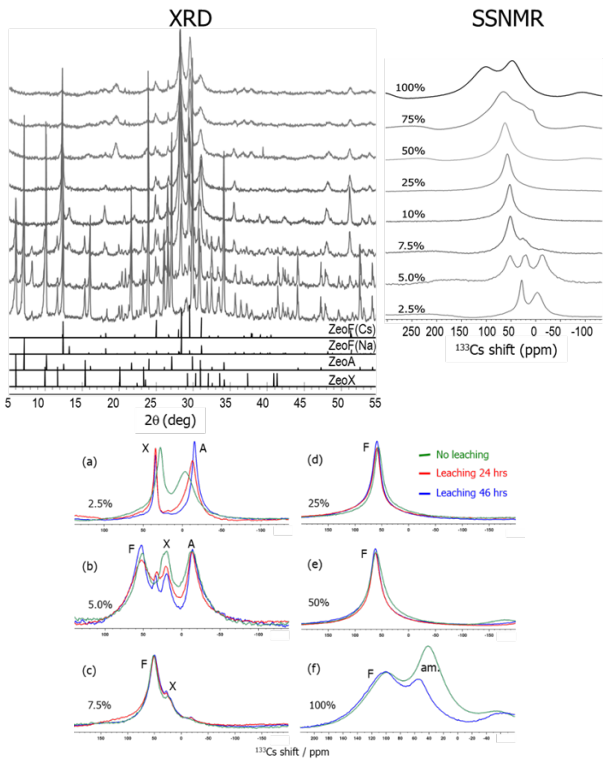

Fig. 1: Top: XRD (Left) and SSNMR (Right) data for samples with varying Cs content. NMR peaks were correlated with Cs ions residing in Zeolite A (right most peak at 2.5% and 5% Cs), zeolite X (left peak at 2.5%, mid peak at 5%, small shoulder at 7.5%), and zeolite F (dominant peak at 7.5% and higher), and the amorphous phase (right peak at 75-100%), all of which were identified in the XRD data. Bottom: Post-leaching NMR spectra (red, 24 hrs; blue, 46 hrs; green, pre-leaching) of the same samples.

The peak due to zeolite F is the dominant feature in the spectrum of the 7.5%Cs sample, and is the sole signal observed in the spectra for samples with 10%-50%Cs. A gradual increase in the corresponding ^{133}Cs chemical shift from 51.6 ppm to 62 ppm may be due to a corresponding increase in Cs content within zeolite F domains. We can thus conclude that in this composition range all of the Cs ions reside within the zeolite F domains phase. Signals at lower chemical shifts, which are assigned to Cs ions residing in the amorphous phase are observed only for the 75%Cs and 100%Cs, probably due to exhaustion of available zeolite F binding sites.

This interpretation of the spectra is further supported by the post-leaching NMR results. The 100%Cs sample lost 14% of its Cs content due to the exposure to deionized water. This resulted in a decrease in the relative intensity of the signal assigned to the amorphous peak. No significant changes were observed in the NMR spectra of the 50%Cs sample or the 7.5%Cs-25%Cs range, where Cs leaching was ~5% and <1%, respectively. The spectral changes observed for samples with low Cs content, despite the low extent of Cs leaching (<1% and ~5% for the 5%Cs and 2.5%Cs samples, respectively) are probably due to the significant leaching out of Na ions (35% and 90% for the 5%Cs and 2.5%Cs samples, respectively) and their replacement by water molecules, which affect both the distribution and mobility of Cs ions within the geopolymer.

The ability to identify the Cs binding sites and follow changes in Cs ion distribution between these sites following leaching experiments confirms our previous hypothesis concerning the efficiency of crystalline zeolite domains for Cs immobilization. We believe that the experimental approach presented here may assist in the future design of immobilization matrices for Cs as well as for other radionuclei.

REFERENCES

1. BLACKFORD, M.G. et al., “Transmission Electron Microscopy and Nuclear Magnetic Resonance Studies of Geopolymers for Radioactive Waste Immobilization”, *J. Am. Ceram. Soc.*, **90**, 1193–1199 (2007).
2. BELL, J. L. et al., “Atomic Structure of a Cesium Aluminosilicate Geopolymer: A Pair Distribution Function Study”, *Chem. Mater.* **20**, 4768–4776 (2008).
3. BERGER, S. et al., “Formulation of Caesium Based and Caesium Containing Geopolymers”, *Adv. Appl. Ceram.*, **108**, 412–417 (2009).
4. CHLIQUE, C. et al., “XRD Analysis of the Role of Cesium in Sodium-Based Geopolymer”, *J. Am. Ceram. Soc.*, **98**, 1308–1313 (2015).
5. ARBEL HADDAD, M. et al., “Formation of Zeolites in Metakaolin-Based Geopolymers and Their Potential Application for Cs Immobilization”, *J. Nucl. Mater.*, **493**, 168–179 (2017).
6. OFER-ROZOVSKY, E. et al., “Cesium Immobilization in Nitrate-Bearing Metakaolin-Based Geopolymers”, *J. Nucl. Mater.*, **514**, 247–254 (2019).
7. CHANG KIM, J. et al., “Base Catalysis by Intrazeolitic Cesium Oxides”, *Microporous Mater.* **2**, 413–423 (1994).
8. KOLLER, H. et al., “Location of Na^+ and Cs^+ Cations in CsNaY Zeolites Studied by ^{23}Na and ^{133}Cs Magic-Angle Spinning Nuclear Magnetic Resonance Spectroscopy Combined with X-Ray Structure Analysis by Rietveld Refinement”, *Microporous Mater.* **5**, 219–232 (1995).

Structural Investigation of the Adsorption von Y(III) on Orthoclase (001) Single Crystals using Resonant Surface X-ray Diffraction

J. Neumann[1], J. Lessing[1], M. Demnitz[1], P.J. Eng[2], J.E. Stubbs[2], T. Stumpf[1], M. Schmidt[1]

[1]*Helmholtz-Zentrum Dresden-Rossendorf, Institute of Resource Ecology, Bautzner Landstraße 400, 01328 Dresden, Germany*
[2] *Center for Advanced Radiation Sources, The University of Chicago, 929 E 57th Street, Chicago, IL 60637, USA*
email: j.neumann@hzdr.de

INTRODUCTION

Transport of radionuclides (RNs), from deep geological repositories for radioactive waste, such as the highly toxic trivalent minor actinides (An(III)) Am and Cm, will be controlled by their interactions with charged mineral phases. Many countries such as Finland, Sweden, and Germany consider a repository in crystalline rock, which contains large amounts of feldspars, e.g. orthoclase (K-feldspar). Hence, reliable risk assessments of potential repository sites depend on a fundamental understanding of sorption quantity and structure of An(III) on feldspars. Typically, those interactions are investigated using mineral powder samples [1], which depict an idealization of the natural system due to the small grain size of the mineral. In those studies, information about macroscopic effects on sorption processes, like crystal orientation or surface roughness, are not accessible.

Therefore, in this work we study the adsorption of Y(III), as an inactive rare earth analogue for An(III), on natural single crystal orthoclase samples of the (001) crystal orientation using the modern synchrotron-based, surface X-ray diffraction technique.

DESCRIPTION OF THE WORK

Natural single crystal orthoclase samples were freshly cleaved along their (001) orientation and reacted overnight in a solution of $[Y^{3+}] = 0.01$ M at pH = 5.0 or 6.9. After the reaction was finished, surface X-ray diffraction (SXRD) was measured *in situ* at beamline 13-ID-C (GeoSoilEnviroCARS) of the Advanced Photon Source at Argonne National Laboratory.

SXRD yields the total electron density profile of the mineral/water interface by measuring crystal truncation rods (CTR). For the first time, resonant anomalous X-ray reflectivity (RAXR) is applied on orthoclase for identification and quantification of sorption species, in our case Y^{3+}. Coverage of adsorbed Y^{3+} is given in units of Y/A_{UC} (area of the orthoclase (001) unit cell = 55.57 $Å^2$).

RESULTS AND DISCUSSION

The study investigates the adsorption of Y^{3+} on orthoclase (001) at two different pH values. RAXR spectra of both samples show strong modulations at the Y X-ray absorption edge (17.038 keV), indicating that Y^{3+} has been adsorbed to the orthoclase surface. Analysis of amplitudes and phases of the RAXR spectra yield information about coverage and distance of the adsorbed species from the surface.

At pH 5.0, two sorption species at a distance of 2.47 (Species A) and 8.35 Å (Species B1) from the uppermost oxygen-atoms (O_{surf}) of the mineral surface are identified. At higher pH (6.9), the adsorbed Y is located at a distance of 1.50 (Species C) and 4.38 Å (B2) from O_{surf}. The Y^{3+} aquo ion has hydration shells in a distance of 2.36 and 4.40 Å. Therefore, Species A can be attributed to an outer-sphere (OS) and species B1 and B2 to extended outer-sphere (EOS) sorption complexes. In contrast, Species C is closer to the surface than any other sorption species observed in this study. At the investigated pH of 6.9, more sites of the orthoclase surface are deprotonated, obviously leading to the release of parts of the hydration shell of Y. Therefore, Species C is interpreted as an inner-sphere (IS) sorption complex. A plausible, bidentate binding motif for Species C is suggested based on the obtained results, where Y^{3+} is bound to two nearest O_{surf} resulting in a Y-O bond length of 2.46 Å in an angle of 39.0°.

While the interfacial speciation between the two samples is different, the total Y coverage is found to be similar for both samples (~0.6 Y/A_{UC}). At pH 6.9 more than 70 % of the adsorbed Y^{3+} is bound as IS complex (Species C, 0.43 Y/A_{UC}). The obtained coverage of the IS complex corresponds to ~2/3 of an adsorbed Y^{3+} monolayer, assuming bidentate coordination to two O_{surf}. Overall, the obtained sorption quantity and interfacial speciation are in good agreement with the powder studies, supporting the applicability of the previously developed SCMs to simulate retention of An(III) by K-feldspar for macroscopic systems.

However, we also identify reasonable amounts of adsorbed EOS complexes that are typically not found in studies using mineral powders and therefore not

considered thermodynamic models. This result points out the need of studies working on macroscopic mineral samples to assess the impact of those species, and more general the controlling parameters relevant for natural systems, such as crystal orientation, surface roughness, and a realistic solid-liquid ratio. In conclusion, the results of this study contribute to a more realistic and reliable prediction of the mobility of trivalent actinides in the environment, and will enable a better risk assessment for deep geological repositories for radioactive waste.

ACKNOWLEDGEMENTS

This work was funded by the Federal Ministry of Economics and Technology in the frame of the SMILE project with grant 02E 11668 B and U.S. Department of Energy, Office of Science, Office of Basic Energy Sciences, Chemical Sciences, Geosciences, and Biosciences Division under Contracts DE-AC02-06CH11357 to UChicago Argonne, LLC as operator of Argonne National Laboratory.

REFERENCES

[1] NEUMANN, J. et al., “A comprehensive study of the sorption mechanism and thermodynamics of f-element sorption onto K-feldspar,” *Journal of Colloid Interface Science*, **591**, 490–499 (2021).
[2] NEUMANN, J. et al., “Sorption of trivalent rare earth elements (Eu, Y) and actinides (Cm, Am) on orthoclase (001) and (010) single crystals”, *in preparation.*

THEREDA - Thermodynamic Reference Database

Xavier Gaona[1], Frank Bok[2], Daniela Freyer[3], Helge Moog[4], Laurin Wissmeier[5]

[1]*Institute for Nuclear Waste Disposal (INE), Karlsruhe Institute of Technology (KIT), 76344 Karlsruhe, Germany*
[2]*Helmholtz-Zentrum Dresden-Rossendorf, Institute of Resource Ecology, 01328 Dresden, Germany*
[3]*Institute for Inorganic Chemistry, TU Bergakademie Freiberg, 09599 Freiberg, Germany*
[4]*Gesellschaft für Anlagen- und Reaktorsicherheit (GRS)mbH, 38122 Braunschweig, Germany*
[5]*CSD Engineers AG, Schachenallee 29A, 5000 Aarau, Switzerland*

email: xavier.gaona@kit.edu

Part of the process to ensure the safety of radioactive waste disposal is the predictive modelling of the solubility of all relevant toxic components in a complex geochemical matrix. To ensure the reliability of thermodynamic equilibrium modelling as well as to facilitate the comparison of such calculations done by different institutions it is necessary to create a mutually accepted thermodynamic reference database. To meet this demand several institutions in Germany joined efforts and created THEREDA [1] (see Fig. 1).

Fig 1. Members of the THEREDA consortium.

THEREDA is a suite of programs at the base of which resides a relational databank. Special emphasis is put on thermodynamic data along with suitable Pitzer coefficients, which allow for the calculation of solubilities in highly-saline solutions. Registered users may either view single thermodynamic data and Pitzer interaction parameters or download ready-to-use parameter files for the geochemical speciation codes PHREEQC, Geochemist's Workbench, CHEMAPP, or TOUGHREACT. The dataset can also be downloaded in a generic JSON-format to allow for the import into other codes. The database can be accessed via the World Wide Web: www.thereda.de (Fig. 2).

Prior to release, the released part of the database is subjected to many tests. Results are compared to results from earlier releases and among the different codes. This is to ensure that by additions of new and modification of existing data no adverse side effects on calculations are caused. Furthermore, the THEREDA website offers an increasing number of examples for applications, including graphical representation, which can be filtered by components of the calculated system.

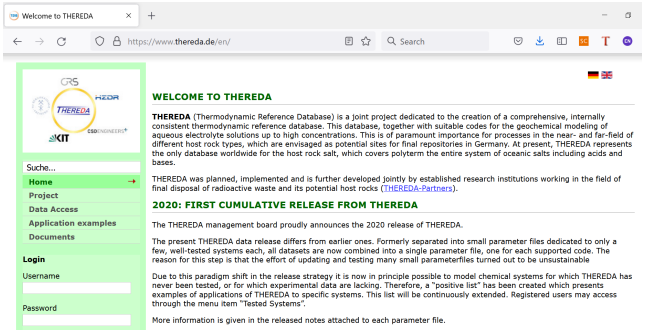

Fig 2. Screenshot of the THEREDA webpage.

ACKNOWLEDGEMENTS

THEREDA is funded by BGE – the federal company for radioactive waste disposal.

REFERENCES

[1] MOOG, H. C. et al. Disposal of Nuclear Waste in Host Rock formations featuring high-saline solutions - Implementation of a Thermodynamic Reference Database (THEREDA). *Appl. Geochem.*, **55**, 72-84 (2015).

Sorption of ^{233}U on ettringite and effects of the presence of isosaccharinic acid, citrate and phthalate.

O. Almendros, T. Missana, Ú. Alonso
Ciemat, Av. Complutense 40, 28040 Madrid, Spain
Oscar.Almendros@ciemat.es

INTRODUCTION

Uranium is a common radionuclide in radioactive waste because its presence in spent nuclear fuel. At present, in Spain, a huge part of this waste that contains uranium is stored in individualized temporary storage facilities (ITS), with the idea to end up storing them in centralized ones (CTS) until the habilitation of the deep geological repository (DGR) (ENRESA, 2006) (IAEA, 2005).

Due to the use of cementitious materials for the immobilization of nuclear waste, being low to intermediate level waste (LLW and ILW) or high-level waste (HLW), it is important to study radionuclide (RN) retention properties of ettringite because of the mineral's presence in the cement structure (ENRESA, 2006).
Cementitious materials are of special importance in LL-ILW and they are known to generate a very alkaline environment.

Ettringite ($Ca_6Al_2(SO_4)_3(OH)_{12}\cdot 26H_2O$) is one of the most common mineral phases of cement, being 10 to 20% of the material's total mass after the hydration process of the clinker (Gascoyne, 2002). The phase presents a structure formed by positively charged cation "columns" of aluminum and calcium ($[Ca_3Al(OH)_6\cdot 24H_2O]^{3+}$). At the same time, interstitial space is formed, called channels, where the charge is neutralized because it's filled with water and sulfate molecules (SO_4^{2-}) (Bokel, 2015).

Inside these repositories different types of organic materials (paper, clothes, etc), composed from cellulose can be found, which degradation products can play an important role towards radionuclide migration capabilities (Glaus, 2008). The main degradation product that comes from cellulose alkaline degradation is isosaccharinic acid (ISA), molecule with a six-carbon structure with carboxylic groups in it. The presence of this organic compound can enhance radionuclides' solubility, complicating their retention and raising the probability of RN migration to the natural environment (Keith-Roach, 2014).

Citric acid (CA) can be found in LLW-ILW because its presence in decontamination sludge (IAEA, 2021). Despite its presence does not tend to be as high as ISA, its relevance as a complexing agent is remarkable. Furthermore, because of its structure, CA is used as an analogue of ISA.

Phthalic acid (FT) may be a product of degradation of specific organic wastes like PVC and, like ISA and CA, may enhance uranium solubility (Vázquez, 2008).

DESCRIPTION OF THE WORK

In this study we analyzed the uranium retention capacity of ettringite and the effect of different organic compounds retention under alkaline conditions.

All the tests were carried out at room temperature and in an anoxic glove box under N_2 atmosphere.
We have synthetized an artificial suspension of ettringite with concentration 1 g/L, following the method described in (Baur, 2003) and used it to undergo the different experimental work with ^{233}U and the different organic compounds.

For the characterization of the solid phase different techniques were used, being the most relevant the X-Ray Diffraction Technique (XRD). Comparing our result with the bibliography (Ghorab, 2014) we can assure that; indeed, our solid phase is ettringite.

Adsorption tests were carried out using the "batch" method. For the sorption isotherms, without organics, ^{233}U was spiked in the ettringite/equilibrium suspension at different concentrations (from 5×10^{-9} to 5×10^{-6}). To achieve higher concentration also stable U was added. The pH of the suspension was approximately 10.

The contact time was 1 week. After this time, the solid and the water were separated by centrifuging (22000·g, 30 min), and three aliquots were taken for the measurement of ^{233}U activity by liquid scintillation.
For evaluating the sorption capability of the material, the distribution coefficient, K_d (E.1), was measured ($mL\cdot g^{-1}$).

$$K_d = \frac{[U]_{solid}}{[U]_{eq}} \quad \textbf{E.1}$$

To analyze the effects of the organics on U retention, the U concentration was fixed to 1E-08 (adsorption zone) whereas the concentration of organic was varied from 1×10^{-5} to 1×10^{-2} M.

RESULTS AND DISCUSSION

Results of uranium isotherm on ettringite are shown in Figure 1. The plot shows the log(K_d) evolution vs. the logarithm of the uranium concentration at the equilibrium. At the equilibrium U concentration from $10^{-8.45}$ to $10^{-6.4}$ M the distribution coefficient is stable (Log(K_d)= 4.4). The tendency breaks when the log$[U^{6+}]_{eq}$ is -6, point where an important increase of log(K_d) value is observed.

The reason behind this is attributed to a potential precipitation of the uranium because of its high concentration at the last samples.

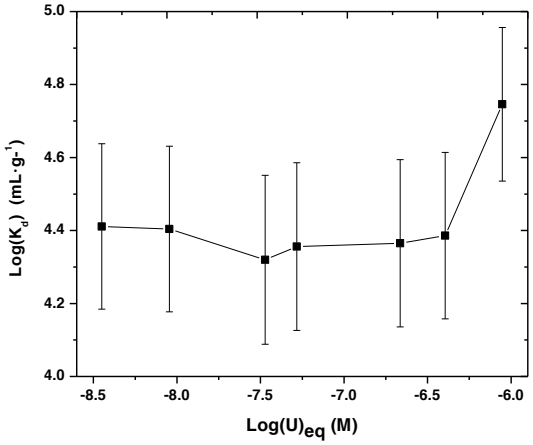

Fig. 1: Uranium Sorption isotherms in ettringite.

Figure 2 presents the results of the uranium sorption on ettringite in the presence of ISA, CA and FT.

When initial organic concentration is raised inside the suspension samples, a clear fall of uranium's log(K_d) can be observed. This tendency is shared between the three organic compounds studied, with higher or minor degree. The aforementioned could be justified because of the analogy between ISA and CA. Phthalic acid, on the other hand, because of its low solubility in water (0.6 g/100 ml), could not reach an initial concentration higher than 1×10^{-3} M in the samples. That is the reason why FT is not displayed in the full range of concentrations in the figure.

Comparing both Figures (1 and 2), one can observe that the sorption decrease is clear when the studied organic compounds are present; reaching a difference of two orders of magnitude of logK_d between both figures when ISA and CA concentration are highest (comparing the initial point without organic presence and the last point with maximum organic concentration). This comparative demonstrates that the studied organic compounds do interact in some way with uranium present in the analyzed environment, diminishing the sorption capabilities of ettringite towards the radionuclide.

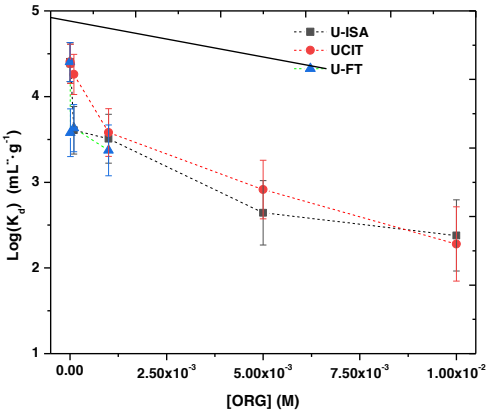

Fig. 2: Log(K_d) of uranium vs. organic concentration [ORG] in ettringite.

REFERENCES

1. BAUR I., JOHNSON C. A., "Sorption of Selenite and Selenate to Cement Minerals". *Environ. Sci. Technol*. **37**, 3442-3447 (2003).
2. BORKEL C., "Understanding the mobility of cesium, nickel and selenium released from waste disposal: chemical retention mechanisms of degraded cement" Ph.D. Thesis, Universitat Politècnica de Catalunya (2015).
3. ENRESA. "Sexto Plan General de Residuos Radiactivos". Ministerio de Industria, Turismo y Comercio (2006).
4. GASCOYNE M., "Influence of grout and cement on groundwater composition". Posiva Oy (2002).
5. GLAUS M. A., VAN LOON L.R., "Degradation of Cellulose under Alkaline Conditions: New Insights from a 12 Years Degradation Study". *Environ. Sci. Technol*. **42**, 2906–2911 (2008).
6. GHORAB H., MABROUK M, HERFORT D., ABDELTAWAB OSMAN Y. " Infrared investigation on systems related to the thaumasite formation at room temperature and 7 °C". *Cement, Wapno, Beton*. **19**, 252-261 (2014).
7. KEITH-ROACH M., LINDGREN M., "Assessment of complexing agent concentrations in SFR". SKB (2014).
8. IAEA, "Disposal Options for Disused Radioactive Sources". International Atomic Energy Agency (2005).
9. VAZQUEZ, G.J., DODGE, C.J., FRANCIS, A.J., "Interaction of Uranium (VI) with Phthalic Acid". *Inorg. Chem*. **47**, 10739–10743 (2008).

Solubility of niobium(V) in cementitious systems: identification of the solubility-controlling solid phases in hyperalkaline systems containing Ca

Yongheum Jo[1], Nese Cevirim-Papaioannou[1], Krassimir Garbev[2], Benny de Blochouse[3], Marcus Altmaier[1], Xavier Gaona[1]

[1]*Institute for Nuclear Waste Disposal, Karlsruhe Institute of Technology, Karlsruhe, Germany*
[2]*Institute for Technical Chemistry, Karlsruhe Institute of Technology, Karlsruhe, Germany*
[3]*ONDRAF/NIRAS, Sint-Joost-ten-Node, Belgium*
email: Yongheum.jo@kit.edu

INTRODUCTION

Cementitious materials are ubiquitous in disposal systems for radioactive wastes and constitute engineered barriers and structural materials of repositories. The contact with groundwater results in the gradual degradation of cement, with the consequent buffering of the pore water conditions (in non-saline systems) to $10 \leq pH \leq 13.3$ and $0.02\ M \geq [Ca] \geq 10^{-4}\ M$.

^{94}Nb is a long-lived activation product ($t_{1/2} = 2 \cdot 10^4$ yr) generated in nuclear reactors by neutron activation of stable ^{93}Nb present in structural components, *e.g.* Inconel alloy and stainless steel. Niobium is predominantly found in the +V oxidation state within the stability field of water, whereas the formation of Nb(III) is only expected under very acidic and very reducing conditions. $Nb_2O_5(s)$ is the solid phase controlling the solubility of Nb(V) in acidic to weakly alkaline pH conditions. The solubility of $Nb_2O_5(s)$ is significantly enhanced in alkaline to hyperalkaline systems due to the formation of $Nb(OH)_6^-$, $Nb(OH)_7^{2-}$ or polyniobiates at [Nb] above ≈ 1 mM. In NaCl-NaOH systems, the formation of highly soluble Na-polyniobiate solid phases, *e.g.* $Na_8Nb_6O_{19} \cdot 13H_2O(s)$, has been described in the literature [1]. In contrast to pure Na-systems, dissolved Nb concentrations significantly drop in cement pore water solutions containing calcium ([Nb] ≈ 10^{-7} – 10^{-8} M) [2], but a conclusive characterization of the solid phase/s controlling the solubility of Nb(V) in these conditions is still missing.

In this context, this work aims at quantitatively investigating the solubility of Nb(V) and characterizing the solubility-controlling solid phase/s in aqueous systems representative of cementitious pore water as well as in synthetic pore water corresponding to the degradation stage I of cement. Future dedicated experimental efforts at KIT–INE will target the thermodynamic description of the aqueous speciation and solubility of Nb(V) in alkaline systems containing Ca.

DESCRIPTION OF THE WORK

All preparation, treatment, and handling of samples were conducted in an Ar-glove box (O_2 < 1 ppm) at room temperature (T = 22 ± 2 °C). The Nb and Ca stock solutions for solubility experiments were prepared by dissolution of $NbCl_5$ in 0.02 M NaOH and $CaCl_2 \cdot 2H_2O$ in Milli-Q water, respectively. The naturally occurring stable ^{93}Nb isotope was used throughout these studies. After 1 week, the total dissolution of $1.3 \cdot 10^{-3}$ M Nb was observed in the Nb stock solution. The initial concentration of Nb in the solubility samples was varied between $1 \cdot 10^{-5}$ M and $5 \cdot 10^{-4}$ M, with $10 < pH_m < 12$ and $0.03\ M > [Ca] > 5 \cdot 10^{-3}$ M. An additional experimental solubility series was prepared in 1 M $CaCl_2$. The pH was adjusted by adding HCl and NaOH, and was measured by a combination pH electrode. An artificial cement pore water representative of the degradation stage I of cement was prepared with pH = 13.5, [Na] = 0.14 M, [K] = 0.37 M, [Ca] = $3.5 \cdot 10^{-4}$ and $1.4 \cdot 10^{-3}$ M and $[CO_3^{2-}]_{tot} = 3.4 \cdot 10^{-4}$ M (young cement pore water containing Ca, *i.e.* YCWCa) [3]. After contact times of 32, 57, and 200 days, an aliquot of the supernatant solution of each sample was taken, and potential colloids or suspended particles were removed by 10 kDa ultrafiltration. The dissolved concentration of Nb was quantified by ICP-MS. Nb solid phases were characterized after attaining equilibrium conditions (defined by constant pH_m and [Nb]). Solid phases were washed with ethanol 3 to 5 times and dried under Ar-atmosphere before characterization by powder X-ray diffraction (XRD), scanning electron microscopy with energy dispersive spectroscopy (SEM-EDS) and quantitative chemical analysis (after dissolution with a mixture of 2 % HNO_3 and 0.1 % HF).

RESULTS AND DISCUSSION

In contrast to the stable stock solution in the pure NaCl–NaOH system ($[Nb(V)] = 1.2 \cdot 10^{-3}$ M, pH = 12.3), a clear drop of the initial concentration of niobium is observed in all samples prepared in Na-Ca-Nb(V)-Cl-H_2O systems, with $[Nb(V)]_{eq} < 1.3 \cdot 10^{-7}$ M (see Fig. 1). A significant decrease of the initial Nb concentration is also observed in the YCWCa, with [Nb] ≈ $8 \cdot 10^{-7}$ – $2 \cdot 10^{-6}$ M. These observations support the formation of sparingly soluble Nb(V) solid phases, expectedly in the form of ternary solid phases containing Ca.

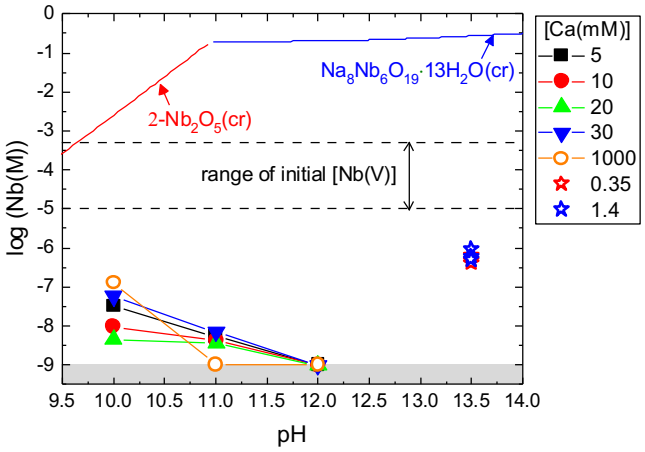

Fig. 1: Nb(V) solubility determined in alkaline to hyperalkaline systems with the initial concentrations of Ca. Symbols at pH 13.5 exhibit $[Nb(V)]_{eq}$ in YCWCa. Dashed lines are the upper and lower limits of initial [Nb(V)] range which was not held constant in the experiments. Solid lines display solubility of β-Nb_2O_5(cr) and $Na_8Nb_6O_{19}·13H_2O$(cr) calculated in 0.1 m and 0.3 m $NaClO_4$ solutions, respectively [1]. Grey area represents the detection limit of ICP-MS in the conditions of this study.

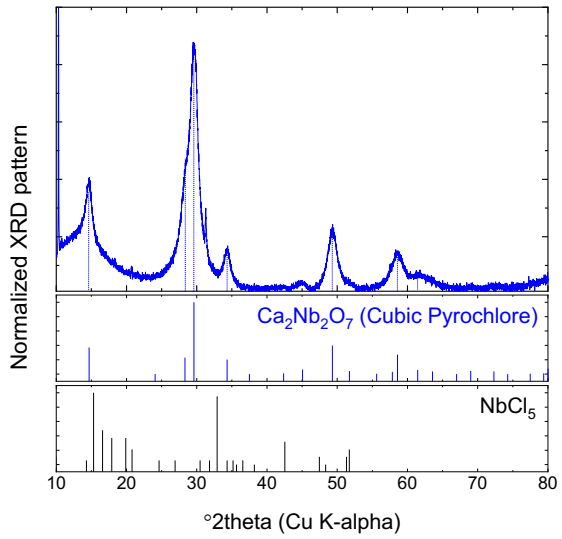

Fig. 2: XRD pattern of Nb(V) solid phase equilibrated in YCWCa (pH 13.5, [Ca] = $1.4·10^{-3}$ M) and reference patterns reported for $Ca_2Nb_2O_7$(cr) and $NbCl_5$(cr).

The results of the quantitative chemical analysis of Nb solid phases dissolved in HNO_3 + HF confirm that all solid phases contain Ca and Nb with no significant contribution of Na. The XRD pattern collected for the sample equilibrated in YCWCa is exemplarily displayed in Fig. 2, and shows a good agreement with the patterns reported for the cubic pyrochlore $Ca_2Nb_2O_7$(cr).

Our results confirm the low solubility of Nb(V) in hyperalkaline pH conditions containing Ca representative of cementitious systems. Quantitative chemical analysis and XRD unequivocally support the key role of Ca in the formation of the solid phases controlling the solubility of Nb(V) under the investigated boundary conditions. The potential implications of these results in the assessment of the Nb(V) source term in cement-based repositories for nuclear waste disposal will be discussed in this contribution.

ACKNOWLEDGEMENT

This work was partially funded by the Belgian National Agency for Radioactive Waste and enriched Fissile Material (ONDRAF-NIRAS).

REFERENCES

1. C. PEIFFERT et al., "Solubility of B-Nb_2O_5 and the hydrolysis of niobium(V) in aqueous solution as a function of temperature and ionic strength", *J. Solution Chem.*, **39**, 197-218 (2010).
2. C. TALERICO et al., "Solubility of niobium(V) under cementitious conditions: importance of Ca-niobates", *Mat. Res. Soc. Symp. Proc.,* **824**, 443-448 (2004).
3. C. CACHOIR et al., "Preparation of Evolved Cement Water (ECW) and Young Cement Waters (YCW and YCWCa) for the Supercontainer experiments" *IW.W&D.0099,* 1-8 (2006).

Influence of EDTA on the sorption of Am(III), Th(IV) and Pu(IV) on hardened cement paste

Janina Stietz[1], S. Herz[1], S. Amayri[1], T. Reich[1]

[1] *Johannes Gutenberg-Universität Mainz, Department Chemie, 55099 Mainz*
jastietz@uni-mainz.de

INTRODUCTION

Cementitious materials are part of the technical barrier in a deep geological nuclear waste repository. Due the degradation of cement, organic ligands present in the form of cement additives or as cementitious waste components could possibly influence the migration behaviour of actinides (An) in the host rock of the repository. The competition and synergetic effect in the ternary system (organic / radionuclide / cement) was investigated by batch experiments in cement degradation state I (pH > 12.5) [1] using artificial cement pore water (ACW; 0.11 M NaOH & 0.18 M KOH) [2] as background electrolyte.

Ethylenediaminetetraacetic acid (EDTA) is used as a decontamination reagent in radioactive waste reprocessing for its ability to form stable complexes with a wide range of cations, including actinides and was therefore chosen as a model organic ligand system. Under the reducing conditions that are expected in a nuclear repository, the tri- and tetravalent species of actinides will dominate. Therefore, the actinides Am(III) and Th(IV) were used as analogous of redox sensitive actinides such as Pu. For comparison, an additional experiment was performed with Pu(IV).

DESCRIPTION OF THE WORK

Initially, the sorption of ^{14}C-labelled EDTA on hardened cement paste (HCP) was investigated as a binary system. The batch experiments were performed as a function of a solid-to-liquid-ratio (S/L) (c_0 (EDTA) = const. = 0.01 M; S/L = 0.5 - 20 g/L) and as sorption isotherm of EDTA (S/L = const. = 5 g/L; c_0 (EDTA) = $1x10^{-1}$ - 1×10^{-9} M).

In experiments with the ternary system, the influence of EDTA (c_0 (EDTA) = 0.01 M) on the sorption of actinides (c_0 (An) = $1x10^{-8}$ M) ^{232}Th(IV) and ^{239}Pu(IV) as well as ^{241}Am(III) on HCP (S/L = 5 g/L) was investigated as a function of addition order after a contact time of 72 h: (i) (An + HCP) + EDTA, (ii) (EDTA + HCP) + An, and (iii) (An + EDTA + HCP).

Also, in an additional experiment of sorption isotherms with Th(IV) (c_0(Th(IV)) = 1×10^{-6} - 1×10^{-11} M) on HCP (S/L = 0.09 g/L), the influence in the presence and absence of EDTA (c_0 (EDTA) = 0.01 M) was studied.

Furthermore, "screening batch experiments" with other relevant organic ligands (e.g. isosaccharinic acid (ISA), phthalate, oxalate, citrate) were carried out and the results will be presented.

RESULTS AND DISCUSSION

The results for the binary system (EDTA / HCP) indicate a low sorption of EDTA ($S_{\%} \leq 7\%$) on HCP. Therefore, no blocking of sorption sites by EDTA on HCP is assumed.

In experiments with the ternary system (EDTA / An / HCP) a quantitative sorption ($S_{\%} > 99\ \%$) of ^{241}Am(III), ^{232}Th(IV) and ^{239}Pu(IV) on HCP was observed in all cases in the presence of EDTA. The order of addition shows no influence of actinide retention. The investigation of the sorption isotherms with Th(IV) show a difference between the obtained two plots of the binary and the ternary system (see Figure 1). This could indicate an influence of the EDTA on the sorption of Th(IV) on HCP, which may due to the formation of a quaternary complex (Th(IV)-EDTA-OH-Ca) as recently described for the Pu(IV) by DiBlasi et al. [3].

In the screening experiments, only a difference of the sorption of the order of addition was determined for the organic ligand ISA. For all other ligands, a quantitative sorption of was also observed.

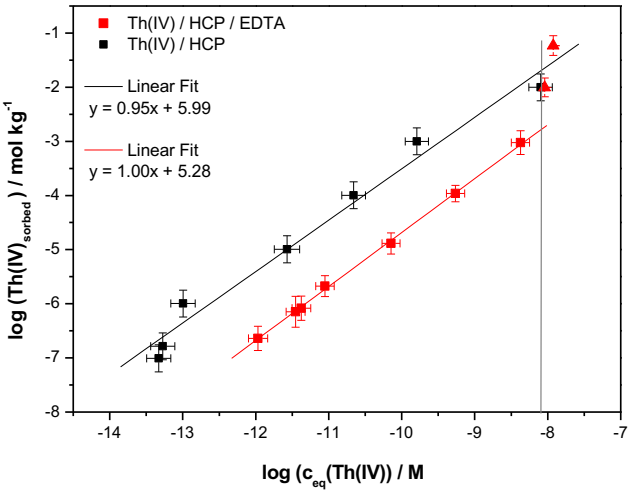

Fig. 1: Sorption isotherms of Th(IV) on HCP (S/L = 0.09 g/L) in the presence (red) and absence (black) of EDTA (c_0 (EDTA) = 0.01 M) at pH 13.

ACKNOWLEDGMENT

This work was performed within the EURAD project - WP CORI, which receives funding from the EU Horizon 2020 Research and Innovation Program under grant agreement No 847593.

REFERENCES

1. OCHS, M., et al., *Radionuclide and Metal Sorption on Cement and Concrete*, Vol. 2, p. 1 and p. 12, Springer (2016).
2. WIELAND, E., et al., "Experimental evidence for solubility limitation of the aqueous Ni(II) concentration and isotopic exchange of ^{63}Ni in cementitious systems", *Radiochim. Acta,* **94**, 29-36, (2006).
3. DIBLASI, N.A., et al., "Impact of Ca(II) on the aqueous speciation, redox behavior, and environmental mobility of Pu(IV) in the presence of EDTA", *Science of the Total Environment,* **783**, 146993 (2021).

Atomistic computer simulation of the structure and properties of iodide-containing hydrocalumite (AFm phase)

Andrey G. Kalinichev[1,2], Artem A. Glushak[2], Evgeny V. Tararushkin[2,3]

[1]*Laboratoire SUBATECH (UMR 6457 - IMT-Atlantique, Université de Nantes, CNRS), France*
[2]*National Research University Higher School of Economics, Moscow, Russian Federation*
[3] *Russian University of Transport, Moscow, Russian Federation*
email: kalinich@subatech.in2p3.fr

INTRODUCTION

^{129}I is one of the major dose-determining radionuclides present in low and intermediate level radioactive waste [1,2]. It is highly solvable in water in the anionic form of I^- and, therefore, highly mobile. Cementitious AFm phases (calcium aluminates) are considered as good candidates for immobilization of the I^- anions, but experimental investigation of their capabilities to do so effectively has just started recently [3].

In recent years, atomistic computer simulations have increasingly proved to be a highly useful tool to study such kind of materials and processes on the fundamental molecular scale and to quantitatively investigate the molecular mechanisms controlling adsorption, retention, and diffusional mobility of aqueous species in the structure and at interfaces of many practically important materials [4,5]. In fact, a very similar chloride-containing AFm phase – hydrocalumite – has been simulated in significant molecular detail already 20 years ago [6,7].

Here we report first results of a similar atomistic simulations study for the iodide-containing AFm phase.

DESCRIPTION OF THE WORK

Molecular computer simulations of two AFm phases of hydrous Ca-aluminates were performed in parallel for comparison of their structural and adsorptive properties: $[Ca_2Al(OH)_6]\,Cl{\cdot}2H_2O$ (also called hydrocalumite or Friedel's salt) and $[Ca_2Al(OH)_6]\,I{\cdot}2H_2O$. The layered structure of hydrocalumite is formed by distorted Ca-hydroxide and Al-hydroxide octahedra. Its interlayers are formed by a highly ordered arrangement of Cl^- anions and H_2O molecules. It is structurally one of the best understood of the layered double hydroxides (LDHs) and can serve as a good model for other less ordered natural and synthetic LDH phases important for a wide variety of technological applications, including environmental remediation.

The earlier atomistic simulations of hydrocalumite [6,7] were among the first successful applications of the ClayFF force field model that is capable to realistically describe all interatomic interactions in such kind of systems [4]. Here we are taking advantage of the new updated parametrization of ClayFF, which can now more accurately account for the bending of Al−O−H and Ca−O−H angles in the mineral structure [5].

RESULTS AND DISCUSSION

The structural and dynamic properties of interlayer and surface species (Cl^-, I^-, H_2O) of the simulated AFm phases were calculated from classical molecular dynamics simulations using standard relationships and approaches [5,7]. Two sets of systems were simulated: bulk crystalline AFm phase and the same crystals in contact with ~0.6M aqueous solutions of CsCl or CsI.

The highly ordered interlayer structure observed earlier for Cl-AFm phase [6,7] is equally well preserved when Cl^- ions are fully replaced by I^- (Fig.1). This indicates that the iodide can be very efficiently retained in the interlayers of the AFm phase.

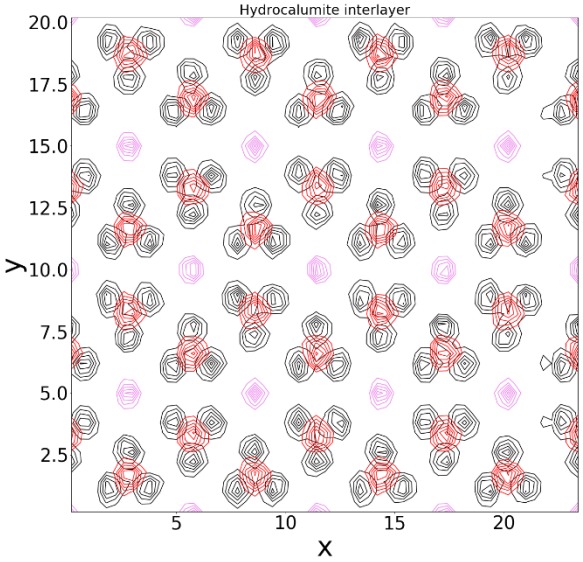

Fig. 1: The time-averaged atomic density distribution of aqueous species in the interlayer of iodide-containing AFm phase (hydrocalumite). Red contours – atoms of O_{H2O}, black contours – atoms of H_{H2O}, pink contours – I-anions. H_2O molecules can assume three different orientations simultaneously donating hydrogen bonds to two out of three neighboring anions [7].

On the AFm surface, the adsorption of I^- is somewhat less strong than that of Cl^- (Fig.2), but the adsorption is still very strong and most iodides can be significantly immobilized by surface adsorption.

The diffusion coefficients of aqueous species could have only been qualitatively evaluated at this time because of the poor statistics due to the relatively small size of the simulated systems and relatively short simulation times. However, these preliminary estimates clearly confirm earlier results [6,7] indicating that the anionic diffusion rate at the surface is about an order of magnitude lower than in the bulk aqueous solution and at least two orders of magnitude lower for the anions retained in the interlayer. These dynamical results are consistent with the structural picture presented in Figs.1,2.

More accurate quantitative calculations are currently in progress and will be reported later.

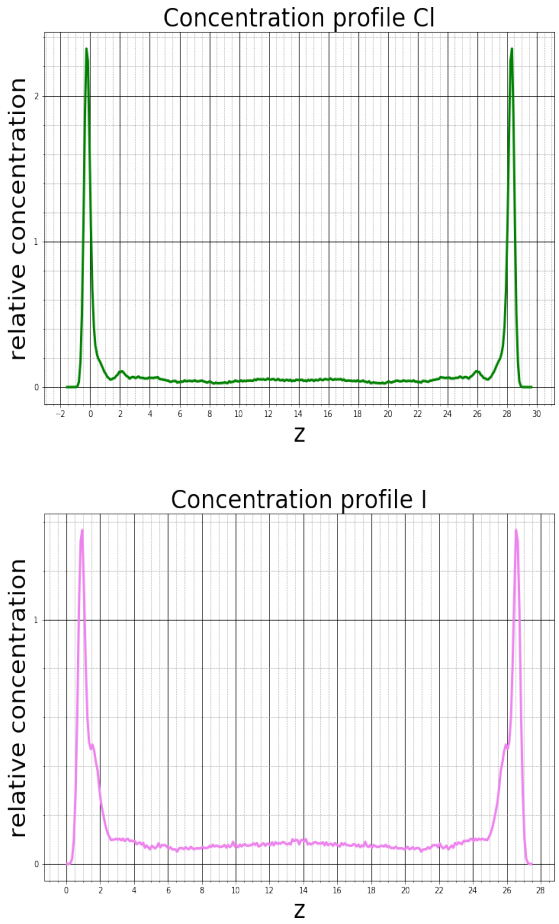

Fig. 2: The time-averaged atomic density profiles of Cl^- (top) and I^- (bottom) anions across a 30 Å-thick layer of aqueous solution. Differences in surface adsorption are distinctly visible and can be largely attributed to the differences of ionic sizes of the two species.

REFERENCES

1. GRAMBOW, B., "Mobile fission and activation products in nuclear waste disposal", *J. Contam. Hydrol.,* **102**, 180-186 (2008).
2. GRAMBOW, B. et al., "Retention and diffusion of radioactive and toxic species on cementitious systems: Main outcome of the CEBAMA project", *Appl. Geochem.,* **112**, 104480 (2020).
3. NEDYALKOVA, L. et al., "Uptake of iodide by calcium aluminate phases (AFm phases)", *Appl. Geochem.,* **116**, 104559 (2020).
4. CYGAN, R.T. et al., "Molecular models of hydroxide, oxyhydroxide, and clay phases and the development of a general force field", *J. Phys. Chem. B,* **108**, 1255-1266 (2004).
5. CYGAN, R.T. et al., "Advances in Clayff molecular simulation of layered and nanoporous materials and their aqueous interfaces", *J. Phys. Chem. C,* **125**, 17573-17589 (2021).
6. KALINICHEV, A.G. et al., "Molecular modeling of the structure and dynamics of the interlayer and surface species of mixed-metal layered hydroxides: Chloride and water in hydrocalumite (Friedel's salt)", *American Mineralogist,* **85**, 1046-1052 (2000).
7. KALINICHEV, A.G. et al., "Molecular dynamics modeling of chloride binding to the surfaces of calcium hydroxide, hydrated calcium aluminate, and calcium silicate phases", *Chem. Mater.,* **14**, 3539-3549 (2002).

Overview of the EURAD-CORI (Cement-Organics-Radionuclides-Interactions) project

M. Altmaier[1], D. Garcia[2], P. Henocq[3], N. Mace[4], T. Missana[5], D. Ricard[3], J. Vandenborre[6]

[1]*Karlsruhe Institute of Technology, Institute for Nuclear Waste Disposal, Karlsruhe – Germany*
[2] *DEN, CEA, Université Paris-Saclay, F-91191 Gif-sur-Yvette – France*
[3]*Amphos 21 Consulting S.L., c/ Veneçuela, 103. 2nd floor. 08019 Barcelona – Spain*
[4]*AGENCE NATIONALE POUR LA GESTION DES DÉCHETS RADIOACTIFS (ANDRA), 1-7, rue Jean-Monnet - 92298 Châtenay-Malabry cedex – France*
[5]*CIEMAT, Avda. Complutense 40 - 28040 Madrid – Spain*
[6]*SUBATECH, UMR 6457, Institut Mines-Télécom Atlantique, CNRS/IN2P3, Université de Nantes; 4, Rue Alfred Kastler, La chantrerie BP 20722, 44307 Nantes cedex , – France*
email: marcus.altmaier@kit.edu

The CORI (Cement-Organics-Radionuclides-Interactions) Workpackage integrated into EURAD [1] performs research to improve the knowledge on the organic release issues which can accelerate the radionuclide migration in the context of the post closure phase of geological repositories for ILW and LLW/VLLW including surface/shallow disposal. The R&D in CORI extends the current state-of-the-art and will contribute to optimize disposal solutions and consider questions of regulatory concern. CORI results will help member states to further develop their national R&D programs and support programs at an early implementation stage.

CORI research addresses topics in the context of cement-organics-radionuclides-interactions. Organic materials are present in some nuclear waste and as admixtures in cement-based materials and can potentially influence the performance of a geological disposal system, especially in the context of low and intermediate level waste disposal. The potential effect of organic molecules is related to the formation of complexes in solution with some radionuclides of interest (actinides + lanthanides) which can (i) increase radionuclide solubility and (ii) decrease radionuclide sorption. Organic substances require special attention since a significant quantity exists in the waste and in the cementitious materials, with a large degree of chemical diversity. Cement-based materials will be degraded with time, leading to specific alkaline pH conditions under which the organics can degrade, thus increasing their impact on repository performance. CORI has prepared a State-of-the-Art document [2] which gives an introduction to the main research topics targeted in CORI.

The three R&D Tasks in CORI are:

ORGANIC DEGRADATION**.** Focus is on the characterization of soluble organic species generated by radiolytic and hydrolytic degradation of selected organics (PVC, cellulose, resins, superplasticizers). Studies also include the analysis of degradation and stability of small organic molecules such as carboxylic acids and the determination of degradation rates.

ORGANIC-CEMENT-INTERACTIONS. Studies focus on investigating the mobility of selected organic molecules in cement-based materials. Mobility of organic molecules includes sorption and transport properties. Organics will also include small ^{14}C bearing molecules as identified in the EC EURATOM project CAST. Both retention on individual cement phases and cementitious systems are investigated.

RADIONUCLIDE-ORGANIC-CEMENT-INTERACTIONS. Consistent with the set of organics, individual cement phases and materials identified in the above two Tasks, radionuclide migration processes are studied in the ternary system. The role of organic molecules on the transfer properties of radionuclides are investigated through sorption and transport experiments. Selected radionuclides cover a range of chemical characteristics and redox states relevant for conditions in L/ILW disposal.

REFERENCES

1. EURAD – European Joint Programme on Radioactive Waste Management. https://www.ejp-eurad.eu/
2. The CORI State-of-the-Art report is available at the EURAD Website at: https://www.ejp-eurad.eu/publications/eurad-deliverable-31-cori-sota-cement-organic-radionuclide-interactions-content-lilw.

ACKNOWLEDGEMENT

The project leading to this application has received funding from the European Union's Horizon 2020 research and innovation programme under grant agreement No 847593.

Towards nuclear waste confinement: solid solutions and phase stability in (Th/Ce)-Y-zirconia systems

Volodymyr Svitlyk[1,2], Stephan Weiss[1], Christoph Hennig[1,2]

[1]*Helmholtz-Zentrum Dresden-Rossendorf, Institute of Resource Ecology, 01314 Dresden, Germany*
[2]*Rossendorf Beamline (BM20), European Synchrotron Radiation Facility, 38000 Grenoble, France*
email: v.svitlyk@hzdr.de

INTRODUCTION

Safe disposal of spent nuclear fuel (SNF) requires matrix materials with strong resistance against corrosion and dissolution over a period of 10^6 years. Derivatives of zirconium-based ceramics, in particular zirconia, ZrO_2, are promising materials for these applications since these phases are known to remain stable in geological cycles of up to 10^9 years. Here scientific and technological goals are to obtain zirconium-based ceramic materials containing maximum possible tetravalent actinides (An) without Zr/An phase separation. In addition, structural stability of these phases under various external parameters, e.g. temperature (*T*), pressure (*P*), irradiation and leaching resistance is essential in order to exclude possible discharge of the incorporated radioactive elements over a long time scale.

Five different structural modifications of zirconia are known to exist. At ambient pressure undoped ZrO_2 phase exhibits three different polymorphs as a function of temperature - low-temperature (*LT*) monoclinic (7-fold coordination of Zr atoms, $P2_1/c$) and parent *HT* tetragonal (T > 1440 K), and cubic (T > 2640 K) forms (8-fold coordination, $P4_2/nmc$ and $Fm\text{-}3m$, respectively) [1]. Upon application of high pressure (*HP*) monoclinic modification of zirconia transforms into orthorhombic-I phase (*Pbca*, 7-fold coordination of Zr atoms similar to that observed for the parent monoclinic $P2_1/c$ phase) at pressure of ~ 4 GPa [2]. Upon further compression at P > 25 GPa orthorhombic-I modification transforms into orthorhombic-II phase (*Pnma*, 9-fold coordination) [3] and this phase was found to be stable up to at least 100 GPa [4].

Various properties of ZrO_2 can be efficiently controlled by doping. In particular, introduction of Y^{3+} ions is known to significantly influence phase stability range of zirconia and to stabilize desired HT modifications. Specifically, tetragonal Y-stabilized zirconia (YSZ) phases, denoted as *t*′, can be obtained at ambient temperature for Y content of ~ 3 - 15 at.% and the cubic YSZ phase can be stabilized for Y content > ~15 at.% [5]. The YSZ phases are, however, much more poorly studied as a function of temperature and pressure compared to the parent ZrO_2 compound and the reported results are sometimes contradictory. In this work we present synchrotron radiation diffraction studies on incorporation of Th and Ce atoms in various YSZ phases as a function of composition, temperature and pressure.

DESCRIPTION OF THE WORK

Five series of samples have been synthesized for the current study: $Zr_xY_{0.11}Th_yO_{2-z}$ (y = 1 – 7%, ~ 1% step), $Zr_xY_{0.14}Th_yO_{2-z}$ (y = 4, 7, 10, 12%), $Zr_xY_{0.21}Th_yO_{2-z}$ (y = 0 – 11%, ~ 3% step), $Zr_xY_{0.10}Ce_yO_{2-z}$ (y = 0 – 8%, ~ 1.5% step) and $Zr_xY_{0.16}Ce_yO_{2-z}$ (y = 0 – 8%, ~ 1.5% step). All samples have been obtained via precipitation of the corresponding metal salts by increasing the pH (pH equal 8 for Th- and 11 for Ce-containing samples, correspondingly). Obtained suspensions were subsequently centrifuged and the residues were dried at 350 K. Final oxide phases were formed by annealing at 1673 K for two hours with further quenching.

Ambient, *T*- and *P*-dependent *in situ* synchrotron radiation diffraction experiments were performed at the ROBL BM20 beamline [6] at ESRF, Grenoble. *HT* was obtained with hot gas blower and *HP* was generated using diamond anvil cells (DAC). Diffraction data were collected on high resolution XRD1 (Pilatus 100k) and multipurpose XRD2 (Pilatus3 X 2M, *HT* and *HP* experiments) diffractometers of ROBL [6].

RESULTS AND DISCUSSION

For the tetragonal $Zr_xY_{0.11}Th_yO_{2-z}$ and $Zr_xY_{0.14}Th_yO_{2-z}$ series maximum Th intake was found to be ~ 10 at.%, as concluded from the corresponding expansion of the unit cell volume as a function of % Th (Fig. 1, left). In addition, appearance of ThO_2 in the sample with 12 at. % Th also confirms this solubility limit.

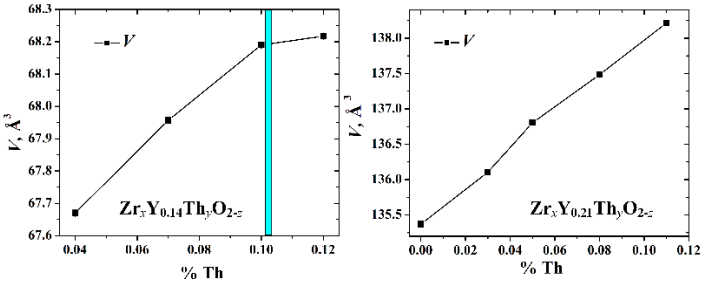

Fig. 1: Evolution of the unit-cell volumes in tetragonal $Zr_xY_{0.14}Th_yO_{2-z}$ (left) and cubic $Zr_xY_{0.21}Th_yO_{2-z}$ (right).

Introduction of Th atoms into the YSZ system induces flattening of the ZrO8 polyhedra (Fig. 2). This behaviour

is explained by the larger ionic radius of Th^{4+} compared to Ce^{4+} (1.19 vs. 0.98 Å, respectively, in 8-fold coordination [7]). Thus, insertion of Th atoms introduces additional volume in the unit cell allowing for the coordinating oxygen atoms to arrange in a more symmetrical way with more equilibrated Zr-O distances. Accordingly, the higher Th at. % content may be expected to be favoured by higher (cubic) symmetry. Indeed, cubic $Zr_xY_{0.21}Th_yO_{2-z}$ system featured intake of Th up to at least 11 at.%, as concluded from the corresponding expansion of the unit cell volume (Fig. 1, right). Investigations in the cubic YSZ system for higher Th content are in progress.

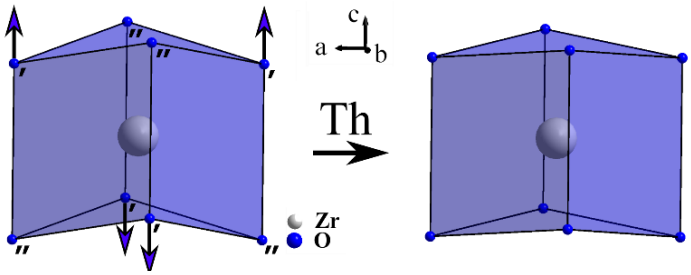

Fig. 2: Evolution of ZrO8 polyhedra upon introduction of Th atoms.

Structural stability of An-containing compounds is one of key requirements for introduction of these materials in the underground nuclear waste repositories (NWR) for long-term storage. This includes resistance against corrosion and internal irradiation. While the underground *T*-*P* conditions at the NWR level (typically 500 m below the ground) are rather mild (T ~ 310 K, P ~ 100 bars (or 0.01 GPa)), partial subduction of NWR over a period of million years can not be excluded. This would expose An-containing phases to more extreme temperatures and pressures. In addition, elevated T can be produced in case of a fire outbreak. Therefore, studies of structural stabilities of the corresponding matrix materials under extreme *T*-*P* conditions allow to simulate and accelerate processes which can possibly occur during the storage period.

For the corresponding studies we have synthesized Ce-containing YSZ series. Ce is widely used as surrogate atom to simulate tetravalent radioactive elements like Th, U or Pu. *In situ* *T*-dependent diffraction studies on tetragonal $Zr_xY_{0.10}Ce_yO_{2-z}$ and cubic $Zr_xY_{0.16}Ce_yO_{2-z}$ series in a *RT*-1150 K range revealed excellent structural stability for all the studied compounds. In particular, occupancy of Ce^{4+} atoms as a function of temperature does not decrease in these systems (Fig. 3, $Ce_{0.05}Y_{0.10}Zr_{0.85}O_{1.95}$ phase is shown as an example) indicating that the mobility of these ions does not increase with temperature. Within the error range unit cell volume increases linearly for all the phases. The corresponding coefficients of thermal expansion, defined as $\alpha = 1/V_0*((V-V_0)/(T-T_0))$, with $V_0(V)$ and $T_0(T)$ being the initial (final) unit cell volume and the sample temperature, are listed in Table 1. Cubic Ce-YSZ samples are slightly stiffer than the corresponding tetragonal phases.

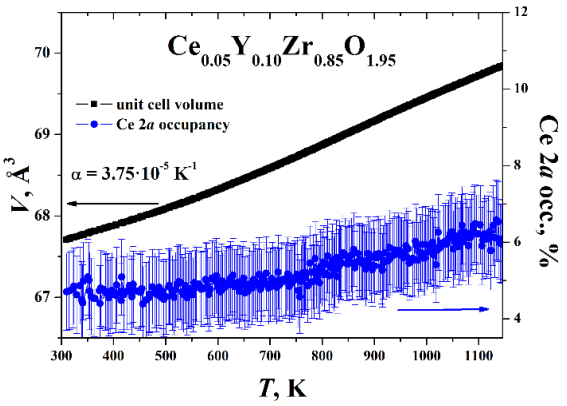

Fig. 3: Unit cell volume (V, left ordinate) and occupancy of Ce atoms on 2*a* site (right ordinate) as a function of T for tetragonal $Ce_{0.05}Y_{0.10}Zr_{0.85}O_{1.95}$.

Table 1. Coefficients of linear thermal expansion ($x10^{-5}$) for tetragonal (*t*) and cubic (*c*) Ce-YSZ phases

t-Ce-YSZ, at. % Ce	α, K^{-1}	*c*-Ce-YSZ, at. % Ce	α, K^{-1}
0	3.66	0	3.52
2.4	3.62	2.2	3.52
4.9	3.75	4.7	3.53
7.0	3.72	6.9	3.53
8.2	3.90	8.6	3.61

Application of external pressure on the $Ce_{0.05}Y_{0.10}Zr_{0.85}O_{1.95}$ phase induced a structural transformation to a higher cubic symmetry around the P ~ 8.5 GPa. Interesting, occupancy of Ce^{4+} remains stable throughout the transition. This together with *T*-dependent data indicates excellent affinity of Ce atoms with the host YSZ matrices. The parent YSZ phases are, therefore, promising candidates as host matrices for radiotoxic tetravalent elements like U, Th or Pu.

ACKNOWLEDGEMENTS

We acknowledge the Federal Ministry of Education and Research (Germany) for the support of this project (BMBF grant 02NUK060).

REFERENCES

1. M. BOCANEGRA-BERNAL *et al.*, "Phase transitions in zirconium dioxide and related materials for high performance engineering ceramics," *J. Mater. Sci.*, **37**, 4947-4971 (2002).
2. O. OHTAKA *et al.*, "Structural Analysis of Orthorhombic ZrO_2 by High Resolution Neutron Powder Diffraction," *Proc. Jpn. Acad. Ser. B*, **66**, 193-196 (1990).

3. J. HAINES *et al.*, "Crystal Structure and Equation of State of Cotunnite-Type Zirconia," *J. Am. Ceram. Soc.*, **78**, 445-448, (1995).
4. O. OHTAKA *et al.*, "Phase relations and equation of state of ZrO_2 to 100GPa," *J. Appl. Crystallogr.*, **38**, 727–733 (2005).
5. H. G. SCOTT, "Phase relationships in the zirconia-yttria system," *J. Mater. Sci.*, **10**, 1527 (1975).
6. A. C. SCHEINOST *et al.*, "ROBL-II at ESRF: a synchrotron toolbox for actinide research," *J. Synchr. Rad.*, **28**, 333-349 (2021).
7. R. D. SHANNON, "Revised effective ionic radii and systematic studies of interatomic distances in halides and chalcogenides," *Acta Crystallogr. Sect. A*, **32**, 751-767 (1976).

Investigation of the Solubility, Redox Behavior, and Aqueous Speciation of the Ternary Plutonium-EDTA-Calcium System

Nicole A. DiBlasi[1,2], Agost G. Tasi[2], Xavier Gaona[2], David Fellhauer[2], Michael Trumm[2], Andreas Schnurr[2], Kathy Dardenne[2], Jörg Rothe[2], Donald T. Reed[3], Amy E. Hixon[1], and Marcus Altmaier[2]

[1]*Department of Civil & Environmental Engineering & Earth Sciences, University of Notre Dame, Notre Dame, IN, USA*
[2]*Karlsruhe Institute of Technology, Institute for Nuclear Waste Disposal, Karlsruhe, Germany*
[3]*Los Alamos National Laboratory, Actinide Chemistry and Repository Science Program, Carlsbad, NM, USA*
email: nicole.diblasi@kit.edu

INTRODUCTION

Understanding the formation, stability, and behaviour of aqueous complexes formed by Pu(III/IV), ethylenediaminetetraacetic acid (EDTA), and competing cations is essential for accurate geochemical modelling of plutonium (Pu) in underground repository systems in cases where significant inventories of EDTA are expected. In the absence of competing cations, the formation of Pu(III)- and Pu(IV)-EDTA aqueous complexes in reducing to anoxic conditions is described in the literature.[1-9]

Calcium (Ca) is expected to be present in geological repositories due to the use of concrete in some disposal concepts and because of its prevalence in environmental systems and in the mineralogy found near geological repositories.[10] For example, it is estimated that upon water intrusion into the Waste Isolation Pilot Plant (WIPP) in Carlsbad, NM, Ca concentrations will be 7–20 mM.[11] In this context, Ca is expected to compete with Pu for EDTA complexation due to high Ca:Pu:EDTA ratios and the stability of the $CaEDTA^{2-}$ complex, which prevails over a very broad pH-range (~3–14).[3] For other chelating ligands (L), such as gluconate (GLU), isosaccharinic acid (ISA), or citrate, the formation of ternary complexes (e.g., Ca-$Pu^{III/IV/VI}$-L) has been described.[12-15] Similarly, ternary Ca-Pu-EDTA complexes may also be present in such systems.

EDTA has also been shown to impact Pu redox chemistry, resulting in the preferential stabilization of Pu(IV)-EDTA complexes regardless of initial oxidation state.[2,6,8,17] This contribution aims at evaluating the solubility, complexation, redox, and competition phenomena of the Pu(III)-Pu(IV)-EDTA-Ca system.

DESCRIPTION OF THE WORK

Pu-EDTA complexation was investigated using undersaturation experiments conducted under inert gas atmosphere (Ar) with < 2 ppm O_2 at T = (22 ± 2) °C. Undersaturation solubility experiments were performed using well-defined ^{242}Pu solid phases ($Pu(OH)_3$(am) or PuO_2(ncr,hyd); (ncr) indicates nanocrystallinity) equilibrated in aqueous solutions with constant EDTA concentration (10^{-3} M), constant pH_c (9 or 11, where $pH_c = -\log[H^+]$), and varied Ca concentration (0–3.5 M). Redox conditions were buffered with either hydroquinone (HQ, moderately reducing), tin(II), or sodium dithionite (Sn(II), DT, very reducing). A series of experiments with PuO_2(ncr,hyd) and EDTA was also performed at $1.5 \leq pH_c \leq 11$ in the absence of Ca and redox buffers and with PuO_2(ncr,hyd) and $Pu(OH)_3$(am) at pH_c = 9 in WIPP-specific brines buffered by HQ and DT, respectively. pH_c and pe were measured at regular time intervals and Pu concentrations were monitored as a function of time after 10 kD ultrafiltration via inductively coupled plasma mass spectrometry (ICP-MS). Vis-NIR spectra of selected samples were collected to evaluate the aqueous-phase oxidation state of Pu and to examine the extent of Pu-EDTA complexation.[2,6,8,16-19] Speciation of both solid and solution phases was probed with X-ray absorption spectroscopy (XAS), utilizing both X-ray absorption near edge structure (XANES) for Pu oxidation state determination and extended X-ray absorption fine structure (EXAFS) for determination of the coordination environments in the complexes and solid phases controlling the solubility.

On the basis of the similar ionic radii of Pu^{3+} and Cm^{3+} (1.00 Å and 0.97 Å, respectively)[19-21] and the favourable spectroscopic properties of Cm, a series of Cm(III)-EDTA experiments were conducted using time resolved laser fluorescence spectroscopy (TRLFS) to determine the impact of Ca on An(III)-EDTA complexation. Aqueous solutions were prepared at constant EDTA concentration (10^{-3} M), pH (7, 9, 11, or 12), and Cm(III) concentration (10^{-7} M). Ca was titrated into experimental solutions ($0 \leq [Ca(II)]_{tot} \leq 3.5$ M) and TRFLS measurements were taken after each progressive titration.

RESULTS AND DISCUSSION

Fig. 1 shows the solubility of PuO_2(ncr,hyd) in the presence of 1 mM EDTA and variable Ca concentrations (0–3.5 M). These solubility measurements are compared to the Rai et al.[6] solubility model calculated with $[EDTA]_{tot}$ = 1 mM, $[Ca]_{tot}$ = 0–0.02 M, and I = 0.1 M. Data in the absence of Ca (Fig. 1a) shows that Pu

concentrations decrease with increasing pH following the trend of the Rai et al.[6] model, indicating stepwise hydrolysis of Pu(IV)-EDTA complexes. However, the model consistently overpredicts the solubility data by 1.0–1.5 $\log_{10}$ units. The nearly pH-independent trend observed for the solubility data in the presence of Ca (Fig. 1b) suggests the formation of novel Ca-containing complex(es) within the Ca-Pu(IV)-H_2O-EDTA system. Model re-evaluation to update the Pu(IV)-OH-EDTA formation constants and include quaternary Ca-Pu(IV)-OH-EDTA complex(es) was also performed for these data.

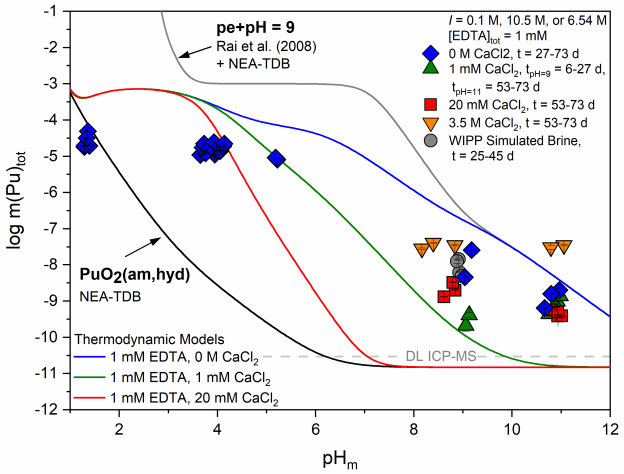

Fig. 1: Solubility of PuO_2(ncr,hyd) in experiments containing 1 mM EDTA and variable Ca concentrations as compared to the Rai et al.[6] Pu(IV)-EDTA speciation model.

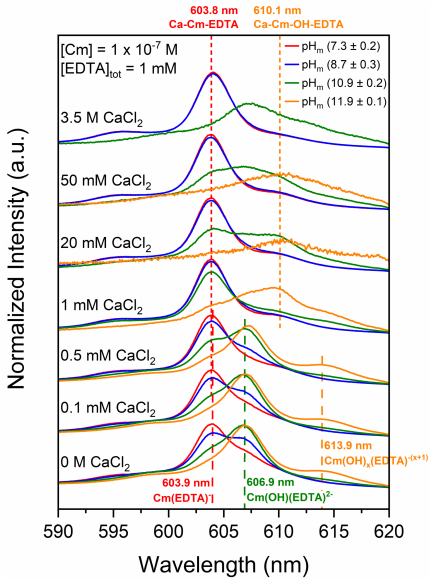

Fig. 2: Cm(III)-TRLFS spectra in experiments containing 1 mM EDTA as a function of pH (7, 9, 11, or 12) and increasing Ca concentration (0–3.5 M).

Fig. 2 shows Cm(III) TRLFS spectra as a function of pH and increasing Ca concentrations in the presence of 1 mM EDTA. In the absence of Ca, these spectra suggest the hydrolysis of Cm(III)-EDTA complexes and allow the estimation of a formation constant for the complex $Cm(OH)(EDTA)^-$. Analogous ternary complexes have been reported for Am(III) and Eu(III), but not yet for Pu(III).[22-24] The impact of Ca addition indicates that, again, Ca behaves in an additive fashion forming Ca-Cm(III)-EDTA complexes under these experimental conditions. In combination with the TRLFS study, undersaturation solubility experiments to determine the impact of hydrolysis and/or Ca stabilization in the Pu(III)-EDTA system were completed and will be discussed.

Additional experimental results including data on redox speciation (pe-pH, Vis-NIR, XAS), aqueous and solid phase characterization (TRLFS, XAS), and a thermodynamic description including novel Ca-containing complex(es) will be discussed in this contribution.

ACKNOWLEDGMENT

This work was performed as part of a collaboration between the university of Notre Dame, LANL, and KIT-INE, and was supported, in part, by an appointment to the DOE Scholars Program (funded by the WIPP Project, DOE-CBFO).

REFERENCES

1. RAI et al., *Radiochim. Acta,* **89**, 69-74 (2001).
2. BOUKHALFA et al., *Inorg. Chem.,* **43**, 5816-5823 (2004).
3. HUMMEL et al., *Chemical Thermodynamics,* **9** (2005).
4. POCZNAJLO, *Radioanal. Nucl. Chem.,* **148**, 295-307 (1991).
5. FOREMAN and SMITH, *J. Chm. Soc. Resumed*, 1752-1758 (1957).
6. RAI et al., *J. Solution Chem.,* **37**, 957-986 (2008).
7. KABANOVA, *Anal. Chim. Acta,* **22**, 66-75 (1960).
8. DIBLASI et al., *Chemosphere,* **274**, 129741 (2021).
9. DIBLASI et al., *Sci. Tot. Environ.,* **783**, 146993 (2021).
10. 40CFR191. Code of Federal Regulations, Part 191, Title 40 (2017).
11. LUCCHINI et al., U.S. Department of Energy, LA-UR-13-20620 (2013).
12. TITS et al., *Appl. Geochem.,* **98**, 2082-2096 (2005).
13. GAONA et al., Migration 2015 Proceedings (2015).
14. FELIPE-SOTELO et al., *J. Hazard Mater.,* **300**, 553-560 (2015).
15. TASI et al., *Appl. Geochem.,* **98**, 351-366 (2018).
16. MEYER et al., *Comptes Rendus Chim.,* **10**, 929-947 (2007).
17. ALMAHAMID et al., *Radiochim. Acta,* **74**, 129-164 (1996).
18. RAI et al., *J. Solution Chem.,* **39**, 778-807 (2010).
19. CLARK et al., *The Chemistry of the Actinide and Transactinide Elements,* **2**, 813-1264 (2010).
20. LUMETTA et al., *The Chemistry of the Actinide and Transactinide Elements,* **3**, 1397-1443 (2010).
21. SHANNON, *Acta Cryst.,* **A32**, 751-767 (1976).
22. GRIFFITHS et al., *Inorg. Chem.,* **52**, 3728-3737 (2013).
23. SHALINETS et al., *Sov. Radiochem.,* **14**, 285-289 (1972).
24. CERNOCHOVA et al., *Radiochim. Acta,* **93**, 733-739 (2005).

Impact of inorganic and organic ligands on the solubility and redox chemistry of Tc under reducing saline conditions

Sarah Duckworth, Xavier Gaona, Kathy Dardenne, Jörg Rothe, Dieter Schild, Marcus Altmaier and Horst Geckeis

Institute for Nuclear Waste Disposal (INE), Karlsruhe Institute of Technology (KIT), P.O. Box 3640, 76021 Karlsruhe/DE
e-mail: sarah.duckworth@kit.edu

INTRODUCTION

^{99}Tc is one of the main fission products of ^{235}U and ^{239}Pu in nuclear reactors. Due to its long half-life ($t_{1/2}$ ~ $2.1 \cdot 10^5$ a), redox sensitive character and large inventory in spent nuclear fuel, ^{99}Tc is of great relevance in the context of safety assessment for radioactive waste repositories. Tc is expected as the sparingly soluble $Tc^{IV}O_2$(am, hyd) under the reducing conditions foreseen in deep-underground disposal. Under oxidizing and redox-neutral conditions, Tc(VII) is the predominating oxidation state forming the soluble and mobile pertechnetate anion, TcO_4^-.

Sulfate is an abundant component in groundwater and one of the most relevant anions (besides chloride) in brines eventually forming in salt-rock formations, where concentrations of up to 0.2 M can be observed. Tc(IV) expectedly forms weak complexes with sulfate, although the latter may outcompete hydrolysis and increase Tc(IV) solubility when present in high concentrations.

Sulfide is a ubiquitous anion in the environment. It is occasionally found in the form of pyrite (FeS_2) in the context of repositories for waste disposal (*e.g.* as minor component in bentonite or certain clay materials). Very stable compounds of Tc(IV) and sulfide are described in the literature [1], although no thermodynamic description is available to date for this system.

Gluconic acid (GLU, $C_6H_{12}O_7$) is a polyhydroxocarboxylic acid commonly used as additive in cement formulations. It is known to form strong complexes with hard Lewis acids such as tetravalent actinides, An(IV) [2]. In the field of medicine, gluconate has been described to stabilize other oxidation states of technetium beyond the "conventional" +IV and +VII prevailing in aqueous systems in the absence of complexing ligands.

In this context, the present work aims at obtaining a better understanding of both fundamental processes at the molecular level and an improved quantitative thermodynamic model description of Tc(IV) systems with inorganic and organic ligands using the concepts of established solution thermodynamics. The studies likewise allow a deeper insight into Tc redox processes and redox speciation.

DESCRIPTION OF THE WORK

All experiments were performed at t = (22 ± 2) °C in Ar gloveboxes with < 2 ppm O_2. The effect of sulfate on the solubility of Tc(IV) was investigated from undersaturation conditions with TcO_2(am, hyd) in 0.3, 1.0 and 5.0 M NaCl–Na_2SO_4–NaOH, 4.5 M $MgCl_2$–$MgSO_4$, and 4.5 M $CaCl_2$–$CaSO_4$ solutions with $[SO_4^{2-}] = 0.001–1.0$ M and $4.0 \leq pH_m \leq 12.5$. In the case of the sulfide system, both oversaturation (with $[Tc(VII)]_0 = 10^{-5}$ M) and undersaturation (with TcO_2(am, hyd)) samples were prepared with $11 \leq pH_m \leq 14$ and 10^{-3} M $\leq [Na_2S]_{tot} \leq$ 0.1 M at I = 0.5 and 5.0 M NaCl + Na_2S. Selected samples included also $Na_2S_2O_4$ as reducing agent besides Na_2S.
The impact of gluconate on the solubility of Tc was investigated from under- and oversaturation conditions with TcO_2(am, hyd) and (in-situ reduction of) Tc(VII), respectively. Solubility samples were prepared in 0.1–5.0 M NaCl solutions with $9 \leq pH_m \leq 14$ and 10^{-4} M $\leq [GLU]_{tot} \leq 0.5$ M. Reducing conditions were chemically set for each independent sample with $Na_2S_2O_4$, Sn(II), hydrazine or Fe powder., except for a limited number of samples that remained redox-unbuffered.

Concentration of Tc, pH_m and E_h values were monitored at regular time intervals, and thermodynamic equilibrium was assumed after repeated measurements with constant [Tc] and pH_m. After attaining equilibrium conditions, the redox speciation of technetium in the aqueous phase of selected samples was investigated by L- and K-edge XANES measurements. Solid phases of selected solubility experiments were characterized by XRD, SEM–EDS as well as EXAFS analysis. XAFS spectra were recorded at the INE-Beamline and ACT-Beamline at KIT Synchrotron (KARA), KIT Campus North, in Karlsruhe (Germany).

RESULTS AND DISCUSSION

No significant changes in the solubility of TcO_2(am, hyd) are observed in the presence of $[SO_4^{2-}] \leq 1.0$ M within the investigated pH_m conditions, compared to the sulfate-free system. Although the formation of Tc(IV)-sulfate complexes has been described in very acidic conditions,[3] sulfate complexation cannot outcompete hydrolysis within

the pH_m-range of relevance in the context of nuclear waste disposal.

In contrast to the sulfate system, preliminary results obtained in the oversaturation experiments with Tc(VII) in the presence of Na_2S show a significant decrease in the initial concentration of Tc, accompanied by the formation of a black/brownish solid in some of the samples. Above $pH_m \approx 12$, the concentration of Tc decreases well below the solubility defined by TcO_2(am, hyd), thus supporting the formation of a secondary phase beyond the known Tc(IV) hydrous oxide. First evidence obtained from XPS measurements hints to predominance of Tc-S compounds in these conditions.

The presence of gluconate significantly enhances the solubility of TcO_2(am, hyd) compared to GLU-free conditions (Figure 1). Experimental solubility data in the presence of gluconate show also a different slope in the pH_m-range 10–14, providing indirect evidence on the change in the aqueous speciation, which is dominated by $TcO(OH)_3^-$ under reducing conditions but absence of gluconate. Tc L_3-edge XANES and K-edge EXAFS measurements of selected samples support the predominance of Tc(IV)-GLU aqueous species in the very reducing conditions defined by Sn(II), but the predominance of a Tc(V)-GLU complex in the absence of Sn(II) (Figure 2). These novel findings are also analyzed by complementary theoretical calculations. Preliminary chemical and thermodynamic models are derived based on the combination of solubility data, solid phase characterization and spectroscopic observations (see red line in Figure 1).

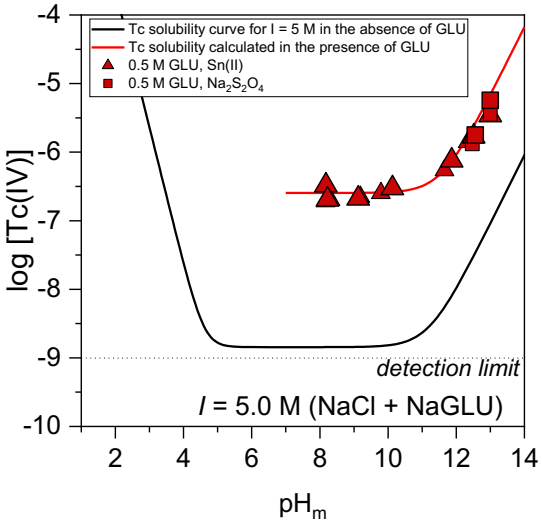

Fig. 1: Experimental solubility data of Tc(IV) in 5.0 M NaCl–NaGLU solutions with [GLU] = 0.5 M. Red and black solid lines corresponds to the solubility of $TcO_2 \cdot 0.6H_2O$(am) in 5.0 M NaCl in the presence and absence of gluconate. Model calculations performed using thermodynamic data derived in this work or reported by Yalçıntaş et al., [4] respectively.

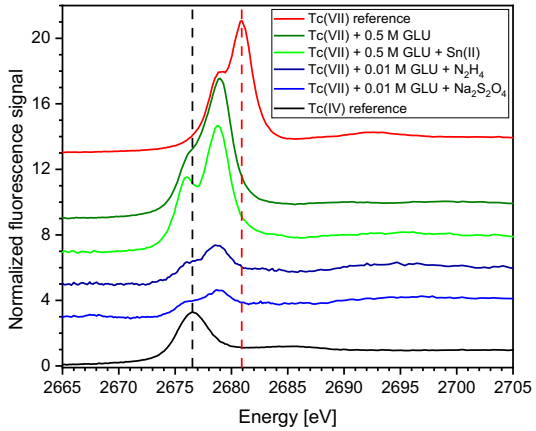

Fig. 2: Measured L_3-edge XANES spectra of selected Tc-GLU samples.

This work highlights a combined approach including classical wet-chemistry methods (measurements of pH, E_h, [Tc]), advanced spectroscopic techniques (K-, L-edge XAFS) and theoretical methods for the characterization of Tc aqueous systems of relevance in the context of nuclear waste disposal and other environmental applications.

ACKNOWLEDGEMENTS

This work is partly funded by the German Ministry of Economic Affairs and Energy (BMWi) within the framework of the VESPA II project (contract numbers 02E11607C). We acknowledge the KIT light source for provision of instruments at the INE-Beamline/ACT experimental station operated by the Institute of Nuclear Waste Disposal and we would like to thank the Institute for Beam Physics and Technology (IBPT) for the operation of the storage ring, the Karlsruhe Research Accelerator (KARA).

REFERENCES

1. PEARCE et al., “Technetium Stabilization in Low-Solubility Sulfide Phases: A Review” *ACS Earth and Space Chemistry,* **2**, 532-547 (2018).
2. HUMMEL et al. “Vol. 9. Chemical Thermodynamics of complexes and compounds of U, Np, Pu, Am, Tc, Zr, Ni and Se with selected organic ligands, OECD Nuclear Energy Agency Data Bank, Eds.” *North Holland Elsevier Science Publishers B. V., Amsterdam, The Netherlands* (2005).
3. PARKER et al., “Complexation of Tc(IV) with SO_4^{2-} in NaCl Medium” *Journal of Solution Chemistry*, **47**, 1192–1201 (2018)
4. 4. YALCINTAS et al. “Thermodynamic description of Tc(IV) solubility and hydrolysis in dilute to concentrated NaCl, $MgCl_2$ and $CaCl_2$ solutions.” *Dalton Trans.,* **45**, 8916–8936 (2016).

Solubility and structural characterization of M(IV) hydrous oxides: the case of Zr(IV) and Th(IV)

C. Kiefer[1], X. Gaona[1], T. Suzuki-Muresan[2], N. Cevirim-Papaioannou[1], O. Dieste Blanco[1], D. Schild[1], T. Kobayashi[3], M. Altmaier[1], B. Grambow[2], H. Geckeis[1]

[1]*Karlsruhe Institute of Technology, Institute for Nuclear Waste Disposal, Karlsruhe, Germany*
[2]*SUBATECH – IMT Atlantique, Université de Nantes, CNRS/IN2P3, Nantes, France*
[3]*Department of Nuclear Engineering, Kyoto University, Kyoto, Japan*
email: christian.kiefer@kit.edu

INTRODUCTION

Tetravalent metals M(IV) (*e.g.* actinides, Zr, Tc) have a strong tendency to hydrolyse in aqueous systems. Cationic hydrolysis species, $M_x(OH)_y^{4x-y}$ (with $y < 4x$), are expected to control the aqueous speciation of M(IV) under (sufficiently) acidic conditions, whereas the neutral species $M(OH)_4(aq)$ (or analogous neutral polynuclear moieties) predominate from acidic to alkaline pH conditions [1]. For some tetravalent transition metals (*e.g.* Zr, Tc) the predominance of anionic hydrolysis species $M(OH)_y^{4-y}$ or $MO(OH)_z^{2-z}$ (with $y > 4$ and $z > 2$) is reported in hyperalkaline pH systems [2-3].

In connection with their strong hydrolysis, M(IV) form sparingly soluble amorphous hydrous oxides, MO_2(am, hyd), which control M(IV) solubility in aqueous media over a broad range of pH from acidic to hyperalkaline conditions. The ageing or exposure of these solid phases to elevated temperatures expectedly results in increased crystallinity (*i.e.* larger particle size), and thus in a decreased solubility in aqueous systems [4-5].

The present studies systematically investigate the impact of temperature on the crystallinity/particle size and hydrate content of ThO_2(am, hyd) and ZrO_2(am, hyd) solid phases, and further the solubility and thermodynamic properties of these solid phases in acidic and hyperalkaline conditions, respectively. For this purpose, a combination of solubility batch experiments and comprehensive solid phase characterization is used. As overarching objective, this work intends to shed light on the mechanisms for the potential transformation of amorphous hydrous oxides into thermodynamically more stable crystalline phases of M(IV) relevant in the context of nuclear waste disposal.

DESCRIPTION OF THE WORK

All experiments were conducted in Ar glove boxes. The starting solid phase used in the Th study, ThO_2(am, hyd, fresh), was prepared by slow titration of a ≈ 0.05 M $ThCl_4$ solution with 1.0 M carbonate-free NaOH. Aliquots of the freshly precipitated solid phase were equilibrated at T = 80°C in 0.1 M NaCl solutions at pH_m = 3 and 12.8 (pH_m = –log [H^+]) in undersaturation solubility studies. After contact times of 1, 2, 4.5 or 5.5 months the solid phases were each characterized by XRD, TG-DTA, SEM-EDX and XPS to evaluate the impact of temperature with time. Undersaturation solubility samples were prepared by equilibrating 5–20 mg of the Th(IV) solid phase, either freshly precipitated or aged (T = 80 °C for 1–4.5 months), with 0.1 M NaCl solutions with pH_m = 2.3–6 at T = 22 °C. The concentration of Th(IV) in the aqueous phase was quantified by ICP-MS after 10 kD ultrafiltration.

The starting solid phase used in the Zr study, ZrO_2(am, hyd, fresh), was prepared by slow titration of a ≈ 0.02 M $ZrOCl_2$ solution with 0.1 M carbonate-free NaOH. After washing 3-4 times with the corresponding solution, aliquots of the freshly precipitated solid phase were equilibrated at T = 80°C in 0.2 M $CaCl_2$-$Ca(OH)_2$ or 0.001 M NaOH solutions at pH_m = 11.0. For both systems, experiments targeting contact times of 4, 8, 10 and 18 months were initiated in December 2020. First insights obtained from the characterization by XRD, TEM, SAXS, XPS, SEM-EDX and TG-DTA of fresh and aged (4 months) solid phases will be presented in this contribution, and compared to the results obtained in the work for Th(IV).

RESULTS AND DISCUSSION

Solid phase characterization confirms the amorphous character of the freshly precipitated ThO_2(am, hyd, fresh). However, after only one month of equilibration time at T = 80 °C, the aged solid phases show broad but well-defined XRD patterns in agreement with the ThO_2(cr) reference. The increased crystallinity correlates with a markeddecrease in solubility (Figure 1) at T = 22 °C (approximately 1 to 3 log_{10}-units), consistent with previous evidence reported by Kobayashi and co-workers [6]. Differences between solid phases aged at pH_m = 3 and 12.8 are observed both for solid phase characterization and solubility measurements, suggesting that the aging process evolves differently at the two pH_m values investigated.

Figure 2 shows the number of hydration waters determined in this work for fresh and aged ThO_2(s, hyd) and ZrO_2(s, hyd) as a function of the ageing time, compared to data reported in the literature for TcO_2(am, hyd, aged) [3] and UO_2(ncr, hyd, aged) [8]. The figure shows a clear trend to decrease the number of hydration with ageing time, which in turn is related to the decrease in the solubility product of the corresponding solid phase.

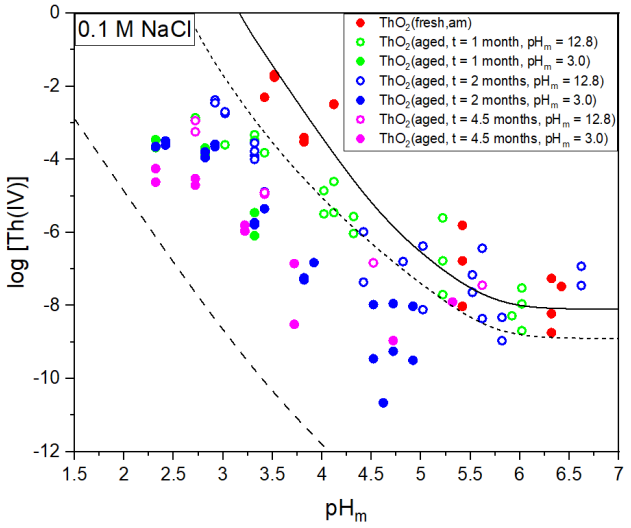

Fig. 1: Solubility data obtained for freshly precipitated ThO_2(am, hyd, fresh) and for ThO_2(ncr, hyd, aged) aged at T = 80 °C for t = 1, 2, 4.5 m with pH_m = 3 and 12.8. Solid, dotted and dashed lines correspond to the solubility of ThO_2(am, fresh), ThO_2(am, aged) and ThO_2(cr) calculated using thermodynamic data reported in the NEA-TDB [7].

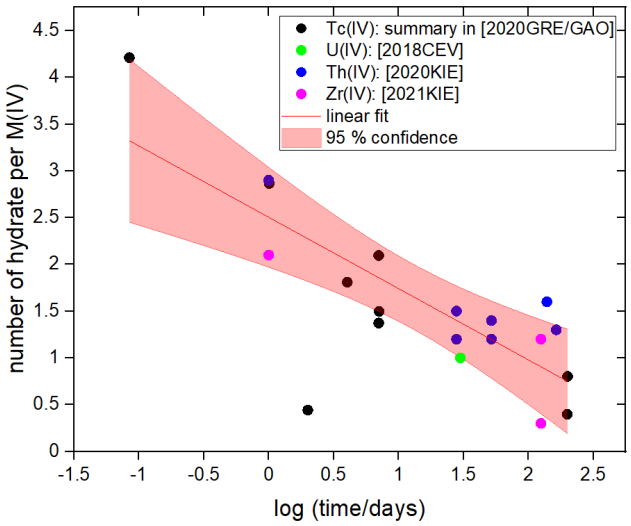

Fig. 2: Number of hydration waters determined in this work and in the literature for ThO_2(s, hyd) and reported in the literature for MO_2(s, hyd) with M = Tc, Th, U, Zr [3,7].

Solid phase characterization of the ZrO_2(s, hyd, aged) samples aged for t = 4 months shows significant differences between the solid aged in 0.001 M NaOH and in 0.2 M $CaCl_2$-$Ca(OH)_2$. In addition to a clear decrease in the number of hydration waters with respect to the fresh solid ($n_{H_2O} \approx 0.3$ *vs.* ≈ 2.1), the ZrO_2(s, hyd, aged) sample equilibrated in NaOH shows well-defined XRD patterns in good agreement with monoclinic ZrO_2(cr), comparable with previous experimental work reported by Kobayashi and co-workers in $HClO_4$–NaOH systems [9]. The increased crystallinity of the sample equilibrated in NaOH is also reflected in the particle size quantified by XRD and TEM, *i.e.* ≈ 30 nm (as compared to ≈ 3–4 nm for the fresh solid). A less crystalline material is obtained for the ageing of ZrO_2(am, fresh) in $CaCl_2$-$Ca(OH)_2$, with a particle size of ≈ 11–12 nm and $n_{H_2O} \approx 1.2$. In contrast to NaOH systems, XRD patterns collected for this sample show an excellent agreement with cubic/tetragonal ZrO_2(cr). Note that the stabilization of tetragonal ZrO_2(cr) with cationic doping has been previously reported in the literature [10].

Fig. 3: XRD pattern from the ZrO_2 samples aged in 0.2 M

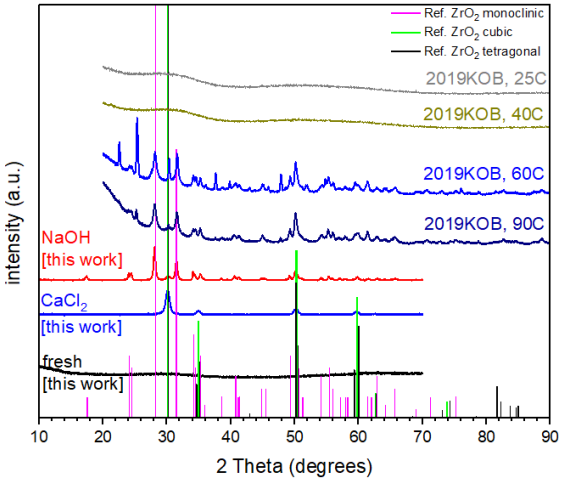

$CaCl_2$/0.001 M NaOH compared to measurements by Kobayashi and co-workers [9].

Experimental results from the on-going experiments will be extensively discussed in this contribution, in combination with data available for other M(IV).

ACKNOWLEDGEMENTS

This work was partially funded by the German Federal Ministry for Education and Research (BMBF), ThermAc project, under the contract number 02NUK039A.

REFERENCES

[1] ALTMAIER et al., *Chem. Rev.*, **113**, 901-943 (2013).
[2] BROWN et al., *NEA OECD Publishing* (2005).
[3] GRENTHE et al., NEA *OECD Publishing* (2020).
[4] RAI et al., *Radiochim. Acta*, **88**, 297-306 (2000).
[5] KOBAYASHI et al., *Radiochim Acta*, **101**, 645-651 (2013).
[6] KOBAYASHI et al., *Journal of Nuclear Science and Technology*, **53**, 1787-1793 (2016).
[7] RAND et al., *NEA OECD Publishing* (2007).
[8] CEVIRIM-PAPAIOANNOU, KIT Ph.D. Thesis, Karlsruhe (2018).
[9] KOBAYASHI et al., *Langmuir*, **35**, 7995−8006 (2019).
[10] DELL'AGLI et al., J. Mat. Sc., **35**, 661–665 (2000).

Converting thermodynamic data using the Pitzer approach for the geochemical code TOUGHREACT

Torben Weyand[1], Holger Seher[2], Guido Bracke[1]

[1] *Federal Office for the Safety of Nuclear Waste Management (BASE), Schwertnergasse 1, 50667 Cologne, Germany*
[2] *Gesellschaft für Anlagen- und Reaktorsicherheit (GRS) gGmbH, Schwertnergasse 1, 50667 Cologne, Germany*
torben.weyand@bfe.bund.de

INTRODUCTION

For the ongoing site selection process for a repository for high-level radioactive waste in Germany possible host rocks are rock salt, clay and crystalline rock. The pore water of these rocks contains saline solutions with high ionic strengths. To model the speciation and/or migration of radionuclides in long term safety analyses for nuclear waste disposal, a geochemical code that includes thermodynamic data suitable for saline solutions is needed. Thermodynamic equilibria in saline solutions with high ionic strengths is usually modelled using the Pitzer approach [1].

DESCRIPTION OF THE WORK

Within the context of nuclear waste disposal, the THEREDA project [2] provides thermodynamic data for some widely used geochemical codes (PHREEQC, Geochemist's Workbench, ChemApp, and EQ 3/6) using the Pitzer approach. However, modelling in long term safety analyses for nuclear waste disposal also uses the well-known geochemical code, TOUGHREACT [3]. Therefore, scripts were needed and developed to convert thermodynamic data from the THEREDA project to be applicable in TOUGHREACT.

RESULTS AND DISCUSSION

The scripts were validated by benchmark tests and by comparing calculations. PHREEQC and TOUGHREACT [4] were used. In total, 50 different benchmark tests were performed considering three specific geochemical systems, which are relevant to long term safety analyses: (1) oceanic salt system, polythermal: K, Mg, Ca - Cl, SO_4 - H_2O(l); (2) actinide system, isothermal: Am(III), Cm(III), Nd(III) - Na, Mg, Ca - Cl, OH - H_2O(l); and (3) carbonate system, isothermal: Na, K, Mg, Ca - Cl, SO_4 - HCO_3/CO_2(g) - H_2O(l). Each benchmark test considered specific ion concentrations in solution and in gaseous phases in presence of specific minerals. The benchmark tests derived the geochemical equilibria and the results of both codes were compared among each other and to experimental data. The results of the calculations agree well for both codes (see Fig.1 as an example). Minor deviations are explainable by technical differences of the codes.

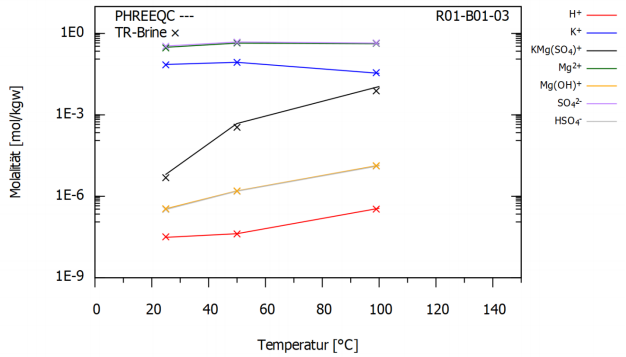

Fig. 1: Molality of aquatic species versus temperature for the system K-Mg-SO_4 calculated by the geochemical codes PHREEQC (lines) and TOUGHREACT (crosses) using the database from THEREDA.

REFERENCES

[1] K. S. PITZER, "Activity Coefficients in Electrolyte Solutions" *CRC Press* (1991).
[2] H. C. MOOG et al., "Disposal of Nuclear Waste in Host Rock formations featuring high-saline solutions - Implementation of a Thermodynamic Reference Database (THEREDA)" *Appl. Geochem.,* **55**, 72-84 (2015).
[3] T. XU et al., „TOUGHREACT V3.32 Reference Manual, A Parallel Simulation Program for Non-Isothermal Multiphase Geochemical Reactive Transport" Lawrence Berkeley National Laboratory (LBNL), LBNL-DRAFT, March 2017.
[4] T. WEYAND et al., „Verwendung von temperaturabhängigen thermodynamischen Daten in TOUGHREACT" *GRS-622*, 111-148 (2021).

THE COMPLEXATION AND THERMODYNAMICS OF Cm(III) WITH F^- AT T = 25 TO 200 °C STUDIED BY TIME RESOLVED LASER FLUORESCENCE SPECTROSCOPY

C. Koke[2], A. Skerencak-Frech[1], P. Panak[1,2], M. Altmaier[1], H. Geckeis[1]

[1] *Karlsruhe Institute of Technology (KIT) – Institute of Nuclear Waste Disposal (INE), 76021 Karlsruhe, Germany*
[2] *Heidelberg University – Institute of Physical Chemistry, 69120 Heidelberg, Germany*
email: Andrej.skerencak@kit.edu

INTRODUCTION

The safety case of a repository for high-level radioactive waste encompasses relevant information on the geochemistry of actinides in the near- and far-field of the repository. A comprehensive modelling of the migration behaviour of the actinides requires accurate thermodynamic data concerning all occurring chemical reactions. While literature data is widely available for ambient temperatures [1], information at elevated temperatures is rare and mostly limited to T < 100 °C.[2,3] Due to the radioactive decay of the stored nuclear waste and the related release of energy, temperatures well above 100 °C may occur in the near-field of a repository for high-level waste in some disposal concepts. Geochemical data for actinide speciation at elevated temperatures are, therefore, required when early canister failure scenarios are considered.

Some studies on Cm(III) fluoride complexation have been performed at temperatures up to 90 °C with laser spectroscopic techniques, yielding standard-state complexation constants (log β^0_n) and thermodynamic functions ($\Delta_rH^0_m$, $\Delta_rS^0_m$).[4] Studies at temperatures above 100 °C have not been reported so far for this system.

DESCRIPTION OF THE WORK

In the present work the formation of Cm(III) fluoride complexes is investigate by time-resolved laser fluorescence spectroscopy (TRLFS) at high temperatures and pressures. For this, a new high-temperature and high-pressure cell was developed and custom-built at KIT-INE, which enables spectroscopic measurements of aqueous solutions over a broad range of different experimental parameters at temperaturs up to 200 °C.

The chemical speciation of the Cm(III) fluoride system is determined as a function of the equilibrium fluoride concentration, the ionic strength (NaCl, $NaClO_4$) and the temperature. Using linear slope analyses the formation of the complexes $[CmF]^{2+}$ and $[CmF_2]^+$ is verified. The conditional log β'_1(T) values are extrapolated to zero ionic strength using the SIT approach [1], yielding the thermodynamic functions (log β^0_n(T), $\Delta_rH^0_m$, $\Delta_rS^0_m$) for the complexation reaction.

RESULTS AND DISCUSSION

In Figure 1 the molar fractions of the Cm(III) species with increasing $[F^-]_{eq}$ (I_m = 0.1 (NaCl)) are given at 25 and 140 °C. At room temperature, only the formation of the 1:1 complex is observed. Increased temperatures results in a shift of the chemical equilibrium towards the higher complexes leading to the formation of the 1:2 species.

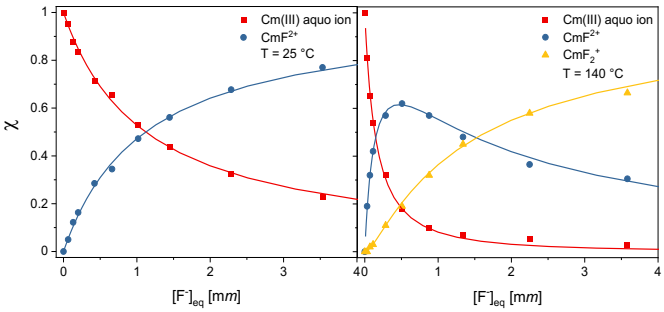

Fig. 1: Molar fractions of the $[CmF_n]^{3-n}$ complexes (n = 0, 1, 2) as function of $[F^-]_{eq}$ (I_m = 0.1 (NaCl). Right: T = 25 °C, left: T = 140 °C.

Both temperature dependent conditional stability constants (log β'_n(T), n = 1 ,2) increase by approximately one order of magnitude with the temperature, reflecting the observed shift of the chemical equilibrium towards the complexed species. Hereby, the log β'_2(T) is determined only at T > 75 °C. The log β^0_1(25 °C) = 3.69 ± 0.05 increases by about 1.5 with increasing temperature resulting in a log β^0_1(200 °C) = 5.26 ± 0.15. As the log β^0_1(T) are linearly correlated with T^{-1} their temperature dependency is fitted according to the integrated Van't Hoff equation, giving the standard reaction enthalpy ($\Delta_rH^0_{1,m}$) and entropy ($\Delta_rS^0_{1,m}$). The results show an endothermic reaction ($\Delta_rH^0_m$ = 23.23 ± 1.32 kJ mol^{-1}) which is driven by a high gain of reaction entropy ($\Delta_rS^0_m$ = 147.1 ± 3.7 J mol^{-1} K^{-1}). Additionally, the SIT specific $\Delta\varepsilon_{0n}$(T) values are determined as function of the

temperature. As no noticeable temperature dependency of this parameter is found, $\Delta\varepsilon_1 = -0.17 \pm 0.04$ kg mol^{-1} is assumed as the median value applicable in the investigated temperature range.

REFERENCES

1. R. GUILLAUMONT et al. Chemical Thermodynamics Vol. 5. "Update on the Chemical Thermodynamics of Uranium, Neptunium, Plutonium, Americium and Technetium". Elsevier , Amsterdam (2003).
2. G.R. CHOPPIN, P.J. UNREIN, Thermodynamic Study of Actinide Fluoride Complexation, in: Proc. Transplutonium Elements 1975 (Eds. W. Müller, R. Lindner, p. 97-107, North Holland Publ. Co., Amsterdam (1976).
3. W. AAS, et al, *Radiochim. Acta*, **84**, 85-88 (1999).
4. A. SKERENCAK, et al, *J. Phys Chem. B*., **114**, 15626-15634 (2010).

Structural and modeling study of the retention of trivalent f-elements (Am, Cm, Eu) by natural and synthetic Ca-feldspars

J. Lessing[1], J. Neumann[1], F. Bok[1], J. Bezzina[1], J. Lützenkirchen[2], V. Brendler[1], T. Stumpf[1], M. Schmidt[1]

[1]*Helmholtz-Zentrum Dresden-Rossendorf e.V., Institute of Resource Ecology, Bautzner Landstraße 400, 01328 Dresden, Germany, email: j.lessing@hzdr.de*
[2]*Karlsruher Institut für Technologie (KIT), Hermann-von-Helmholtz-Platz 1, 76344 Eggenstein-Leopoldshafen, Germany*

INTRODUCTION

Deep geological repositories are considered as a safe disposal strategy for radioactive waste due their ability to isolate toxic components from the biosphere over hundreds of thousands of years. Minor actinides and Pu dominate the radiotoxicity of spent nuclear fuel over these long time scales. Due to the expected reducing conditions in the underground repository, the trivalent oxidation state is dominant for Am and Cm, and will also be relevant for Pu. For investigations of the mobility of the trivalent actinides Am(III) and Cm(III), the less toxic trivalent rare earth elements, in particular Eu(III), are commonly used.

In Germany and many other countries, crystalline rock is being considered as a possible host rock. Therefore, there is a need for understanding the sorption behavior of radionuclides on this material. Crystalline rock (*e.g.* granite), consists mainly of quartz, feldspars, and mica. Recently, the retention of trivalent actinides by K-feldspar was investigated from a thermodynamic and structural point of view.[1] Here, we extend this study towards Ca-feldspars (plagioclases), which may show a different sorption behavior due to their different elemental composition, crystal structure, and surface charge behavior.

DESCRIPTION OF THE WORK

Synthetic Ca-feldspar and natural plagioclases of different Ca amounts were used for zeta potential measurements and batch sorption experiments under different geochemical conditions ($[M^{3+}]$ = 52 nM – 10 µM; solid-liquid ratio = 1 – 3 g/L, I = 0,1 M NaCl, pH = 3 – 9) to quantify the uptake of Am(III) and Eu(III). For analysis of the sorption structure of trivalent *f*-elements on the molecular level, time-resolved laser-induced spectroscopy (TRLFS) using Cm(III) as a luminescent probe was carried out on synthetic Ca-feldspar. The obtained data were used to develop a surface complexation model (SCM) and to derive surface complexation parameters for the spectroscopically identified surface complexes.

RESULTS AND DISCUSSION

Zeta potential investigations of all Ca-feldspars show a decrease of the potential for pH = 2 – 4 due to surface site deprotonation. In contrast to the previously reported trend for K-feldspar, the zeta potential increases for pH = 4 – 7, with a stronger increase with higher Ca^{2+} concentration in the crystal lattice of the investigated plagioclases, even reaching positive values in the case of the synthetic Ca-feldspar. This effect can be traced to dissolved Al^{3+}: Due to differences in solubility, Al^{3+} concentration in solution increases with increasing Ca^{2+} in the crystal lattice. Experiments on K-feldspar with added Al^{3+} reveal a connection between its concentration and the increase of the zeta potential.

All observed Ca-feldspars show a strong sorption uptake of trivalent f-elements for pH > 6. K- and Ca-feldspars seem to have a similar sorption behavior for low $[M^{3+}]$.[1] In contrast, Ca-feldspar has a slightly stronger sorption affinity when the metal concentrations is increased. This leads to a steeper sorption edge with increasing Ca^{2+} concentration in the crystal lattice of the mineral.

Spectroscopic studies with Cm(III) on synthetic Ca-feldspar reveal three sorption complexes: one inner sphere complex (IS) and its two hydrolysis forms, which have the same band positions as previously determined for K-feldspar.[1] Therefore, it can be concluded that the structure of the formed IS complexes is independent on the feldspar type. Differences are only observed for the quantitative contributions of the surface complexes. In particular, hydrolysis of the IS complex is stronger in the case of the Ca-feldspar.

Batch sorption data and the information about spectroscopically identified surface complexes were then combined to develop a SCM for Ca-feldspar that describes the experimental data. The formation constants of the surface complexes were determined to be −8.37; −10.81, and −16.35, respectively and are very similar to those of the K-feldspar.[1]

From the applied multi-method approach, we conclude that the sorption of trivalent f-elements on K- and Ca-feldspar is most likely comparable for relevant, natural conditions. Therefore, it may be possible not to distinguish between the two minerals in reactive transport

simulations, which will reduce calculation resources needed for a reliable risk assessment of repositories for radioactive waste.

ACKNOWLEDGEMENTS

This work was funded by the Federal Ministry of Economics and Technology in the frame of the SMILE project with grant 02E 11668B and 02E 11668C.

REFERENCES

[1] J. NEUMANN et al., "A comprehensive study of the sorption mechanism and thermodynamics of *f*-element sorption onto K-feldspar," *Journal of Colloid Interface Science*, **591**, 490–499 (2021).
[2] J. NEUMANN et al., "Structural and modeling study of the retention of trivalent *f*-elements (Am, Cm, Eu) by natural and synthetic Ca-feldspars", in preparation.

Surface complexation models for rough and heterogeneous surfaces – the charge regulation concept applied to simple 2D geometries

Frank Heberling[1], Teba Gil-Díaz[1,2], Johannes Lützenkirchen[1]

[1] *Karlsruhe Institute of Technology, Institute for Nuclear Waste Disposal, Hermann-von-Helmholtz Platz 1, 76344 Eggenstein-Leopoldshafen, Germany,*
[2] *Friedrich-Schiller-University Jena, Institute of Geosciences, Burgweg 11, 07749 Jena, Germany*
email: frank.heberling@kit.edu

INTRODUCTION

Electrostatic surface complexation models (SCMs) are commonly used to simulate the adsorption behaviour of ions at mineral-water interfaces and the charging behaviour of mineral surfaces. Classical SCMs use mathematical formulations, specific to certain simple surface geometries like flat surfaces, or surfaces of spherical- or cylindrical particles. The models generally imply that the electrostatic potential approaches zero away from the surface in the bulk solution, and is not influenced by potentials originating from other surfaces [1].

In natural or technical systems, however, like the ones encountered in the multi-barrier system around nuclear waste in high level radioactive waste disposal sites, mineral surfaces exhibiting roughness down to the nanometre-scale or patch wise heterogeneities will be commonly present. Thus, lateral contributions to the electrostatic potential, sometimes referred to as spill-over effects, should actually be expected. In nanoporous systems, as encountered in clay (bentonite as well as clay-rock) or cementitious materials, mineral surfaces will often be in so close proximity that the decay of the surface potential to zero in the pore-solution cannot simply be presumed.

The most accurate way of simulating electrostatic interactions between mineral surfaces on a mean field level is by coupling electrostatic SCMs via the so-called charge regulation approach [2]. Mean field here means that ions are treated as point charges and the solution as a continuous dielectric medium. For 1D systems of opposing mineral surfaces, a charge-regulation code has recently been developed and benchmarked [3]. The model is capable of simulating the potential throughout the pore space, the pore-solution chemistry as affected by the electrostatic potential, and changes in surface speciation caused by the mutual influence of charged surfaces in close proximity to each other. Further parameters provided by the model are electrostatic interaction forces between mineral surfaces and the osmotic pressure inside a pore.

Here we present the next step in this code development, where we transfer the charge regulation concept to simple 2D-geometries.

MODEL DESCRIPTION

The 2D Poisson Boltzmann (PB) equation for arbitrary electrolytes is solved by a Finite-Element method (FEnics, Python). The FE-based electrostatic calculation is coupled to a Python based code capable of solving aqueous- and surface-speciation problems. Presently, Triple-Layer SCMs are implemented. Activity corrections are performed on the basis of the Davies equation. Simple examples of the 2D code were benchmarked against PhreeqC [4] (planar homogeneous surface) and analytical solutions for the PB equation (1:1 electrolyte).

Examples presented here use surface complexation models for Eu(III) adsorption on quartz [5] for the example representing a corner formed by quartz surfaces, and the silica model by Hiemstra et al. [6] with modifications thereof for the example simulating a patch-wise heterogeneous surface.

RESULTS AND DISCUSSION

Fig. 1 highlights selected results for adsorption of Eu(III) on a corner formed by quartz surfaces as a function of pH. The simulation results summarized in Fig. 1c show that depending on the conditions, Eu(III) adsorption may increase by a factor of three in a corner compared to adjacent flat surfaces. The speciation plot (Fig 1d) highlights that this effect is most prominent for pH around 5 at which positive Eu-surface species dominate. At higher pH, where neutral Eu-surface species dominate, the effect of the corner vanishes.

The mechanistic model demonstrates the effect of geometry on interfacial electrostatics, and how it affects adsorption. It highlights how roughness may create chemical heterogeneity on a surface which is homogeneous with respect to the surface functional groups.

Further examples, shown on the Poster, highlight the impact of Eu(III) concentrations on the corner effect, and the electrostatic spill over on a patch-wise heterogeneous surface. All these effects may have important implications for pore-scale transport processes as they affect the distribution of adsorbed ions (i.e. radionuclides) on rough and heterogeneous surfaces. To date, however, pore scale

modelling codes are not capable of including charge regulation type interactions.

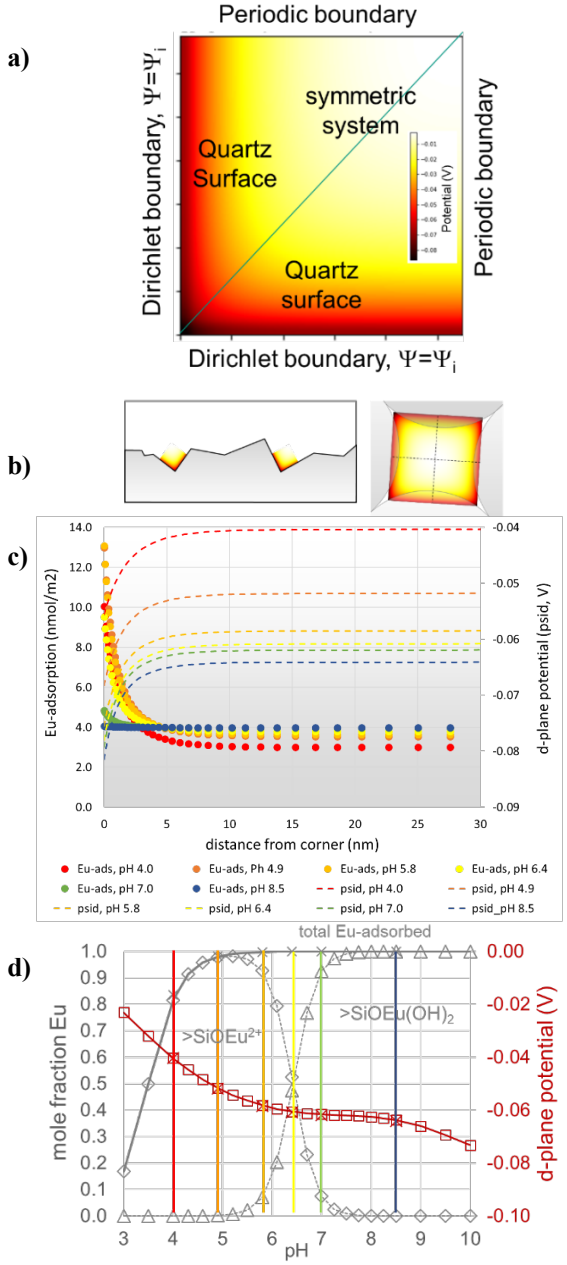

Fig. 1: Eu(III) adsorption on a corner formed by quartz surfaces as a function of pH. a) Layout of the simulation cell concerning boundary conditions and symmetry. b) Application examples for the corner type simulations, i.e. to represent nano-scale roughness on a natural quartz surface or as a simplified representation of pore-throats formed by quartz grains. c) Eu concentration as function of distance from the corner for various pH values, as well as the corresponding d-plane potentials. d) Eu surface speciation as function of pH (calculated using PhreeqC). Coloured lines mark pH values at which the 2D simulations were run. The crosses mark values obtained at the flat ends of the 2D simulation cell.

ACKNOWLEDGEMENTS

We acknowledge funding received through the iCross project from the German Federal Ministry of Education and Research (02NUK053C) and the Helmholtz association (SO-093).

REFERENCES

1. LÜTZENKIRCHEN, J., Surface complexation modelling. Academic press; Vol. 11 (2006).
2. NINHAM, B. W. and PARSEGIAN, V. A., Electrostatic potential between surfaces bearing ionizable groups in ionic equilibrium with physiologic saline solution, *Journal of Theoretical Biology*, **31**, 405 – 428 (1971).
3. GIL-DÍAZ, T., et al. Charge regulated solid-liquid interfaces interacting on the nanoscale: Benchmarking of a generalized speciation code (SINFONIA). *Advances in Colloid and Interface Science*, **294**, 102469 (2021).
4. PARKHURST, D. L and APPELO, C., Description of input and examples for PHREEQC version 3—a computer program for speciation, batch-reaction, one-dimensional transport, and inverse geochemical calculations. US geological survey techniques and methods**,** 6 (2013).
5. GARCÍA D. et al., Sorption of Eu(III) on quartz at high salt concentrations, *Colloids and Surfaces A: Physicochemical and Engineering Aspects*, **578**, 123610 (2019).
6. HIEMSTRA, T., et al., Multisite proton adsorption modeling at the solid/solution interface of (hydr) oxides: A new approach: I. Model description and evaluation of intrinsic reaction constants. *Journal of Colloid and Interface Science*, **133**, 91-104 (1989).

Understanding tetravalent actinide oxide formation, stability, and dissolution under far field environmental conditions

Brian. A. Powell[1,2], Kathryn Peruski[1], Connor Parker[1], Melody Maloubier[1], Daniel I. Kaplan[1,2], Annie B. Kersting[3], Mavrik Zavarin[3]

[1] Clemson University, Anderson, SC, USA 29625
[2] Savannah River National Laboratory, Aiken, SC, USA 29808
[3] Lawrence Livermore National Laboratory, Livermore, CA USA 94550
email: bpowell@clemson.edu

INTRODUCTION

Comprehensive thermodynamic understanding of nuclear materials is paramount for long-term management of legacy nuclear waste and commercial spent nuclear fuel. Actinide oxides (AnO2(s)) are ubiquitous materials throughout the nuclear fuel cycle, yet existing thermodynamic data has noticeable discrepancies, creating uncertainty in environmental prediction of the fate of nuclear materials.

DESCRIPTION OF THE WORK

In this work, we have deployed a variety of neptunium and plutonium solid phases in a series of field lysimeter experiments at the Department of Energy Savannah River Site. The Radionuclide Field Lysimeter Experiment (RadFLEx) testbed is equipped to deploy highly characterized radionuclide source terms into natural settings for periods from months to years by deploying the sources at the center of 10 cm x 50 cm soil columns which are subject to rainfall infiltration and natural atmospheric and temperature fluctuations. Thus, RadFLEx allows us to examine how these solid phases may age in the environment.

RESULTS AND DISCUSSION

All plutonium sources are transforming to disordered PuO_{2+x} type phases regardless of the initial oxidation state and the extent of transformation to disordered PuO_{2+x} phases appears to be accelerated in the field lysimeter sources relative to the archived sources. Comparison of the downward migration of each source indicates some notable differences between lysimeters with different initial Pu and Np sources. These differences were further studied with laboratory studies examining the influences of the grain boundary microstructure on the oxidative dissolution of NpO_2(s). This work demonstrated the sizable differences in dissolution of NpO_2(s) based on process conditions, such as the temperature at which the material is calcined and resultant particle size, and the need for more thorough evaluation of the microstructure of solid phases used to generate thermodynamic data of actinides and understand environmental fate. The current working hypothesis to explain these differences is that colloidal PuO_{2+x} and NpO_2 phases are forming during the chemical/physical transformations of the source materials and downward migration is enhanced by these colloidal phases. Thus, the extent of transport appears to be somewhat dependent on the initial chemical/physical state of the source.

The contribution of Natural Analogue Studies to the Safety Assessment of Nuclear Waste Repositories

Jordi Bruno

Amphos 21Group, Barcelona, Spain
email: jordi.bruno@amphos21.com

INTRODUCTION

One of the main objectives of the design of radioactive waste repositories is to provide adequate long-term isolation of the waste from the biosphere. The ability of the repository materials and the surrounding host-rock in retarding the possible migration of radionuclides from the repository system is therefore of especial relevance. Due to the long-term time scales inherent to the long-lived material deposited, it is not possible to conduct experimental tests that adequacy of the concept designed to contain the wastes has to seek for evidence outside the perfectly controlled world of the laboratory tests, in terms of both spatial scale, time perspective, and complexity. Processes occurring in nature can provide this adequate frame of space, time and complexity needed for the assessment of the performance of the repository system.

Not all examples from nature are relevant for this purpose, only those presenting a certain level of analogy to the features, events or processes expected to be present or to occur in a repository or its surroundings, and these examples are known as natural analogues (NNAA).

Natural analogue (NNAA) studies have thus become an integral part in the performance assessment (PA) of nuclear waste repositories [1].

DESCRIPTION OF THE WORK

This presentation will focus on NNAA studies that have contributed to the development of radionuclide migration models and predictive tools to assess retention/migration processes of radionuclides in a repository system.

The main objective of this presentation will be to emphasize the extent of application of NNAA investigations in radionuclide migration concepts and their quantification.

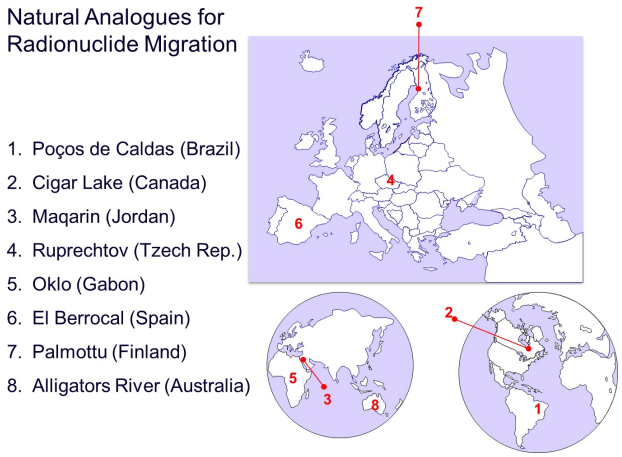

Fig. 1: Geographic location of the NNAA study sites [1]

REFERENCES

1. DURO L. & BRUNO, J. Natural analogues of nuclear waste repositories: Studies and their implications for the development of radionuclide migration models, in Radionuclide Behaviour in the Natural Environment: Science, Implications and Lessons for the Nuclear Industry, pp. 411-445 (2012).

Reactive transport and retention of solutes in pores media: Current state of the art and the challenges

Sergey V. Churakov

Paul Scherrer Institute Forschungsstrasse 111, 5232 Villigen PSI
email: sergey.churakov@psi.ch

INTRODUCTION

Deep geological disposal of nuclear waste is considered as the most reliable and sustainable long-term solution worldwide. The disposal cell is a complex geochemical system. The radionuclide mobility and consequently radiological impact depend not only on their chemical speciation but also on the background concentration of other stable nuclides and their behaviour in the natural environment. The safety assessment of the repository is thus a complex multidisciplinary problem requiring knowledge in chemical thermodynamics, structural chemistry, fluid dynamics, geo- and radiochemistry. Broad aspects of radionuclide thermodynamics and geochemistry have been investigated in state-of-the-art radiochemical laboratories at the Paul Scherrer Institute for more than 30 years. This research has resulted in improved understanding of the radionuclides release, retention and transport mechanism in the repository system [1].

Safety and performance of repository system need to be evaluated for a very long time-period not accessible experimentally. Furthermore, the petro physical properties of geological and engineered barriers are expected to evolve due to chemical and physical interactions. Temporal and spatial extend of such processes can only be assessed based on reactive transport models employing mechanistic coupling between relevant physical phenomena.

Reactivity of minerals and rocks is controlled by chemical processes acting at different time- and length scales. Accordingly, each of these phenomena need to be addresses via multi-scale modelling approach, in which effective material parameters form small-scale high resolution models are used to feed the larger scales simulations (Fig. 1). Most fundamental aspects of mineral reactivity are provided by atomic scale simulations. Pore scale simulations on the other hand, offer an elegant way to link atomistic description of chemical reaction at mineral fluid interfaces with structural and compositional heterogeneities of natural systems. Such modelling allows predicting transport parameters of reactive materials and provide these as input for the large-scale reservoir models. Several numerical and theoretical challenges need to be resolved before such approach can be used to a full extend. This contribution will summarizes the current molecular-scale knowledge on mineral-fluid interface the system behavior chemistry, obtained from complementary coarse-grain simulation approaches [2].

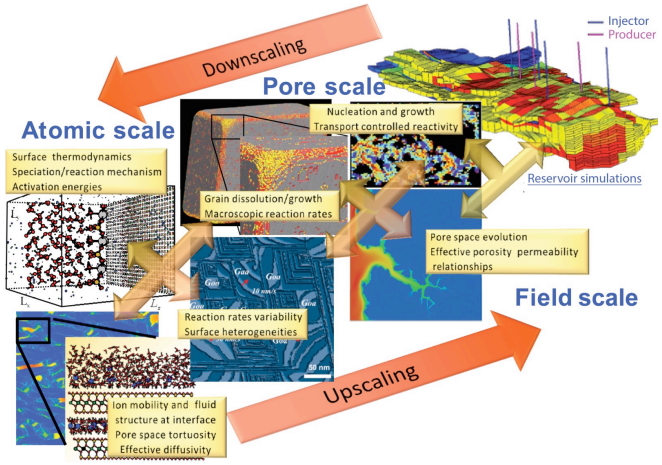

Fig. 1: Conceptualization of process couplings and parameter upscaling in multiscale reactive transport modelling [2].

DESCRIPTION OF THE WORK

The main challenges for an integrated mechanistic description of precipitation/dissolution phenomena are the process couplings and the transfer of parameters controlling the system evolution between different scales. Taking into account the system's complexity, we believe that a breakthrough in the quantitative description of the mineral reactivity in complex mineral systems can be achieved with due account for the mechanistic understanding of the reaction controlling processes and their couplings. The key factors controlling these processes are [2]:

1. The atomistic mechanism of surface reactions and molecular mass transport
2. The chemical speciation on surface sites and in the near-surface fluid
3. The morphology and reactive site density of mineral surfaces
4. The pore-scale transport and the pore space evolution

5. The macroscopic mineral reactivity and rock textures

RESULTS AND DISCUSSION

The presentation will cover recent examples of using multiscale simulation to address various aspects of reactive transport processes in porous media, ion adsorption and diffusion mechanism. New insights in the mechanism of mineral dissolution have been obtained by quantum mechanical simulations using explicit solvent molecules [3]. These data helps to understand mechanism of mineral reactivity and kinetics. Molecular scale nature of sorption on edge surface of clay minerals has been revealed combining spectroscopic studies and atomistic modelling [4]. These results help to explain experimentally measured ion competition effect in clay minerals. Effect of electrostatic interaction and pore scale ion transport has been revealed combination of molecular simulations and Lattice Boltzmann Modelling in cementitious materials [5, 6]. Macroscopic reactive transport models are applied to reveal the mineral transformation and porosity evolution at cement clay interface [7]. Finally, we will address the application of machine learning algorithms and deep neural networks for improving the performance of reactive transport simulations [8].

REFERENCES

1. CHURAKOV S.V., et al., “Fundamental Research on Radiochemistry of Geological Nuclear Waste Disposal.”, *Chimia,* **74**, 1000-1009 (2020).
2. CHURAKOV S.V. & PRASIANAKIS N.I. “Review of the current status and challenges for a holistic process-based description of mass transport and mineral reactivity in porous media.”, *American Journal of Science*, **318**, 921–948 (2018).
3. SCHLIEMANN, R. & CHURAKOV, S.V. Atomic scale mechanism of clay minerals dissolution revealed by ab initio simulations. *Geochimica et Cosmochimica Acta* **293**, 438-460 (2021).
4. KERI, A., et al., Iron Adsorption on Clays Inferred from Atomistic Simulations and X-ray Absorption Spectroscopy. *Environmental Science & Technology* **54**, 1886-11893 (2020).
5. KRATTIGER, N., et al. “Sorption and electrokinetic properties of ASR product and C-S-H: A comparative modelling study.” *Cement and Concrete Research,* **146**, 106491 (2021).
6. YANG, Y., et al. Multiscale modeling of ion diffusion in cement paste: Electrical double layer effects. *Cement and Concrete Composites* **96**, 55–65 (2019).
7. GIMMI T. & CHURAKOV S.V. Water retention and diffusion in unsaturated clays: Connecting atomistic and pore scale simulations. *Applied Clay Science,* **175**, 169-183 (2019).
8. PRASIANAKIS N.I., et al. Neural network based process coupling and parameter upscaling in reactive transport simulations. *Geochimica et Cosmochimica Acta* **291**, 126-143 (2020).

Coupled radionuclide transport reactions in shale rocks interpreted based on laboratory diffusive tests and data modelling – a novel approach

Raphael A.J. Wüst[1], Luc R. Van Loon[2], Martin Glaus[2], Xiaoshuo Li[1], Thomas Kämpfer[1], Gerhard Mayer[3]

[1]Nagra, Hardstr. 73, 5430 Wettingen, Switzerland
[2]PSI-LES, Forschungsstr. 111, 5232 Villigen PSI, Switzerland
[3]CSD Ingenieure AG, Schachenallee 29A, 5000 Aarau, Switzerland
email:Raphael.wuest@nagra.ch

INTRODUCTION

Low permeability rocks, such as shales, are the target of several exploratory programs and studies around the world for geological disposal of radioactive waste. The rocks form the geological barrier and contribute significantly to repository safety, i.e. long-term safe storage with negligible radiological impact on the environment.

Radionuclide transport through such rocks is dominated by slow diffusive processes. In order to determine diffusivity based on laboratory analysis and/or data modelling, various sample material is tested and compared with various rock properties.

DESCRIPTION OF THE WORK

Here we present a new approach for determining effective diffusion coefficients for clay-rich shales and calcareous mudstones in northern Switzerland. This has been established based on >60 samples from various formations of Triassic- to Jurassic ages. The data is based on new exploratory core analysis within two siting areas of the ongoing site selection program. Correlations between mineral components and porosity-permeability are provided and show dependency of property parameters. The data allow modelling approaches using newly developed formulas and fixed parameters that illustrate links to transport characteristics.

RESULTS AND DISCUSSION

The importance of understanding the methodological approaches and method development and therefore data output is that better knowledge allows proper upscaling of datasets and obtaining meaningful input data for modelling studies. Upscaling challenges are illustrated and discussed und sensitivities shown which have implications for long-term safety assessments of such geological repositories for radioactive waste.

Cationic and anionic species calculations are separated, and data compared with clay to non-clay content ratios and surface diffusion effects are taken into account. Examples of long-term diffusive analysis based on obtained information and rock properties are illustrated in the presentation.

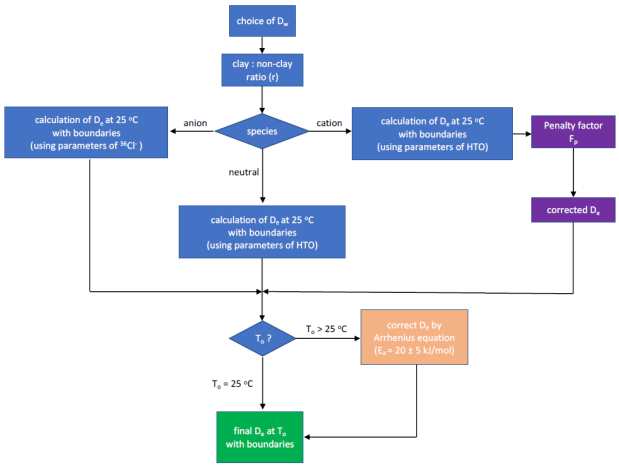

Figure 1

Fig. 1: General scheme for estimating effective diffusion coefficients for radionuclide species in argillaceous rocks (incl. upper and lower limits or bounds).

A hybrid pore-scale and continuum-scale model for solute transport and local precipitation in porous media

Yuankai Yang[1], Renchao Lu[2], Jenna Poonoosamy[1], Guido Deissmann[1], Haibing Shao[2], Dirk Bosbach[1]

[1]*Institute of Energy and Climate Research (IEK-6): Nuclear Waste Management and Reactor Safety, Forschungszentrum Jülich GmbH, 52425 Jülich, Germany*
[2]*Department of Environmental Informatics, Helmholtz-Zentrum für Umweltforschung GmbH, 04318 Leipzig, Germany*
Email: y.yang@fz-juelich.de

INTRODUCTION

Precipitation growth and solute transport are involved in many geological processes. Critical examples include radionuclide reactive transport in the context of nuclear waste disposal, wastewater treatment, and concrete degradation. Mineral precipitation changes the solid structures of porous media, and thus affects the transport pathway of solutes. Normally, if the precipitation reaction is not strong, this alteration can be modeled by the classical continuum-scale theory with a simple power-law function of the effective diffusivities with the porosity. However, when the reactive rate of precipitation is much quicker than the transport, the chemical heterogeneity becomes significant and the continuous media assumption fails. Hence, the alteration of solute fluxes caused by the local precipitation may not be easily simulated by the continuum-scale models (1,2). In this situation, the pore-scale simulations are usually used to accurately capture the dynamics of liquid-solid interfacial reactions and the corresponding solute transport. However, the pore-scale computation is very expensive and time-consuming. In comparison, a hybrid pore-scale and continuum-scale model is a balanced way between the computational cost and the accuracy (3).

DESCRIPTION OF THE WORK

In this work, a hybrid pore-scale and continuum-scale model has been recently developed to consider the solute reactive transport with local precipitation in porous media. In the region with high chemical heterogeneity, a pore-scale reactive transport model based on the lattice Boltzmann method (LBM) is employed in order to accurately capture the dynamics of liquid-solid interfacial reactions, and in the other regions, it is adequate to apply the continuum-scale standard simulations by using the OpenGeoSys (OGS-6).

RESULTS AND DISCUSSION

Fig. 1 shows a classical mesh for our hybrid model, where the red grids are used for the two-dimensional LBM and the black is for the one-dimensional OGS. The code implementation of the proposed hybrid model has been verified through several one-dimensional benchmarks including a conservative diffusion example, a solute degradation example, and a diffusion-dissolution example. For instance, Fig. 2 compares the profiles of solute concentration in a parallel-plate channel simulated by the finite element method (FEM) and our hybrid model, respectively. The results given by our hybrid model agree well with those by FEM.

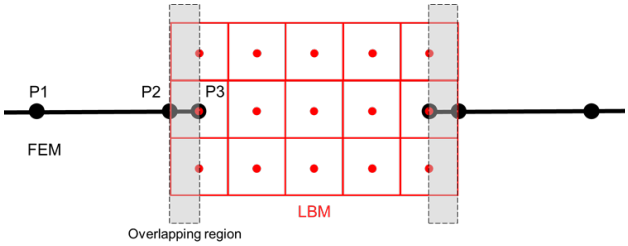

Fig. 1: Sketch of the computational discretization in the hybrid model, where the red region is the grids for LBM at pore scale and the black region is that for FEM at the continuum scale. These two regions have an overlapping part (grey region) designed for the data transformation.

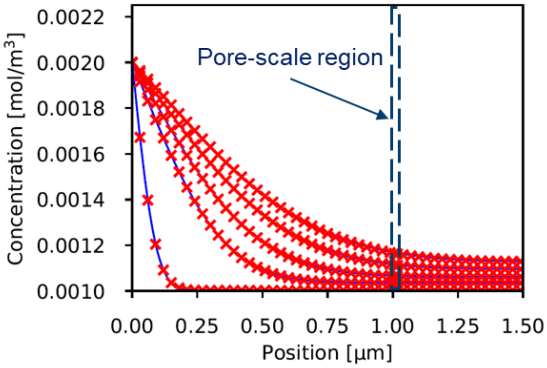

Fig. 2: Comparison of finite element and hybrid models for simulation of the coupled diffusion-dissolution process in a reactive parallel-plate channel.

As mentioned before, when the reactive rate of precipitation is much quicker than the diffusion of solutes,

the chemical heterogeneity becomes significant and the continuous media assumption fails. An example of the solute diffusion in a straight channel with local precipitation around x=0.55 m (shown in Fig.3A) is designed to show the difference between the continuum-scale model and the hybrid model to calculate the tracer diffusion in a channel after local precipitation. The concentration profile computed by our hybrid model has a significant drop caused by the local precipitation, but the continuum-scale model does not capture this.

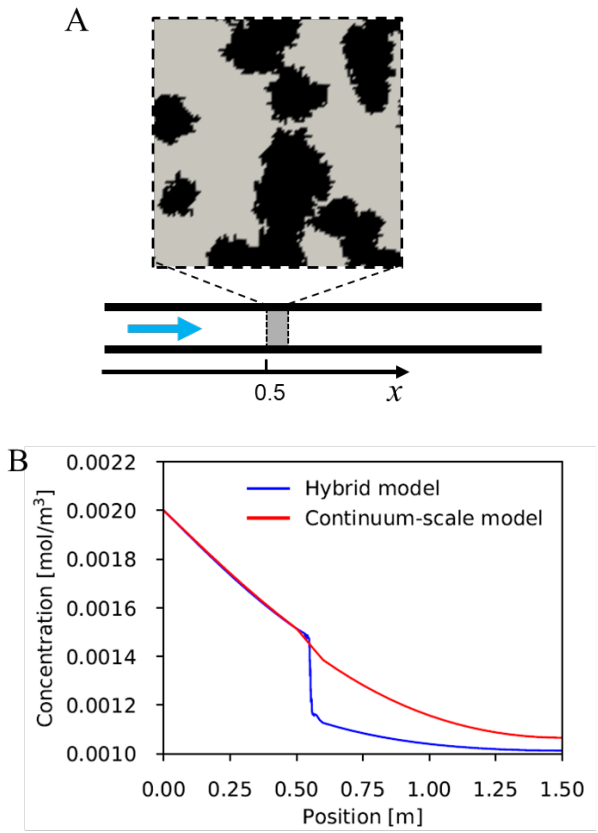

Fig. 3: A) a sketch of the domain with local precipitation for simulations. B) Comparison of finite element and hybrid models for simulation of the tracer diffusion in the channel from B.

REFERENCES

1. DENG, H., et al., "A Pore - Scale Investigation of Mineral Precipitation Driven Diffusivity Change at the Column - Scale", *Water Resources Research*, **57**, 2020wr028483 (2021).

2. BATTIATO, I., et al., "On breakdown of macroscopic models of mixing-controlled heterogeneous reactions in porous media", *Advances in Water Resources*, **32**, 1664-1673 (2009).

3. TANG, Y., A.J. "Valocchi, and C.J. Werth, A hybrid pore-scale and continuum-scale model for solute diffusion, reaction, and biofilm development in porous media", *Water Resources Research*, **51**, 1846-1859 (2015).

Numerical modeling and simulation of diffusive transport of radionuclides in the sandy facies of Opalinus Clay using multi-scale digital rock physics

Tao Yuan[1], Yuankai Yang[2], Guido Deissmann[2], and Cornelius Fischer[1]

[1]*Institute of Resource Ecology, Helmholtz-Zentrum Dresden-Rossendorf (HZDR), 04318 Leipzig, Germany*
[2]*Forschungszentrum Jülich GmbH (FZJ) – Institute of Energy and Climate Research (IEK-6), 52428 Jülich, Germany*
email: t.yuan@hzdr.de

INTRODUCTION

Accurate modeling and simulation of radionuclides migration in host rocks such as Opalinus Clay (OPA) play a key role in the safety assessment of disposal concepts for nuclear waste. At the continuum scale, the representative elementary volume (REV) is a fundamental parameter for the quantification of the effective diffusivity, which is critical in the diffusive transport calculations. Therefore, meaningful modeling of heterogeneous diffusion in the sandy facies of OPA at the continuum scale requires an accurate estimation of the REV. In this study, we first utilize digital rock physics and an upscaling workflow that integrates nm- and µm-scale simulations to estimate the effective diffusivity of radionuclides in the sandy facies of OPA [1]. Second, we determine the REVs for the effective diffusivity and porosity by using the classical sampling theory [2]. The resulting REV provides critical insight into the heterogeneity of the diffusivity in the sandy facies of OPA, utilized to enhance the predictability of radionuclide migration.

METHODOLOGY

DIFFUSIVITY PARAMETERIZATION. The effective diffusivities of radionuclides are determined using multi-scale digital rock physics and an integrated upscaling workflow. The digital rocks include two types of materials at the pore scale, in which the pore space and pore network in the clay mineral aggregates at the nm scale (Fig. 1a) and mineral complexity in shales at the µm scale (Fig. 1b) are considered. As a starting point, the lattice Boltzmann method (LBM) is used to solve the Poisson-Nernst-Planck (PNP) equation at the nm scale [3]. The nm-scale results are then used as input parameters in the µm-scale model for diffusive transport calculations. At this scale, the three-dimensional (3D) diffusion-sorption equation is numerically solved by a previously developed numerical simulator [4]. The diffusivity is calculated using the proposed upscaling approach, which is validated with published experimental data that confirm the general applicability of the models.

DETERMINATION OF REV. We determine the REVs for effective diffusivity and porosity using the classical sample theory [2]. In order to do so, we first constructed a synthetic microstructure of OPA with a size of 150^3 µm^3, which contains 80 % clay mineral aggregates and 20 % of other sedimentary components including quartz, calcite, and pyrite. We then extracted the various sub-regions with different volumes. For the same volume, all sub-regions are non-overlapping and evenly distributed within the entire domain, resulting in the 10^3, 5^3, 3^3, and 2^3 sub-regions with volumes of 15^3, 30^3, 50^3, and 75^3 µm^3, respectively (Fig. 2). For each subset, the effective diffusivity is calculated as explained above. Based on the classical sampling theory, the relative error on the exact mean value of a given property M_D is defined as $\varepsilon = 2\sigma_D(\mathrm{V})/M_D$, where σ_D is the standard deviation of the property for the subsets with the identical volume of V. The REV for the given property can be determined with a predefined relative error, e.g., $\varepsilon = 10\%$ [5, 6].

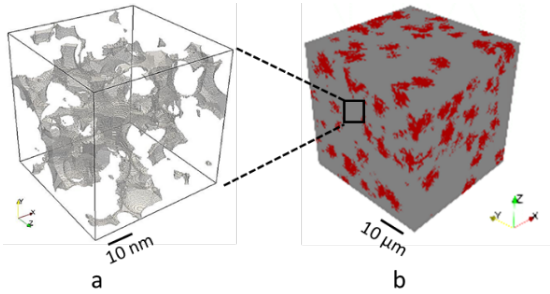

Fig. 1: a: Digital rock model of the rock structure built-up of clay mineral aggregates (transparent) and pores (gray color). b: Reconstructed digital rock with clay mineral aggregates (gray color) and other sedimentary and diagenetic components (red color) including quartz, calcite, and pyrite.

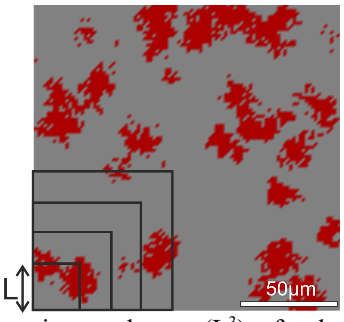

Fig. 2: The various volumes (L^3) of sub-regions on a synthetic microstructure of OPA for REV determination. The volumes of the microstructure and extracted sub-regions are 150^3, 75^3, 50^3, 30^3, and 15^3 µm^3, respectively. For each volume, all sub-regions are non-overlapping and evenly distributed within the entire domain.

RESULTS AND DISCUSSION

Fig. 3 illustrates the calculated relative errors of porosity and effective diffusivity as a function of the volume of the subset, which shows a linear correlation on a log-log scale (R^2 = 0.99 for porosity, R^2 = 0.98 for diffusivity). As expected, the relative errors of both properties decrease with increasing the volume because the measured properties become more statistically representative with a larger volume. With a suggested relative error of 10 %, the REV for porosity is about 92^3 µm^3 and the REV for diffusivity is about 330^3 µm^3. The significantly different REVs for porosity and diffusivity suggest that the REV for diffusivity instead of that for porosity should be utilized for 3D numerical modeling of the diffusive transport of radionuclides at the continuum scale. The REV analysis improves the understanding of heterogeneous diffusion in the sandy facies of OPA at the core scale, which contributes to an enhanced predictability of radionuclide migration at the field scale.

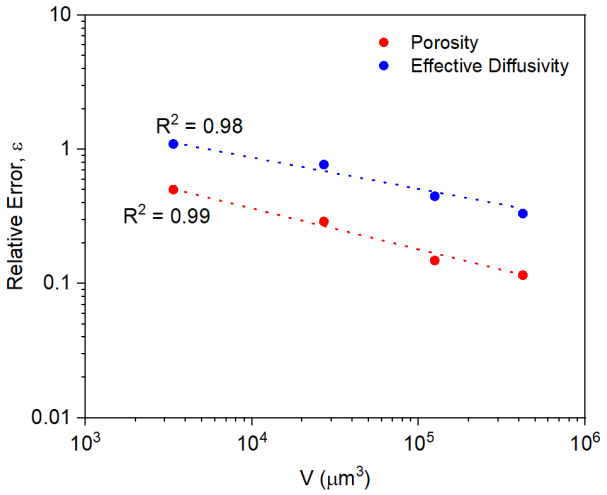

Fig. 3: Relative errors of porosity (red dots) and effective diffusivity (blue dots) versus the volume of the sub-region. The red and blue dash lines represent the calibration curves for porosity and diffusivity, which show the linear curves with the coefficients of determination, R^2 = 0.99 and R^2 = 0.98 on a log-log scale, respectively.

ACKNOWLEDGEMENTS

We gratefully acknowledge funding by the German Federal Ministry of Education and Research (BMBF), grant 02NUK053B and the Helmholtz Association, grant SO-093 (iCross).

REFERENCES

[1] YUAN, T., FISCHER, C., "Effective Diffusivity Prediction of Radionuclides in Clay Formations Using an Integrated Upscaling Workflow", *Transp. Porous Med.*, **138**, 245-264 (2021).

[2] KANIT, T. et al., "Determination of the size of the representative volume element for random composites: statistical and numerical approach", *Int. J. Solids Struct.*, **40**, 3647-3679 (2003).

[3] YANG, Y. et al., "Multiscale modeling of ion diffusion in cement paste: Electrical double layer effects", *Cem. Concr. Compos.*, **96**, 55-65 (2019).

[4] YUAN, T. et al., "A Numerical Simulator for Modeling the Coupling Processes of Subsurface Fluid Flow and Reactive Transport Processes in Fractured Carbonate Rocks", *Water*, **11,** 1957 (2019).

[5] KELLER, LM. et al., "Pore space relevant for gas permeability in Opalinus clay: Statistical analysis of homogeneity, percolation, and representative volume element", *J. Geophys. Res. Solid Earth*, **118**, 2799-2812 (2013).

[6] HOUBEN, M.E. et al., "A comparative study of representative 2D microstructures in Shaly and Sandy facies of Opalinus Clay (Mont Terri, Switzerland) inferred form BIB-SEM and MIP methods", *Mar. Pet. Geol.*, **49**, 143-161 (2014).

Autoradiography and SEM–EDX analysis of diffusion samples of sandy facies of Opalinus Clay

Claudia Joseph, Dieter Schild, Stephanie Kraft, Horst Geckeis

Institute for Nuclear Waste Disposal (INE), Karlsruhe Institute of Technology (KIT), P.O. Box 3640, 76021 Karlsruhe, Germany
email: claudia.joseph@kit.edu

INTRODUCTION

Natural clay is discussed and investigated as host rock for high-level nuclear waste repositories in several countries such as Switzerland, Belgium, and France. For instance, the Opalinus Clay formation is considered as host rock in the Swiss disposal concept. In this regard, Opalinus Clay is accessible to international partners for research in manifold scientific questions in the so-called Mont Terri Project in an underground rock laboratory (URL) in Mont Terri, Switzerland. In the last decades, in particular the Opalinus Clay shaly facies were well-characterized and well-studied. In 2018, a new gallery was excavated in the URL providing access to more experiments in the sandy facies of Opalinus Clay. This is a more complex part of the clay formation. The sandy facies is characterized by large sand layers and carbonate lenses. It contains half as much clay minerals (e.g., illite, kaolinite) but about twice as much calcite and quartz than the shaly facies. Its heterogeneity mimics clay formations present in Germany which could be discussed as host rocks of a potential site for a high-level waste repository.

The focus of this study was to investigate the influence of heterogeneities of the sandy facies of Opalinus Clay on the radionuclide diffusion. Diffusion is the dominating transport process in clay rock for water-mediated waste-released radionuclides. Through-diffusion experiments with HTO and $^{36}Cl^-$ were conducted with bore core pieces of the Opalinus Clay. Subsequently, the diffusion samples were analyzed by autoradiography to identify the preferred radionuclide transport paths. Outstanding features were closer studied by scanning electron microscopy (SEM) combined with energy dispersive X-ray spectroscopy (EDX).

DESCRIPTION OF THE WORK

The bore core BAD-1, drilled in the sandy facies of Opalinus Clay parallel to the bedding in July 2018, was obtained from the URL Mont Terri, Switzerland. Diffusion specimens of about 25 mm in diameter and about 10 mm in length were prepared from BAD-1 to study the HTO and $^{36}Cl^-$ diffusion perpendicular to the clay bedding in two different types of diffusion cell: 1. the well-known diffusion cell [1], where the clay specimen is sandwiched between two stainless steel filter plates and two polyether ether ketone (PEEK) end plates inside a surrounding PEEK cylinder; except the clay sample was glued to the PEEK cylinder by a 2-component PEEK glue; 2. an optimized diffusion cell consisting of the clay cylinder jacket embedded in EpoFix (Struers) resin sandwiched between two borosilicate glass filters and two PEEK end plates.

Each diffusion cell was connected to a high concentration reservoir (HCR) and a low concentration reservoir (LCR) containing synthetic Opalinus Clay pore water [2] (pH 7.2, I = 0.22 mol/L). Before the diffusion was initiated by adding the appropriate amount of radioactive tracer to the HCR solution (1000 Bq/mL HTO, 1000 Bq/mL $^{36}Cl^-$), the samples were equilibrated for about one month with pore water.

The diffusion experiments were stopped after about one month (1. diffusion cell type) and five months (2. diffusion cell type). Subsequently, each central clay specimen was sawed into two halves. The surfaces were placed onto a MultiSensitive storage phosphor screen (Perkin Elmer) for $^{36}Cl^-$ detection. After 22 h (1. diffusion cell type) and 73 h (2. diffusion cell type), the samples were removed, the screen scanned (Cyclon® Plus Imaging System, Perkin Elmer) and the scans analyzed by OptiQuant™ Image Analysis software.

Selected surfaces were coated by a several nanometer thick carbon film and imaged by a FEI Quanta 650 FEG environmental scanning electron microscope. SEM–EDX spectra of selected areas were acquired using a Thermo Scientific NORAN System 7 microanalysis system, software Pathfinder version 2.8.

RESULTS AND DISCUSSION

The radionuclide migration data showed significant advective flow using the 1. diffusion cell type. The autoradiographic images of the respective samples revealed dominant radionuclide transport across the sample rim (Fig. 1). The sandy facies contain relatively large aggregates of non-swellable minerals. The clay rock itself seems to be not able to close the gap between the clay specimen and the surrounding PEEK cylinder by swelling during the equilibration of the diffusion sample. However, the autoradiographic analysis identified areas of low $^{36}Cl^-$ activity (blue, Fig. 1), which is equated with low anion permeability of the heterogenous clay rock. This was attributed to white mineral aggregates in the clay. A SEM-EDX analysis of one of these white areas (Fig. 2)

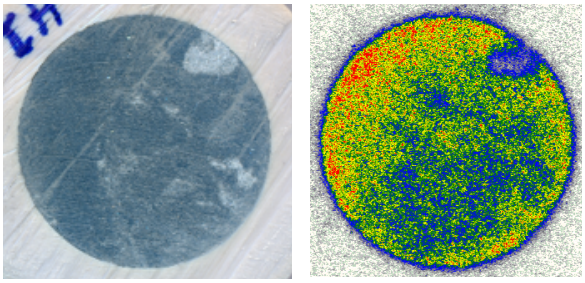

Fig. 1: Photo scan (left) and autoradiographic image (right) of Opalinus Clay sandy facies diffusion sample (1. diffusion cell type). Color scale ranges from areas of low $^{36}Cl^-$ activity (blue) to areas of high activity (red).

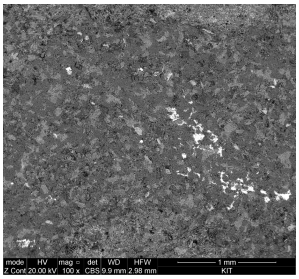

Fig. 2: Backscattered electron image of the area with low activity (1. diffusion cell type) showing material contrast.

showed that it consists mainly of quartz (dark grey in the backscattered electron image) cemented with calcite (light grey). The bright white mineral in Fig. 2, caused by elements with high Z, was identified as $(Sr,Ba)SO_4$. In particular celestite is known to block the diffusion accessible pores in clay for anionic tracers[3], which could be the explanation for the observed behavior.

After the improvement of the diffusion cell setup by embedding the clay specimen in resin (2. diffusion cell type), the diffusion data of the second experiment showed diffusion through the specimen as dominant radionuclide transport process. However, the autoradiographic images showed still some rim transport (not shown), but also revealed areas of high $^{36}Cl^-$ activity, meaning high anion permeability, in the clay (Fig. 3). The lower right-hand side high-activity spot in Fig. 3 was compared to an area of mean activity (green) via SEM. Both areas significantly differed by their morphology. The high-activity area was more homogenous and fine-grained, the green area showed larger mineral aggregates apparently cemented in clay. The respective EDX analysis of both areas did not show significant differences in chemical composition. However, the high-activity area contained less large calcite grains, indicating a calcite leaching due to higher flow. SEM images of high-activity areas at higher resolution revealed the presence of pore structures below the surface (Fig. 4). EDX analysis identified elevated amounts of carbon and Fe, but no S. Either these were remains of fossils, where iron oxide or hydroxide precipitated or siderite as described elsewhere [4].

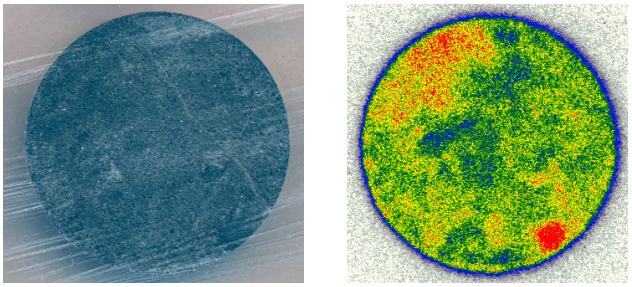

Fig. 3: Photo scan (left) and autoradiographic image (right) of Opalinus Clay sandy facies diffusion sample (2. diffusion cell type). Color scale ranges from areas of low $^{36}Cl^-$ activity (blue) to areas of high activity (red).

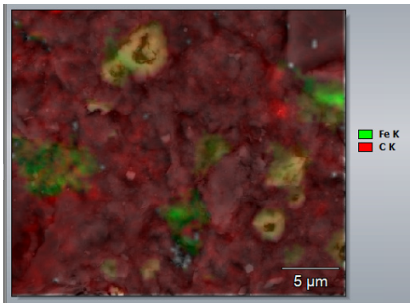

Fig. 4: SEM image of the area with high activity (2. diffusion cell type) combined with false color representation of the main elements identified via EDX mapping.

These pores seem to be the reason for the high permeability, since they were found only in areas of high activity.

ACKNOWLEDGEMENTS

The authors thank the Federal Ministry of Education and Research (Grant 02 NUK 053 C) and the Helmholtz Association (Grant SO-093) for financial support.

REFERENCES

1. L. R. VAN LOON et al., "Diffusion of HTO, $^{36}Cl^-$ and $^{125}I^-$ in Opalinus Clay samples from Mont Terri - Effect of confining pressure", *J. Contam. Hydr.,* **61**, 73-83 (2003).
2. T. GIMMI et al., "Anisotropic diffusion at the field scale in a 4-year multi-tracer diffusion and retention experiment - I: Insights from the experimental data", *Geochim. Cosmochim. Acta,* **125**, 373-393 (2014).
3. A. CHAGNEAU et al., "Complete restriction of $^{36}Cl^-$ diffusion by celestite precipitation in densely compacted illite", *Env. Sci. Techn. Letters,* **2**, 139-143 (2015).
4. B. LAURICH et al., "Microstructures and deformation mechanisms in Opalinus Clay: insights from scaly clay from the Main Fault in the Mont Terri Rock Laboratory (CH)", *Solid Earth,* **8**, 27-44 (2017).

Migration behaviour of Ra-226 in the sandy facies of Opalinus Clay

Naila Ait-Mouheb[1], Luc R. Van Loon[2], Martin A. Glaus[2], Yuankai Yang[1], Guido Deissmann[1], Dirk Bosbach[1]

[1]*Institute of Energy and Climate Research (IEK-6): Nuclear Waste Management and Reactor Safety, Forschungszentrum Jülich GmbH, 52425 Jülich, Germany*
[2]*Laboratory for Waste Management, Paul Scherrer Institut, CH-5232 Villigen PSI, Switzerland*
email: n.ait.mouheb@fz-juelich.de

INTRODUCTION

A reliable and consistent assessment of the safety of a deep geological repository for heat generating radioactive waste over time scales of hundred thousand of years requires an advancement of process understanding and simulation tools for a close-to-reality description of repository evolution scenarios. This is notably required due to the challenging task to compare and assess the safety of different repository concepts in different host rocks within the German site selection process. Thus, within the collaborative project iCross, a coordinated programme of dedicated laboratory-scale experiments is currently being performed in support of the development of a multi-scale approach to describe and analyse the integrity of nuclear waste repository systems across scales.

DESCRIPTION OF THE WORK

Opalinus Clay (OPA) is proposed as host rock formation for a geological disposal facility for radioactive waste in Switzerland and is also being considered in the recently started site selection procedure for a high-level radioactive waste repository in Germany. In this context, we evaluated the effect of the natural heterogeneity of the sandy facies in the Opalinus Clay formation on radionuclide transport. Here, we address the migration behaviour of Ra-226 as a critical radionuclide to be considered in safety cases for the deep geological disposal of spent nuclear fuel. However, data on the sorption and diffusion behaviour of Ra-226 in clay rocks is so far mainly derived from analogies with Ba or Sr.

RESULTS AND DISCUSSION

In this study, we report results on the impact of the natural heterogeneity of sandy OPA facies on the Ra-226 uptake in bore core samples from the Mont Terri underground rock laboratory. The investigated bore cores BAD-1 and BMB-A7 are oriented parallel and inclined to the bedding, respectively. Different samples were selected from the two bore cores which were representative for their chemical heterogeneity. The samples were carefully characterized with respect to mineralogy and geochemistry using, e.g., XRD and SEM/EDS. The amounts of quartz, carbonates, and clay minerals present in the samples ranged from 58 to 65 wt. %, 13 to 35 wt.% and 5 to 25 wt.%, respectively. Precipitates of (Ba, Sr)-sulphates were identified in the clay matrix by SEM-EDX.

The uptake behaviour of Ra-226 was evaluated using batch sorption experiments. In all samples the distribution ratio R_d for Ra-226 was in the range of 20 L kg^{-1} < R_d < 120 L kg^{-1} after 30 days, when sorption steady state conditions were reached. The uptake of Ra-226 is associated with cation exchange and surface complexation reactions, the possible formation of solid solutions during the recrystallization of (Ba, Sr)-sulphates and/or uptake/co-precipitation with carbonate minerals.

The results of the time-dependent Ra-226 batch sorption experiments for all samples are shown in Fig. 1. An increase of Ra-226 retention over time is observed, indicating a kinetically controlled sorption process. This implies that diffusion or incorporation of Ra-226 into carbonates through a co-precipitation reaction may occur. The co-precipitation reaction is characterized by slow reaction kinetics, particularly for samples containing higher contents of carbonates. The experimental work is supported with PhreeqC calculations [1], where a bottom-up approach has been used to model the sorption data, with the assumption that illite and illite/smectite mixed layers are the main sorbing phases in the sandy OPA (cf. [2]).

Currently, the retention of radionuclides due to co-precipitation with secondary solid phases is often not included in safety assessments of radioactive waste repositories. However, this study indicates that the bottom-up approach assuming sorption only by clay minerals is not applicable for Ra-226 sorption on sandy OPA with high amounts of carbonate minerals. Thus, with respect to the robustness of the approach and to reduce uncertainties and conservatisms in the assessment of Ra-226 sorption in clay rocks with higher carbonate contents, the formation of Ra-226 bearing carbonates should be considered in such systems and further investigated.

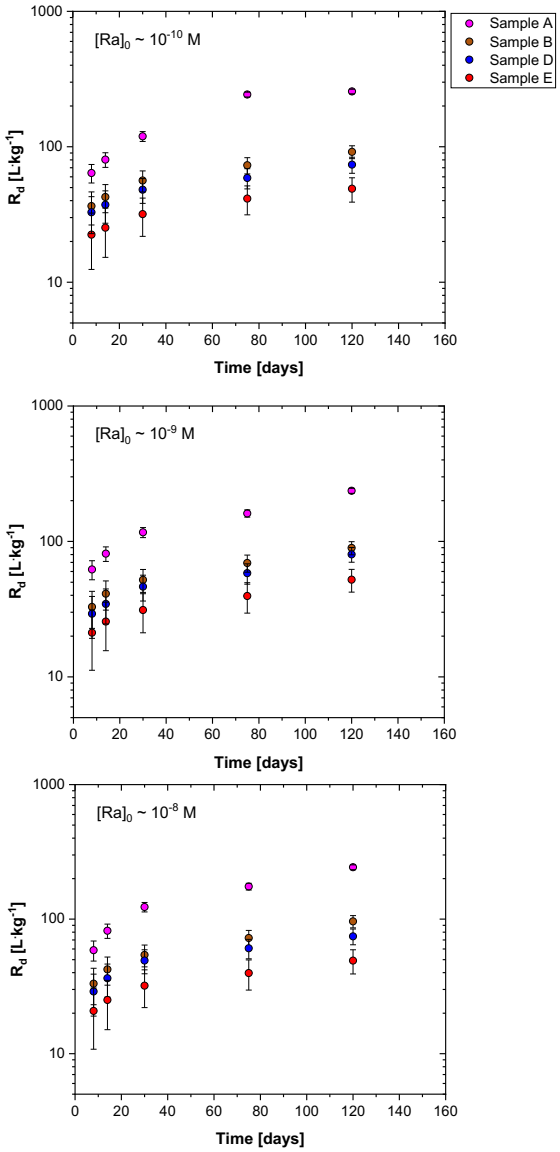

Fig. 1: Sorption of Ra-226 on selected samples from the sandy OPA facies from Mont Terri (BAD-1 bore core) as function of time (S/L ratio = 117 g L^{-1}; c_0(Ra) ~10^{-8} mol·L^{-1} - 10^{-9} mol·L^{-1} - 10^{-10} mol·L^{-1}). The amounts of carbonates and clay minerals present in the "sample A" were 35 wt.% and 5.1 wt.%, respectively, in the "sample B" were 13.5 wt.% and 25.6 wt.%, respectively, in the "sample D" were 22.4 wt.% and 12.4 wt.%, respectively, and in the "sample E" were 15.2 wt.% and 20.8 wt.%, respectively,

ACKNOWLEDGEMENTS

The research leading to these results has received funding from the German Federal Ministry of Education and Research (BMBF, grant agreement 02NUK053A) and from the Initiative and Networking Fund of the Helmholtz Association (HGF grant SO-093) within the iCross project.

REFERENCES

1. PARKHURST & APPELO, "Description of input and examples for PHREEQC version 3: a computer program for speciation, batch-reaction, one-dimensional transport, and inverse geochemical calculations", *US Geological Survey* (2013).
2. BRADBURY & BAEYENS, "Predictive sorption modelling of Ni(II), Co(II), Eu(IIII), Th(IV) and U(VI) on MX-80 bentonite and Opalinus Clay: A "bottom-up" approach", *Applied Clay Science*, **52**, 27-33 (2011).

Long term bentonite erosion experiments in an artificial fracture: Radionuclide diffusion in FEBEX bentonite

Y. Kouhail[1], F. Rinderknecht[2], F. Geyer[1], E. Soballa[1], D. Schild[1], F. Quinto[1], V. Metz[1], T. Schäfer[3], H. Geckeis[1]

[1]*Karlsruhe Institute of Technology (KIT), Institute for Nuclear Waste Disposal (INE), Karlsruhe, Germany*
[2]*Karlsruhe Institute of Technology (KIT), Training Center for Technology and Environment (FTU), Karlsruhe, Germany*
[3]*Friedrich-Schiller-Universität Jena (FSU), Institute for Geosciences (IGW), Applied Geology, Jena, Germany*
email: yasmine.kouhail@kit.edu

INTRODUCTION

Natural bentonite is envisaged to be used as engineered barrier for repositories of high-level radioactive waste in, e.g., crystalline rocks [1]. Steel canisters with or without copper coating containing the spent fuels rods are planned to be emplaced in a host rock with bentonite surrounding the canisters as a backfill material. In some disposal concepts (e.g. the Scandinavian concept), glacial melt water intrusion scenarios are discussed. The intrusion of low mineralized water would lead to the swelling and the erosion of the bentonite [2], with consecutive formation of bentonite colloids. These would in term act as carrier for radionuclides, increasing their mobility, in such cases, where the container corrodes and loses integrity. The present study investigates radionuclide diffusion through the bentonite, bentonite erosion and the colloid-associated radionuclide migration.

DESCRIPTION OF THE WORK

FEBEX bentonite erosion experiments have been conducted in an artificial horizontal fracture set-up (mock-up experiments) to simulate the intrusion of groundwater in a repository. A ring of compacted bentonite (40 mm inner diameter, 80 mm outer diameter, 25 mm height) was emplaced between two Plexiglas plates spaced by a 1 mm height aperture to simulate a parallel fracture around the bentonite. Groundwater from the Grimsel Test Site, pumped through the fracture at a flow rate of 50 µL/min, led to bentonite swelling and formation of a gel in the aperture [3]. This inactive experiment was carried out under atmospheric conditions.

A similar experiment was performed with Zn-labelled montmorillonite, a cocktail of radionuclide tracers (containing ^{241}Am(III), ^{137}Cs(I), ^{242}Pu(III), ^{45}Ca(II), ^{75}Se(IV), ^{99}Tc(VII), ^{233}U(VI), ^{237}Np(V)) and a conservative tracer, Amino-G, that was mixed with a bentonite slurry and inserted in open glass vials within the bentonite. This active experiment was carried out in an argon glove box. In the collected effluent, analysis of colloids, elemental composition and radionuclide breakthrough were performed [3].

The Plexiglas boxes containing the radioactive and the inactive mock-up test were opened after ca. 5 years from the end of the experiments for post mortem analysis.

RESULTS AND DISCUSSION

In the inactive experiment, coarse grains of accessory minerals of various colors were visible in the bentonite gel and sampled for SEM-EDX and XRD analysis. Some minerals that were originally present in the bentonite (i.e. gypsum) were not identified, suggesting the dissolution of these minerals− in agreement with enhanced SO_4 concentrations in the collected water samples, while some other secondary phases were formed in the ring.

In the active experiment, 49 ± 2% of the Amino G tracer was released from the bentonite source. Radionuclide release was detected in case of ^{99}Tc, and ^{237}Np. In the post mortem analysis of the active experiment aiming at the investigation of other radiotracers, the bentonite ring and gel were preserved as two samples of the same size that adhere onto the two Plexiglas plates (top and bottom plates of the Plexiglas box as seen in Fig. 1). Two of the vials were intact and the two others broken due to the pressure rise during the experiment. Autoradiography was performed on the ring sample adhering to the top plate to detect gamma-emitter radionuclide tracers (namely ^{241}Am and ^{137}Cs). Two different types of diffusion distances were identified as shown in Figure 1. For the intact vial, the radionuclides were still mostly contained in the vial, with diffusion at a millimeter scale around the vial. In the case of the broken vial, the radionuclides were diffusing further away from the source on a centimeter scale. Autoradiographs of gamma emitting radionuclides could not be taken to represent diffusion profiles due to the relatively long range of gamma radiation. Such picture of the gamma-emitters distribution in the proximity of the vials will, however, allow planning the forthcoming steps of sample preparation and analysis by other analytical methods. In particular, in order to investigate the diffusion profiles of the actinide tracers at different distances from the vials, the bentonite sample will be cut into ca. 100 µm slices by abrasive peeling. After desorption of the actinide tracers

with concentrated nitric acid, their concentration will be determined with (SF)ICP-MS.

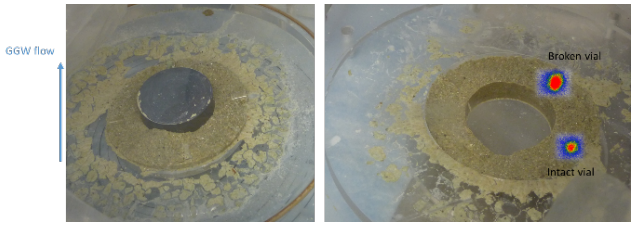

Fig. 1: Post mortem analysis of the FEBEX erosion experiment containing the radioactive tracer cocktail. Autoradiography images of the bentonite ring on the right.

REFERENCES

[1] SHELTON et al., SKB Technical report TR-17-17 (2018).
[2] BOUBY et al., *Applied Clay Science*, **198**, 105797, (2020).
[3] RINDERKNECHT, Doctoral thesis, KIT (2017).

Radionuclide transport modelling: The Smart K_d-concept in reactive transport codes

M. Stockmann[1], R. Lu[2], A. Gehrke[3], V. Montoya[2], U. Noseck[3], V. Brendler[1]

[1]*Helmholtz-Zentrum Dresden-Rossendorf (HZDR) e.V., Institute of Resource Ecology, Dresden, Germany*
[2]*Helmholtz Centre for Environmental Research - UFZ, Department of Environmental Informatics, Leipzig, Germany*
[3]*Gesellschaft für Anlagen- und Reaktorsicherheit (GRS) gGmbH, Braunschweig, Germany*
email: m.stockmann@hzdr.de

INTRODUCTION

A key component of performance assessment for radioactive waste repositories in deep geological formations is the long-term prediction of potential radionuclide transport to the geosphere over periods longer than 100,000 years. Radionuclide sorption on minerals (host rocks and geotechnical barriers) is one of the most important retardation process. One big challenge for radionuclide transport calculations with large-scale heterogeneous geochemical compartments is the integration of realistic physico-chemical models and their parameters at affordable computational costs.

In performance assessment, sorption is an important retardation process and typically considered by constant distribution coefficients (K_d) that can be easily included in transport codes. One of the advantage of this approximation is their computational efficiency, but it cannot reflect changes in geochemical conditions. On the other hand, mechanistic surface complexation models used for process understanding can be directly coupled to transport codes with geochemical solvers, but usually only at high computational costs. An effective alternative to the above mentioned approaches is provided by the smart K_d-concept (www.smartkd-concept.de) [1, 2], specifically developed to describe variable radionuclide sorption in transport models as consequence of changing geochemical conditions in time.

The fundamental strategy of the smart K_d-concept is to firstly compute multidimensional matrices (namely look-up tables) of distribution coefficients based on surface complexation and cation exchange models. The smart K_d-values are computed for different radionuclides as a function of a wide range of geochemical parameters. Such parameters are typically pH, ionic strength, and dissolved ions, e. g. calcium, carbonate. The look-up table is generated using the geochemical code PhreeqC [3].

The information stored in the look-up table can then be accessed by reactive transport codes at each point in time and space. This approach was already implemented in the d^3f^{++} code [4]. Here, an additional implementation and validation of the smart K_d-approach in OGS6 [5, 6] is demonstrated. For this purpose, three benchmark test were defined with increasing complexity. Complexity is mainly related to the number of components (radionuclides) included in the simulation. Results obtained with the OGS6 were compared with OGS6#PhreeqC3.5.0, PHAST [7] and d^3f^{++}.

DESCRIPTION OF THE WORK

MODEL SETUP. A 20 m long and 3 m high 2D domain was defined. A constant inflow of $3{\cdot}10^{-5}$ m s^{-1} (pH = 7.0, $CaCl_2$ dilute solution) in a 1 m wide window is stablish (see Fig. 1, above) and open boundary is assumed at the end of the domain. After 10,000 s different radionuclides (shown exemplarily for uranium in Fig. 1, below) at different concentrations are injected. The domain is considered as homogeneous porous media (porosity = 0.2 and permeability = $1.01{\cdot}10^{-11}$ m^2) with a reactive surface associated to quartz, feldspar, mica, Fe(III)-oxides/hydroxides and 2-layer clay minerals. In addition, it is assumed that calcite is present in the entire domain, being the only mineral that may dissolve or precipitate from solution changes over time.

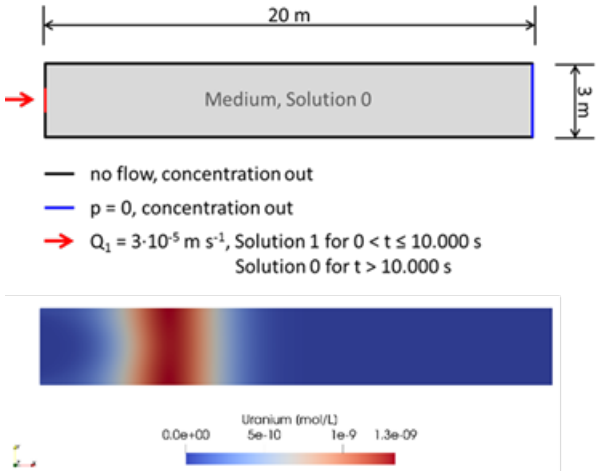

Fig. 1: Model domain dimensions (above) and boundary conditions as well as transport of uranium through the model domain (below).

RESULTS AND DISCUSSION

In the first benchmark, a non-sorbing tracer transport was simulated with consideration of the reactive transport equation in saturated porous media implemented in OGS6

and d³f++. Similar results were obtained with both transport codes for the flow and tracer calculations and verified the model setup.

In a second benchmark, Np(V) was taken as injected radionuclide (concentration = $1 \cdot 10^{-7}$ mol L^{-1}) that could sorb on the different minerals. In Fig. 2, the spatial distribution of Np(V) is shown after 100,000 s (~1 h) calculated with the new implemented smart K_d-OGS6 approach and with direct coupling OGS6#PhreeqC. As can be seen, the Np(V) profiles lie nearly perfectly one upon another. This implies that the look-up table approach works well.

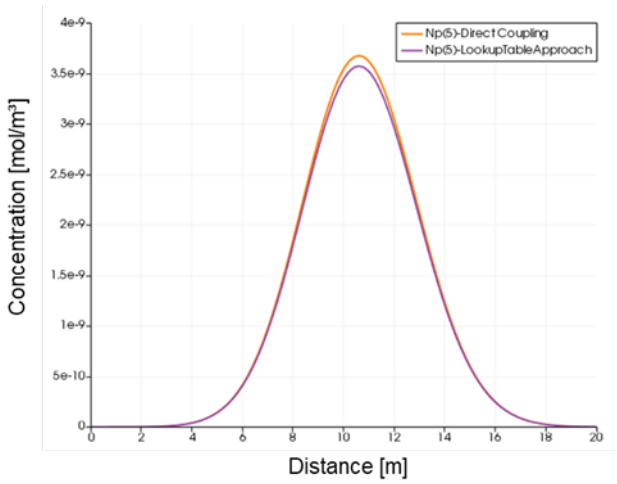

Fig. 2: Spatial distribution of Np(V) after 100,000 s (~1h) calculated with OGS6#PhreeqC and Smart-K_d-OGS6 approach

In a third benchmark, a case similar to the previous one was modelled but apart from Np(V), six additional radionuclides, Cs, Am, Th, Ni, U(VI) and Ra were included simultaneously (concentrations between $1 \cdot 10^{-6}$ and $1 \cdot 10^{-8}$ mol L^{-1}). In that case, comparison was performed between OGS6#PhreeqC and PHAST. Good agreement between both codes is observed. The spatial distributions after 500,000 s (~6h) reflect a radionuclide-specific retardation effect as can be seen clearly in Fig. 3. Neptunium has the weakest sorption of all considered radionuclides with the peak maximum at a distance of 10 m from the inflow. Cesium, Americium and Thorium have the strongest sorption and accumulated nearby the injection boundary (therefore not shown in Fig. 3).

We are able to reflect the radionuclide-specific retardation effect. This real application case serves as a comprehensive proof-of-concept and as a benchmark for field-scale transport simulations.

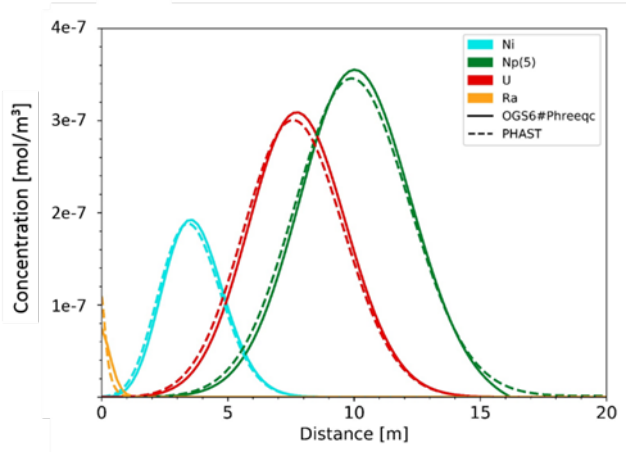

Fig. 3: Spatial distribution of the radionuclides after 500,000 s (~ 6h).

ACKNOWLEDGEMENTS

This work based on two projects: The iCross project is funded by the German Federal Ministry of Education and Research (BMBF) (Grant 02NUK053B) and the Helmholtz Association (Grant SO-093). The SMILE project is funded by the German Federal Ministry for Economic Affairs and Energy (BMWi) under contract Nos. 02E11668A-C.

REFERENCES

1. STOCKMANN et al., *Chemosphere*, **187**, 277-285 (2017).
2. NOSECK et al., Report GRS-500 (2018).
3. PARKHURST and APPELO, U.S.G.S. Report 6-A43 (2013).
4. SCHNEIDER et al., Report GRS-392 (2016).
5. JANG et al., OpenGeoSys Tutorial III, 103 (2018).
6. KOLDITZ et al., *Environ. Earth Sci.*, **67**, 589-599 (2012).
7. PARKHURST et al., U.S.G.S. Report 6-A35 (2010).

Anion transport mechanisms: applications to radionuclide migration and cementitious systems

Teba Gil-Díaz[1,2], Frank Heberling[2], Johannes Lützenkirchen[2], Thorsten Schäfer[1]

[1]*Teba Gil-Díaz, Institute of Geosciences, Friedrich-Schiller-Universität Jena, Burgweg 11, 07749 Jena, Germany*
[2]*Karlsruhe Institute of Technology (KIT), Institute for Nuclear Waste Disposal, Hermann-von-Helmholtz-Platz 1, 76344 Eggenstein-Leopoldshafen, Germany*
email: teba.gil-diaz@uni-jena.de

INTRODUCTION

Detailed knowledge on aquatic chemistry and mineral-solution interaction is necessary to understand and better predict radionuclide transport through narrow pores. This is of particular interest in the multi-barrier system around high-level waste (HLW) repositories, where several minerals and their surfaces within geo-technical, geological, and cementitious systems, determine transport and fate of radionuclides on the long term (> 10^4 y).

Among the ubiquitous radioisotopes in HLW repositories, ^{79}Se ($t_{1/2}$ = 3.27.10^5 y), ^{90}Sr ($t_{1/2}$ = 28.9 y) and ^{36}Cl ($t_{1/2}$ = 30.1.10^4 y) are expected to be released, among others, on the very long-term from both matrix and instant release fractions towards the overburden, contributing to the estimated total cumulative radioactive dose [1]. Mineral phases present in the containment providing rock zone and associated cementitious systems include silica and iron oxyhydroxides. In addition, migration of chlorine through cementitious systems, simulated by silica phases, is of general interest regarding steel depassivation [2].

Modelling approaches help understand and predict radionuclide adsorption onto mineral phases. In particular, surface speciation and electrostatic effects of single mineral surfaces can be accounted for via Surface Complexation Models (SCMs) [3]. Overlapping of electric double layers (EDL) at interacting surfaces are most efficiently accounted for by calculating the electric field in-side the pore space via Charge Regulation (CR) [4]. This concept implies that surface speciation, interfacial charges and potentials are adjusted in accordance with the distance between the surfaces based on generally valid intrinsic equilibrium constants (K_{int}) and mean-field type Poisson-Boltzmann (PB) theory. Currently, freely available or commercial (geo-)chemical speciation codes (e.g., PHREEQC, ECOSAT, FITEQL, Visual MINTEQ) do not include surface interactions through CR, and other codes that do, are not publicly available.

DESCRIPTION OF THE WORK

This work presents the application of a recently published, free-access speciation code SINFONIA (Speciation and INter-particle FOrces for Nanoscale InterActions) [5] that enables CR type simulations and extends SCMs to a four-layer model (FLM) involving interactions of both, equal and unequal mineral surfaces, with a numerical solution for the PB equation for arbitrary electrolytes. In this exemplary case study, the code is applied to simulate SeO_3^{2-}/Sr^{2+} and Cl^- interactions, adsorption and solution concentrations inside nanopores composed of either goethite or silica, respectively, based on published parameters [6,7].

RESULTS AND DISCUSSION

Calculations using SINFONIA to simulate Cl migration in silica nanopores at pH 9 show that pore sizes < 30 nm favor anion exclusion (fraction < 1, Fig. 1), particularly at low ionic strength (e.g., case study at 0.001 M NaCl) where electrostatic effects are stronger. Similar results are obtained for higher pH values, related to the negatively charged silica surface at higher than circumneutral pH.

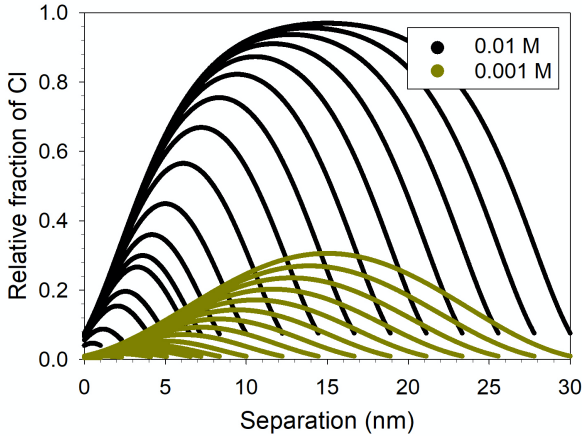

Fig. 1: Profiles of relative fractions of total aqueous Cl in interstitial pore water compared to bulk solution between silica surfaces at different separation distances for pH 9 and two ionic strengths (NaCl).

In pores composed of goethite at pH 9 (i.e., close to the isoelectric point), and in the presence of SeO_3^{2-} and Sr^{2+} (c_0 = 2.5.10^{-4} M), a change in the ionic strength of the pore solution from 0.01 M to 0.001 M will shift the

transport pore regime from anion exclusion (fraction < 1) to enhanced anion migration (fraction > 1, Fig. 2). The strongest effects occur in the smallest pores (e.g., < 20 nm) where even the mid-plane composition is modified by the overlapping EDLs.

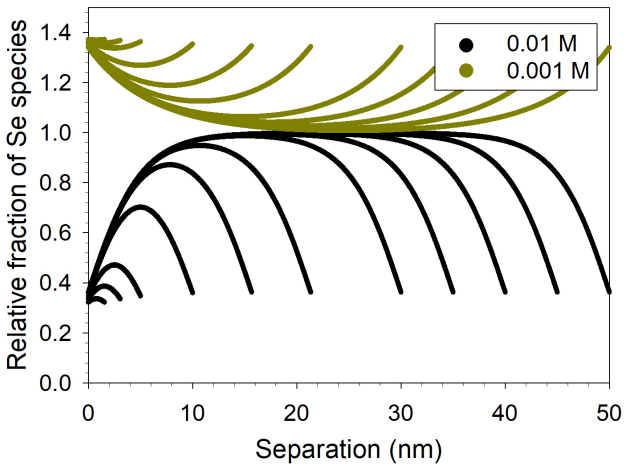

Fig. 2: Profiles of relative fractions of total aqueous Se in interstitial pore water compared to bulk solution between goethite surfaces at different separation distances for pH 9 and two ionic strengths (NaCl).

These examples imply that changes in the ionic strength of nano-porous media occurring over time due to input/mixing with renewed solution (e.g., glacial melt water) could entail shifts in the transport regime of the geological system with respect to radionuclides, with potential implications for radionuclide release from geological repositories.

REFERENCES

1. ANDRA, Dossier 2005 Argile (2005).
2. G. DE VERA, "Determination of the selectivity coefficient of a chloride ion selective electrode in alkaline media simulating the cement paste pore solution", *J Electroanal Chem*, **639**, 43-49 (2010).
3. J. LÜTZENKIRCHEN, "The Constant Capacitance Model and Variable Ionic Strength: An Evaluation of Possible Applications and Applicability", *J Colloid Interf Sci*, **217**, 8-18 (1999).
4. B.W. NINHAM, V.A. PARSEGIAN, "Electrostatic potential between surfaces bearing ionizable groups in ionic equilibrium with physiologic saline solution", *J Theor Biol*, **31**, 405-428 (1971).
5. T. GIL-DÍAZ *et al.,* "Charge regulated solid-liquid interfaces interacting on the nanoscale: Benchmarking of a generalized speciation code (SINFONIA)", *Adv Colloid Interfac*, **294**, 102469 (2021).
6. Z. NIE *et al.,* "Adsorption of Selenium and Strontium on Goethite: EXAFS Study and Surface Complexation Modeling of the Ternary Systems" *Environ Sci Tech*, **51**, 3751-3758 (2017).
7. D. GARCÍA et al., "Sorption of Eu(III) on quartz at high salt concentrations " *Colloid Surface A*, **578**, 123610 (2019).

Deciphering mineral precipitation induced porosity clogging in diffusion-controlled porous media

Mara I. Lönartz, Jenna Poonoosamy, Guido Deissmann, Dirk Bosbach

Institute of Energy and Climate Research: Nuclear Waste Management and Reactor Safety (IEK-6), Forschungszentrum Jülich GmbH, 52425 Jülich, Germany
email: m.loenartz@fz-juelich.de

INTRODUCTION

Understanding mineral dissolution-precipitation reactions and their effect on macroscopic transport properties in porous media is essential for describing and assessing various subsurface systems. In a diffusion-controlled porous medium, chemical and thermal gradients can lead to localized mineral precipitation, resulting in a reduction of porosity and potentially leading to porosity clogging, which can significantly affect the diffusivity [1-4]. Although in the context of radioactive waste disposal a reduction of porosity may appear desirable to inhibit radionuclide migration, it can also be detrimental, particularly in the case of gas pressure build up due to canister corrosion or bacterial activity [5,6].

The implementation of porosity clogging into continuum scale reactive transport codes represents a challenging task due to the complexity of precipitation mechanisms and kinetics and the evolving microstructure of the porous media [7]. Recent 1D continuum scale simulations of diffusion experiments have shown that even revised versions of Archie's law to describe the diffusivity-porosity relationship still fail to capture the experimentally observed effective diffusivity and the amounts of precipitates in case of porosity clogging [2,3]. Currently, there is very little data available for systems with changing porosity under well-controlled conditions to constrain model input parameters.

DESCRIPTION OF THE WORK

In this context, we developed a "lab on a chip" approach [8-9] which combines time lapse optical microscopy imaging and in-operando confocal Raman spectroscopy (Fig. 1 a - b) to determine (i) whether complete clogging in porous media is possible and can be permanent, (ii) which parameters control the porosity clogging, and (iii) which changes in transport properties of porous media are induced due to porosity clogging. The microfluidic device consists of two supply channels interconnected by porous reaction chambers. The porosity clogging process is fostered by the precipitation of celestine ($SrSO_4$) due to counter-diffusive mass transport of the reactants (Fig. 1c). As the system becomes clogged, isotopic tracers (e.g., D_2O) are injected to assess the evolving diffusivity of the confined porous medium (Fig. 1d).

In order to assess the diffusive or advective nature of mass transport, the flow fields and the solute concentration fields in the complete microfluidic reactor were modelled using the software COMSOL Multiphysics 5.6, which is based on the finite element method (FEM).

The experimental data sets will be used to predict the effective diffusivity by pore-scale modelling and to upscale the derived key relationships for continuum-scale reactive transport models.

RESULTS AND DISCUSSION

The very first results of the ongoing microfluidic experiments already demonstrated the complex nature of pore-scale dynamics, pointing to a non-permanent clogging of the system due to re-dissolution reactions and microporosity of the precipitates. This setup will provide new insights into the phenomenon of porosity clogging and its impact on the diffusivity-porosity relationship at the pore scale.

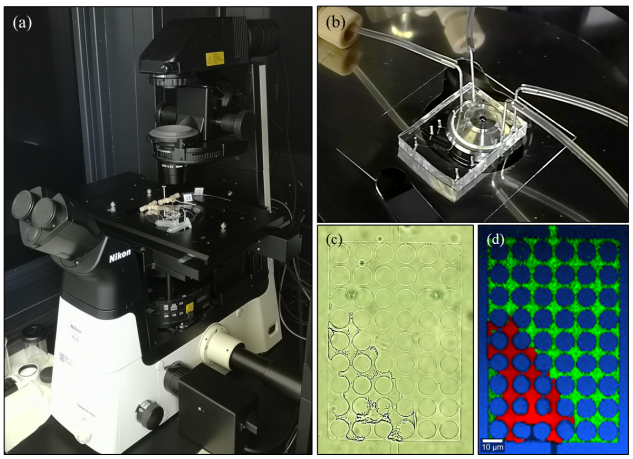

Fig. 1: (a) Microfluidic experimental setup in combination with optical microscopy imaging and confocal Raman spectroscopy. (b) Microfluidic polydimethylsiloxane (PDMS) chip placed on automatically moving x-y-z stage. (c) Optical image of celestine precipitates inside the diffusive reaction chamber. (d) Raman-spectroscopic phase distribution image of precipitated celestine (red), PDMS (blue) and deuterated sulfate solution (green) after ~ 2 hours reaction time.

ACKNOWLEDGEMENTS

The research leading to these results has received funding from the German Federal Ministry of Education and Research (BMBF, grant agreement 02NUK053A) and from the Initiative and Networking Fund of the Helmholtz Association (HGF grant SO-093) within the iCross project.

REFERENCES

1. SEIGNEUR et al., "Reactive transport in evolving porous media", *Reviews in Mineralogy and Geochemistry*, **85**, 197-238 (2019).
2. CHAGNEAU et al., "Mineral precipitation-induced porosity reduction and its effect on transport parameters in diffusion-controlled porous media", *Geochemical Transactions,* **35**, 13 (2015).
3. DENG et al. "A pore-scale investigation of mineral precipitation driven diffusivity change at the column-scale", *Water Resources Research*, **57**, 1-16 (2021).
4. RAJYAGURU et al., "Experimental characterization of coupled diffusion reactions mechanisms in low permeability chalk", *Chemical Geology*, **503**, 29-39 (2018).
5. SHAO et al., "Reactive transport modeling of the clogging process at Maqarin natural analogue site", *Physics and Chemistry of the Earth*, **64**, 21-31 (2013).
6. XU et al., "Corrosion-induced gas generation in a nuclear waste repository: reactive geochemistry and multiphase flow effects", *Applied Geochemistry*, **23**, 3423-3433 (2008).
7. POONOOSAMY et al., "Benchmarking of reactive transport codes for 2D simulations with mineral dissolution–precipitation reactions and feedback on transport parameters", *Computational Geosciences*, **25**, 1337-1358 (2021).
8. POONOOSAMY et al., "A microfluidic experiment and pore scale modelling diagnostics for assessing mineral precipitation and dissolution in confined spaces", *Chemical Geology*, **528**, 119264 (2019).
9. POONOOSAMY et al., "Microfluidic flow-through reactor and 3D Raman imaging for: In situ assessment of mineral reactivity in porous and fractured porous media", *Lab on chip*, **14**, 1-10 (2020).

Processes Contributing to Rock Matrix Diffusion in Fractured Crystalline Rock

B.W.D. Yardley[1], R.Metcalfe[2], A.E. Milodowski[3], L.P. Field[3], R.Wogelius[4], S. Norris[5]

[1]*School of Earth and Environment, University of Leeds, Leeds LS2 9JT, U.K.*
[2]*Quintessa Limited, Videcom House, Newtown Road, Henley-on-Thames, Oxfordshire RG9 1HG, UK*
[3]*British Geological Survey, Environmental Science Centre, Nicker Hill, Keyworth, Nottingham, NG12 5GG, UK*
[4]*School of Earth, Atmospheric, and Environmental Sciences, University of Manchester, Manchester, M13 9PL, UK*
[5]*Radioactive Waste Management Limited, Didcot, Oxfordshire, OX11 0GD, UK*
email: B.W.D.Yardley@leeds.ac.uk

INTRODUCTION

For many years Rock Matrix Diffusion (RMD) has been considered a possible means of retarding radionuclide transport from a deep geological repository for radioactive wastes constructed in fractured crystalline rocks e.g. [1,2,3]. Laboratory and in situ experiments e.g. [4,5] have been used to estimate the rate at which radionuclides would be taken up by fracture wall rocks and the results have provided a basis for modelling studies. Generally, these indicate that extensive take-up of radionuclides is possible. In contrast, veins in naturally fractured rocks commonly show very limited evidence for interactions with wall rocks. Our earlier results [6], showed that take up of radionuclides and other elements in the studied crystalline rocks was limited to damage zones around fractures with mineralogical alteration. This implies that in fractured crystalline rocks, mineral growth and dissolution kinetics may be rate-limiting for long term radionuclide uptake, after any initial adsorption on mineral surfaces. Here we show that the pattern of alteration and the O isotope composition of secondary minerals around fractures in a granite, further constrain the potential for RMD to chemically modify wall rocks.

DESCRIPTION OF THE WORK

A sample of Mountsorrel Granite, Leicestershire, UK was investigated. This is a biotite granodiorite of Lower Palaeozoic age, which has been uplifted and buried multiple times since the Caledonian orogeny. The sample is from just over 200 m below both the present surface and the Middle Triassic unconformity.

The granodiorite is composed of plagioclase, quartz and perthitic K-feldspar with minor biotite and hornblende and is cut by a thin (mm-scale) vein, occupying a fracture. The vein is predominantly of calcite and dolomite, but quartz and K-feldspar are present at vein walls and secondary K-feldspar is also intergrown with vein carbonates (Fig. 1). Veinlets mark minor fractures around the main one. The wall rocks are altered within <15mm of the vein. While quartz and K-feldspar are unaltered, even where cut by the vein, plagioclase is often rimmed by secondary albite. Next to the vein, the calcic plagioclase interior is often intensely altered to secondary K-feldspar and clay minerals (Fig. 1). Less-altered plagioclase has calcite and secondary porosity. Biotite and hornblende alter to chlorite, but often incompletely, even where cut by the vein. Chemical changes include addition of K, Ca, Mg and CO_3, and removal of Si and Na, but are limited to a damage zone a few millimetres across. This zone developed enhanced permeability due to subsidiary microfractures and secondary porosity after plagioclase (Fig. 1).

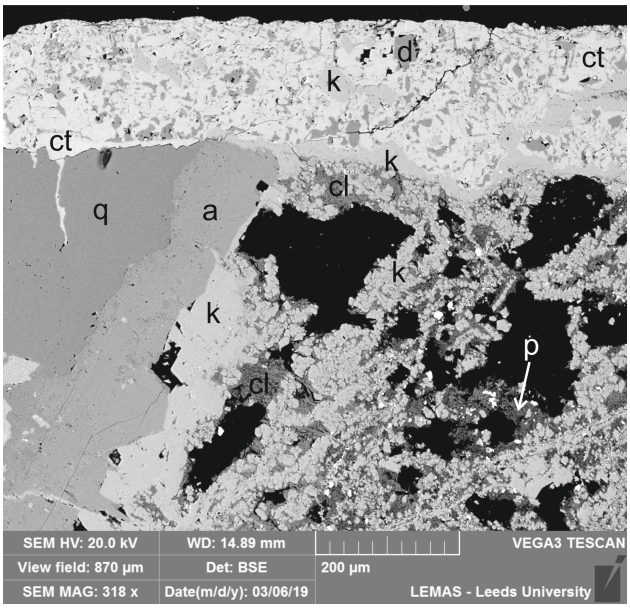

Fig. 1: BSEM image of vein with calcite (ct), dolomite (d) and K-feldspar (k), cutting primary quartz (q) and plagioclase. The plagioclase has a rim of albite (a) but the interior is replaced by K-feldspar and clay (cl) with interstitial porosity (p). The large black "pores" are largely due to plucking in preparation.

Oxygen isotope analysis of calcite from veins or secondary pores within partially altered plagioclase have been performed using a Cameca 1270 Ion Probe at the

Edinburgh Ion Micro-Probe Facility, under the guidance of John Craven. Analysed spots are c. 15 µm in diameter and the analyses have an analytical uncertainty < 0.5 ‰.

RESULTS AND DISCUSSION

Fig. 2 illustrates the analysed calcite vein. 17 vein calcite analyses gave mean $\delta^{18}O_{SMOW}$ of +19.0 ‰ and +20.9 ‰ for the two vein portions while 7 points on secondary calcite replacing vein wall plagioclase gave +19.7 ‰. The differences are insignificant. Primary minerals could not be analysed, but probably have $\delta^{18}O_{SMOW}$ <+10 ‰, based on data for other Caledonian granodiorites.

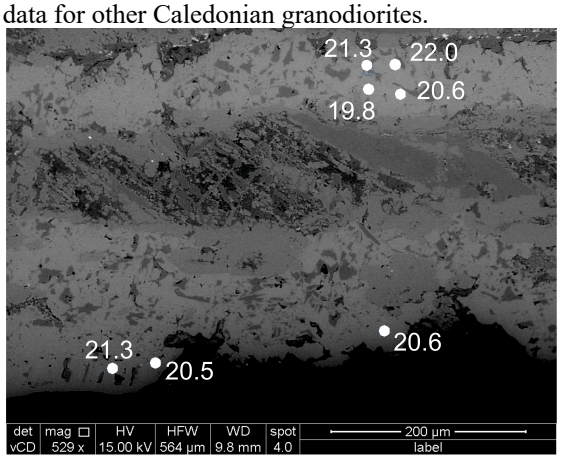

Fig. 2: BSEM image of a calcite vein section with $\delta^{18}O_{SMOW}$ in per mil shown at analysis locations in the calcite.

If the species introduced by water flowing in the fracture simply diffused perpendicularly into the wall rocks, there would be a different front for each introduced species and a gradient in oxygen isotopic composition. If, however, transport was dominated by flow in, and parallel to, the fracture and adjacent damage zone, fronts for different species should coincide and oxygen isotopes in secondary minerals should be uniform. The similar calcite oxygen values and the confinement of chemical change to the narrow damage zone strongly support the conclusions in [7] that water/solute movement is focused along, not perpendicular to fractures. The occurrence of fresh primary minerals more than a few millimetres from the fracture suggests that water penetration to the matrix was limited, since these minerals are unstable in free water.

Any oxygen contribution from primary minerals would lower calcite $\delta^{18}O$, so the measured calcite values are minima. Given fractionation factors in [7], if the introduced water had an isotopic composition like seawater (0‰), calcite would have grown at < 100 °C, while a reasonable groundwater composition (-7 ‰) yields 30-40 °C. Vein and alteration therefore formed at temperatures little higher than those of a granite-hosted waste repository.

CONCLUSIONS

No evidence was found for diffusion of aqueous species from fractures into fresh wall rocks over distances of more than a few millimetres. Chemical changes are only extensive near the fracture where smaller cracks and secondary porosity created by mineral reactions have enhanced permeability. The oxygen isotopic composition of secondary calcite reflects that of the introduced water, unmodified by water-rock reactions. Hence mineral dissolution and growth were too slow to significantly change the isotopic composition of the water. In contrast experimental studies typically imply more rapid reactions. The different timescales over which natural and experimental chemical changes occur may explain the difference. Fast initial take-up of introduced species from water may not be sustained after initial saturation of fresh mineral surfaces. The common assumption that wall rocks are completely saturated with water may also be incorrect.

REFERENCES

1. NERETNIEKS, I. Diffusion in the rock matrix: an important factor in radionuclide retardation. *Journal of Geophysical Research,* **85**, 4379-4397 (1980).
2. BAKER, A., JACKSON, C.P., JEFFERIES, N.L. and LINEHAM, T.R. The role of rock matrix diffusion in retarding migration of radionuclides from a radioactive waste repository. *Nirex Report***, N/051,** 101 pp (2002).
3. SKB. Radionuclide transport report for the Safety Assessment SR-Site. *SKB Technical Report* **TR-10-50,** 317 pp (2010).
4. TACHI, Y., EBINA, T., TAKEDA, C., SAITO, T., TAKAHASHI, H., OHUCHI, Y., MARTIN, A.J. Matrix diffusion and sorption of Cs^+, Na^+, I^- and HTO in granodiorite: laboratory-scale results and their extrapolation to the in situ condition. *Journal of Contaminant Hydrology*, **179**, 10–24 (2015).
5. VOUTILAINEN, M., KEKÄLÄINEN, P., POTERI, A., SIITARI-KAUPPI, M., HELARIUTTA, K., ANDERSSON, P., NILSSON, K., BYEGÅRD, J., SKÅLBERG, M., YLI-KAILA, M., KOSKINEN, L., Comparison of water phase diffusion experiments in laboratory and in situ conditions. *Journal of Hydrology* **575,** 716–729 (2019).
6. WOGELIUS, R.A., MILODOWSKI, A.E., FIELD, L.P., METCALFE, R., LOWE, T., VAN VEELEN, A., CARPENTER, G., NORRIS, S., YARDLEY, B. Mineral reaction kinetics constrain the length scale of rock matrix diffusion. *Nature Scientific Reports*, **10**, 8142 (2020).
7. ZHENG, Y-F. On the theoretical calculations of oxygen isotope fractionation factors for carbonate-water systems. *Geochemical Journal* **45,** 341-354 (2011).

Flow channelling and dispersion in discrete fracture networks with internal fracture roughness and implications for large-scale numerical modelling

A. Frampton and B. Stock

Department of Physical Geography, Stockholm University, Sweden
email: andrew.frampton@natgeo.su.se

INTRODUCTION

There is a need for improved understanding of the mechanisms controlling flow and transport in fractured crystalline rocks in order to address long-term safety analysis of repositories for spent nuclear fuel. Due to the notable geological complexity of fractured bedrock, there are still significant challenges in understanding the effects heterogeneity in hydraulic and material properties at different scales have on flow, flow channelling, dispersion, and solute and reactive transport [1,2].

Fractures have significant variability in their aperture structure because of surface roughness [3], which leads to great variability in permeability. Several studies have shown that heterogeneous structures can strongly impact flow channelling in single fractures [4,5] and simple networks [6], but the effects of internal fracture variability on flow and transport in fracture networks relevant for repositories is not fully understood [7].

DESCRIPTION OF THE WORK

In this contribution, flow dispersion and channelling in three-dimensional discrete fracture networks with internal heterogeneity in permeability is investigated using a numerical DFN model (Fig. 1). The fracture networks are obtained using field data of sparsely fractured crystalline rock from the Swedish candidate repository site for spent nuclear fuel. Heterogeneity textures with different correlation length and variance are created and mapped to each individual fracture of the network to represent fracture roughness and internal variability in permeability. Then, the flow through the network is calculated and particle tracking is used to analyse flow channelling through the flow field.

RESULTS AND DISCUSSION

We demonstrate how the structure and variability of textures on the scale of individual fractures leads to different dispersion and channelling behaviour at the scale of the network. Key thresholds for cases where channelling is controlled by single-fracture heterogeneity versus network-scale heterogeneity are identified. Implications for large-scale modelling are discussed.

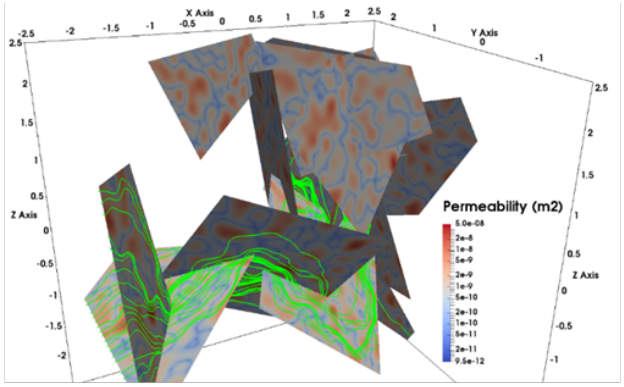

Small network, scale ~ 1 m

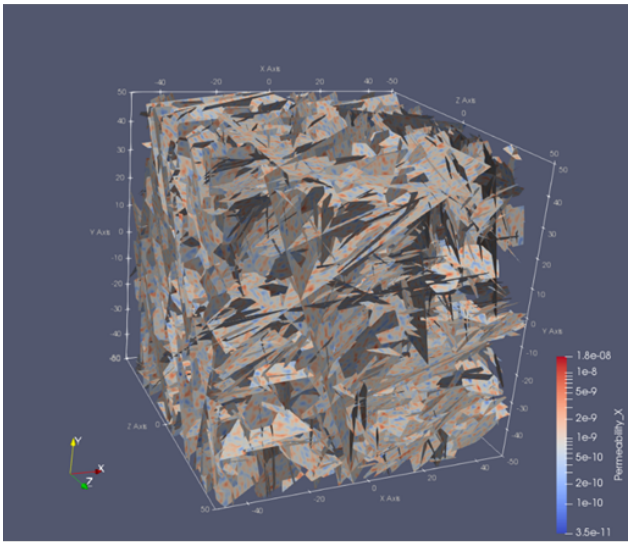

Larger network, scale ~ 100 m

Fig. 1: Internal variability at scale of single fractures and simple networks is used for larger (~100m) scale DFN models. Flow and transport by particle tracking is investigated at the DFN scale of 100 m to study impacts of internal variability in permeability.

REFERENCES

1. NEUMAN, S. P., Trends, prospects and challenges in quantifying flow and transport through fractured rocks. *Hydrogeology Journal*, **13**, 124–147 (2005).

2. TSANG, C.-F., NERETNIEKS, I., & TSANG, Y., Hydrologic issues associated with nuclear waste repositories. *Water Resources Research*, **51**, 6923–6972 (2015).
3. BROWN, S. R., Fluid flow through rock joints: The effect of surface roughness. *Journal of Geophysical Research: Solid Earth*, **92**(B2), 1337–1347 (1987).
4. DETWILER, R. L., & RAJARAM, H., Predicting dissolution patterns in variable aperture fractures: Evaluation of an enhanced depth-averaged computational model. *Water Resources Research*, **43,** W04403 (2007).
5. NICHOLL, M. J., RAJARAM, H., GLASS, R. J., & DETWILER, R., Saturated flow in a single fracture: evaluation of the Reynolds Equation in measured aperture fields. *Water Resources Research*, **35**, 3361–3373 (1999).
6. FRAMPTON, A., HYMAN, J.D., ZOU, L., Advective Transport in Discrete Fracture Networks With Connected and Disconnected Textures Representing Internal Aperture Variability. *Water Resources Research* **55**, 5487-5501 (2019).
7. CVETKOVIC, V., & FRAMPTON, A., Solute transport and retention in three-dimensional fracture networks. *Water Resources Research*, **48**, W02509 (2012).

Diffusion of U(VI) and Am(III) through Opalinus Clay studied down to ultra-trace levels

D. Glückman[1], K. Hain[2], C. Joseph[1], V. Metz[1], F. Quinto[1], P. Steier[2], H. Geckeis[1]

[1]*Institute for Nuclear Waste Disposal, Karlsruhe Institute of Technology, Eggenstein-Leopoldshafen, 76344, Germany*
[2]*Faculty of Physics, University of Vienna, Vienna, 1090, Austria*
email: daniel.glueckman@kit.edu

INTRODUCTION

Clay rock is a potential host rock for the final disposal of nuclear waste in deep geological formations. In the scenario of ground water intrusion into the nuclear waste repository and consecutive corrosion of canisters and waste, possibly released actinides, such as uranium (U) and americium (Am), would be transported through the clay host rock, mainly by diffusion. To our knowledge, the diffusion of U in clay rock has not been investigated below concentrations of 10^{-4} mol/m³ clay [1]. For Am, no diffusion experiments have been performed in a clay rock, considered suitable as host rock, such as Opalinus Clay (OPA). This study aimed at the investigation of the diffusive behavior of U and Am down to ultra-trace concentrations (<< 10^{-4} mol/m³) in OPA.

DESCRIPTION OF THE WORK

Laboratory-scale in-diffusion experiments were conducted with samples of OPA (shaly facies, borehole BLT-14, drilled parallel to bedding), obtained from the Mont Terri URL. Two cylindrical OPA samples (length: 10 mm, diameter: 6 mm) were embedded in poly(methyl methacrylate) (PMMA) sample holders with epoxy resin. They were equilibrated with synthetic pore water (I = 0.22±0.02 mol/L, pH = 7.24±0.10) [2] for 56 days. Subsequently, they were immersed about 2 mm deep into a diffusion reservoir containing 400 mL of pore water spiked with 5×10^{-9} mol/L ^{233}U(VI) and ^{243}Am(III), respectively. The diffusion reservoir was equilibrated with the spiked pore water for 56 days prior to the clay sample immersion.

The first sample was removed after 126 days of diffusion and segmented into thin layers of 20–400 µm using abrasive peeling [3] proceeding backward in the direction of the proximal sample surface immersed in the reservoir. The analysis of the segments indicated unexpectedly high actinide concentrations in the individual layers, especially for diffusion distances deeper into the distal direction. Therefore, the processing procedure for the second OPA sample taken after 240 days was adjusted: prior to the segmentation, the external surface of the PMMA sample holder was removed to a depth of approximately 100 µm. This was necessary in order to prevent cross-contamination of the segmented layers by actinides sorbed on or incorporated into the PMMA. Furthermore, core segments were drilled from 3700 to 5500 µm depth with two corresponding rim segments (Fig. 1, dark and light blue segments, respectively) and from 5500 to 8220 µm with two corresponding rim segments (Fig. 1, red and purple segments, respectively). This allowed for the investigation of potential preferential pathways across the rim of the OPA sample. For sample depth ranges 0–3700 µm and 8220–8600 µm, the full segments were abraded (Fig. 1, green segments; Fig. 2, orange segments). Due to the expected ultra-trace concentrations of ^{233}U and ^{243}Am in the clay segments, analysis was carried out with accelerator mass spectrometry (AMS) [4].

RESULTS AND DISCUSSION

The concentration profile of ^{233}U(VI) was determined down to 10^{-9} mol/m³ of clay and a distance of 8600 µm, as shown in Fig. 1. Core and rim segments followed the general trend of decreasing ^{233}U concentrations with diffusion depth in the fully abraded segments, suggesting that no preferential pathways along the rim of the OPA sample occurred.

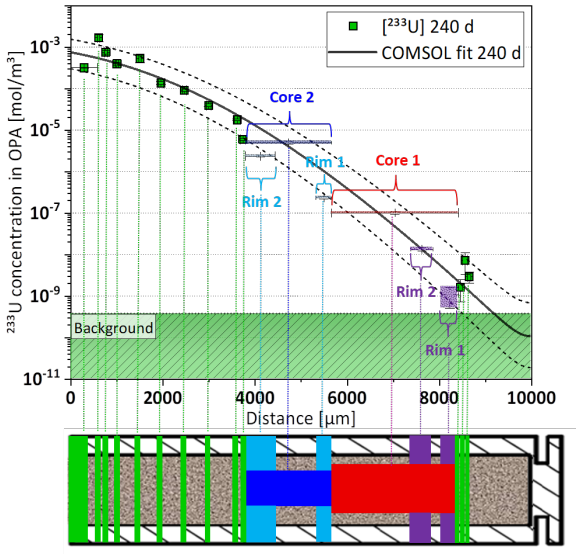

Fig. 1: Concentration profile of ^{233}U(VI) in OPA obtained with AMS after 240 days, comprising fully abraded segments (green), core segments (dark blue & red), and rim segments (light blue & purple).

The transport parameters, distribution coefficient, K_d, and effective diffusion coefficient, D_e, were obtained by fitting the concentration profile with a 1D model in

COMSOL Multiphysics (v. 5.6). The values amounted to K_d = 0.105 (+0.111/–0.065) m³/kg and D_e = 1.6 (+2.0/–1.1) × 10^{-11} m²/s. Joseph et al. [1] reported K_d 0.025±0.003 m³/kg and D_e (1.9±0.4) × 10^{-12} m²/s for U(VI) diffusing perpendicular to the bedding through shaly facies of OPA (BLT-14). Diffusion perpendicular to the bedding is known to be slower than parallel to the bedding with an anisotropy factor of 4–6 for HTO, Cl^- and Na^+.[5] From the present work, this factor can be confirmed also for U(VI). The difference in K_d values can be explained by differences in the experimental setup (through-diffusion [1] vs. in-diffusion). Joseph et al. [1] applied a confining pressure of 5 MPa, while in the present study no confining pressure was applied, which could have caused higher diffusion-accessible porosities.

For ^{243}Am(III), the concentration profile was determined down to ca. 10^{-6} mol/m³ and a distance of about 4000 µm (Fig. 2). For longer distances, the determined ^{243}Am concentrations were consistent with the background (≈ 3 × 10^{-7} mol/m³). The profile of ^{243}Am(III) is featured by two different sections. The first section (about 0–1000 µm depth) exhibits a strong decrease in ^{243}Am concentration, while in the second section (about 1500–4000 µm), the concentration decrease is less distinct. There is currently no explanation for this second "fast-runner" profile. However, a similar diffusion behavior was also observed for Eu(III) in OPA [6]. For the first section of the profile, a K_d of 100±30 m³/kg was determined, which was in fair agreement with literature data (60 m³/kg [6]; 63 m³/kg [7]). The determined D_e value was 2.4 (+2.1/–1.1) × 10^{-10} m²/s. With K_d and D_e, the apparent diffusion coefficient, D_a, can be calculated. It amounts to 1 × 10^{-15} m²/s for Am(III) diffusion parallel to the bedding through OPA.

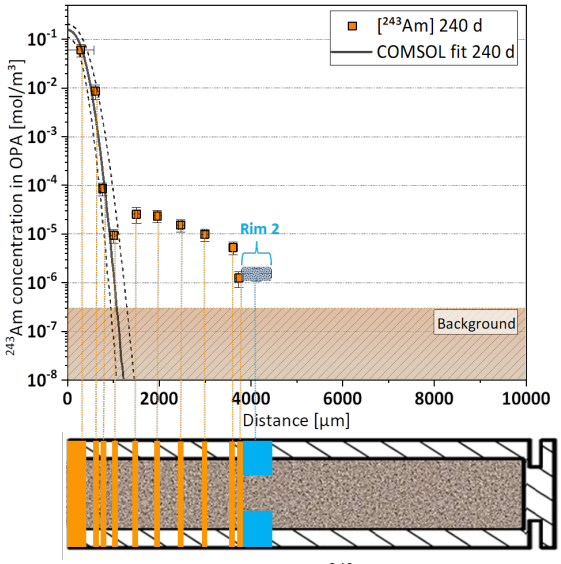

Fig. 2: Concentration profile of ^{243}Am in OPA obtained with AMS after 240 days, comprising fully abraded segments (orange) and rim segments (light blue).

This is more than one order of magnitude higher than D_a = 3.5×10^{-16} m²/s for Eu(III) diffusion through OPA [6] determined assuming a density of 2400 kg/m³ and a porosity of 0.15. Studies are ongoing to explain the different results obtained in our experiments. D_a(Am(III)) from the present study is, however, lower than D_a for Am(III) of 1.7×10^{-14} m²/s diffusing through a sand-bentonite mixture [8]. This can be attributed to the lower density of the mixture with 1600 kg/m³ compared to OPA and differences in the main diffusing species, $[Am(CO_3)]^+$ in the present study vs. $[Am(CO_3)_3]^{3-}$ [8].

ACKNOWLEDGEMENTS

The authors thank the Federal Ministry of Education and Research (Grant 02 NUK 053 C) and the Helmholtz Association (Grant SO-093) for financial support.

REFERENCES

1. C. JOSEPH et al., Diffusion of U(VI) in Opalinus Clay: Influence of temperature and humic acid, *Geochim. Cosmochim. Acta*, **109**, 74–89 (2013).
2. T. GIMMI et al., Anisotropic diffusion at the field scale in a 4-year multi-tracer diffusion and retention experiment - I: Insights from the experimental data, *Geochim. Cosmochim. Acta,* **125**, 373–393 (2014).
3. L. R. VAN LOON, and W. MÜLLER, A modified version of the combined in-diffusion/abrasive peeling technique for measuring diffusion of strongly sorbing radionuclides in argillaceous rocks: a test study on the diffusion of caesium in Opalinus Clay, *Appl. Radiat. Isot.*, **90**, 197–202 (2014).
4. F. QUINTO et al., Multiactinide analysis with accelerator mass spectrometry for ultra-trace determination in small samples: application to an in situ radionuclide tracer test within the colloid formation and migration experiment at the Grimsel test site (Switzerland), *Anal. Chem.*, **89**, 7182–7189 (2017).
5. L. R. VAN LOON et al., Anisotropic diffusion in layered argillaceous rocks: a case study with Opalinus Clay, *Environ. Sci. Technol.*, **38**, 5721–5728 (2004).
6. PSI Progress Report 2019; Laboratory for Waste Management (LES), Paul Scherrer Institut, Villigen, Switzerland (2020).
7. M. H. BRADBURY, B. BAEYENS, Far field sorption data bases for performance assessment of a high-level radioactive waste repository in an undisturbed Opalinus Clay host rock. PSI Technical Report 03-08, Paul Scherrer Institut, Villigen, Switzerland (2003).
8. T. SAWAGUCHI, et al., Diffusion of Cs, Np, Am and Co in compacted sand-bentonite mixtures: evidence for surface diffusion of Cs cations, *Clay Miner.*, **48**, 411–422 (2013).

Pore network and flow field analysis toward improved predictability of diffusive transport in argillaceous host rocks

Till Bollermann, Johannes Kulenkampff, Tao Yuan, Thorsten Stumpf, Cornelius Fischer

Department of Reactive Transport, Institute of Resource Ecology, Helmholtz-Zentrum Dresden-Rossendorf, Germany
email: c.fischer@hzdr.de

INTRODUCTION

Clay rock formations are considered as host rocks for underground radioactive waste disposal sites. Key to evaluate the sealing capacity of argillaceous rocks are reliable predictions about the heterogeneity of the diffusive transport. The predictive power of numerical approaches toward flow field analysis and radionuclide migration depends on the quality of the pore network model. Both sedimentary and diagenetic complexity, including laminations and diagenetic precipitates provide controlling factors to the pore network model across the length scale.

DESCRIPTION OF THE WORK

In this study, we exemplify a scale-crossing approach to reconstruct the pore network geometries of heterogeneous geomaterials. Here, we investigate the sandy facies of the Opalinus clay rock [1]. We identified structural and compositional components based on the concentration of diagenetic carbonates and sulfides as well as on grain size variability of the sediment. We quantified the resulting pore size distribution and pore network geometries. Pore network models (length scale: nm to mm), based on focused ion beam scanning electron microscopy (FIB-SEM), mercury intrusion porosity measurements (MIP), scanning electron microscopy (SEM) and elemental analysis (CHNS), were implemented into computer tomography (µ-CT) data sets. The µ-CT data cover the diagenetic and sedimentary heterogeneity of the sandy facies of the Opalinus clay at the core scale.

The resulting pore network model is utilized in reactive transport modeling. Validation of the simulation calculations is provided using positron emission tomography (PET) for the analysis of the flow field pattern.

RESULTS AND DISCUSSION

The generalized pore network model is implemented into a digital rock model to parameterize the effective diffusivity. It is combined with an upscaling workflow from nanometer-scale transport simulation to micrometer-scale simulation [2]. The transport simulation results show up to two orders of magnitude faster diffusion velocities in the clay rich layers ($D_e = 10^{-11}$ m^2/s) compared to the other subfacies components (sandy laminae: $D_e = 10^{-12}$ m^2/s; carbonate and sulfide lenses: $D_e = 10^{-13}$ m^2/s).

To validate the simulation results, we conducted diffusion experiments. The resulting tomographic PET and µ-CT data sets were statistically analyzed. The diffusion length was calculated based on the radial density standard deviation. This calculation identifies structural and compositional heterogeneity. The resulting effective diffusivities validated the numerical approach.

This study provides a workflow of general applicability for the analysis of pore and pore network data in complex porous media across the length scale, their use in transport modelling, as well as the[i] validation of the simulation results using process tomography.

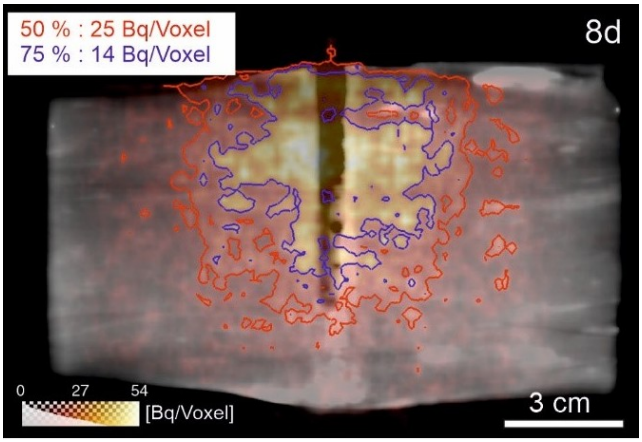

Fig. 1: Axial and radial heterogeneity of the diffusive flow field, visualized using 50 % and 75 % activity isolines; PET data, diffusive transport after 8 days. Density pattern (gray scale visualization) indicating structural and compositional heterogeneity of the sandy facies of the Opalinus clay.

ACKNOWLEDGEMENTS

Funding provided by the German Federal Ministry of Education and Research (BMBF, Grant 02NUK053) and

the Helmholtz Association (Grant SO-093) is acknowledged.

REFERENCES

1. LAUPER, B. et al., Quantification of Lithological Heterogeneity Within Opalinus Clay: Toward a Uniform Subfacies Classification Scheme Using a Novel Automated Core Image Recognition Tool. *Frontiers in Earth Science,* **9** , 645596 (2021).
2. YUAN, T. and FISCHER, C., Effective diffusivity prediction of radionuclides in clay formations using an integrated upscaling workflow. *Transport in Porous Media***, 138**, 245-264 (2021).

Diffusion of HTO, $^{36}Cl^-$, and $^{85}Sr^{2+}$ in compacted natural and reduced-charge dioctahedral smectites

Claudia Joseph[1], Laure Delavernhe[1,2], Martin Glaus[3], Dimitra Zerva[3], Sylvia Moisei-Rabung[1], Vanessa Montoya[1,4], Rainer Schuhmann[2], Thorsten Schäfer[1,5], Katja Emmerich[2]

[1]*Institute for Nuclear Waste Disposal (INE), Karlsruhe Institute of Technology (KIT), P.O. Box 3640, 76021 Karlsruhe, Germany*
[2]*Competence Center for Material Moisture (IMB-CMM), Karlsruhe Institute of Technology (KIT), P.O. Box 6980, 76049 Karlsruhe, Germany*
[3]*Laboratory for Waste Management, Paul Scherrer Institut, 5232 Villigen-PSI, Switzerland*
[4]*Department of Environmental Informatics, Helmholtz Centre for Environmental Research (UFZ), Permoserstr. 15, 04318 Leipzig, Germany*
[5]*Institute of Geosciences, Applied Geology, Friedrich-Schiller-University Jena, Burgweg 11, 07749 Jena, Germany*
email: claudia.joseph@kit.edu

INTRODUCTION

A couple of reference bentonites are studied internationally for their suitability as backfill material in nuclear waste repositories. In this geotechnical barrier, molecular diffusion will be the decisive transport process for waste-released radionuclides. The majority of the bentonites' clay fraction is composed of smectites. Their structure is characterized by layers composed of sheets of octahedrally (O) coordinated Al^{3+} embraced by sheets of tetrahedrally (T) coordinated Si^{4+} – TOT. The space between the T sheets of two adjacent TOT layers is called interlayer. Due to isomorphic substitutions of Al^{3+} and Si^{4+} for metal cations with lower charge, e.g., Al^{3+} by Mg^{2+} or Fe^{2+}, a negative excess charge in the smectite structure is created. This charge is compensated by cations in the interlayers.

The focus of the present work was to study HTO, $^{36}Cl^-$, and $^{85}Sr^{2+}$ diffusion through four different Na-saturated smectites and to compare the results with the diffusion through their four Na-saturated reduced charge derivatives (RCD). RCD contains Li^+ and has collapsed interlayers (Fig. 1), which are no longer accessible for water. The aim was to clarify to which extent smectite properties such as layer charge and particle size distribution determine the tracer diffusion. The study was also aimed to clarify if and how interlayer pores are available for diffusive transport.

DESCRIPTION OF THE WORK

Purified Na-saturated < 0.2 µm-fractions of dioctahedral smectites separated from the bentonites Calcigel®, FEBEX, Bentonite P, Volclay®, referred to as C, S, P, and V, were investigated. From each of these smectite fractions, a Na-saturated RCD was prepared using the Hofmann-Klemen effect [1,2]. The samples were Li-saturated and heated at 300°C for 24 h.

With the four smectite fractions and their four

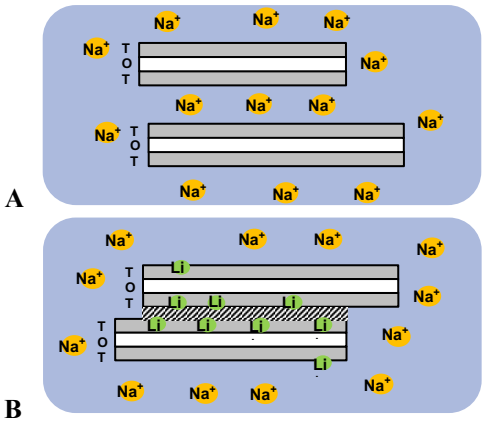

Fig. 1: Schematic structure of Na-saturated smectites (A) and the reduced-charge derivative (B).

respective RCD through- and out-diffusion experiments [3] were performed with HTO, $^{36}Cl^-$, and $^{85}Sr^{2+}$ as tracers. Each smectite or RCD was compacted in diffusion cells to a dry density, ρ_d, of about 1700 kg/m^3, a thickness of about 1 cm, and a diameter of about 2.54 cm. Each cell was connected to a high (HCR) and a low concentration reservoir (LCR) initially containing 0.3 mol/L $NaClO_4$ at pH 5.5 ± 0.5. Through-diffusion was started after an equilibration period with the electrolyte solution for about two months by addition of appropriate amounts of the tracers to the HCR. The experiments were run until a quasi-steady state flux was reached in the LCR. Out-diffusion was subsequently monitored by replacing both reservoirs by tracer-free electrolyte solutions. In both types of diffusion experiments, a near-zero concentration boundary condition was maintained in the target reservoirs by replacing the target reservoir solutions at regular time steps against tracer-free electrolyte solutions.

A 1-dimensional model applying Fick's laws was implemented in COMSOL Multiphysics and used to fit the experimentally determined diffusive fluxes, J [mol/(m^2·s)], in the HCR and LCR and the accumulated

mass in the LCR. For all tracers, the effective diffusion coefficient, D_e [m^2/s], and the rock capacity factor, α [–], were treated as fitting parameters. α is related to the distribution coefficient, R_d [m^3/kg], and the diffusion-accessible porosity, ε_{acc} [–], via the relationship:

$$\alpha = \varepsilon_{acc} + \rho_d \cdot R_d \quad (1)$$

For HTO and $^{36}Cl^-$, $R_d = 0$ was assumed. For $^{36}Cl^-$, a heterogeneous experimentally determined porosity distribution in the clay specimen was taken into account in the model according to Glaus et al. [4]. α forms together with D_e the apparent diffusion coefficient, D_a [m^2/s]:

$$D_a = D_e/\alpha \quad (2)$$

The different diffusive behaviors of the smectites and their respective RCD were tentatively modelled with PhreeqC using a simplified electrical double layer (EDL) model [5]. In such a model, the enrichment of cationic species and the depletion of anions in the Donnan volume is the basis to explain the comparably high D_e values of cationic species and the small D_e values of anionic species. The – rather arbitrary – thickness of the Donnan layer was chosen such that only a negligible fraction of free pore water resulted. This assumption was taken in order to mimic the behavior of the interlayer pore space.

RESULTS AND DISCUSSION

Compared to the three other smectites, smectite V showed a similar ε_{acc}(HTO) of about 0.5, but a two to three times lower D_e(HTO). The deviating parameter values of this material were also observed in the $^{36}Cl^-$ and $^{85}Sr^{2+}$ diffusion data. This behavior was attributed to a higher fraction of interlayer porosity in compacted smectite V due to its larger lateral dimension [2] compared to the other smectites. For V-RCD, no diffusion data could be obtained. The respective diffusion experiment, although even repeated once, showed influence of advection. The data for the HTO and $^{36}Cl^-$ diffusion through the smectite V were in very good agreement with literature values obtained for Na-saturated montmorillonite from Milos (Greece) [6].

For HTO, D_e(RCD) was slightly higher than D_e(smectite), meaning that the J(HTO) through samples with interlayer space was slower than through samples with only interparticle space. D_e(RCD) was still lower than D_e(illite), although illite is expected to have water inaccessible interlayers similar to RCD. However, compared to RCD, the layer charge of illite is higher (0.26–0.37 eq./f.u. vs. 0.75 eq./f.u.), which could be a reason for this difference.

For $^{36}Cl^-$ diffusion, the significant decrease of $\varepsilon_{acc}(^{36}Cl^-)$ to only 11 to 14% of ε_{acc}(HTO) indicated the partial exclusion of the anion from the interlayers. In the case of the RCD, $\varepsilon_{acc}(^{36}Cl^-)$ was significantly larger, since the interlayer space was already blocked, only interparticle space was available. The reduction of ε_{acc} amounted to 40 to 46% of ε_{acc}(HTO), presumably caused by EDL also present at the surfaces of the interparticle pores.

For $^{85}Sr^{2+}$, although R_d(smectites) was higher than R_d(RCD), leading to a more pronounced retardation, also $J(^{85}Sr^{2+})$ through the interlayers of smectite was higher than through the interparticle space of RCD. Both effects compensated each other leading to a similar tracer breakthrough, meaning $D_a(^{85}Sr^{2+})$ for each smectite and its respective RCD were comparable. $R_d(^{85}Sr^{2+})$ obtained by diffusion were consistent with batch sorption data.

Rather good fits of the experimental data were obtained with the EDL model in the representations of the D_e and respective α values as a function of cation exchange capacity. For the case of $^{36}Cl^-$ diffusion, a volume fraction of ≈ 30% of full exclusion of anions, representing the behavior of the interlayers was considered in order to optimize the fits for the untreated smectites. In the case of $^{85}Sr^{2+}$ diffusion, different selectivity coefficients for the exchange of Sr^{2+} against Na^+ had to be considered for the untreated smectites and the RCD, which however, agreed with the behavior of the selectivity coefficients (0.7 vs. 1.1) observed in batch sorption experiments.

REFERENCES

1. U. HOFMANN et al., "Loss on heating of the ability of lithium ions to exchange in bentonite", *Zeitschrift für Anorganische Chemie,* **262**, 95-99 (1950).
2. L. DELAVERNHE et al., "Influence of mineralogical and morphological properties on the cation exchange behavior of dioctahedral smectites", *Colloids and Surfaces A-Physicochemical and Engineering Aspects,* **481**, 591-599 (2015).
3. L. R. VAN LOON et al., "Anion exclusion effects in compacted bentonites: Towards a better understanding of anion diffusion", *Applied Geochemistry,* **22**, 2536-2552 (2007).
4. M. A. GLAUS et al., "Consistent interpretation of the results of through-, out-diffusion and tracer profile analysis for trace anion diffusion in compacted montmorillonite", *Journal of Contaminant Hydrology,* **123**, 1-10 (2011).
5. M. A. GLAUS et al., "Cation diffusion in the electrical double layer enhances the mass transfer rates for Sr^{2+}, Co^{2+} and Zn^{2+} in compacted illite", *Geochimica et Cosmochimica Acta,* **165**, 376-388 (2015).
6. M. A. GLAUS et al., "Comparative study of tracer diffusion of HTO, $^{22}Na^+$ and $^{36}Cl^-$ in compacted kaolinite, illite and montmorillonite", *Geochimica et Cosmochimica Acta,* **74**, 1999-2010 (2010).

Workflow Development for Thermo-Hydro-Mechanical (THM) and Reactive Transport Processes (RTP) and Software Integration for Deep Geological Repository Simulation

OpenGeoSys Developer Team[1,2,3]

[1]*Helmholtz Centre for Environmental Research UFZ, Leipzig, Germany*
[2]*Technische Universität Bergakademie Freiberg, TUBAF, Germany*
[3]*Technische Universität Dresden, TUDD, Germany*
email: olaf.kolditz@ufz.de

INTRODUCTION

Planning, site selections, safety assessment for deep geological repositories (DGR) require a profound understanding of related physical, chemical, and biological processes. For this purpose, specialised modelling tools need to address the complexity of the involved processes at repository scales. Moreover, professional workflows need to be developed, which in addition to sophisticated process modelling provide interfaces to data bases, utilizing high-performance computing, and virtual reality for intuitive representation of complex data and model sets [1] to become useful tools for planning processes.

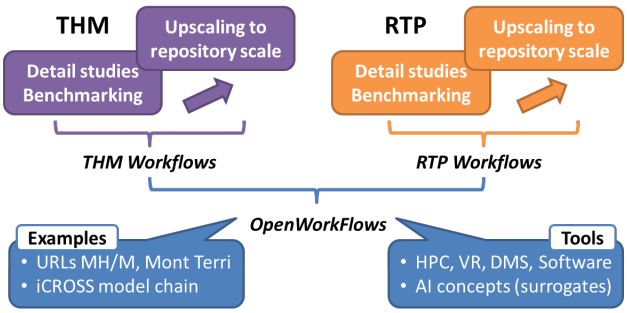

Fig. 1: Workflow development for THM and RTP simulation of DGR and combination with common tools.

Top of Fig. 1 illustrates workflows for THM and RTP modelling branches concerning upscaling from smaller scale (i.e. laboratory experiments) to the repository scales. This requires high-fidelity and efficient numerical modelling tools (see Tools) but also new approaches for modelling concepts, e.g. based on artificial intelligence (AI) approaches.

DESCRIPTION OF THE WORK

We are developing and deploying OpenGeoSys[1] as a central module of the workflow concept. OGS is a multi-purpose open-source platform for the numerical simulation of thermo-hydro-mechanical/chemical (THM/C) processes in porous and fractured media [2]. The basic concept of OGS consist of providing a flexible numerical framework, using primarily the Finite Element Method (FEM) for solving multi-field coupled processes with application in different disciplines. For example, OGS has been successfully applied in the fields of regional hydrogeology, technical and geothermal energy systems, geotechnical engineering, energy storage, CO_2 sequestration/storage and nuclear waste management and disposal. The current version OGS-6 is targeted at developing seamless workflows starting from data integration, using high-performance computing (HPC) for coupled process simulation as well as virtual reality (VR) concepts for data analytics. OGS-6 is developed and maintained platform-independently relying on professional software engineering methods such as continuous code integration[2] and containerization. A strict code review is conducted for quality assurance completed by unit testing and comprehensive benchmarking. OGS provides open interfaces for working closely with other simulators (e.g. mHM, PhreeqC). Moreover, OGS's Python interface ogs6py[3] allows integration into Jupyter notebooks and, therefore, a direct link to the powerful and growing Python ecosystem.

RESULTS AND DISCUSSION

In order to illustrate the workflow development recent benchmark studies and applications to underground research laboratories (URL) in Bure (Meuse/Haut-Marne) and Mont Terri are briefly presented here.

THM: Within the framework of the DECOVALEX 2019 project, Task E was dedicated to upscaling THM models from the laboratory to repository scale. In the context of Callovo-Oxfordian clay [3] a large-scale repository model has been tested for a hypothetical layout according to the French repository concept [4]. These model applications largely benefit from HPC methods and facilities. In addition to model application, new methods have been introduced in OGS-6 such variational phase-fields for fracture mechanics [5] and a fully coupled TH2M model,

[1] www.opengeosys.org
[2] https://code.opengeosys.org
[3] https://github.com/openjournals/joss-reviews/issues/3327

which is under extended benchmarking [6] and proving the concept for gas transport in excavation disturbed zone and clay-rich host rocks [7]. The new models for non-isothermal two-phase flow in deformable porous media are also involved in the new DECOVALEX 2023 phase for simulating the FE experiment in Mont Terri for experimental analysis and verification-based code comparisons.

RTP: Reactive transport processes have been investigated at different scales. Águila et al. [8] presented a benchmark study for cesium migration at small scale in order to better understand its non-linear sorption behavior in Opalinus clay. Based on a new operator-splitting method for coupling transport and reactions processes porosity changes due to chemical reactions have been analyzed for microfluidic experiments [9]. The new coupling scheme at Gauss-point level will also allow for consistent coupling of chemical and mechanical processes. Gas generation and resulting two-phase processes in low- and intermediate level cemented waste packages has been studied at the scale of a repository cell [10].

Currently, these specific studies related to different reactions, buffers materials, and scenarios are organized in so-called RTP model-chains. Radionuclide transport will be simulated along the entire multi-barrier system within a unified modelling framework (see Tools below).

TOOLS: THM and RTP modelling across scales require various tools, e.g. HPC for computational efficiency has been mentioned before. For representation and integration of data and models in a real geological context, Virtual Reality methods have been developed and applied for URL experiments [11]. A first prototype of a digital twin concept based on VR methods has been designed for the URL Mont Terri (Rink and Graebling, personal communication)[4]. For supporting model-chains (see above) Jupyter notebooks will be used for flexible combination of code modules and allowing for user interaction.

CONCEPTS: Further improving modelling methods and tools is necessary and will help to facilitate decision processes in future. Additionally, development of new concepts (out-of-the-box) is essential as for uncertainty quantification in model parametrizations [12]. Predictive power of full-complexity models will be limited to certain extent even with increasing model capacities and computational power. Current progress in AI methods and tools may prepare ground for a new paradigm in complex systems analyses. One basic idea of machine learning approaches is to find surrogate representations (e.g. by neuronal networks) of full-complexity models able to cover main features but performing much faster. The general idea of surrogate modeling is not new, but in conjunction with extreme computational power and progress in fundamental methods (physics-informed networks, deep learning), the potential of AI methods seems huge and needs profound elaboration for DGR simulations.

[4] https://www.ufz.de/index.php?en=46896

ACKNOWLEDGEMENTS

We are very grateful to BGE, BGR, BMBF, BMWi, DECOVALEX, EURAD, Helmholtz Association, iCROSS, swisstopo for funding various projects for the development of open-source software and workflows for applications in environmental geosciences.

REFERENCES

1. KOLDITZ, O. et al., Workflows in environmental geotechnics: Status-quo and perspectives. 119-127. In: Zhan L., Chen Y., Bouazza A. (eds) Proceedings of the 8th International Congress on Environmental Geotechnics Volume 1. ICEG 2018. Environmental Science and Engineering. Springer, Singapore (2019).
2. BILKE, L. et al., *Transport in Porous Media*, **130**, 337–361 (2019).
3. WANG, W. et al., *Int. J. Rock Mech. Min. Sci*., **142**, 104683 (2021).
4. WANG, W. et al., *Eng. Geol.,* **293**, 106265 (2021).
5. YOSHIOKA, K. et al., *Comput. Meth. Appl. Mech. Eng.,* **384**, 113951 (2021).
6. GRUNWALD, N. et al., Non-isothermal two-phase flow in deformable porous media: Systematic open-source implementation and verification procedure. *Geomech. Geophys. Geo-energ. Geo-re* (2021, submitted).
7. MARSCHALL, P. et al., *Oil and Gas Science and Technology*, **60**, 121-139 (2005).
8. ÁGUILA, J.F. et al., *Comput. Geosci,*. **25**, 1405 – 1436 (2021).
9. LU, R. et al., A consistent operator-splitting finite element framework for reactive transport in saturated porous media. *Computers and Geosciences* (2021, submitted).
10. HUANG, Y. et al.. *npj Mater. Degrad.,* **5**, 4 (2021).
11. RAITH, F. et al., Visual analysis of a full-scale-emplacement experiment in the Underground Rock Laboratory Mont Terri using fiber surfaces. In: Dutta, S., Feige, K., Rink, K., Zeckzer, D., (eds.) Proceedings Eurographics/EnvirVis2020. (2020).
12. BUCHWALD, J., et al., *Int. J. Heat Mass Transf.,* **172**, 121127 (2021).

A framework for risk analysis of clayrock fracturing due tohigh gas pressures in repository systems

Jörg Buchwald[1], Mostafa Mollaali[1], Vanessa Montoya[1], Olaf Kolditz[1,2], and Keita Yoshioka[1]

[1]*Helmholtz Centre for Environmental Research - UFZ, Department of Environmental Informatics, Leipzig, Germany*
[2] *Technische Universität Dresden, Dresden, Germany*
email: joerg.buchwald@ufz.de

INTRODUCTION

The engineered barrier concept normally comprises a variety of sub-systems or components, such as waste form (i.e., spent fuel), canisters, buffers (i.e., bentonite), backfills, seals and plugs. Because of the long disposal times and the anaerobic corrosion of the steel-canister, we expect a considerable amount of hydrogen gas generation at the interface between the canister and the bentonite. Even though we expect the gas production to be slow (H_2 flux of 5 $\mu g/m^2y$), gas generation at higher rates could pressurize the engineered barrier system and the host clayrock, and induce discrete pathways (e.g. fracturing). The fractured system increases the permeability of the rock and consequently radionuclides transport in the clayrock. To assess the long term risks of clayrock fracturing, we need to employ complex computer models capable of simulating fracture propagation with high morphological fidelity such as phase-field models [1, 7] (Figs. 1a&b). However, such simulations are typically computationally expensive and the computational cost increases exponentially if we analyze the sensitivity to both physical and operational parameters. To overcome the computational challenges, we design a risk analysis tool using Design of Experiments [4, 5, 6, 3], which generates a computationally inexpensive proxy model based on a set of significant parameters, so called heavy hitters.

DESCRIPTION OF THE WORK

To simulate the clayrock fracturing, we employ a phase-field model which is capable of simulating fracture propagation with high fidelity because of the continuum description of discontinuities [1, 2]. For our risk analysis workflow, we first define parameters (intrinsic permeability, Poisson's ratio, etc.) and their probability distributions that are subject to uncertainty, and an objective function that quantifies the uncertainty of the model or, in our case, the risk of fracturing (Fig. 2). The parameter screening step identifies heavy hitters which are used to build a proxy applying a space-filling design in the subsequent step. Using the proxy model, we analyze a global sensitivity. Also, we can generate a posterior distribution through Monte Carlo sampling to quantify the uncertainty/risk of fracturing with tractable computational costs.

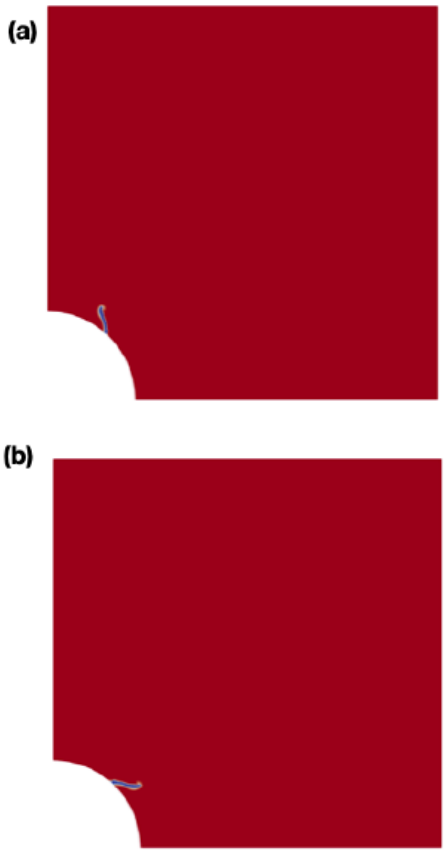

Fig. 1: Fracture propagation induced by gas pressurization in the middle (45°) at t = 100 s when assuming (a) the horizontal stress of 1 MPa and the vertical stress of 0.5 MPa, and (b) the horizontal stress of 0.5 MPa and the vertical stress of 1 MPa.

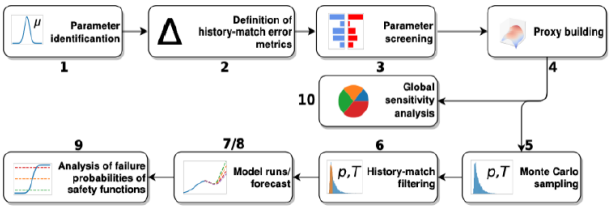

Fig. 2: Design of Experiments workflow [3].

RESULTS AND DISCUSSION

Using experimental designs (Plackett-Burman for screening, latin-hypercube for proxy-building), we obtained the evolution of the fracture length with time as a function of their input parameters (Fig. 3). Although our previous work [3] used experimental data and a history-match error as objective function, this study exclusively used modeling data. We define an objective function as the inverse time for the fracture to reach a specific predefined length, which we call risk of fracture. In the first step, we performed a Plackett-Burman design to study the main effects of various input parameters that are subject to uncertainty. To distinguish between significant and non-significant input parameters, we performed a t-test assuming a p-value of p=.05 to produce a Pareto chart (Fig. 4).

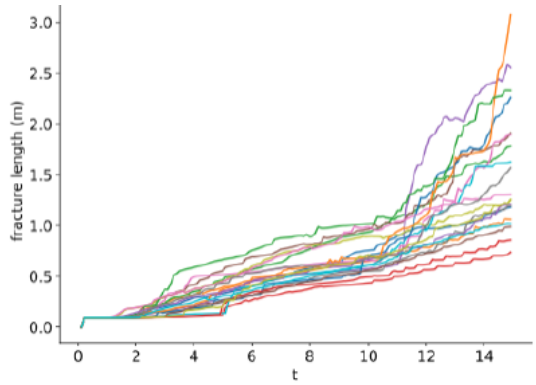

Fig. 3: Fracture length evolution with time.

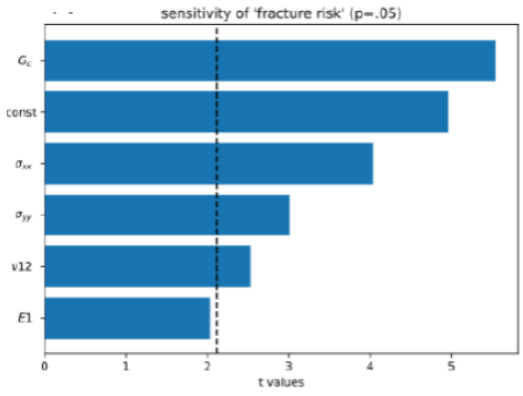

Fig. 4: Sensitivity of the fracture risk measure to different input parameters (Pareto chart).

In our first example, in which the angle of gas injection is at 45, all parameters except for the Young's modulus seem to have a significant impact. As next steps, we will use a space-filing design based on all significant parameters and build a proxy based Gaussian process regression model that will allow us to perform a Monte Carlo sampling to produce a posterior distribution in terms of our input quantities. Furthermore, the proxy will allow us to perform a global sensitivity analysis to assess risk of clayrock fracturing in repository systems.

REFERENCES

[1] B. BOURDIN, C. CHUKWUDOZIE, AND K. YOSHIOKA. A variational approach to the numerical simulation of hydraulic fracturing. SPE Annual Technical Conference and Exhibition. OnePetro (2012).

[2] B. BOURDIN, G.A. FRANCFORT, AND J.-J. MARIGO. Numerical experiments in revisited brittle fracture. *J. Mech. and Phys. of Solids*, **48**, 797-826 (2000).

[3] J. BUCHWALD, A.A. CHAUDHRY, K. YOSHIOKA, O. KOLDITZ, S. ATTINGER, AND T. NAGEL. Doe-based history matching for probabilistic uncertainty quanti_cation of thermo-hydro-mechanical processes around heat sources in clay rocks. *International Journal of Rock Mechanics and Mining Sciences*, **134**, 104481 (2020).

[4] B. LI, E.W. BHARK, T.C. BILLITER, AND K. DEHGHANI. Best practices of assisted history matching using design of experiments. *SPE Journal*, **24**, 1435-1451 (2019).

[5] N.S. POLITIS, P. COLOMBO, G. COLOMBO, AND M.D. REKKAS. Design of experiments (doe) in pharmaceutical development. *Drug development and industrial pharmacy*, **43**, 889-901 (2017).

[6] S.A. WEISSMAN AND N.G. ANDERSON. Design of experiments (doe) and process optimization. a review of recent publications. *Organic Process Research & Development*, **19**, 1605-1633 (2015).

[7] K. YOSHIOKA, F. PARISIO, D. NAUMOV, R. LU, O. KOLDITZ, AND T. NAGEL. Comparative veri_cation of discrete and smeared numerical approaches for the simulation of hydraulic fracturing. *GEM – International Journal on Geomathematics*, **10**, 13 (2019).

Reactive transport model of a low and intermediate-level waste disposal cell evolution in clay rock

Jaime Garibay-Rodriguez[1], Georg Kosakowski[2], Renchao Lu[1]; Olaf Kolditz[1,3], Vanessa Montoya[1]

[1]*Helmholtz Centre for Environmental Research (UFZ), Department of Environmental Informatics, Germany*
[2] *Paul Scherrer Institute (PSI), Laboratory for Waste Management (LES), Villigen, Switzerland*
[3]*Faculty of Environmental Sciences, Dresden University of Technology, Germany*
email: jaime.garibay-rodriguez@ufz.de

INTRODUCTION

In some countries, Low and Intermediate-Level radioactive Waste (L/ILW) is planned to be disposed in deep geological repositories. In these facilities, the waste will be emplaced in disposal cells consisting of the waste surrounded by an Engineered Barrier System (EBS) comprised of several different materials. In turn, waste disposal cells will be surrounded by a natural barrier, the host rock, which will act as a containment barrier for radionuclide migration. These repositories must isolate the nuclear waste from the biosphere for as long as 100,000 years.

Cement-based materials are typically used in the design of L/ILW disposal cells as construction material, as backfill material and for conditioning of wastes. One major aspect affecting the performance of EBS materials and host rock is the long-term chemical evolution of the system. The effects of hydraulic and chemical gradients between the different materials will produce their degradation. Several previous approaches have studied the chemical interaction in cement-claystone interfaces in the context of nuclear waste disposal [1]. However, remaining issues are still present, as indicated in a recent review [1].

In this work, we study a full-scale L/ILW disposal cell evolution consisting of multiple cement-based materials and the Callovo-Oxfordian claystone by reactive transport modelling. In the context of repository performance assessment, the model considers a time scale of 100,000 years. The disposal cell design is as follows: a low-pH liner shotcrete in contact with the Excavation Damage Zone (EDZ) in the host rock, a vault backfill mortar, a mortar to fill the spaces between waste packages, and a waste package concrete wall.

The inside of the waste package (i.e., the waste matrix) is not included in the model. CEMDATA v18.1 updated with new thermodynamic data on iron has been used as the chemical thermodynamic database to obtain the hydrated cement materials as well as performing the reactive transport calculations. Some additional clay minerals that could precipitate in the clay (e.g., saponite) have been imported from ThermoChimie v90b.

DESCRIPTION OF THE WORK

First cement hydration calculations have been carried out to define the initial chemical composition of each cement-based material and its porosity. These calculations have been performed in the GEM-Selektor v3 software. All cement-based materials are based in Portland Cement CEM I 42.5 N, however, each one has a different porosity, porewater, and solid composition due to their different recipes (i.e., binder/water ratios, silica, aggregates and fillers). This information is then fed to the reactive transport model. The mineralogy of the Callovo Oxfordian clay rock has been taken from elsewhere [2]. An EDZ has been assumed to extend up to 1 meter next to the liner with a porosity of 20% compared to the porosity of 18% of the intact host rock.

It is assumed that the disposal cell and the adjacent host rock is fully water saturated. No hydraulic gradients that drive water movements are taken into account, therefore transport of solutes in the system is dominated by diffusion. Several chemical processes are considered (e.g., aqueous complexation, cation exchange, mineral dissolution, and precipitation). All chemical processes are assumed to be thermodynamically controlled. The slow, kinetically-controlled dissolution of clay minerals in Callovo-Oxfordian (e.g., illite) has been neglected. Cation exchange reactions for Ca, Mg, Na, K, Sr, and Fe are included in the clay, whereas only cation exchange of Na and K in the low-pH liner is considered. Cation exchange is neglected for the rest of cement-based materials (due to their reduced cation exchange capacity).

The reactive transport calculations are performed by coupling OpenGeoSys-6 to iPhreeqc using a new operator-splitting approach [3]. In each time step, the iPhreeqc module is called to perform a sequence of geochemical calculations for each element in the computational mesh.
The numerical/computational parameters are:

- 1D (218 elements), $\triangle x_{min}$=0.02 (finer discretization at material interfaces)
- implicit Euler time discretization scheme, $\triangle t$=10a
- no-flux conditions at inner/outer boundaries
- 7h computational time with single CPU core (Intel(R) Xeon(R) @ 2.40GHz)

RESULTS AND DISCUSSION

Figure 1 shows a representation of the initial chemical and mineral composition (in volume fractions) of each cement-based material, as well as the EDZ and the clay host-rock. Additional secondary mineral phases (not initially present) are also included in the model (i.e., that could precipitate), especially near the cement-clay interface (e.g., M-S-H phases). Cement-based materials are primarily C-S-H phases with different Ca:Si ratios, ettringite, and monocarbonate. Portlandite is present in all the cement base materials except the low-pH concrete liner. The inert materials are sand or aggregate and are not considered as reactive in the model calculations. The reactive minerals in the clay rock are mostly calcite and quartz, with smaller proportions of dolomite, celestite, pyrite, and siderite.

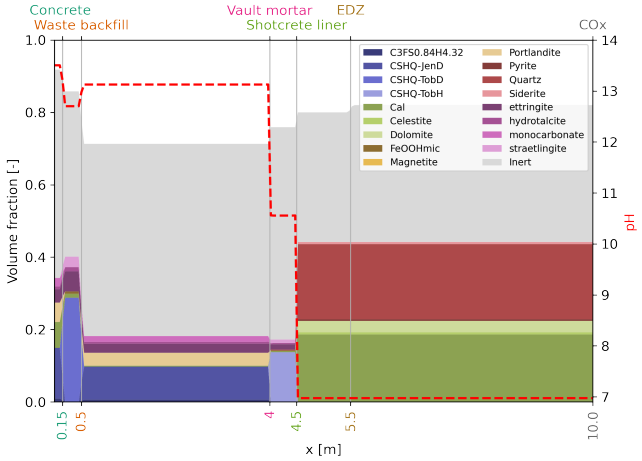

Fig. 1: Initial mineral composition of each cement-based material and the clay rock. The white space represents the porosity of each material.

Figure 2 shows the preliminary results of the reactive transport model at 100,000 years of interaction. As expected, interactions are mainly occurring in the low pH shotcrete/ clay interface. It is observed that the high pH plume moves around two meters from the low pH shotcrete-clay interface, however, the pH-buffering capacity of the clay minerals is still not included in the model and interpretation has to be cautious. Further, the Finite Element approach causes local over and undershooting for steep gradients, which are observed near the EDZ interface. In this case, adding slow dissolution kinetics of clay minerals may be helpful to model pH-buffering and to enable grid convergence (at the expense of more computational resources), which cannot be achieved for equilibrium controlled chemical systems. Furthermore, the precipitation of significant amounts of M-S-H phases occurs in the EDZ. These phases are known to precipitate in cement-clay interfaces [4] and, only recently, related data has been added to CEMDATA.

Precipitation of calcite and quartz in the clay, as well as precipitation of Tobermorite-like phase in the clay rock are major factors affecting the porosity at the shotcrete liner-clay (EDZ) interface. On the other hand, drastically decrease of the porosity at the low-pH shotcrete-clay (EDZ) interface is predicted which will favourably reduce radionuclide mobility, lowering the effective diffusion coefficient almost by one order of magnitude.

In the disposal cell, cement degradation of the vault mortar can be measured by the almost complete dissolution of portlandite, augmenting slightly the pore space in that zone (0.5-4 m).

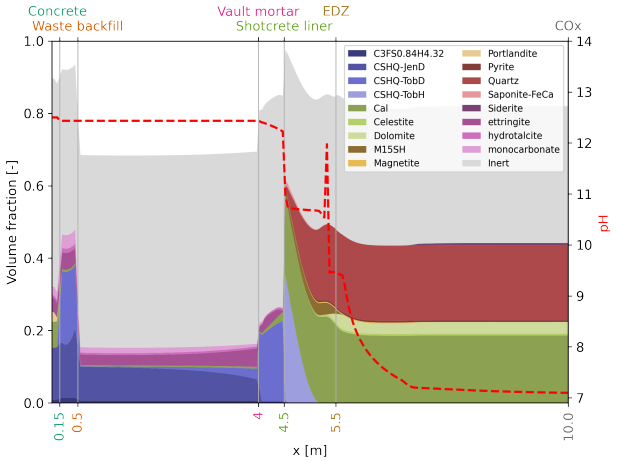

Fig. 2: Mineral composition and pH evolution at the time horizon (100,000 years) of the L/ILW disposal cell in contact with the clay rock. The white space represents the porosity of each material.

ACKNOWLEDGEMENTS

The funding of this work by EURAD-ACED (Grant Agreement No 847593) and iCROSS (grant numbers 02NUK053E / SO-093) projects is greatly acknowledged

REFERENCES

1. WILSON, J. et al. “The impact of cement on argillaceous rocks in radioactive waste disposal systems: A review focusing on key processes and remaining issues”, *Applied Geochemistry*, **130**, 104979 (2021).
2. IDIART, A. et al., “Reactive transport modelling of a low-pH concrete / clay interface”, *Applied Geochemistry,* **115**, 104562 (2020).
3. LU, R. et al., “A consistent integration-point collocation scheme for reactive transport modeling with the operator splitting approach”, *Computer and Geosciences* (under review, 2021).
4. DAUZERES, A. et al., “Magnesium perturbation in low-pH concretes placed in clayey environment—solid characterizations and modeling”, *Cement and Concrete Research,* **79,** 137-150 (2016).

Geochemical gradients within the Opalinus Clay system at Mont Terri (Switzerland) enhance uranium migration

Theresa Hennig[1,2], Michael Kühn[1,2]

[1]*GFZ German Research Centre for Geosciences, Fluid Systems Modelling, Telegrafenberg, 14473 Potsdam, Germany*

email: theresa.hennig@gfz-potsdam.de

[2]*University of Potsdam, Institute of Geosciences, Karl-Liebknecht-Str. 24-25, 14476 Potsdam-Golm, Germany*

INTRODUCTION

In claystones, the disposal concept for spent nuclear fuel mainly consisting of uranium is for the most part based on the isolation of the radionuclides within the effective containment zone due to the high retention capacity of the host rock resulting from the large reactive surface area of the inherent minerals. Transport properties are typically determined in laboratory or in-situ experiments under geochemically controlled and constant conditions.

Previous numerical studies have shown for the Opalinus Clay at Mont Terri (Switzerland), that uranium migration is highly affected by variations in the composition of the pore water resulting from mineralogical heterogeneities [1, 2]. Embedding aquifers are the hydro-geological boundaries between which gradients in the 210 m thick low permeable section established (blue dots, Figure 1) through diffusive exchange over millions of years [3, 4]. Thus, the assumption of homogeneity is no longer applicable as can be seen from the pore water profiles of the potential host rock Opalinus Clay.

By modelling the past history of the pore water using single-component diffusion simulations following Fick's laws, we quantify the impact of the heterogeneous geochemical system on uranium migration by comparison with homogeneous simulations [1] after a simulation time of one million years.

DESCRIPTION OF THE WORK

One-dimensional, reactive transport simulations on the host rock scale (200 m) were performed with PHREEQC [5] in order to quantify uranium diffusion and sorption processes as well as interaction with the inherent minerals considering the geochemical gradient in the Opalinus Clay system. The model applied here coincides with the concept presented in Hennig et al. [1] in terms of incorporated sorption and transport processes following Fick's laws. The underlying chemical thermodynamic data are based on the PSI/Nagra database version 12/07 with the extensions and updates described in Hennig et al. [1].

First, present-day pore water profiles were modelled based on the geological evolution of the Mont Terri anticline, where the Opalinus Clay is embedded between Triassic and Jurassic limestones, marls and shales. According to Pearson et al. [3] and Mazurek et al. [4], fresh-water infiltration into the surrounding aquifers, and with that the activation of the current hydro-geological boundaries of the system, was only possible after uplift of the entire low permeable section (Opalinus Clay and Liassic shales) and overlying stratigraphic layers during the folding of the Jura mountains and subsequent erosion of the latter. The initial conditions and the geochemical system were defined according to the geological evolution.

Secondly, uranium migration from a source term located in the centre of the low permeable section is assessed for one million years taking into account the heterogeneous geochemical system. In order to quantify the impact of the geochemical gradient, migration distances of uranium were compared with results from homogeneous simulations [1].

RESULTS AND DISCUSSION

First, the model was calibrated against the chloride profile [3] measured from field samples (blue dots, Figure 1). The main assumption is an uniform initial chloride concentration of 18.9 g/L across the entire low permeable section [4, 6]. Due to erosion, the surrounding aquifers were flushed with fresh water, what led to diffusive exchange with the embedded clays. Total simulation time was six million years with the footwall aquifer only being active for the last 0.5 million years [4]. The accuracy of our model in relation to the measured data is quantified by the relative Root Mean Square Error (rRMSE). Figure 1 shows, that the modelled chloride profile (blue line) coincides very well with the measured data (blue dots).

Based on the modelled profiles, the impact of the geochemical gradient on uranium migration was quantified. The potential repository is represented by a constant uranium concentration of 1 µmol/L located in the centre of the low permeable section.

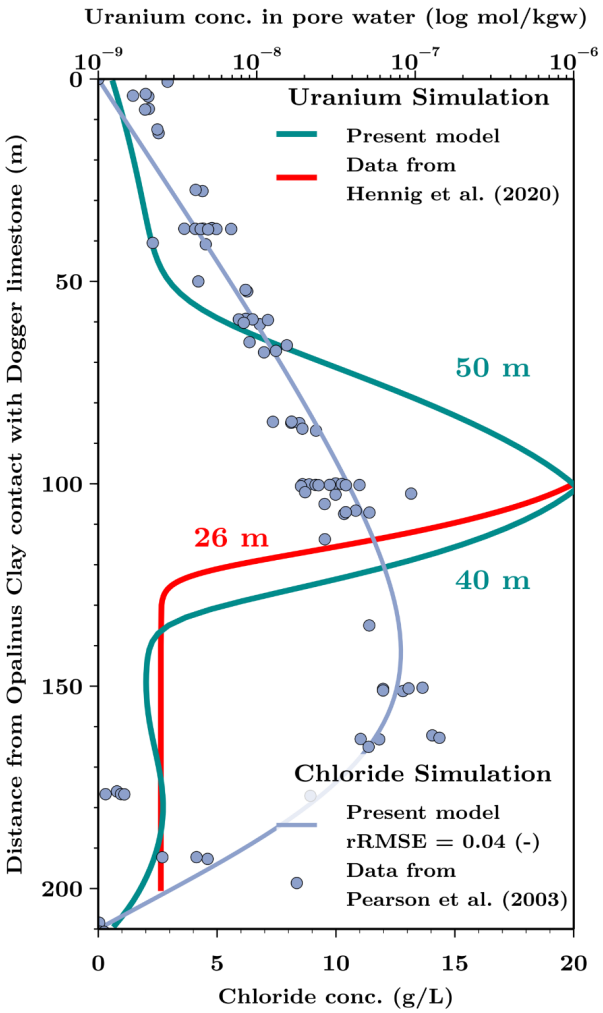

Fig. 1: Geochemical gradients in the Opalinus Clay system at Mont Terri (blue dots) enhance uranium migration (green lines) through the formation compared to homogeneous simulations (red line). Modelled chloride profile (blue line) coincides with measured data, that stems from borehole analysis [3]. The y-axis is the distance perpendicular to the contact between Opalinus Clay and Dogger limestones.

In the heterogeneous simulation (green line, Figure 1), uranium migrated 50 m towards the hanging wall aquifer (Dogger) and 40 m towards the footwall aquifer (Liassic). Thus, uranium migrated up to 24 m farther through the formation considering the geochemical gradients compared to the homogeneous simulations with a maximum of 26 m (red line). Therefore, the geochemical gradients significantly affect uranium migration in terms of increased migration lengths due to a decreased sorption capacity associated with the gradients. This implies, experimentally determined sorption parameters cannot be used for single-component simulations on the host rock scale. Our results show, that uranium is retained within the theoretical effective containment zone of the Opalinus Clay formation and adjacent aquifers are not reached.

REFERENCES

1. HENNIG, T. et al., “Simulation of diffusive uranium transport and sorption processes in the Opalinus Clay”, *Applied Geochemistry,* **123,** 104777 (2020).
2. HENNIG, T. and KÜHN, M., “Surrogate model for multi-component diffusion of uranium through Opalinus Clay on the host rock scale”, *Applied Sciences (Switzerland),* **11**, 1–21 (2021).
3. PEARSON, F.J. et al., “Mont Terri Project–Geochemistry of water in the Opalinus Clay formation at the Mont Terri rock laboratory” *Mont Terri Project Technical Report* 5, Federal Office for Water and Geology, FOWG, Bern, Switzerland (2003).
4. MAZUREK, M. et al., “Natural tracer profiles across argillaceous formations”, *Applied Geochemistry,* **26**, 1035–1064 (2011).
5. PARKHURST, D.L. and APPELO, C.A.J., “Description of input and examples for PHREEQC Version 3 — A computer program for speciation, batch-reaction, one-dimensional transport, and inverse geochemical calculations*” U.S. Geological Survey Techniques and Methods*, vol. 6 chapter A43, page 497 (2013).
6. KOROLEVA, M. and MAZUREK, M., ”Natural Tracer Profile Mont Russelin (NT) Experiment: Natural tracer profiles in the Mont Russelin anticline” *Mont Terri Project, Technical Note 2006-24* (2009).

Breakthrough of ^{99}Tc and actinide tracers from the Long-term-In-situ-Test (LIT)

Francesca Quinto[1], Ingo Blechschmidt[2], Thomas Faestermann[3], Karin Hain[4], Dominik Koll[3], Gunther Korschinek[3], Stephanie Kraft[1], Johanna Pitters[4], Markus Plaschke[1], Georg Rugel[5], Thorsten Schäfer[6], Peter Steier[4], Horst Geckeis[1].

[1]*Karlsruhe Institute of Technology (KIT), Institute for Nuclear Waste Disposal (INE), Karlsruhe, Germany*
[2]*NAGRA (National Cooperative for the Disposal of Radioactive Waste), Wettingen, Switzerland*
[3]*Technical University of Munich (TUM), Physics Department, Garching, Germany*
[4]*University of Vienna, Faculty of Physics, VERA Laboratory, Vienna, Austria*
[5]*Helmholtz-Zentrum-Dresden-Rossendorf, Accelerator Mass Spectrometry and Isotope Research, Dresden, Germany*
[6]*Friedrich-Schiller-Universiy (FSU), Institute for Geosciences (IGW), Applied Geology, Jena, Germany*
email: francesca.quinto@kit.edu

INTRODUCTION

The LIT experiment at the Grimsel Test Site (GTS) in Switzerland consisted in a packer-system containing 16 Febex bentonite rings - four of them spiked with radionuclide (RN) tracers - emplaced in the crystalline rock intersecting a water-conducting shear zone [1]. The saturation of the bentonite with the Grimsel groundwater (GGW) from the shear zone, its consequent swelling with possible release of bentonite colloids and the diffusion of RNs through the bentonite followed by their transport/retention through the shear zone under advective conditions were investigated for a duration of 4.5 years.

DESCRIPTION OF THE WORK

Water samples were collected from two near field boreholes (5.6 cm from the bentonite source). In these samples, composed by bentonite pore water mixing with GGW from the shear zone, the concentration of the radioactive tracers ^{99}Tc, ^{233}U, ^{237}Np and ^{242}Pu, as well as that of the conservative fluorescent tracer Amino-G was analyzed. RN tracers were introduced into a bentonite block as Tc(VII), U(VI), Np(V) and Pu(III). Depending on the redox state establishing during the course of the experiment, they behave as weakly (e.g. Tc(VII)) or relatively strongly (e.g. Pu(IV)) adsorbing elements from which a slow diffusion through bentonite is expected. Consequently, ultra-trace levels are expected in the LIT-GGW samples.

Such analytical challenge was faced with AMS that provides extremely high sensitivity for ^{99}Tc and actinide nuclides. In particular, actinide tracers were analyzed at the 3 MV tandem accelerator of VERA, while ^{99}Tc at the 14 MV tandem accelerator of TUM, enabling quantification at the level of ca. 7×10^4 atoms/sample and ca. 1×10^6 atoms/sample, respectively [2, 3].

A further challenge consisted in the possible background of the shear zone from previous *in situ* RN tracer tests [3, 4]. In order to estimate such shear zone background and identify RNs originating from the LIT, an analysis of the RNs originating from previous *in situ* RN tracer tests was undertaken in GGW samples collected before the emplacement of LIT and from the tailing of the tests in 2012 and 2013 [3].

RESULTS AND DISCUSSION

For both ^{233}U and ^{237}Np the highest breakthrough was observed in the early part of the experiment with concentrations above the estimated shear zone background within 600 days for ^{233}U and 300 days for ^{237}Np. Later, the concentration of ^{233}U decreased down to more than 3 orders of magnitude at the end of the experiment with values below the estimated range of shear zone background, whereas the concentration of ^{237}Np decreased by 2 orders of magnitude with values mostly consistent with the background.

The concentrations of ^{242}Pu had a different trend and were since the beginning mostly consistent with the shear zone background, with only a few data significantly higher especially at 900 days.

The breakthrough of ^{99}Tc (Fig. 1) was always above the estimated shear zone background with a maximum concentration at 200 days followed by a decrease down to 2 orders of magnitude towards the end.

It is important to note that the signal of the conservative tracer was detected already after 20 days and reached the maximum between 400 and 750 days (indicated by the blue box in Fig. 1). Afterwards, the concentration of the conservative tracer decreased by 60% due to the increase of the extraction rate of the water samples from 20 to 50 µl/min at 750 days (indicated by the purple star in Fig. 1). However, the decrease in the concentration of ^{99}Tc is much higher than 60% and cannot be explained only with a dilution effect due to the mixing of bentonite pore water with a higher volume of GGW. In fact, for redox sensitive elements like Tc, the mixing of the bentonite pore water with the reducing GGW (Eh_{SHE} = -200 mV, pH ~ 9.6) may have caused the reduction of Tc(VII) to the less mobile Tc(IV) species. During the experiment we observed slight variations in pH and

fluctuating Eh values. Notably for Tc at least a partly reduction from mobile TcO_4^- to strongly adsorbing reduced Tc(IV) species can be expected which actually will prevail under given conditions.

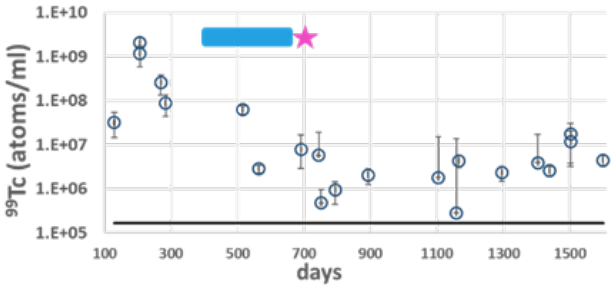

Fig. 1: Concentration of ^{99}Tc in LIT-GGW water samples. The horizontal line indicates the maximum of the estimated shear zone background. The blue box represents the maximum of the conservative tracer and the purple star the increase of the extraction rate of the water samples (see text).

Since all the ^{99}Tc data were above the estimated shear zone background, it is possible to estimate for ^{99}Tc the total number of atoms released from LIT during the test by summing up the number of atoms in the volume of the water samples collected between two consecutive experimental data. In this way, a possible release of ^{99}Tc from LIT equal to ca. 4×10^{12} ^{99}Tc atoms is estimated within the experimental period of 4.5 years and accounting for ca. 8.5×10^{-3} % of the inventory of ^{99}Tc in LIT.

While the obtained results suggest that ^{242}Pu release from the bentonite could not be detected above shear zone background, for other investigated RNs (Tc, Np U) a partly unexpected early appearance was observed. Only for Tc(VII) and Np(V) a significant diffusion can be expected, as both are known to undergo no or only weak sorption. In fact, in the frame of CLAYPOS [1] calculations, K_d values of ca. 0 and 0.11 m^3/kg were adopted for Tc(VII) and Np(V), resulting in a significant diffusion of these species through the bentonite source of LIT up to the bentonite/shear zone interface. Conversely, the other actinide tracers as well as Tc(IV) and Np(IV) present K_d values > 1 m^3/kg and therefore comparatively shorter diffusion lengths are predicted.

The present results can be interpreted assuming an adaption of the initial oxidation states of the applied RN tracers to repository conditions and allow further understanding of the *in situ* RN tracers diffusion through compacted bentonite and consequent migration through a water-conductive feature in granodiorite rock over the time span of 4.5 years.

By using AMS analysis the mobility of even ultra-trace concentration levels of relevant RNs could be detected under given experimental conditions.

ACKNOWLEDGEMENTS

Acknowledments go to : The German Federal Ministry for Economic Affairs and Energy, BMWi, (Grant Number 02E11759B), the International Consortium of the CFM Project, the EU Project RADIATE (Research And Development with Ion Beams – Advancing Technology in Europe).

REFERENCES

1. Kollorado-e2 Final Report. *KIT publications*, Editors: ULRICH NOSECK, THORSTEN SCHÄFER (2019).
2. F. QUINTO et al., "Ultratrace Determination of ^{99}Tc in Small Natural Water Samples by Accelerator Mass Spectrometry with the Gas-Filled Analyzing Magnet System", *Anal. Chem.*, **91**, 4585-4591 (2019).
3. F. QUINTO et al., "Multiactinide Analysis with Accelerator Mass Spectrometry for Ultratrace Determination in Small Samples: Application to an in Situ Radionuclide Tracer Test within the Colloid Formation and Migration Experiment at the Grimsel Test Site (Switzerland)", *Anal. Chem.*, **89**, 7182-7189 (2017).
4. H. GECKEIS et al., "Results of the colloid and radionuclide retention experiment (CRR) at the Grimsel Test Site (GTS), Switzerland - Impact of reaction kinetics and speciation on radionuclide migration", *Radiochim. Acta*, **92**, 765-774 (2004).

Evolution of Radionuclide Transport and Retardation Processes in Uplifting Crystalline Rocks

Richard Metcalfe[1], Daisuke Kawama[2], Steven J. Benbow[1], Yukio Tachi[3]

[1]*Quintessa Limited, Videcom House, Newtown Road, Henley-on-Thames, Oxfordshire RG9 1HG, UK*
[2]*QJScience, 3rd floor, Yokohama Port Side Building, 8-1 Sakaecho, Kanagawaku, Yokohama, 221-0052 Japan*
[3] *Japan Atomic Energy Agency (JAEA), 4-33 Muramatsu, Tokai, Ibaraki, 319-1194, Japan*
email:richardmetcalfe@quintessa.org

INTRODUCTION

A safety case for an underground radioactive waste repository must show that if radionuclides leave the repository, the surrounding geosphere barrier will prevent or adequately retard their migration via groundwater, despite any future environmental changes. Uplift is one such environmental change that may affect some potential repository sites. This may be a particularly important issue in Japan, where a repository site is yet to be selected, but where possibly in future areas undergoing tectonically driven uplift might be considered.

At early stages of a project to site a radioactive waste repository, as at present in Japan, generic safety cases are typically based on simplified/conservative assessment models. However, at an actual repository site, where site-specific conditions are known, more realistic models are needed that account for the long-term geoenvironmental evolution and their impacts on radionuclide migration/retention. Here we review the state of knowledge about evolving properties of fractured crystalline rocks during uplift, based on studies in Japan. Hence, we propose how this knowledge may be used to produce assessment models that appropriately balance realism and with sufficient simplicity to allow exploration of parameter uncertainty.

DESCRIPTION OF THE WORK

Research into groundwater flow and solute transport in uplifting fractured crystalline rock in Japan was reviewed (e.g. [1-4] and references therein). Based on the review, generic conceptual models were developed for radionuclide migration from a hypothetical deep geological repository for higher activity radioactive waste sited in an uplifting fractured granitic rock body. Using Quintessa's computer code CABARET, which has the same functionality as the code QPAC used in many other modelling studies e.g. [5], fully-coupled 2-D reactive transport models were then constructed to represent the key processes controlling radionuclide transport and retardation in these generic conceptual models. The numerical model represents groundwater flow and radionuclide transport through a single 500 m long fracture. Simulations carried out with the model aimed to gain insights into the sensitivity of radionuclide transport to rock matrix diffusion (RMD), sorption, mineral precipitation and dissolution, reaction kinetics, and porosity distribution in the host rock. Model cases were parameterised using realistic transport data obtained from studies of Japanese granitic rocks, principally the Toki Granite of the Tono area in central Japan e.g. [1-3].

RESULTS AND DISCUSSION

Fractured crystalline rocks are assumed to uplift at <90 m / 100,000 years, the repository being sufficiently deep that it remains several 100 m below the surface after 100,000 years. During this uplift erosion will occur and hydraulic gradients are likely to steepen and fractures to dilate, causing increased groundwater fluxes in the rocks around the repository (Fig. 1). Fresh oxidizing meteoric water flushes the crystalline rock and reduces the salinity of deep more saline groundwater near the repository. At the same time, the porosity of rock matrix adjacent to the fracture may increase very near the ground surface.

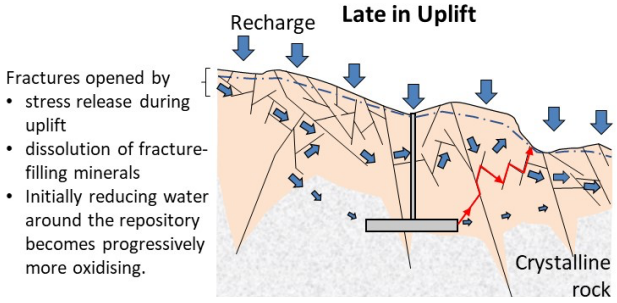

Fig. 1: Schematic illustration showing processes affecting repository in fractured crystalline rock late in uplift. Red line shows a hypothetical radionuclide transport path. The light brown shaded area is an oxidized zone.

As an example Fig. 2. shows model output cases in which reducing saline water transports U at a concentration of 1 x 10^{-6} mol kg^{-1} into a fracture for 10,000 a. Fresh, oxidising water then begins to inflow to the fracture in proportions that increase linearly, such that after 100,000 a all the inflowing water would be of this type. The inflowing fresh water has a U concentration of 1 x 10^{-10} mol kg^{-1}. This situation could occur as the redox

front in Fig. 1 moves downwards into a rock volume through which U has been transported from the repository. In this example model, this period of U transport is 10,000 a; this is not the time after repository closure, which could be much earlier.

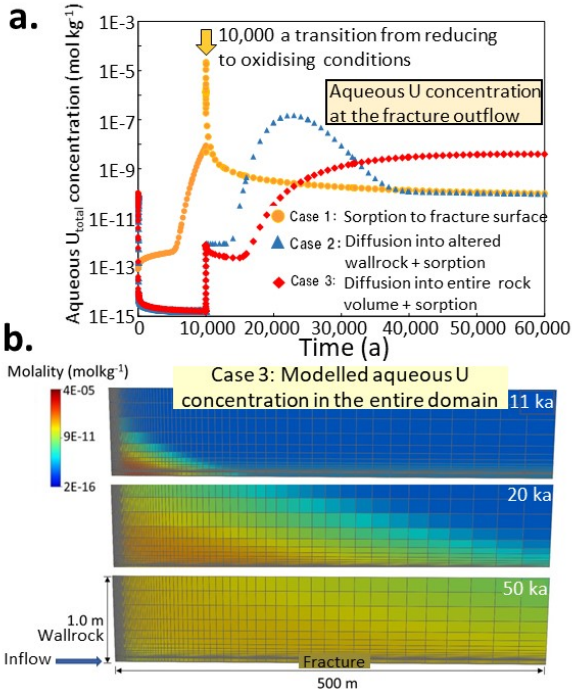

Fig. 2: Example model output. In all cases water in the modelled domain initially contains U = 1 x 10^{-10} mol kg^{-1} and inflowing water is reducing and saline, with U = 1x10^{-6} mol kg^{-1}. From 10,000 a to 100,000 a increasing proportions of oxidising fresh water with U = 1 x 10^{-10} mol kg^{-1} flow into the fracture. **a.** U concentrations in the outflow from a 500 m long fracture. **b.** Aqueous U concentrations at different times throughout the domain.

In Fig. 2, Case 1 involves U retention only by sorption on fracture surfaces. The U breaks through to the end of the fracture rapidly. A spike in U concentration occurs as soon as conditions start to become oxidising. However, outflowing U concentrations fall sharply after this peak. In Case 2, RMD occurs in addition to sorption, but only in 5 cm of rock matrix adjacent to the fracture. In this case U transport through the fracture is retarded and peak U concentrations at the outflow are lower and occur later. After 40,000 a the U concentrations in the fracture outflow are the same as in Case 1. In Case 3, all the rock matrix (1 m thick) is accessible to diffusing U, which can sorb throughout the rock volume. U transport is retarded even more than in Case 2, so that for about half the modelled time (after 30,000 a) U concentrations in Case 3 are higher than in Case 1 or Case 2.

This example illustrates it is challenging to specify conservative behaviour when developing safety assessment models for uplifting fractured rocks owing to many processes involved being coupled. Case 1 might be considered conservative, because there is no RMD, a potentially important retardation mechanism. However, if the spike in U occurs when there is still a sufficient thickness of shallower rock present, there could still be much dispersion of U further along the flow path that would reduce U concentrations at the ground surface. In contrast, Case 3 has maximal RMD but results in higher U concentrations at later times. If erosion during uplift had shortened the flow path by these later times, then potentially U concentrations at the surface could be higher than in Case 1; the maximal RMD case could be conservative. Case 2 results are intermediate, between those of Case 1 and Case 3. Case 2 might be considered the most realistic, based on observations on the length scale of matrix diffusion from the Toki Granite in the Tono area, [4]and references therein.

Modelling the coupled radionuclide transport and retardation processes is computationally intensive. Nevertheless, we have demonstrated that it is possible to simulate these couplings for a single fracture pathway within reasonable computational times (a few hours to days) over realistic length scales (500 m). These kinds of simulations are necessary to identify realistically conservative combinations of processes and parameter values, as precursors to safety assessment calculations.

ACKNOWLEDGMENTS

This study was performed as part of 'The project for validating near-field assessment methodology in geological disposal (FY2018-2020)' supported by the Ministry of Economy, Trade and Industry of Japan (Grant Number: JPJ007597).

REFERENCES

1. JNC, H12: Project to Establish the Scientific and Technical Basis for High-Level Radioactive Waste Disposal in Japan, Supporting Report 1 Geological Environment in Japan, JNC TN1410 2000-002 (2000).
2. IWATSUKI, T. et al., Hydrochemical baseline condition of groundwater at the Mizunami underground research laboratory (MIU), *Applied Geochemistry*, **20**, 2283–2302 (2005).
3. YOSHIDA, H. et al., Retardation capacity of altered granitic rock distributed along fractured and faulted zones in the orogenic belt of Japan, *Engineering Geology*, **106,** 116–122 (2005).
4. WOGELIUS, R.A. et al.. Mineral reaction kinetics constrain the length scale of rock matrix diffusion, *Scientific Reports*, **10**, 8142 (2020).

5. WILSON, J. et al., Reactive transport modelling of a cement backfill for radioactive waste disposal. *Cement and Concrete Research*, **111,** 81–93 (2017).

A new operator-splitting finite element scheme for reactive transport modelling in saturated porous media

Renchao Lu[1], Vanessa Montoya[1], Olaf Kolditz[1,2], Haibing Shao[1]

[1]*Helmholtz Centre for Environmental Research - UFZ, Department of Environmental Informatics, Leipzig, Germany*
[2] *Technische Universität Dresden, Dresden, Germany*
email: renchao.lu@ufz.de

INTRODUCTION

The design of high-level radioactive waste repositories follows the widely recognized multi-barrier concept [1]. The multi-barrier system normally includes the waste canister, the buffer, seals, plugs and the host rock which serves to retard and limit the potential release and migration of radionuclides in the expected disposal period [2, 3]. Over the time scale up to one million years, the near-field engineered barrier system will be perturbed by chemical reactions. This may degrade the durable sealing integrity of the repository which is at the core of performance assessment for high-level waste repositories.

Reactive transport modelling is considered an efficient tool to predict the evolutionary integrity of each component of the multi-barrier system. In this context, a number of reactive transport modelling software packages have been developed in the last years, such as COMSOL-Phreeqc, COMSOL-GEM, CORE^{2D}, CrunchFlow, CSMP++GEM, DuCOM-Phreeqc, FEniCS-Reaktoro, Frachem, HP1/HPx, MATLAB-Phreeqc, MIN3P, OpenGeoSys-5#GEM, OpenGeoSys-5#Phreeqc, ORCHESTRA, Proost, ReactMiCP, and ToughReact among others. A majority of the aforementioned reactive transport codes employ the operator splitting approach in solving reactive transport processes, because of its computational efficiency and its flexibility in the choice of the numerical methods for solving the transport and reaction equations. When we come to the operator-splitting finite element scheme as a subcategory of numerical technique, the long-established workflow (referred as Nodal-OS scheme) works in a way that Gaussian points are taken as the collocation points in discretizing the transport equation in space while the mesh node for the reaction equation.

DESCRIPTION OF THE WORK

In this work, a new uniform collocation scheme has been employed for spatially discretizing the transport and reaction equations. Accurately speaking, the transport and reaction equations both take the Gaussian points as their collocation points (called as IP-OS scheme). Here, we take a one-dimensional radionuclide decay problem in a semi-infinite, fluid-saturated porous medium column as an example to demonstrate the advantage of the IP-OS scheme over the conventional Nodal-OS scheme in numerical accuracy.

Specifically, the radionuclide will decay during its migration. The decay of the radionuclide is assumed to obey a first-order kinetic law (half-life = 42 h). The computational domain is 2-meter long. In this classical problem, we perform three comparable numerical experiments where the global implicit approach, the Nodal-OS scheme, and the IP-OS scheme are employed respectively. The model parameters used in the numerical experiments (i.e. the pore diffusion coefficient, porosity, first-order decay constant, grid spacing, time step size, and initial and boundary conditions) are set according to Valocchi and Malmstead (1992) [4]. Besides, the analytical solution of this problem is also provided as the reference for precision evaluation.

RESULTS AND DISCUSSION

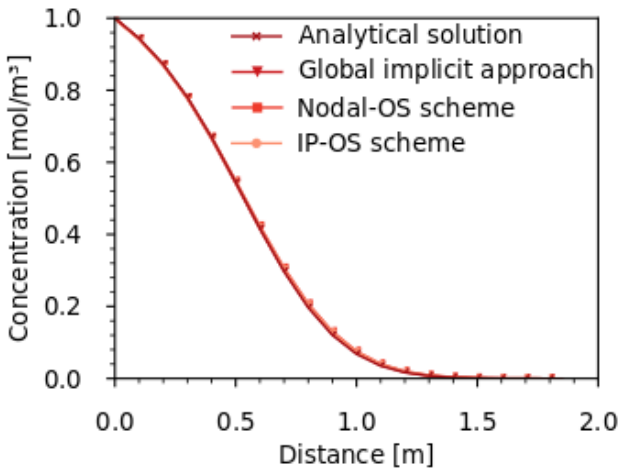

Fig. 1: Comparison of the nodal-OS scheme, IP-OS scheme, and global implicit approach in terms of the radionuclide concentration profile.

Figure 1 illustrates the comparison of the radionuclide concentration profiles obtained from the three numerical experiments against the analytical solution. As expected, all the numerical solutions reach very good agreement with the analytical solution, thereby validating the implementation of the three numerical solution schemes.

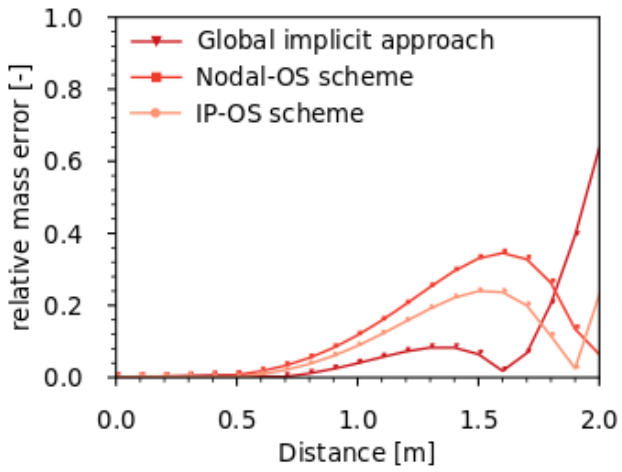

Fig. 2: Comparison of the nodal-OS scheme, IP-OS scheme, and global implicit approach in terms of the spatial distribution of the relative mass error.

Figure 2 shows insight on the relative errors of the three numerical solutions yielded by a comparison to the analytical solution. By comparison of the error profiles, it is indicated that the global implicit approach is superior to the operator splitting approach in terms of numerical accuracy. It is also revealed that among the two OS schemes, the IP-OS scheme yields a numerical solution of higher accuracy than the conventional Nodal-OS scheme. It is generally believed that the loss of accuracy under using the operator-splitting approach is completely caused by the algorithm itself. Whereas, the results in this study as illustrated in Fig. 2 show that the inconsistent choice of collocation points for the transport and reaction equations will cause an extra numerical error and contribute to the loss of accuracy.

Despite a small error in the presented problem, such error may accumulate over time. The accuracy of numerical solutions may become increasingly important when we come to the assessment of long-term evolution radionuclides on waste repositories. This study recommends to unify the choice of collocation points in numerically treating the transport and reaction equations in such a way that accuracy of the numerical solution can be improved.

ACKNOWLEDGEMENTS

We acknowledge the funding support by the iCROSS-Project (Integrity of nuclear waste repository systems – Cross-scale system understanding and analysis) by the Federal Ministry of Research and Education (BMBF) (grant number 02NUK053E) and the Helmholtz Association (Helmholtz-Gemeinschaft e.V.) through the Impulse and Networking Funds (grant number SO-093).

REFERENCES

1. CLARET. F. et al., “Modelling the long-term stability of Multi-barrier system for Nuclear Waste Disposal in Geological Clay Formations”. In Xiao et al.: John Wiley & Sons (2018).
2. JEDINÁKOVÁ-KŘIŽOVÁ, V., “Migration of radionuclides in the environment”, *Journal of Radio-analytical and Nuclear Chemistry*, **229**, 13-18 (1998).
3. KRAUSKOPF, K.B., “Geology of high-level nuclear waste disposal”, *Annual Review of Earth and Planetary Sciences*, **16**, 173-200 (1988).
4. VALOCCHI, A.J. AND MALMSTEAD, M., “Accuracy of operator splitting for advection-dispersion-reaction problems”, *Water Resources Research*, **28**, 1471–1476 (1992).

INE Scientific Working Documents
ISSN 2701-262X

www.kit.edu